University of Zagreb

Faculty of Transport and Traffic Sciences

Lucija Bukvić

MODELLING THE RESILIENCE PARAMETER AND COST PREDICTION OF THE INTERMODAL TRANSPORT SYSTEM USING THE CONGESTION GAME APPROACH

DOCTORAL DISSERTATION

Zagreb, 2025

University of Zagreb

Faculty of Transport and Traffic Sciences

Lucija Bukvić

MODELLING THE RESILIENCE PARAMETER AND COST PREDICTION OF THE INTERMODAL TRANSPORT SYSTEM USING THE CONGESTION GAME APPROACH

DOCTORAL DISSERTATION

Supervisor: Prof. Borna Abramović, Ph.D.

Zagreb, 2025

Sveučilište u Zagrebu

FAKULTET PROMETNIH ZNANOSTI

Lucija Bukvić

MODELIRANJE PARAMETRA OTPORNOSTI I PREDVIĐANJE TROŠKOVA INTERMODALNOG PRIJEVOZA KORIŠTENJEM PRISTUPA IGRE ZAGUŠENJA

DOKTORSKI RAD

Mentor: Prof. dr. sc. tech. Borna Abramović

Zagreb, 2025.

Contents

Acknowledgements

Pursuing a Ph.D. is often a long and always a difficult journey, filled with challenges, learning, and continuous personal growth. This dissertation is the result of not only academic effort but also the support and encouragement from my colleagues and friends that I received along the way. First, my deepest gratitude goes to my advisor, Prof. Borna Abramović, for his invaluable guidance, patience, and continuous support throughout all of my doctoral journey, even though he was not officially mentoring my work from the start. His expertise, insightful feedback, kind and encouraging words were crucial at the very last stage of this journey.'We should train the AI Ph.D. advisors on his work database, so that other struggling PhD students can receive words of encouragement any time.'

I am especially grateful to my Department of Intelligent Transport Systems, where I've enriched my perspective, and to those kind people who helped me shape a key part of this dissertation. Many thanks to our ITS boss Pero with all the help he provided since I'm officially a part of the Department. I would also like to thank the members of both research groups in Zagreb and Cork, Ireland for their intellectual contributions and collegial spirit.

To my friends and fellow Ph.D. candidates, thank you for your encouragement, your humour in difficult times, and the shared understanding of this challenging but rewarding path. Thank you for all the coffee breaks that kept us all above the surface level.

Sincere thanks go to my colleagues at the Faculty of Transport and Traffic Sciences, University of Zagreb, for stimulating collaborative work environment, and many shared moments that made this journey more enjoyable.

I owe my deepest gratitude to my mom Đurđica, sister Maja for their unconditional love, patience, and belief in me. Big thanks also go to my friends, Doroteja and Dominik, for their long-term support and lifelong friendship. Many thanks to my Sunshine island Croatian crew for encouragement and making new strategies every week, its pool of ideas inspired me to apply game theory in the first place. Last but not least, my greatest thanks goes to my dearest Jure whose love and knowledge guided me through the darkest days. Your support has been my foundation and strength throughout this journey.

About the mentor:

Borna Abramović was born on September 20, 1977 in Slavonski Brod. He completed primary and secondary railway technical school in Zagreb. He graduated from the Faculty of Transport Sciences, University of Zagreb with the topic "Formal methods in the analysis of safety of railway level crossings". He successfully defended his scientific master's thesis in 2007 with the topic "Technological model of charges for railway infrastructure". He successfully defended his doctoral dissertation entitled "Modeling demand in the function of railway transport" in 2010. He was elected to the scientific title of scientific advisor and the scientific teaching title of full professor. At the Faculty of Transport Sciences in Zagreb, he is the head of the Department of Railway Transport. He is the president of the Croatian Chamber of Transport and Transport Technology Engineers. He is an ambassador for the "Railway Talents" project of the International Union of Railways. At the Faculty of Transport Sciences, he teaches the following courses: Organisation of Railway Transport, Transport of Goods by Rail, Management in the Railway System and Organisation of Passenger Transport by Rail. At the doctoral level, he is the course leader for Applied Statistics for Transport Research, Innovative Intermodal Technologies and the Research Seminar on the Organization of Integrated Passenger Transport. At the Faculty of Electrical Engineering and Computing, University of Zagreb, he is the course leader for Railway Safety Signaling and Communication Systems. At the Department of Geography, Faculty of Science, University of Zagreb, he is a guest lecturer for the course Transport and Spatial Organization. He is a guest lecturer at the following higher education institutions: University of Žilina (Slovakia), University of Pardubice (Czech Republic), University of Palermo (Italy), Carolo-Wilhelmina Technical University in Braunschweig (Germany), University of Ljubljana (Slovenia), University of Košice (Slovakia), University of Novi Sad (Serbia), Institute of Technology and Business in České Budějovice (Czech Republic), University of Newcastle (United Kingdom), Budapest University of Technology and Economics (Hungary), Gediminas Technical University in Vilnius (Lithuania), Polytechnic University of Bucharest (Romania), University of Gdansk (Poland), Lumière Lyon 2 University (France) and Iran University of Science and Technology. His areas of scientific interest are: railway transport organization, railway infrastructure charges, rail freight transport, railway service market, integrated passenger transport, traffic forecasting, transport demand and game theory. He is an active researcher and has participated in a large number of scientific projects of the European Union and Croatia, as well as a large number of studies and reports in Croatia. In total, he has published five book chapters, four university textbooks (two in English), one scientific monograph, 60 scientific papers in international journals, 25 invited lectures at international scientific conferences, and 97 papers in internationally peer-reviewed conference proceedings.

O mentoru:

Borna Abramović rođen je 20. rujna 1977. u Slavonskom Brodu. Osnovnu i srednju Željezničku tehničku školu završio je u Zagrebu. Diplomirao je na Fakultetu prometnih znanosti Sveučilišta u Zagrebu na temu „Formalne metode u analizi sigurnosti željezničkih cestovnih prijelaza u razini". Znanstveni magistarski rad uspješno je obranio 2007. na temu „Tehnološki model pristojbi za željezničku infrastrukturu". Doktorsku disertaciju pod nazivom „Modeliranje potražnje u funkciji prijevoza željeznicom" uspješno je obranio 2010. godine. Izabran je u znanstveno zvanje znanstvenog savjetnika i znanstveno nastavno zvanje redovnog profesora. Na Fakultetu prometnih znanosti u Zagrebu predstojnik je Zavoda za željeznički promet. Predsjednik je Hrvatske komore inženjera tehnologije prometa i transporta. Ambasador je projekta „Željeznički talenti" Međunarodne željezničke unije. Na Fakultetu prometnih znanosti nositelj je kolegija: Organizacija željezničkog prometa, Prijevoz robe željeznicom, Gospodarenje u željezničkom sustavu i Organizacija prijevoza putnika željeznicom. Na doktorskom studiju nositelj je kolegija Primijenjena statistika za istraživanja u prometu, Inovativne intermodalne tehnologije i Istraživačkog seminara iz organizacije integriranog prijevoza putnika. Na Fakultetu elektrotehnike i računarstva Sveučilišta u Zagrebu izvođač je kolegija Željeznički sigurnosno signalni i komunikacijski sustavi. Na Geografskom odjelu Prirodoslovnog fakulteta Sveučilišta u Zagrebu gost predavač je na kolegiju Promet i organizacija prostora. Gost predavač je na sljedećim visokoobrazovnim ustanovama: Sveučilište u Žilini (Slovačka), Sveučilište u Pardubicama (Češka), Sveučilište u Palermu (Italija), Tehničko sveučilište Carolo-Wilhelmina u Braunschweigu (Njemačka), Sveučilište u Ljubljani (Slovenija), Sveučilište u Košicama (Slovačka), Sveučilište u Novom Sadu (Srbija), Institut za tehnologiju i poslovanje u Českim Budějovicama (Češka), Sveučilište u Newcastleu (Ujedinjeno Kraljevstvo), Sveučilište za tehnologiju i ekonomiju u Budimpešti (Mađarska), Tehničko sveučilište Gediminas u Vilniusu (Litva), Politehničko sveučilište u Bukureštu (Rumunjska), Sveučilište u Gdanjsku (Poljska), Sveučilište Lumière Lyon 2 (Francuska) i Iransko sveučilište za znanost i tehnologiju. Područja interesa u znanosti su: organizacija željezničkog prometa, pristojbe za željezničku infrastrukturu, prijevoz robe željeznicom, tržište željezničkih usluga, integrirani prijevoz putnika, prognoziranje prometa, prijevozna potražnja i teorija igara. Aktivni je istraživač te je sudjelovao u velikom broju znanstvenih projekata Europske unije i Hrvatske te velikom broju studija i elaborata u Hrvatskoj. Ukupno je objavio pet poglavlja u knjizi, četiri sveučilišna udžbenika (od toga dva na engleskom jeziku), jednu znanstvenu monografiju, 60 znanstvenih radova u međunarodnim časopisima, 25 pozvanih predavanja na znanstvenim međunarodnim skupovima i 97 radova u zbornicima skupova s međunarodnom recenzijom.

Abstract

The fundamental problem of intermodal transport is route optimisation and the choice of transport mode, which affect the interests of logistics companies and end customers. The possibility of organising more frequent, consolidated transports and the coordinated use of the freight transport network results in savings in overall costs for carriers when forming a coalition, along with modal shift and a more favourable impact on the environment. Such an approach is called the congestion game. Game theory represents a framework for making decisions that must result in an efficient and rational outcome. Cooperativeness in the game contributes to the minimisation of costs if the costs of the terminal are also observed, especially in case of complete closure of certain parts of the route. Through an example of freight transport from three seaports to a certain intermodal terminal, it is presented that it is possible to find the lowest transport cost on different routes for each carrier (player), considering total transport and terminal handling costs. The transport cost in the extended network will be predicted by applying reinforcement learning to the congestion game model, where the state of the players is defined with a unique resilience parameter. To mitigate the resulting negative impacts in the intermodal network, selected congested routes are 'punished' and the choice of terminals with a higher level of service is 'rewarded'.

Keywords: intermodal transport; game theory; congestion game; reinforcement learning; carriers; transport costs

Sažetak

Temeljni problem intermodalnog prijevoza jest optimizacija usmjeravanja i odabir prijevoznog moda, koji utječu na interese logističkih poduzeća i krajnjih korisnika. Mogućnost organiziranja češćih, konsolidiranih prijevoza te usklađenog korištenja mreže teretnog prijevoza rezultira uštedama u ukupnim troškovima za prijevoznike pri formiranju koalicije, uz promjenu moda prijevoza i povoljniji utjecaj na okoliš. Takav se pristup naziva igrom zagušenja. Teorija igara predstavlja okvir za donošenje odluka koje moraju rezultirati učinkovitim i racionalnim ishodom. Kooperativnost u igri doprinosi minimizaciji troškova ako se promatraju i troškovi terminala, osobito u slučaju potpunog zatvaranja pojedinih dijelova rute. Na primjeru teretnog prijevoza iz tri morske luke do određenog intermodalnog terminala prikazuje se da je moguće pronaći najniži trošak prijevoza na različitim rutama za svakog prijevoznika (igrača), uzimajući u obzir ukupne troškove prijevoza i manipulacije u terminalu. Trošak prijevoza u proširenoj mreži predviđat će se primjenom pojačanog učenja (reinforcement learning) na model igre zagušenja, pri čemu je stanje igrača definirano jedinstvenim parametrom otpornosti. Kako bi se ublažili nastali negativni učinci u intermodalnoj mreži, odabrane zagušene rute se „kažnjavaju“, dok se odabir terminala s višom razinom usluge „nagrađuje“.

Ključne riječi: intermodalni prijevoz; teorija igara; igra zagušenja; pojačano učenje; prijevoznici; prijevozni troškovi

Chapter 1

Introduction

Vulnerability and resilience are two key concepts that are often used in different contexts, including those related to people, organisations, society, ecology and technology. The connection is that the notion of resilience operates as a response to vulnerability as it often plays a key role in mitigating vulnerability. If an individual, organisation, or system can adapt or recover from challenges, vulnerability can be reduced. In the last few years, research on the vulnerability of the transport network has attracted increasing attention due to the possible negative consequences it can have on the daily functioning of transport. System vulnerability is a key concept used to analyse network structure and is defined in different forms [1]. A recent study [2] examines the vulnerability of the public transport network. The proposed methods integrate stochastic supply and demand models, dynamic route selection and limited operational capability [3]. Dynamic agent modelling of network performance enables the coverage of cascading effects as well as the adaptive redistribution of passenger or freight flows [4]. The topological attributes of the transport system significantly influence its resilience to incident events in terms of flow, connectivity or compactness [5]. There are several ways to assess and model cascading effects in transport infrastructure that can be found in the literature, which aim to provide an overview of methods for assessing infrastructure use as part of risk and vulnerability analysis. [6] One of the methods of quantitative risk assessment is defined as the product of frequency and consequences, based on parameters: frequency, probability, extent, number of people affected by the unavailability of the service and duration, the period of time when the service is unavailable. Vulnerability of the public transport network through cascading effects can be observed through graph theory applied to the public transport network and the analysis of the possible vulnerability of the service due to relevant disturbances, such as the closure and unavailability of one or more nodes. Integrating reinforcement learning with game-theoretic modelling offers a powerful approach to simulate and optimise complex intermodal transport networks. Modelling carriers as strategic agents and enabling them to learn adaptive cost-minimising behaviours leads to more resilient, efficient, and decentralised logistics systems. As shown in various research fields, multiagent reinforcement learning is a promising avenue for artificial intelligence (AI) research, as agents have been documented to collaborate at human-level performance in three-dimensional multiplayer games. [7],[8] Such interactions can be modelled as congestion games, where each player represents a freight carrier. When carriers play rationally and utilise their operational data collaboratively, the resulting models can achieve higher complexity. In this context, rationality acts as an objective function that drives each carrier to select strategies minimising its transport cost (or maximising utility), given the congestion level and behaviour of other players, ensuring that no unilateral deviation gives a better outcome. While it is impressive that multiagent collaboration at human-level performance is now possible using a game theoretic approach, it also raises the inevitable question of whether human beings have the skill and will to collaborate with AI agents in the future. Consequently, we need to find our appropriate co-existing strategy, or the optimal combination of collaboration and competition, if we are to co-exist with AI agents. Or to paraphrase the famous Danish scientist and artist Piet Hein: It is a question of 'co-existence or no existence'.

This dissertation presents real-world intermodal networks, focussing on the North Adriatic Port Association (NAPA) ports and Central European corridors, which are used to validate the model. A congestion game framework models route selection under limited capacity and cooperative payoff distribution (via Shapley values), while reinforcement learning, augmented with Graph Attention Networks (GAT), enables adaptive cost prediction in dynamic environments. Through simulation and empirical analysis, the dissertation demonstrates how integrating resilience-aware parameters leads to smarter decision-making, more robust transport flows, and cost-efficient re-routing strategies under disruption scenarios. This multidisciplinary approach contributes both to theoretical transport network modelling and practical digitalisation strategies aligned with EU Green Deal and sustainable freight goals.

This research is grounded on two hypotheses:

It is possible to apply a new resilience parameter on the intermodal network to improve route selection in the congestion game. Thus, a novel resilience parameter can be integrated into intermodal transport networks to enhance route selection within a congestion game framework.

Transport costs can be predicted by applying reinforcement learning in the congestion game using a new resilience parameter. Transport costs in intermodal systems can be predicted using reinforcement learning (RL), using GAT and the new defined resilience parameter within a disrupted node in the intermodal network.

To test these hypotheses, the study introduces a resilience parameter that captures the dynamic robustness of nodes and links within the intermodal transport network. This parameter is based on network capacity surplus, vulnerability metrics (entropy-based demand-capacity distributions), and node criticality under disruption scenarios. The resilience parameter is integrated into a congestion game model, where each agent (carrier) competes for route selection under limited capacity, dynamically influenced by the system's resilience.

A reinforcement learning model, based on a multi-agent architecture, is developed to simulate adaptive agent behaviour in selecting cost-effective, resilient routes. The RL model incorporates both static network attributes and dynamic resilience feedback, allowing it to learn optimal strategies in environments subject to congestion and disruption.

Scientific Contribution

Identification of a new resilience parameter of the intermodal transport system: A quantitative parameter is proposed to reflect the surplus capacity and vulnerability of network nodes, derived from entropy-based formulations and time-to-survive (TTS) metrics under disruption scenarios. This resilience parameter enables a measurable comparison of node robustness in distribution, incorporating robustness, adaptability and recoverability of a certain node.

Congestion game model based on a new resilience parameter with the aim of cost optimisation in the intermodal transport system: The intermodal transport system is modelled as a non-cooperative congestion game, where agents' payoffs (i.e., transport cost minimisation) are dynamically modulated by the resilience parameter. This leads to adaptive equilibrium route choices that reflect not only congestion levels but also the systems' vulnerability.

Reinforcement learning based model for cost prediction in the intermodal transport system using a new resilience parameter: A Graph Attention Network (GAT)-based reinforcement learning framework is applied to predict transport costs. The model learns from state-action interactions, demonstrating that cost-effective routing decisions emerge more reliably when the resilience parameter is embedded into the RL training environment.

Simulation results show that incorporating the resilience parameter leads to more balanced flow distributions, avoiding structurally weak nodes and reducing the risk of cascading failures. The RL model trained with resilience-aware features consistently outperformed baseline models in cost prediction accuracy and adaptive route selection. Comparative experiments across disruption scenarios confirmed that resilience-guided routing maintains lower overall transport costs and higher system continuity compared to traditional shortest-path or load-based approaches.

Chapter 2

Intermodal transport system

Intermodal transport is defined as the movement of freight-standardised units, intermodal transport units (ITU), without freight handling in changing transport modes. It combines the accessibility of inland transport modes with the long-haul capabilities of railway and seaport shipping. The benefits of intermodal transport systems can be seen in the rise of these specific freight operations, resulting in various changes in the organisation of transport. Geographical and transport infrastructure differences, economic development at different levels characterise every continent's transport system. A operational intermodal transport system consists of key elements which are listed in this chapter, and the meaning of each element will be shown on the example of the intermodal system in the Republic of Croatia and Europe's biggest shipping ports.

2.1 Introduction to intermodal transport system

Intermodal transport has been created as an answer to the question of how to transport freight to its destination and end users as efficiently and quickly as possible, with as little expense, freight manipulation and human labour. Whether the ITU is a container, swap body or a freight vehicle, intermodal transport is characterised by the fact that the freight in the ITU is not handled when changing transport modes. Less energy and time is thus spent on transport, with a greater effect at the same time, because the ITU is at the same time a storage unit that is being handled. In other words, the transport process is optimised and its reliability is ensured. [9] In the process of globalisation, international trade has grown because of increased sourcing activities, diffused production facilities, yearly increasing freight volume and decreased transport costs. Carriers and logistics service providers have to supply more rapidly and with reliability of delivering services to minimize shippers' costs associated with warehousing, inventory holding, and other aspects of production and distribution. All these elements can be collectively classified into terminal handling cost (THC) [10]. European Commission provided a definition of intermodal transport in 2002 as follows: 'Intermodal freight transport provides transport for consolidated loads such as containers, swap-bodies and semi-trailers by combining at least two modes.' [11] One example of an intermodal freight chain is shown in Figure 2.1 where the two seaports are connected with a hinterland container terminal by railway, inland waterway, and roads.

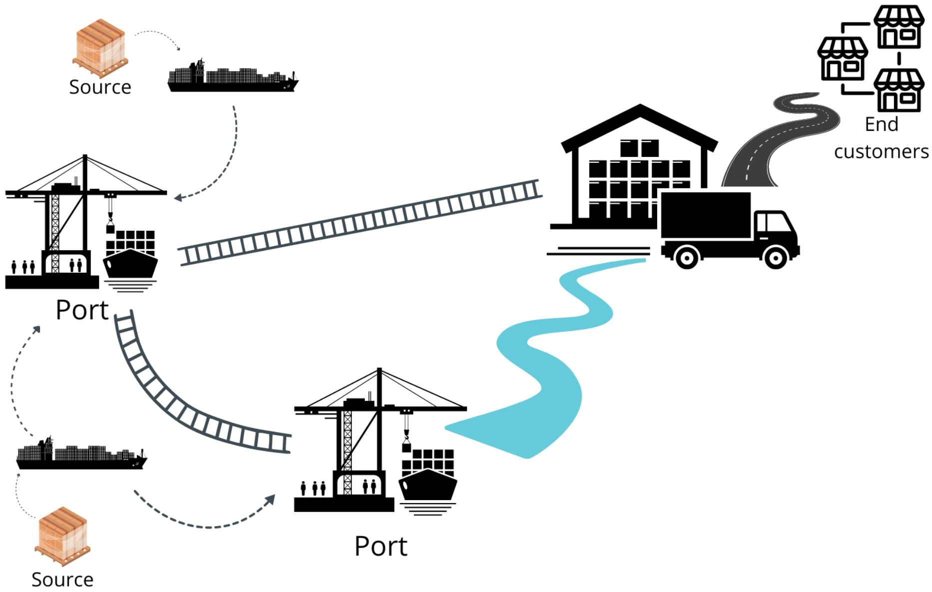

Figure 2.1: Example of an intermodal freight transport logistic chain.

Intermodal transport is supported by legislative actions of the European Union. Actions, directives and financial support are the results of the provisions of the White Paper issued in 2011 named 'Plan for a Single European Transport Area'. The development of intermodal transport is particularly evident in EU countries such as Germany, France, and the Netherlands. In Western European countries, this type of transport accounts for about 40 per cent of the total volume. What has been neglected is the information and IT infrastructure . The shipper's selection of intermodal transport largely hinges on the availability of comprehensive information regarding its various options, terms, and pricing structures, given its complex multi-service provider nature. The implementation of a collective procurement entity for intermodal transport services appears to hold the potential to expedite its advancement. Determining the optimal terminal location is of great importance. It necessitates positioning at the convergence point of diverse transport modes, including mainline railways and highways. Location considerations categorise terminals into three types:

- port terminals,
- rail terminals,
- intermodal terminals (serving as rail-road or rail-road-waterway terminals).

These terminals are frequently situated within logistics hubs and primarily manage freight flow to and from these centres. Collaborative efforts involving the United Nations Economic Commission for Europe (UN/ECE), the European Parliament, the European Commission, and the European Conference of Ministers of Transport (ECMT) have explored the prospect of instituting international legislation for modal transport. Since the 1950s, Europe has witnessed a surge in endeavours supporting intermodal transport development. Rail transport became economically viable for distances exceeding 500 kilometres. However, this scenario underwent a dramatic shift during the oil crises triggered by The Organisation of Arab Petroleum Exporting Countries (OAPEC) member state embargoes and subsequent events. Consequently, customers and shippers began gravitating towards rail transport, mainly because of the extensive electrification initiatives financed by governments. This transition was prompted by the recognition of adverse effects associated with truck deliveries, such as noise pollution, road accidents, exhaust emissions, and road congestion caused by heavy vehicles. From the late 1970s, Western Europe observed a reversal in transport trends, prompting many countries to address the broader ramifications of excessive reliance on-road vehicles. Measures such as restricting or suspending road transport on weekends and nights, special tolls for highway usage by trucks, and designating certain roads, especially those in tourist destinations, off-limits to heavy vehicles were implemented. Alpine countries, due to their transit positions, were particularly stringent in imposing restrictions and encouraging freight shift from road to rail. The development of intermodal transport has been fostered by successive favourable legal acts in force throughout the EU. The most important ones for intermodal transport are listed as follows. [12]

- Directive 92/106/EEC on the establishment of common rules for certain types of combined transport of freight between Member States;
- Regulation 913/2010/EU of 22 September 2010 on a European rail network for competitive freight transport;
- White Paper. Roadmap to a Single European Transport Area - Towards a competitive and resource-efficient transport system of 28.03.2011;
- Directive 2012/34/EU of the European Parliament and of the Council of 21.11.2012 establishing a Single European Railway Area;
- Regulation 1316/2013 of the European Parliament and of the Council of 11.12.2013 establishing the Connecting Europe Facility;
- Regulation 1315/2013 of the European Parliament and of the Council of 11.12.2013 on Union guidelines for the development of the trans-European transport network and repealing Decision No 661/2010/EU (Article 51).

In one of its most widely accepted interpretations, intermodal freight transport denotes a multimodal sequence of container transport services. This sequence typically connects the initial shipper with the ultimate consignee of the container (referred to as door-to-door service) and extends across considerable distances. Transport is frequently facilitated by multiple carriers. Illustratively, in a scenario of an intercontinental intermodal trip, containers depart from a shipper's premises via road truck either directly to the port or to a rail terminal, from where a train will convey them to the port. Subsequently, a vessel will transport the containers from this initial port to a port on the opposite continent, where they will be delivered to the final destination via a single or a blend of land transport methods: truck, rail, coastal, or waterway transport. This chain encompasses various intermodal terminals, including the initial and concluding seaport container terminals facilitating the transfer between sea and land transport modes, along with inland terminals such as rail yards and river ports, which offer freight transfer hubs between coastal transport modes. [13] A typical port fleet comprises vessels of different sizes and configurations, e.g., in terms of the number of refrigerated containers that can be carried. Vessels are becoming larger and larger to increase their unit efficiency, meaning that the risk of delay from equipment failure is increasingly concentrated on a few vessels. Container vessels carry standardised containers in a restricted set of sizes and types. Standard containers are called dry and refrigerated reefers. The amount of containers carried is measured using the twenty-foot equivalent unit (TEU), which represents a single twenty-foot container, or the forty-foot equivalent unit (FEU/FFE), with 2 TEU = 1 FEU, as shown in Figure 2.2. [14]

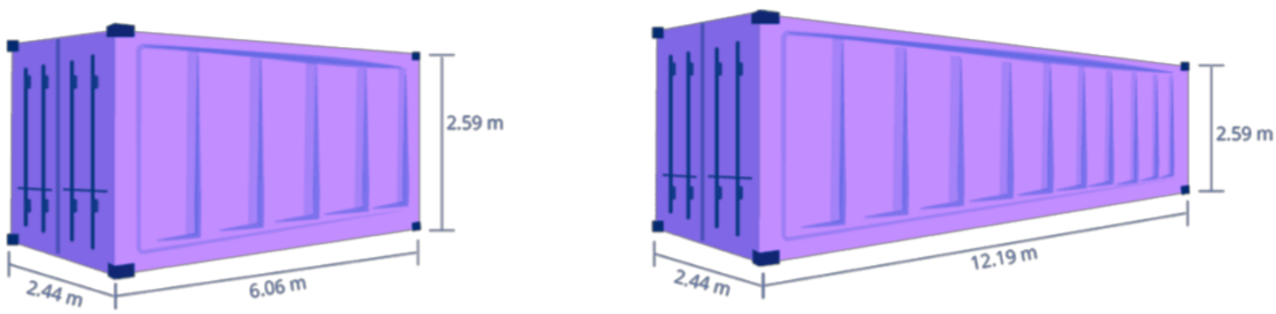

Figure 2.2: Dimensions of a twenty-foot (left) and forty-foot (right) equivalent unit. [13]

2.1.1 Intermodal infrastructure and location

Terminals come in several designs and sizes and may be specialised for particular transport modes and the handling of specific products, or may offer a complete set of services. Major operations performed in consolidation terminals include vehicle loading and unloading, freight and vehicle sorting and consolidation, convoy make-up and breakdown, and vehicle transfer between services [13]. Transport networks inherently have a node and link structure, where the links represent linear features providing for movement, such as highways and rail lines, and the nodes represent intersections. Thus, the principal data content of a node is its name or number and location. Links usually have characteristics such as length, direction, number of lanes, and functional class. Flow capacity, or some characteristics enabling ready estimation of the capacity, are included. The whole assemblage of nodes and links is identified with a particular mode. Another representational decision to be made is whether the network links will be straight lines or shape points, depicting their true geography. Early network models were called stick networks, which are topologically accurate but lacking in topographic accuracy. For many types of analyses, this is of no concern; a software system that deals only with link-node incidences, paths, and network flows will yield the same answer whether or not the links have accurate shapes. However, to produce recognisable network maps and for certain types of proximity analysis, topographically accurate representations are needed (see Figure 2.5). Hence, most large-scale network models currently utilise shape points because of the energy consumption cost estimations. This comes at a price, in that much more data storage is required, and plots or screen renderings are slowed. Fortunately, advances in computing power and geographic information systems (GIS) have minimised these drawbacks to a large extent. Topological representation and characteristics of the Rijeka intermodal terminal are shown in Figure 2.3 and 2.4. These representations are used for further analysis of energy and fuel consumption calculations at the Rijeka use case scenarios.

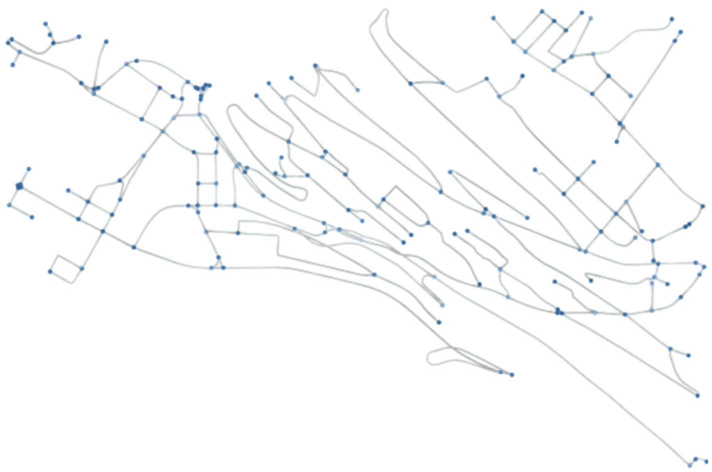

Figure 2.3: Intermodal terminal node selection at Rijeka location.

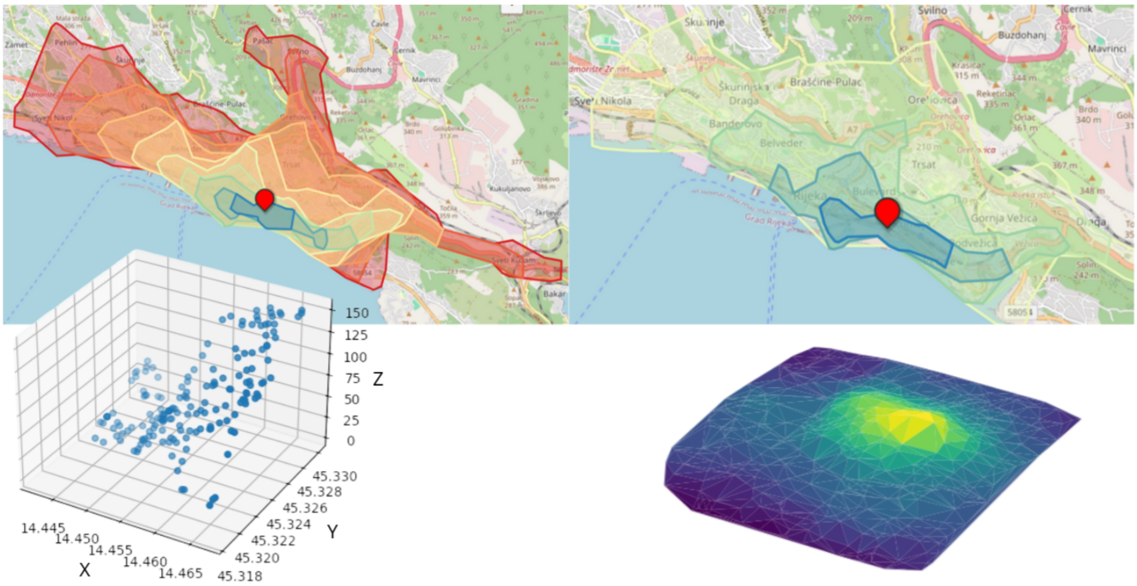

Figure 2.4: Rijeka terminal distance-based isochrones and elevation.

In some networks, this is stated directly for each link, in units such as vehicles per hour or tons per day. A schematic presentation of the nodes prepared for reinforcement learning (RL) models can be seen in Figure 2.6. To use this in a supply chain setting, the behaviour of the other agents needs to be simulated when the other agents' initial conditions and decisions are unknown. To handle that lack of knowledge of the starting conditions, these uncertainties need to be seen as random variables and samples from a distribution. It is possible for an agent to have, for example, no inventory and a substantial backorder. [15] In other, the functional class of a link points to an attribute table that has default capacity values. In the case of an oil pipeline, for example, the diameter of the pipe could be used to estimate flow capacity for various fluid properties. Nodes are modelled as capacity-constrained, but in principle can be (and have been) treated in the same way as links. [16]

Some key concepts governing this research area include robustness, resilience, criticality, and vulnerability. The application of such concepts to transport networks is relatively new, thus, the field has seen an expansion in terms of the metrics used to quantify criticality and the methodologies used to apply them. To date, the majority of research efforts in the area of network robustness have often been limited to examining the issue from a single facet, such as network topology. The Network Robustness Index (NRI), originally proposed in [17], overcomes this limitation by simultaneously accounting for the network-wide effects due to link closure with respect to network topology, link capacity, and origin-destination demand. While the NRI has been successfully implemented in the analysis of urban road networks, its application characterising the robustness of entire multi-regional freight networks has not been explored in past studies. Conclusively, the problem of the resilience parameter is proposed in this research to

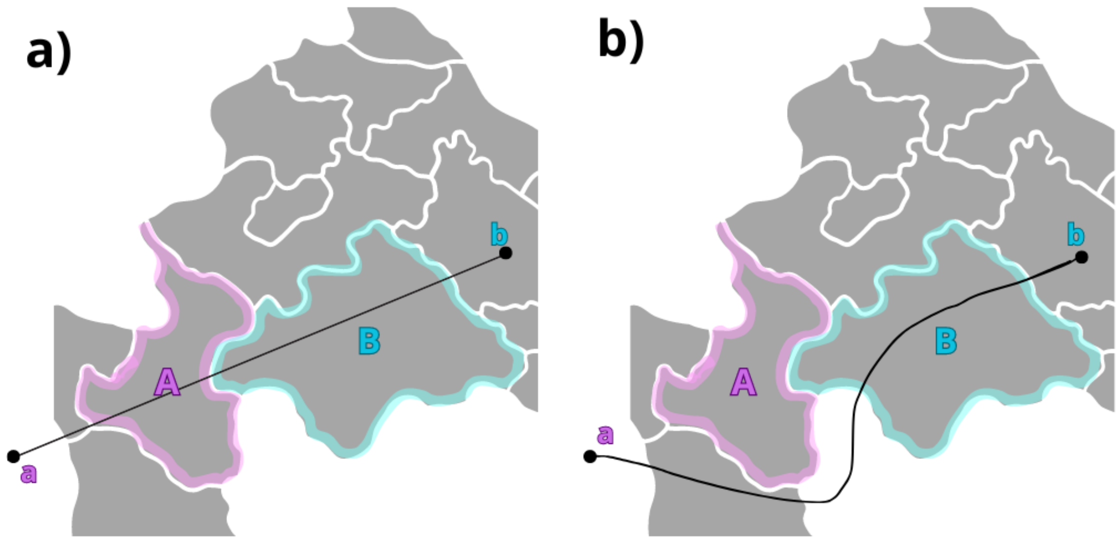

Figure 2.5: Example of a) link passing through two regions; b) link passing through one region.

model the types of events for this analysis which represent severe events that disable one network segment for a prolonged period of time, such that drivers must find alternative routings to reach their destinations. Examples of such events are road closures, and the collapse of important structural roadway elements, considering the impacts of an ageing infrastructure, such events can have severe and far-reaching implications. Modelling these disruptions and their impacts on network segments provides insights into the operating characteristics of the network and regions of potential criticality for freight flows. [18]

2.1.2 Terminal infrastructure and superstructure

Port terminals, including container terminals, are composed of integrated infrastructure and superstructure systems. The construction, maintenance, and upgrade of these elements require substantial capital investment. This research is focusing on NAPA terminals (North Adriatic Port Association) where main transport intermodal routes can be seen in Figure 2.7. [19]

Port terminal infrastructure investments can be divided into three main categories: infrastructure, superstructure and regulatory. [20]

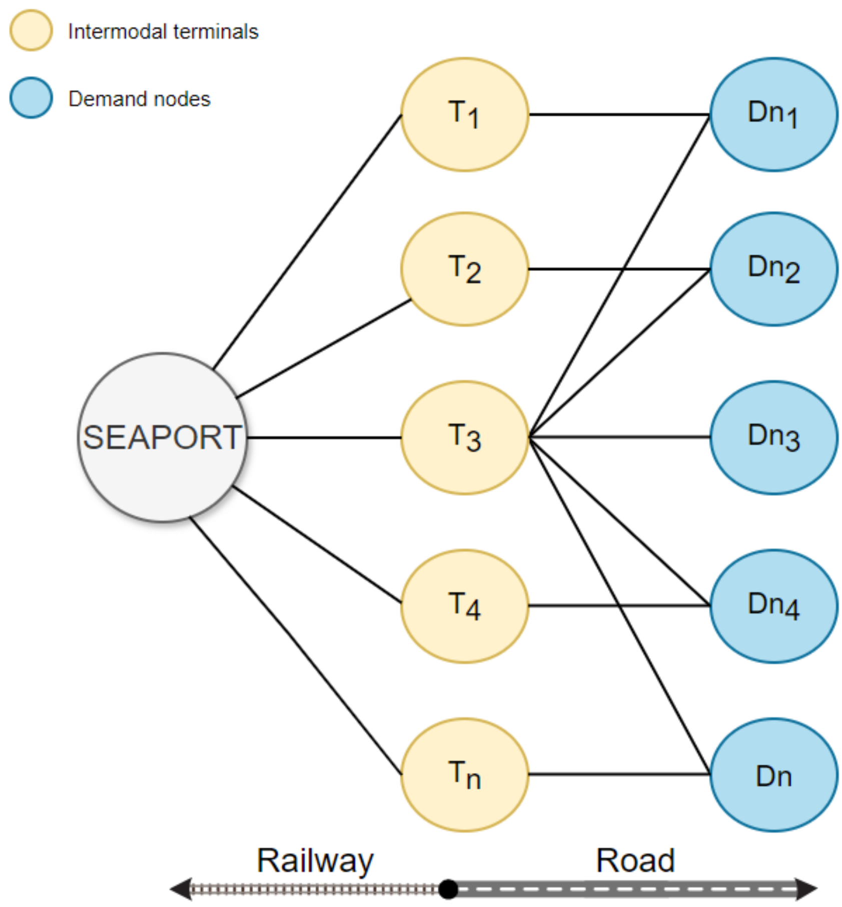

Figure 2.6: Schematic representation of intermodal terminal integration in a transport network.

Infrastructure

- Land reclamation works.
- Capital dredging and maintenance dredging of access channels and basins.
- Quay-wall construction and maintenance.
- Apron, mooring equipment and fenders.

Superstructure

- Terminal handling equipment (ship-to-shore cranes, yard equipment, etc.).
- Electric installations and wiring.
- Telecommunication installations and wiring.
- Paving of the terminal.
- On-terminal rail facilities (yards and spurs).

Figure 2.7: Ports of Koper, Rijeka and Trieste connected with the Central European states through main transport routes. [19]

- Roads on the terminal.
- Warehouses and technical buildings.
- Fencing and video surveillance (port security).
- Truck gates and inspection.
- Office buildings.

Regulatory

Intermodal terminals across the EU, including those in Croatia, are subject to an evolving regulatory framework aimed at minimising environmental impacts, particularly noise pollution and air emissions. Under EU legislation, the Environmental Noise Directive (2002/49/EC) sets requirements for strategic noise mapping and action plans around major transport hubs, which apply to intermodal terminals located near urban areas or critical infrastructure. To comply, terminals must implement noise mitigation measures such as acoustic barriers, low-noise handling equipment, and restrictions on night-time operations. In terms of emissions, the Non-Road Mobile Machinery (NRMM) Regulation (EU 2016/1628) establishes emission limits for terminal equipment like cranes, reach stackers, and shunting locomotives, while Euro VI standards apply to heavy-duty vehicles involved in road transport. These are reinforced in Croatia by national laws, including the Environmental Protection Act and the Air Protection Act, which align Croatian environmental governance with EU directives. Terminals are increasingly adopting electric or hybrid equipment, investing in on-site energy monitoring, and enabling modal shifts to rail in order to meet these environmental standards. These measures are essential for achieving compliance, securing operational permits, and contributing to broader EU Green Deal goals for decarbonised and sustainable freight transport.[21]

2.1.3 Intermodal technologies

The use of intermodal technologies in transport systems and their specific features, based on the integration of different modes of transport allows to reduce the costs of the transport process and increase its efficiency, and at the same time allows to prepare a lower-price offer for the customer. It is also possible to organise transport in a variety of ways and to improve the quality of services by making faster deliveries, improving access to transport services simplifying the procedures for moving freight and taking over the organisation, implementation and management of transport processes by an intermodal transport operator. In combined transport there is an internal integration of transport processes on the planes [22]:

- technical - including the adaptation of line and point infrastructure and means of transport of various branches, as well as transhipment facilities and machinery to handle intermodal loading units,
- organisational - consisting in the presence of specialized entities performing the functions of operators involved in the implementation of complex transport processes and one transport document along the entire delivery route,
- functional - in point infrastructure elements (intermodal terminals) there is an integration of functional areas of the terminal such as unloading, storage and loading zones for

handling intermodal loading units.

Transhipment terminals are a basic point infrastructure in intermodal transport networks and are equipped with appropriate transhipment equipment and machines, enabling transhipment of intermodal units between different modes of transport and stationary service in the terminal. Figure 2.8 is a methodological framework for building simulation models and evaluating performance at an intermodal logistics hub (transhipment or intermodal terminal) connected to an information and communication platform for data integration. The input data of the simulation model shown in light grey are freight transport demand, derived from observations of terminal operativity and terminal conditions in terms of available equipment and possible disturbances (temporary closure of a yard block for scheduled maintenance of the road surface or yard cranes). The principal output in darker grey is a set of selected key performance indicators (KPIs) which are evaluated to compare the terminal performance in alternative situations, also according to the implementation of potential control actions on terminal operations. [22], [23]

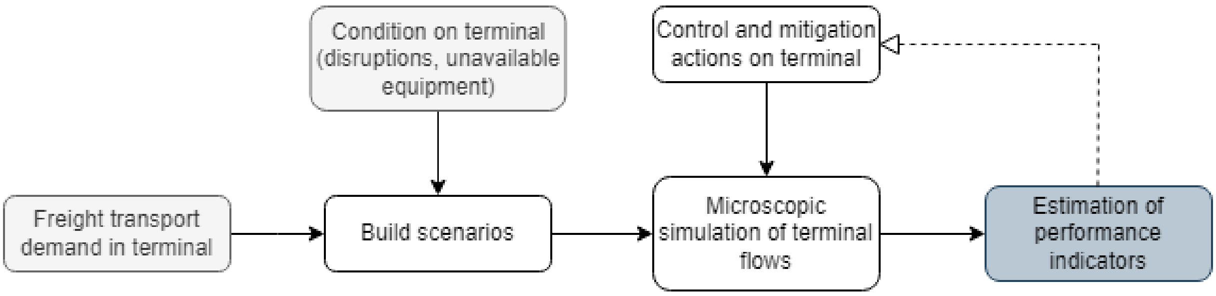

Figure 2.8: A methodological framework for building scenarios and evaluating terminal performance.

The implementation of intermodal services requires close cooperation between different stakeholders, including rail infrastructure managers, intermodal terminal managers and combined transport operators, who manage the entire transport process and can offer finished services to customers. All activities are connected with incurring significant costs by individual participants of the whole transport process, which implies various types of restrictions. On the one hand, these are the technical constraints of the transport network, financial, environmental, social, etc. On the other hand, there are different points of view of the various actors involved in the transport process, each of which seeks to maximise its benefit. Intermodal transport brings together the strengths of different modes of transport and creates synergies in terms of increased transport efficiency and reduced external costs. As a result of technological progress, transport technology and the role of individual branches in the movement of freight is systematically developed. Customers who want to satisfy their transport needs have a choice of different forms and types of freight transport, using:

- various modes of transport,

- various forms of transport organisation,
- different technologies,
- different means of transport within a single mode of transport.

The dominant factor in assessing the usefulness of particular forms of transport and types of freight transport, especially transport technologies, is the provision of comprehensive logistics services according to the needs reported by customers. [13],[22]

2.1.4 Stakeholders in transport

The basic objective for decision-makers is to formulate recommendations for simpler and more transparent information services when choosing the mode of transport in complex intermodal chains. It's deemed that recommendations for decision-makers work best when there is stability in the market, i.e., when there is a balance between supply and demand for transport services. Therefore, the price and reliability of services in the transport chain are constant. As soon as disruptions occur, as we experienced in 2021 with the Suez Canal shipping congestion and in 2020 with the COVID-19 pandemic, the supply chains are disrupted and so is the market equilibrium. In such cases, other criteria such as transport time, cost and supply become much more important than environmental criteria. Thus, it can be concluded that recommendations for more environmentally friendly transport can only be considered when the market is stable. Based on the elaborated decision-makers in the supply chain, three main groups of stakeholders are determined:

1. logistics companies,
2. manufacturers,
3. end-customers.

Manufacturers and logistics companies are direct decision-makers on the mode of transport and influence the design of intermodal transport chains. End-customers or product buyers form a separate category, as they usually have no influence on the design of the transport process and thus the possibility to choose a more environmentally friendly mode of transport. However, they can buy products whose transport causes the lowest greenhouse gas (GHG) footprint and achieves a higher energy efficiency. The efficiency of a port is part of a continuum that includes maritime, terminal, and hinterland operations as shown in Figure 2.9. These dimensions are interrelated since inefficiencies in one dimension are likely to impact the others. For instance, issues in terminal operations are most likely to negatively impact maritime and hinterland operations with delays. Authors in [24] investigate a dynamic shipment matching (DSM) problem in which a platform provides online matches between shipment requests and transport services.

An online synchromodal matching platform is proposed that receives contractual and spot (regular) shipment requests from shippers, and receives transport services from carriers, as shown in Figure 2.10. Shippers are entities that search for services to transport their shipments. When each transport operator can change planned actions up until the time the action is carried out, co-planning between transport operators must happen in real-time. One planning problem in a synchromodal transport network is co-planning between truck operators responsible for routing trucks and delivering containers on time, and a barge operator responsible for barge departures. [25]

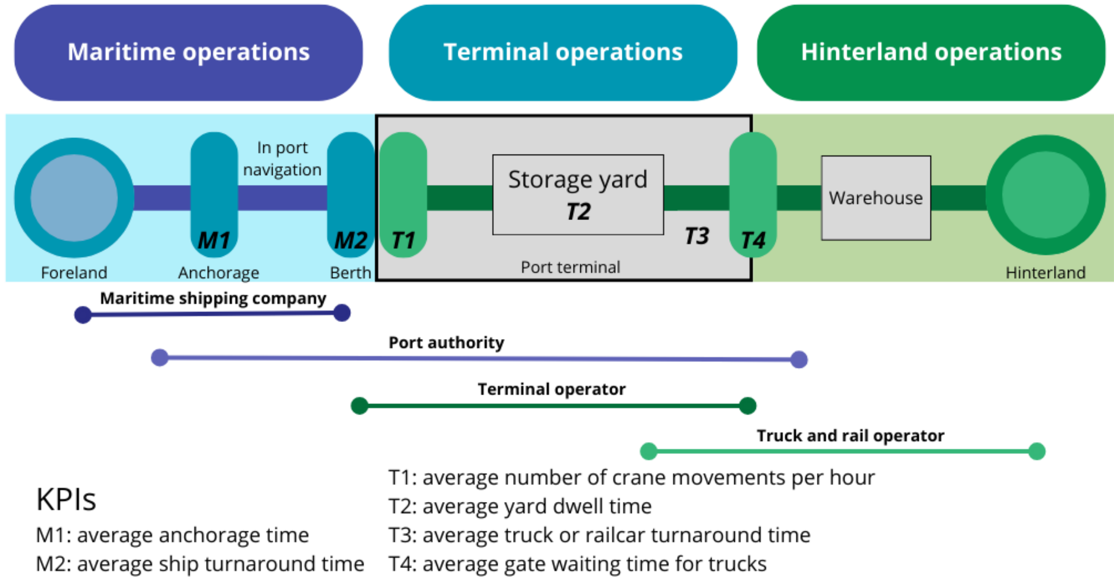

Figure 2.9: Intermodal terminal stakeholders and operations' key performance indicators.

Intermodal transport matching platform involves a number of stages [11]:

1. collection in the origin zone and transport by truck to the origin intermodal terminal located in the shipper area;
2. transhipment at the origin intermodal terminal from truck to the trunk-haul, non-road transport mode (rail, inland waterways, air);
3. line-haul transport between the origin and destination intermodal terminals by the trunk-haul mode;
4. transhipment at the destination intermodal terminal in the receiver area from the trunk-haul mode to trucks;
5. distribution from the destination intermodal terminal to the destination zone by truck.

In the road transport network movement of loads between shippers and receivers is carried out directly by the same truck in three steps: collection in the origin zones; line-hauling from the border of the origin to the border of the destination zone; and distribution within the destination zones [26].

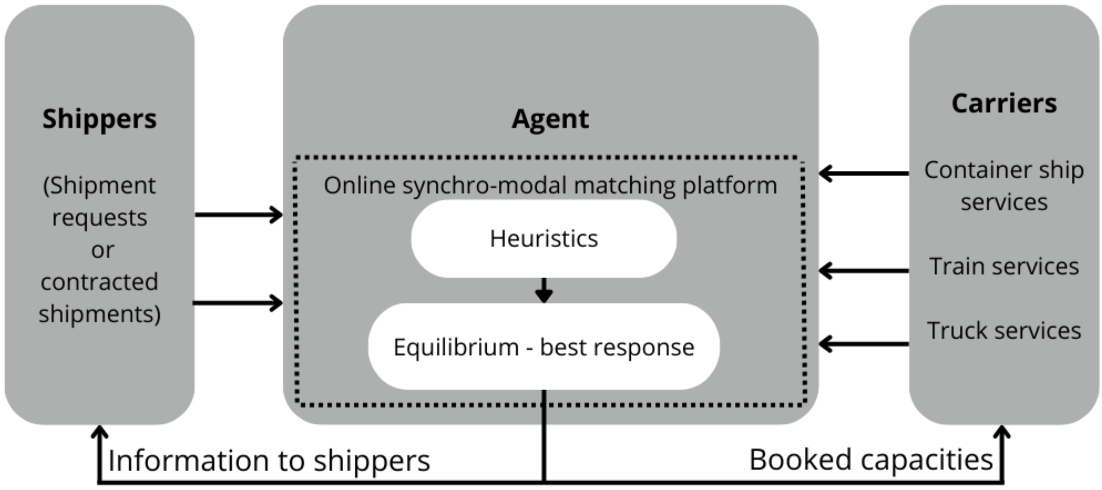

Figure 2.10: Illustration of an online transport services matching platform.

2.1.5 Data collection for intermodal networks

The sources of data listed in Table 2.1 provide essential data for modelling intermodal transport networks. OpenStreetMap (OSM) serves as the base layer for spatial network representation, containing road and rail infrastructure. The General Transit Feed Specification (GTFS) offers scheduled transit data, enabling accurate representation of public transport routes and transit time estimation. The Automatic Identification System (AIS) contributes real-time vessel tracking data, allowing maritime route optimisation. Eurostat and UIC rail freight datasets provide statistical insights into freight flows, infrastructure utilisation, and congestion levels. Weather and Traffic APIs provide external conditions affecting costs. Real-time freight APIs complement historical datasets by integrating dynamic routing information from trucking, railway, and maritime operators. By combining these datasets, an intermodal transport network is modelled as a graph, where nodes represent terminals, ports, and key interchanges, while edges correspond to different transport links. This enables the development of data-driven reinforcement learning models for routing optimisation, congestion prediction, and cost estimation.

The collected data is preprocessed into a structured format suitable for GAT to use in reinforcement learning-based intermodal routing model. The preprocessing steps include the following:

1. **Spatial data extraction:** Conversion of OSM data into a directed graph where nodes represent intermodal hubs, and edges represent transport links.

Table 2.1: Sources of data for intermodal transport network

Dataset	Source	Description
OpenStreetMap (OSM)	`www.openstreetmap.org`	Road, rail, and port network data
GTFS	Various transit agencies	Public transport schedules and routes
AIS Data	MarineTraffic, ExactEarth	Real-time ship tracking and port calls
Eurostat Transport Data	`ec.europa.eu/eurostat`	Freight flows, modal split, and emissions
UNECE Transport Statistics	`w3.unece.org`	Rail, road, and inland waterway statistics
Truck traffic data	[27]	Road trucking data for Europe in 2019 and syntethic data for 2030 predictions
Google Distance Matrix	`developers.google.com/maps`	Road transport distances and estimated travel times
OpenRailwayMap	`www.openrailwaymap.org`	Detailed railway network infrastructure

2. **GTFS data parsing:** Extraction of schedules, route structures, and transfer times from GTFS feeds, converting them into a graph-compatible adjacency matrix.

3. **AIS data aggregation:** Processing real-time vessel movements to estimate maritime link travel times and delays.

4. **Eurostat/UIC data integration:** Statistical data with network nodes to assign realistic capacities, freight demand, and congestion levels to transport links.

5. **Feature engineering:** Construct node and edge features, including:

   - *Node features:* terminal type, capacity, processing time.
   - *Edge features:* distance, cost, transit time, congestion factor.

6. **Graph construction:** Assembling of an intermodal transport graph where nodes correspond to terminals, ports, and major logistics hubs, while edges represent rail, road, and sea connections with associated transport costs.

7. **Normalisation and encoding:** Normalisation of numerical features (cost, transport time) and encoding categorical variables (transport mode) to prepare data for model training.

The processed dataset is then used as input for GAT-based reinforcement learning models, enabling efficient adaptive routing in intermodal networks.

In this table from Figure 2.11 are the head rows and the end rows of the dataset of 480 biggest global seaports. From this dataset, it is analysed what are the most important features in a seaport terminal and how they affect the performance of the model. The first step in further feature importance analysis is the preprocessing of the data, where is detected which are continuous and categorical variables. The number of arrivals and departures in the last 24 hours shows a very high correlation with the expected arrivals in the port shown in Figure 2.12. The Spearman's rank correlation coefficient (ρ) is a measure of monotonic correlation between two variables and is therefore better at catching nonlinear monotonic correlations than Pearson's r. Its value lies between -1 and +1, -1 indicating total negative monotonic correlation, 0 indicating

Unnamed: 0	Country	Port Name	UN Code	Vessels in Port	Departures(Last 24 Hours)	Arrivals(Last 24 Hours)	Expected Arrivals	Type
0	China	SHANGHAI	CNSHG	2420	1376	1626	644	Port
1	China	NANTONG	CNNTG	1572	1173	1287	234	Port
2	China	CJK	CNCJK	1529	343	370	310	Anchorage
3	China	NANJING	CNNKG	1414	667	1060	203	Port
4	China	JIANGYIN	CNJIA	1112	1076	1070	166	Port
...	...	...	...	...	...	...	...	...
475	Korea	ONSAN	KRONS	51	121	121	26	Port
476	China	PENGLAI	CNPLI	51	63	61	22	Port
477	USA	PORT EVERGLADES	USPEF	51	23	21	22	Port
478	India	KAKINADA	INKAK	51	8	10	21	Port
479	Japan	NAHA	JPNAH	51	33	42	15	Port

Figure 2.11: Dataset of the 480 biggest seaports.

no monotonic correlation and 1 indicating total positive monotonic correlation. To calculate (ρ) for two variables X and Y, one divides the covariance of the rank variables of X and Y by the product of their standard deviations. Pearson's correlation coefficient (r) is a measure of linear correlation between two variables. Its value lies between -1 and +1, -1 indicating total negative linear correlation, 0 indicating no linear correlation and 1 indicating total positive linear correlation. Furthermore, r is invariant under separate changes in the location and scale of the two variables, implying that for a linear function, the angle to the x-axis does not affect r. To calculate r for two variables X and Y, one divides the covariance of X and Y by the product of their standard deviations.

Table 2.2: Statistics on the dataset of 480 shipping ports

Dataset statistics	
Number of variables	12
Number of observations	480
Missing cells	12
Missing cells (percentage)	0.2%
Duplicates	0
Total size in memory	45.1 kB
Average record size in memory	96.3 B
Variable types	
Numeric	5
Categorical	7

After the normalisation of the input data and elimination of missing values, formed dataset

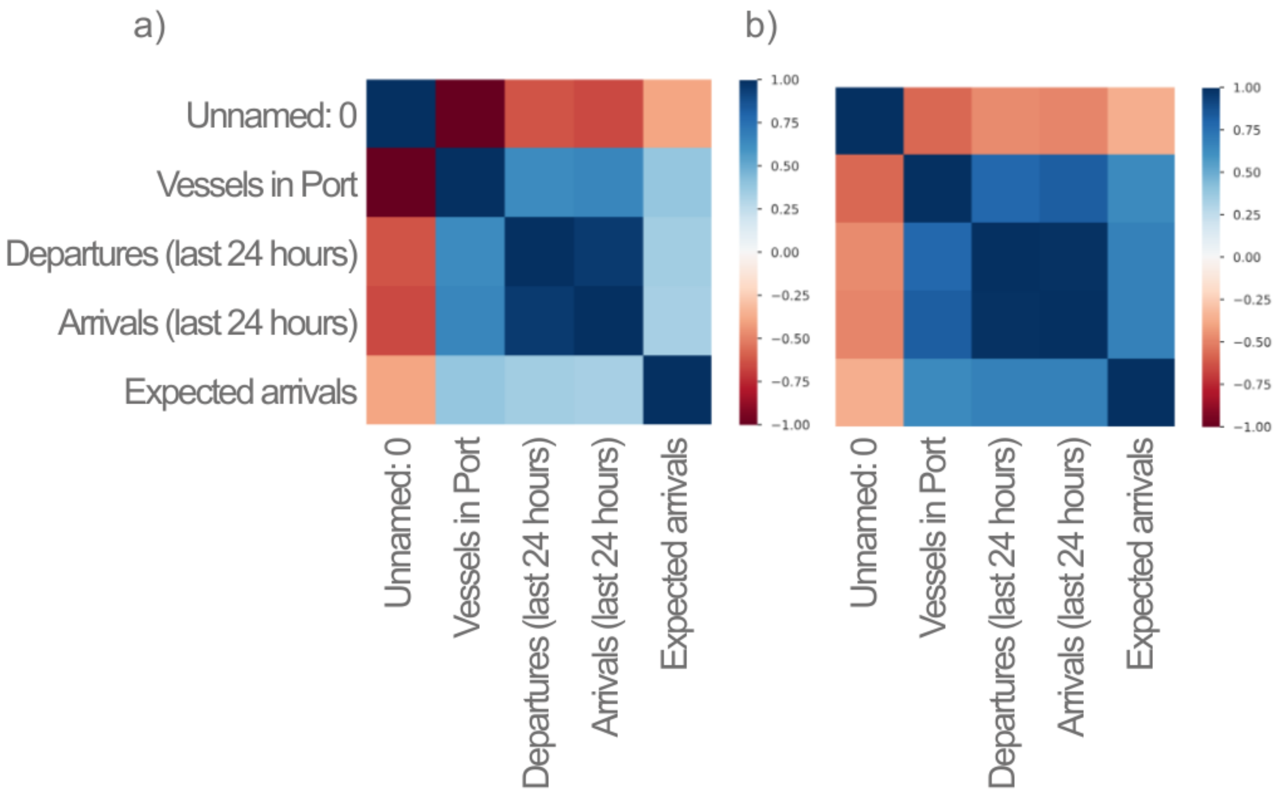

Figure 2.12: a) Spearman's ρ and b) Pearson's r coefficient of correlation on important dataset features.

statistics are shown in Table 2.2. For every target variable in the dataset, the comparative of performance is done on 27 models and a TabNet model. Those models are predefined and trained models on feature importance stored in a Python package (XGBoost Feature Importances). Output model performance and processed data are then stored in CSV (comma-separated value) format for every new output dataset. [28] The dataset contains four shipping port categories; port, anchorage, marina and canal, shown in Figure 2.13. Maritime ports receive and distribute the largest amount of freight daily, so for further assessments, only 391 shipping maritime ports are used for distributing freight flows and analysis. More than 30 % of biggest seaports are located in China.

A defining feature of transport networks in Central and Southeast Europe is their legacy as components of formerly larger transport networks (e.g. the former Austro-Hungarian Empire, and the Former Yugoslavia). Present-day borders have in many respects created "unnatural" impediments to these former networks. However, the signing of the "Treaty establishing the Transport Community" in 2017 offers a critical tool for the reintegration of transport in the

Table 2.3: Dataset description

	count	mean	std	min	25%	50%	75%	max
Unnamed	480.00	239.50	138.71	0.00	119.75	239.50	359.25	479.00
No. of vessels in seaport	480.00	153.31	217.30	51.00	63.00	86.00	144.00	2420.00
Departures (Last 24 Hours)	480.00	98.98	170.50	0.00	26.75	48.00	102.00	1682.00
Arrivals (Last 24 Hours)	480.00	108.66	185.36	1.00	30.00	56.00	106.25	1748.00
Expected arrivals	480.00	39.23	82.39	0.00	3.00	16.00	40.25	1205.00

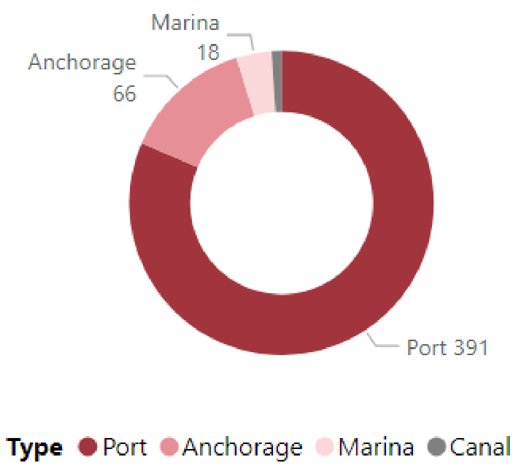

(**a**) Total number of ports by category

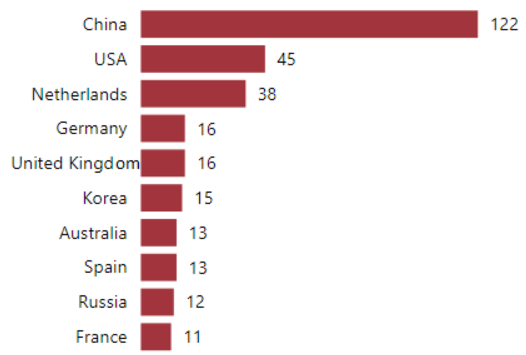

(**b**) Top 10 countries with highest number of seaports

Figure 2.13: Seaport dataset overview. [28]

sub-region. Treaty terms effectively apply some of the most critical transport sector elements of the EU acquis throughout the Western Balkans. In the case of railways, this includes open and non-discriminatory access to infrastructure for both passenger and freight operations. In the case of roads, inland waterway transport, and maritime transport, this means convergence on operating standards and regulations that apply to shippers. In addition, the treaty envisages extensive customs cooperation and facilitation of border crossings for freight and passengers. The potential impact of these changes on Croatia's transport sector is significant given that Croatia shares borders with three of the six Western Balkans signatories to the treaty. In the longer-term future, there is also the prospect of EU accession of Croatia's regional neighbours. The medium and long-term trends implied by both the new Treaty and the prospect of EU enlargement suggest that Croatia's transport networks will increasingly be integrated with international freight and passenger flows. [29] In the context of the management of a heterogeneous fleet of containers by an international maritime shipping company, the intermodal terminal location problem with balancing requirements was first introduced by Crainic et al. [13] The land operations of the carrier proceed as follows. Once a ship arrives at port, the company has to deliver loaded containers, which may come in several types and sizes, to designated in-land destinations. Following their unloading by the importing customer, empty containers are moved to a depot. From there, empty containers may be delivered to customers who request them for subsequent shipping of their own products. In addition, empty containers are often moved, or repositioned, to other depots. These inter-depot movements are a consequence of regional imbalances in empty container availabilities and needs throughout the network: some areas lack containers of certain types, while others have surpluses. These balancing movements of empty containers among depots differentiate this problem from classical location–allocation applications. Inter-depot movements are performed by high-density transport (rail, typically) and their unit transport cost is lower than for other types of movements. The general problem is, therefore, to locate depots and allocate customer depots (for each type of container and direction of movement) in order to collect the supply of empty containers available at customers' sites and to satisfy the customer requests for empty containers while minimizing the total operating costs: the costs of opening and operating the depots, and the costs generated by customer-depot and inter-depot movements. The container terminal in Rijeka Brajdica, Croatia is an example of customer and inter-depot transport of freight with its railway station connection as shown in Figure 2.14. This representation is generated in SUMO as a model configuration and simulations of a few scenarios extracted from statistical data were made. Simulation of Urban MObility (SUMO) is an open-source, highly portable, microscopic and continuous traffic simulation package designed to handle large networks. It allows for intermodal simulation including pedestrians and comes with a large set of tools for scenario creation. [30] Transport simulations of annual freight flows were generated for further output usage in the research, where the seaport of Rijeka is an origin point, transferring freight to a railway terminal for inland distribution of long-haul contract transports, or road terminal for shorter, spot-contract continental distribution. The main difference between the generated scenarios is the disruption of the transport infrastructure or more precisely the closing of a road or railway sections in the route. In Figure 2.15 are locations of cranes at the terminal Rijeka, yard cranes represent the locations of manipulation equipment for input and output vehicles (delivery trucks) and quay cranes represent the docking stations for unloading the container ships and loading the site vehicles for freight manipulation. The location of transhipment terminals in the transport network is a determining factor for the efficient and effective functioning of intermodal transport. The specificity of intermodal transport consisting of the handling of freight in long-distance transport by rail, sea and inland waterway transport, with the simultaneous provision of service areas with a small ratio of local terminals operated by road transport, requires the organisation of hierarchical multi-territory systems. Such systems are characterised by the existence of terminals of different importance and their role in the hierarchy. In multi-territory hierarchical systems, there are central, regional and local terminals, between which transports are carried out in an efficient way with comprehensive and fast customer service. [22]

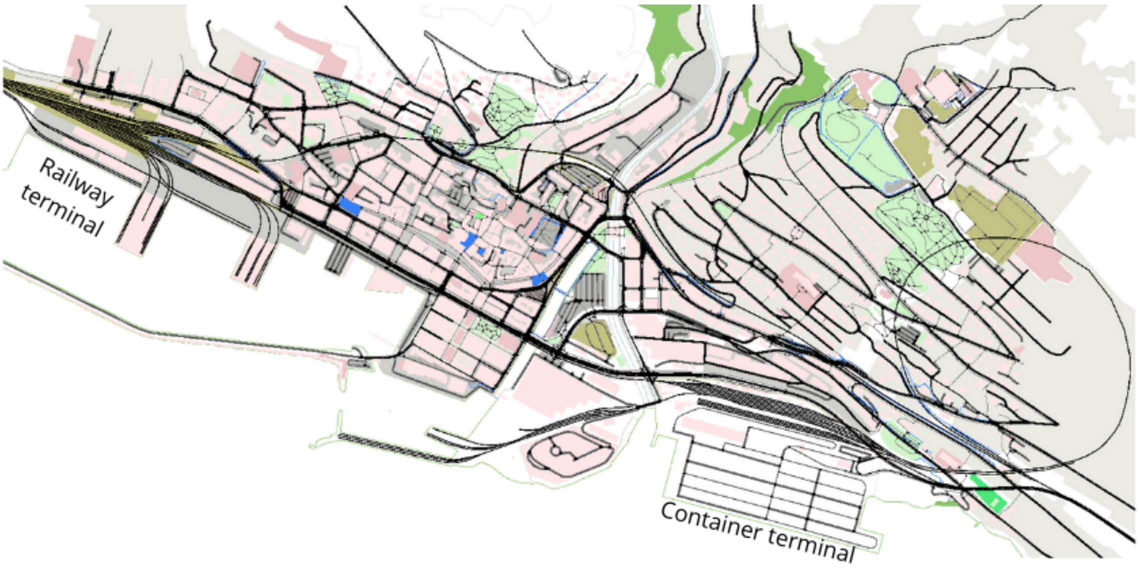

Figure 2.14: Rijeka container terminal (Brajdica) and railway connection terminal.

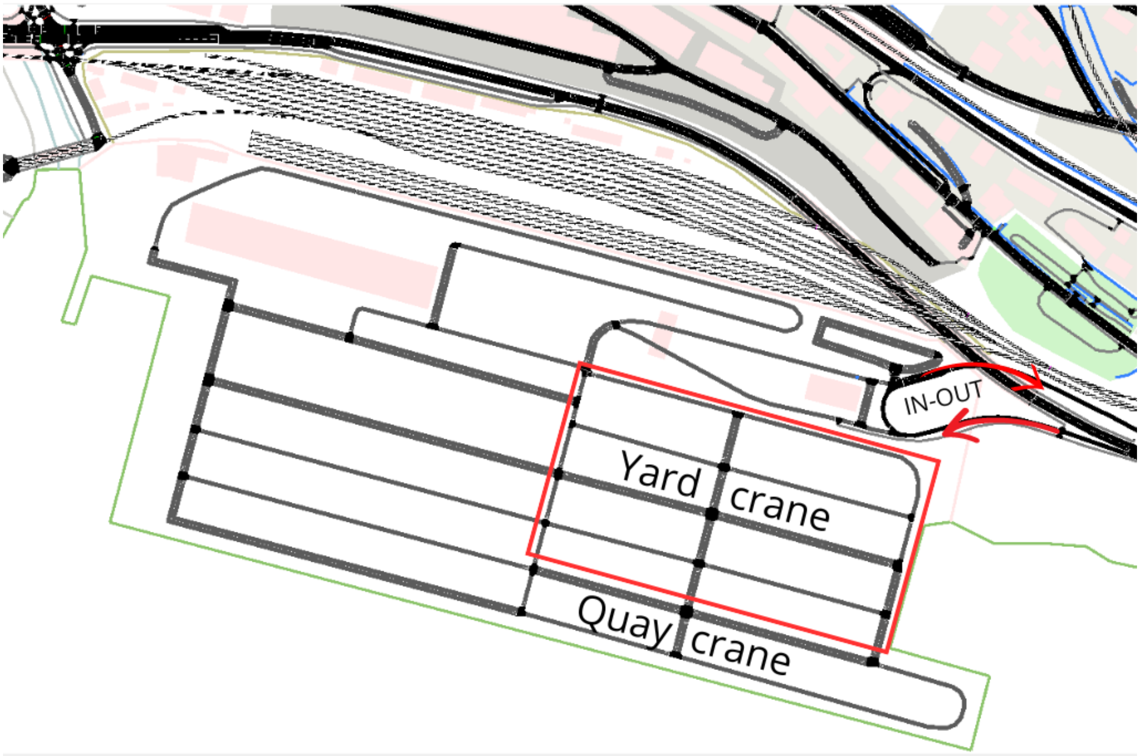

Figure 2.15: Position of yard and quay cranes; input and output of road trucks at Rijeka container terminal (Brajdica).

It is important to have areas for expansion in order to ensure that the site is sustainable for future growth. A site that can contain future growth will avoid a future necessary reallocation.

The locations of seaports in Croatia fulfil this criterion; at the same time, there is little competition with areas for residence. Area for expansion also provides flexibility in enabling further expansion of rail infrastructure and rail-connected plots and businesses. [31]

To simulate the allocation of freight vehicles under yard cranes, vehicle types were classified into four classes: (1) left external trucks, (2) right external trucks, (3) left internal trailers, and (4) right internal trailers. This classification is required to assign vehicles to the two specific traffic flows and to realistically reproduce various vehicle loading and unloading operations under cranes. Freight flows were modelled, adapting the operations of freight transport lines with established routes and stops at specific points. However, external and internal flows were simulated differently, external vehicles are modelled as vehicles that are continuously generated, whereas the flow generated by internal trailers was modelled as a predefined number of vehicles that carry out a certain number of activities [23]. Terminal layout in the micro-simulation model, detailing the location of yard and quay services in a loop. Linear public transport lines and circular public transport lines were used to model the behaviour of vehicles. In the proposed model for maritime terminals, each stop represents a vehicle's activity in the terminal at a specific location along the route in a certain amount of time, to comply with an assigned task. In particular, public transport stops with specific waiting times were used to model the duration of activities performed by quay cranes and gate-out operations. Loading and unloading operations performed by yard cranes were instead simulated using simulation objects called metering, which are linked to detectors to identify vehicle types and apply different service times (waiting times at the metering) depending on the type of vehicle on arrival. The time needed by yard cranes to pick up operations on trailers is usually shorter than the time required for delivery operations on external trucks. Finally, the gate-in service was modelled with metering, which can delay the arrival of trucks to modify the incoming distributions of the simulated public transport lines. Each micro-simulation experiment consists of ten replications for a one hour simulation period, consistent with the duration of peak congestion detected in a port terminal. To avoid the empty network state at the initial simulation time, a warm-up period equal to 30 minutes before the simulation period was used.

2.2 Decarbonisation of transport

The decarbonisation of freight transport in Europe is a critical component of the EU's broader climate goals. This report synthesizes key regulations and initiatives aimed at reducing greenhouse gas (GHG) emissions from heavy-duty vehicles (HDVs), shipping, and other transport sectors. The focus is on recent regulatory measures and their implications for achieving a sustainable and climate-neutral transport system by 2050. The simplest way to incorporate multiple objectives into optimisation model is to take one or several objectives and convert everything into a single unit. Emissions are defined in tons of CO2, so conversion into a monetary value is needed, or factor that represents the social cost of emissions. The factor is calculated by €50 per ton of CO2. Even though Croatia has a negative value of social cost of carbon which is beneficial, value of €50 is average if we combine transport paths with the destination nodes in countries with higher social cost [32]. In a defined single objective model, the function is set to minimise total costs and monetised emissions. The results are 31% of road-only transport and 68% of rail-road. Those results are similar to the cost-only optimisation where the shares were 32.67% for road-only, and rail 67.33%. But there are other sources that indicate that we might have a different conversion factor. The study reference shows that the social cost of emissions is sometimes estimated to be €180 per ton. The model will still minimise total emissions and total costs, simply using a different conversion factor. In that case, the result for road-only transport is 24%. The rail-road terminals have better performance in terms of the cost-effectiveness and emissions when transporting over larger distances. Objectives are not competing and the output values are in the same direction looking at the minimisation function. The cost versus duration in other cases, if ocean freight and air freight transport are compared, objectives evolve in a different direction. To date, there is a scarce amount of literature that addresses planning and decision problems in intermodal transport while at the same time calculating and presenting emissions data in such a way that a calculation can be used to provide regular and credible guidance at the operational level. There are several areas in the literature that attempt to solve the problem of minimising emissions from the perspective of comparing entire intermodal transport chains and their efficiency, as well as their individual transhipment points as intermodal terminals. The NSA survey launched by the French and Swiss NSAs, concerning the impact of climate change on railway systems, investigated methods to identify weather risks, and whether NSAs had some interfaces with other organisations involved in identifying and/or analysing risks linked to extreme weather. The findings show that 40 % of NSAs have interfaces with other organisations, and 30 % of them have developed or are developing some methods of identifying weather risks. For example, in Sweden, there is a project facilitating cooperation between the competent authorities (meteorological, hydrological, and civil protection authorities, decision-makers, climate change specialists, etc.) for the warning and prediction of natural events at the national level. In Poland, these skills are directly developed within railway companies. In Germany, natural-hazard-driven risk analysis and cross-modal analysis (with roads and waterways) are run. [33]

2.2.1 Regulations

Heavy-duty vehicles (HDVs) are significant contributors to road transport emissions in the EU, responsible for over a quarter of GHG emissions from this sector. Figure 2.16 shows the ratio of GHG emissions in the transport sector of Croatia. To address this, the EU has implemented stringent CO_2 emission standards for HDVs, which will become progressively stricter over time. The first EU-wide CO_2 emission standards for HDVs were established by Regulation (EU) 2019/1242, setting a 15% reduction target by 2025. Revised targets aim for a 45% reduction by 2030, 65% by 2035, and 90% by 2040.

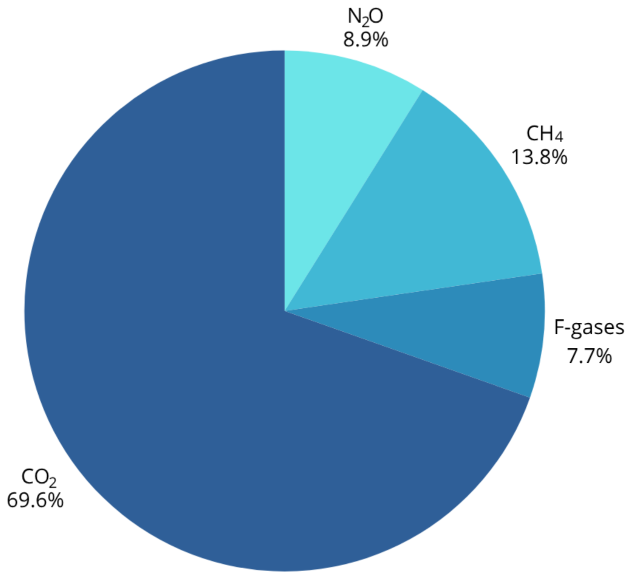

Figure 2.16: GHG emissions percentage in the transport sector of Croatia in 2023. [34]

The amended regulation covers nearly all emissions from HDVs, including heavy and medium trucks, city buses, coaches, and trailers. It mandates that 90% of new city buses must be zero-emission by 2030, with all new city buses meeting this requirement by 2035. An incentive mechanism for zero and low-emission vehicles (ZLEV) is also included to support the transition. To ensure effective implementation, the EU will assess the robustness of reference CO_2 emissions, collect and monitor real-world fuel consumption data, and introduce in-service verification tests. Financial penalties will be applied for non-compliance with CO_2 targets. Manufacturers are required to determine CO_2 emissions and fuel consumption of new HDVs and trailers in accordance with Certification Regulations.

Shipping emissions are a significant concern, with global shipping emissions reaching 1,076 million tonnes of CO_2 in 2018. The EU aims to include maritime emissions in its Emissions Trading System (ETS), covering CO_2 emissions from all large ships entering EU ports. This system will cover 50% of emissions from trips starting or ending outside the EU and 100% of emissions between two EU ports. Shipping companies must purchase and surrender EU ETS emission allowances for each tonne of reported CO_2 emissions. The MRV (Monitoring, Reporting and Verification) Maritime Regulation was revised in 2023 to include maritime transport emissions within the EU ETS scope. Additionally, the FuelEU Maritime Regulation aims to boost the demand for marine renewable and low-carbon fuels. The revised 2023 strategy sets a goal of net zero emissions from ships by around 2050, with indicative checkpoints of at least 20% reduction by 2030 and 70% by 2040. The International Maritime Organisation (IMO) has also agreed to adopt additional GHG reduction measures by 2025 to meet these targets. The European Green Deal aims for a 90% reduction in transport-related GHG emissions by 2050. The European Climate Law requires all emissions regulated in the EU, including shipping, to be reduced to net zero by 2050 at the latest. The EU has adopted various policy packages to accelerate the transition to cleaner fuels and ensure a growing share of renewable energy in the transport sector. The EU's Emissions Trading System (ETS) has been extended to cover CO_2 emissions from large ships and will include road transport from 2027. This system aims to reduce the industry's carbon emissions and includes a Carbon Border Adjustment Mechanism to apply a carbon levy on imports of certain freight from outside the EU. The EU is revising the Renewable Energy Directive (RED) to accelerate the supply of renewables and the Directive on Deployment of Alternative Fuels Infrastructure to support the transition. These measures are crucial for achieving the EU's climate goals and reducing the environmental impacts of transport, where maritime transport is still the main generator of freight transport (Figure 2.17). The EU has set ambitious targets and implemented comprehensive regulations to decarbonise freight transport. These measures include stringent CO_2 emission standards for HDVs, the inclusion of maritime emissions in the ETS, and various initiatives under the European Green Deal. Achieving these goals will require continued efforts and collaboration across sectors to ensure a sustainable and climate-neutral transport system by 2050. [34]

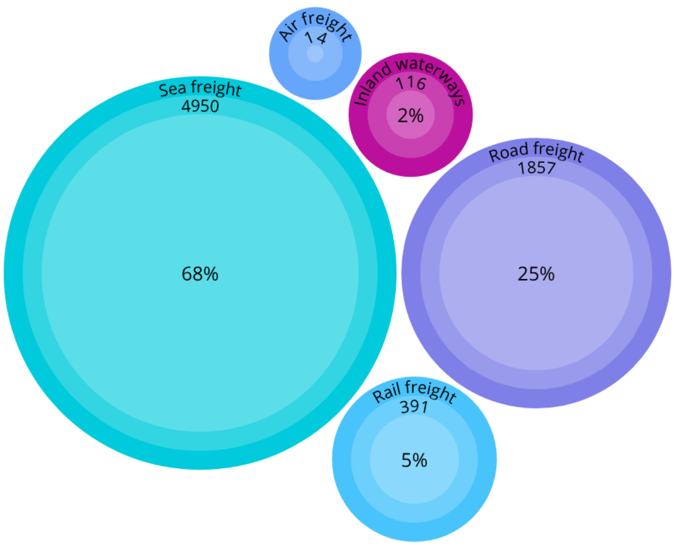

Figure 2.17: EU region freight tonne-kilometres in millions with corresponding shares according to mode of transport in 2021. [34]

2.2.2 Global environmental effects of container shipping

Container shipping plays a pivotal role in facilitating seamless movement along the supply chains of manufactured freight, the most valuable product group. In 2020, container ships carried approximately 149 m TEUs, making up nearly 17% of the total seaborne cargo in terms of volume. The goal of reducing environmental impact is not only to solve the technical issue of computing emission volume but also to comprehensively analyse emission patterns in maritime transport. Recent environmental policies have highlighted the necessity to monitor emissions in an individual fleet. For example, an IMO's (International Maritime Organisation) measurement, which comes into effect in November 2022, concerns the annual update on the carbon intensity of operators' ship fleets. The European Union has recently considered incorporating shipping in its emissions trading system to combat climate change.[35]

2.2.3 Carriers and emissions

The competitive context of business continues to change, bringing new complexities and general concerns for management. Because of the constant changes, many strategic issues are confronting all logistics organisations today. Carriers in the hinterland are confronted with a complex and ambiguous market situation, while the weak market position of carriers and fierce competition among logistics providers restrict collaboration, standardisation and cost pressure drive collaboration for reducing empty-truck trips and improving logistical efficiency. These initial observations on the specifics of hinterland collaboration can be underlined by the few qualitative studies on the subject, in a study on hinterland collaboration in New Zealand and Bangladesh that identifies a lack of trust, coordination between carriers and lack of flexibility at the ports as constraints to truck-sharing. Comparing motives for collaboration of shippers and carriers, operational efficiency is the most important motive for both, while sustainability and safety in transport are rated as more important by shippers than by carriers. It can be subsumed that, while the studies have demonstrated the importance of trust and the motives and challenges for engaging in horizontal collaboration in logistics, the current literature has not yet provided comprehensive insights into the carriers' perception of collaboration in the hinterland, which due to its peculiarities requires special attention. Therefore, the focus is to explore hinterland carriers' perceptions in European countries, where seaports and supply chains play an important role due to their size and potential for optimisation. [36] In real-world operations, carriers are facing decisions regarding the tradeoff between distribution cost and safety. It is important for them to be able to quantify the "price of safety", i.e., the effect of the unloading constraints on the distribution cost, approximated by the total distance travelled by the distribution fleet. Prescriptive analytics (decision optimisation) technology recommends actions that are based on desired outcomes. It takes into account specific scenarios, resources, and knowledge of past and current events. With this insight, your organisation can make better decisions and have greater control of business outcomes. Prescriptive analytics is the next step on the path to insight-based actions. It creates value through synergy with predictive analytics, which analyses data to predict future outcomes. Prescriptive analytics takes that insight to the next level by suggesting the optimal way to handle that future situation. Organisations that can act fast in dynamic conditions and make superior decisions in uncertain environments gain a strong competitive advantage. Trucking carriers look for a model for their businesses that assigns the correct number of trucks to each route in order to minimise the cost of transhipment and meet the volume requirements. With prescriptive analytics, complex problems can be solved by [37]:

- Automation of the complex decisions and trade-offs to better manage your limited resources.
- Taking advantage of a future opportunity or mitigating a future risk.
- Proactively update recommendations based on changing events.
- Meet operational goals, increase customer loyalty, prevent threats and fraud, and optimise business processes.

For every kind of transport optimisation problem, the business problem needs to be mathematically formulated and modelled with constraints. An integrated multi-level intermodal network design in operations research is proposed based on a sequential decision-making game. On the upper level, a stakeholder as the agent with environmental, economic, and social concerns decides whether or not to establish intermodal terminals and rail corridors, considering budget limitation and minimisation of both internal and external costs. On the lower level, freight shippers as the players decide how to transport their freight shipments through rail or road, considering rail accessibility, capacity constraints and internal cost minimisation. A mathematical programming model is developed to formulate the shippers' best response to the decisions adopted by the stakeholders. For the business problem of a trucking company, the solution was investigated on the following example. A trucking company has a hub and spoke system, meaning that has a main feeder terminal which covers the neighbouring distribution centres. The shipments to be delivered are specified by an originating spoke, a destination spoke, and a shipment volume. The trucks have different types defined by maximum capacity, speed, and cost per kilometre. The model assigns the correct number of trucks to each route in order to minimise the cost of transhipment and meet the volume requirements. There is a minimum departure time and a maximum return time for trucks at a spoke, and a load and unload time at the hub. Trucks of different types travel at different speeds. Therefore, shipments are available at each hub in a timely manner. Volume availability constraints are taken into account, meaning that the shipments that will be carried back from a hub to a spoke by a truck must be available for loading before the truck leaves. For the sake of the mathematical model, the assumptions are [37]:

- Exactly the same number of trucks that go from A to B return from B to A,
- Each truck arrives at a terminal as early as possible and leaves as late as possible,
- The shipments can be broken arbitrarily into smaller packages and shipped through different paths.

The model was developed in the Python programming language and to run the scenarios, the Decision Optimization CPLEX Modelling library was imported. This library contains two modelling packages, Mathematical and Constraint Programming. Data in this scenario is stored in JSON format for easier customisation of the parameters. All the parameters of the trucking company distribution model with delivery windows are:

- parameters: maxTrucks, maxVolume
- location: name
- spoke: name, minDepTime, maxArrTime
- truckType: truckType, capacity, costPerKm, KmPerHour
- loadTimeInfo: hub, truckType, loadTime
- routeInfo: spoke, hub, distance
- triple: origin, hub, destination
- shipment: origin, destination, totalVolume

Trucks are divided into teams to preprocess the dataset. This type of assessment was conducted on two sets of test problems involving 50 and 75 customers, denoted by TP50 and TP75 respectively. Each of the above sets consists of 20 test problems, demand and capacities are shown in litres. The types of vehicles and the customers' orders are shown in Table 2.4. The vehicles used were distinguished into three types [38]:

1. Truck_1, net weight: 16,000 kg, maximum volume: 4800 L, fuel consumption 21.6-31.1L/100 km;
2. Truck_2, net weight: 28,000 kg, maximum volume: 4900 L, fuel consumption 29.9-31.6L/100 km;
3. Truck_3, net weight: 29,000 kg, maximum volume: 6100 L, fuel consumption 32.6-34.3L/100 km;

Table 2.4: Results of the TP50 and TP75 scenarios

Type ID	Average demand (L)	No. of Truck_1	No. of Truck_2	No. of Truck_3
TP50-75% demand	521,550	2	5	5
TP50-95% demand		3	6	6
TP75-75% demand	818,750	4	7	8
TP75-95% demand		5	9	10

Type ID	Total capacity (L)	Average total distance (km)	No. of routes
TP50-75% demand	395,100	925.2	13.7
TP50-95% demand	487,200	919.7	13.8
TP75-75% demand	612,700	1364.1	21.2
TP75-95% demand	775,100	1362.8	20.9

In both TP50 and TP75, increasing demand from 75% to 95% leads to: An increase in truck counts, especially for $Truck_3$, which has the highest capacity. A proportional increase in total capacity to match the higher demand needs. Interestingly, the average total distance per scenario stays nearly the same, suggesting optimisation of routes even as demand scales. $Truck_2$ and $Truck_3$ are used more frequently than $Truck_1$: Reflects a preference for higher capacity trucks to reduce the number of trips. More cost-effective when factoring volume per km per fuel unit. Average number of routes slightly increases with demand, but not linearly. This indicates that the model successfully consolidates shipments to reduce route count even as demand increases. (Figure 2.18) TP75-95% has 775,100 L capacity across 20.9 routes, while TP50-75% has 395,100 L across 13.7 routes. Despite a near doubling of volume from TP50 to TP75 scenarios, the average total distance increases only moderately (from 920 km to 1360 km). This indicates efficient spatial clustering and terminal optimisation, likely due to the constraints around earliest arrival and latest departure being well managed. The model effectively balances fleet composition, cost, and operational constraints to deliver ITUs at increasing demand levels (congested environment). It favours larger trucks ($Truck_2$ and $Truck_3$) for cost-efficiency and volume consolidation.

2.3 Intermodal transport terminals in Europe

Ports or terminals, as the interface of water-land transports and value-adding activities play an indispensable role in international trade. Areas served by a port are referred to as its hinterland, over which port users, including all types of shippers and receivers, choose the port as the transfer connection on water-land intermodal paths and coordinate and oversee the en-

Figure 2.18: Truck assignment and fuel costs per scenario.

tire freight delivering process on the paths. The first step in tackling port congestion is staying informed. [39] Shippers are facing worsening equipment shortages in China due to soaring export demand and disruption to both long-haul and intra-Asia services caused by the ongoing vessel diversions around southern Africa. While the impact varies by carrier, the worst-affected ports are Ningbo, Dalian and Guangzhou, while inland hubs including Wuhan and Chongqing are also experiencing container shortages. Carriers are facing equipment issues in China, especially for 40-foot and 40-foot high cube containers and the shortages are worse by every week. As China is the biggest exporter of various products, those freight flows are spilling over to other worldwide destinations, including Europe. The road truck transport network with flows data for 2019 is shown in Figure 2.19. Flows are divided into five categories from very low to very high flow. As for the further analysis, only the high and very high freight flows are presented in the map because of the excessive congestion, which causes the intermodal terminal disruptions.

Intermodal terminals are essential for creating efficient and competitive intermodal supply

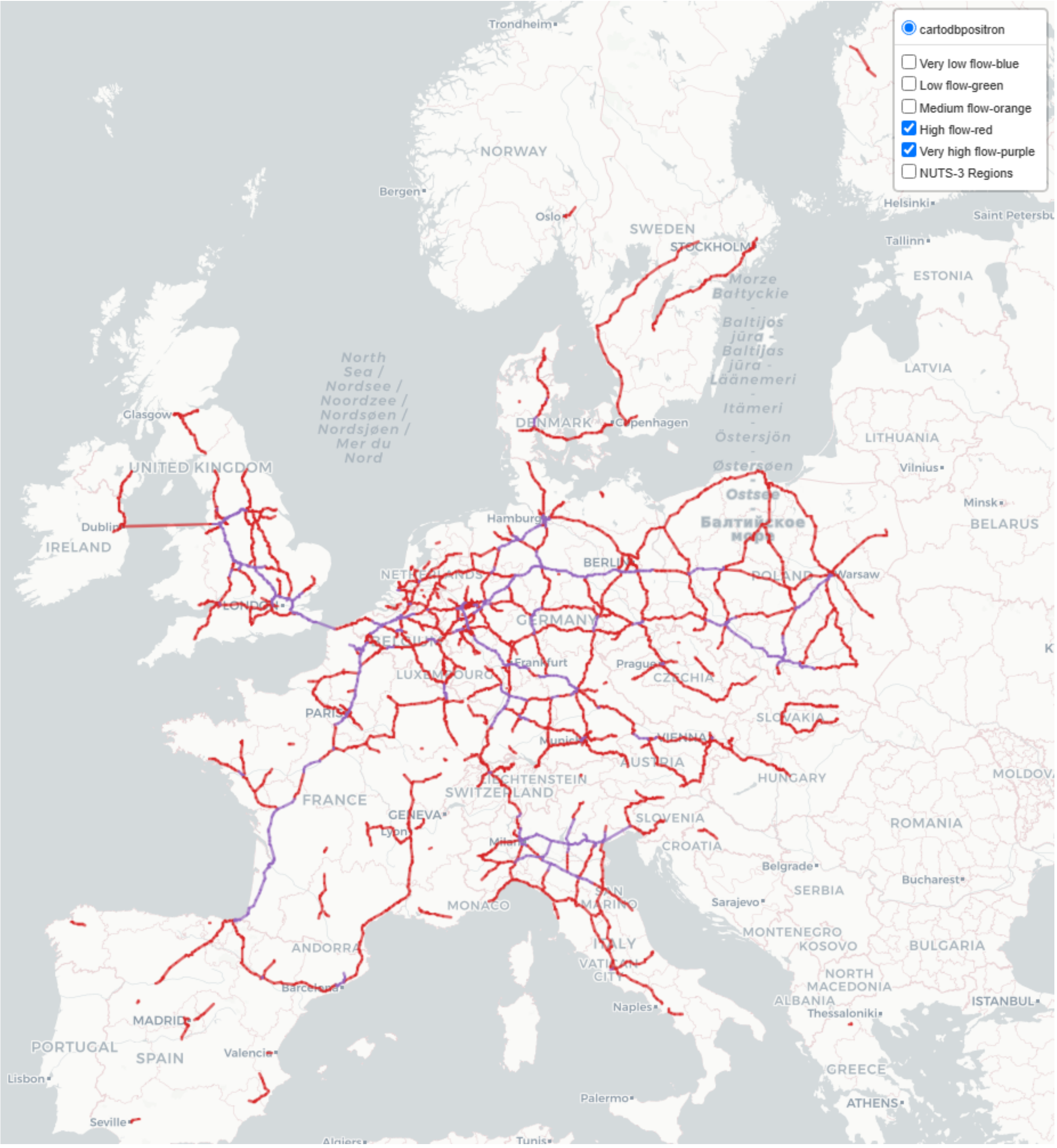

Figure 2.19: Freight flows by truck road traffic in . [27]

chains across Europe, which is a key strategy for sustainable development and reducing urban congestion. Figure 2.20 shows the density of intermodal terminals across Europe and northern countries in the EU with the biggest number of terminals per square kilometre are Germany, Denmark, Netherlands, Belgium and Luxembourg. The European Green Deal emphasizes the need to shift a significant portion of inland freight from road to rail and inland waterways, necessitating efficient transhipment facilities and technologies. Despite the advantages, intermodal freight transport faces challenges such as regulatory and infrastructure barriers, which hinder its competitiveness compared to road transport. The development of intermodal terminals in Europe is supported by various EU initiatives and funding programs, including the Trans-European

Figure 2.20: Intermodal terminal density in Europe. [40]

Transport Network (TEN-T) regulation and the Connecting Europe Facility (CEF). These initiatives aim to enhance the infrastructure and operational efficiency of intermodal terminals, thereby promoting a modal shift towards more sustainable transport options. However, the lack of easily accessible information on intermodal terminals and real-time network capacities remains a significant barrier. Europe also boasts a significant share in the intermodal freight transport market, driven by its extensive rail and inland waterway networks. [40]

Key features of European intermodal terminals include:

High Efficiency: European terminals are known for their high efficiency and integration with various transport modes, supported by the European Green Deal and other EU initiatives.

Strategic Locations: Terminals are strategically located to facilitate seamless transfers between rail, road, and waterways, enhancing the overall efficiency of the supply chain.

For many businesses, transhipments are an unavoidable part of shipping their freight from A to B. With the right logistics partner, transhipments can contribute positively to the resilience and stability of a supply chain. With a combination of high-performing transhipment hubs, advanced technologies, solid partnerships, strong risk assessment practices, and a commitment to continuous improvement, transhipments can be smooth, reliable and deliver for business and supply chains.

2.3.1 Container throughput and management

The 'Network of the Future' covers the ocean freight network on East and West trades of all the biggest shipping companies (Maersk and Hapag-Lloyd) and went live in February 2025. The ambition is to reduce network complexity with mostly single-operator loops and fewer port calls per service and incorporate terminals with the highest level of productivity and operational efficiency. The improved Asia Mediterranean network (2.21) provides an overall transit time reduction of 3 days for most corridors and multiple weekly connections from Asia to key Mediterranean gateways in Spain, Italy, the Adriatic and Turkey. Valencia and Barcelona experience improved transit times of 4 days on average. North China and South Korea enjoy at least 1 week of improved transit times by deploying dedicated and lean shuttle services where costs are decreased by sharing the fleet with cooperative stakeholders. [41] Dedicated shuttle services for the Mediterranean area are shown in Figure 2.22.

Croatia's geographical position offers significant advantages for further development of intermodal transport, particularly through its maritime, river, and railway networks. The strategic location of Croatia makes it a vital link in the European transport corridor network, which is essential for the success of its intermodal terminals. The development of intermodal transport in Croatia is seen as a crucial factor for its integration into European traffic flows.

Determining suitable locations for intermodal terminals in Croatia involves evaluating several criteria, including legislative, environmental, freight flow, spatial, technical-technological, and organisational factors. Among these, the criterion of freight flows has the most significant impact on the selection of terminal locations, followed by spatial considerations. Quality indicators for intermodal terminals in Croatia include flexibility, safety and security, reliability, time, and accessibility.

One of the main challenges in the development of intermodal transport in Croatia is the delay in the intermodal transport chain, which affects its competitiveness in the international

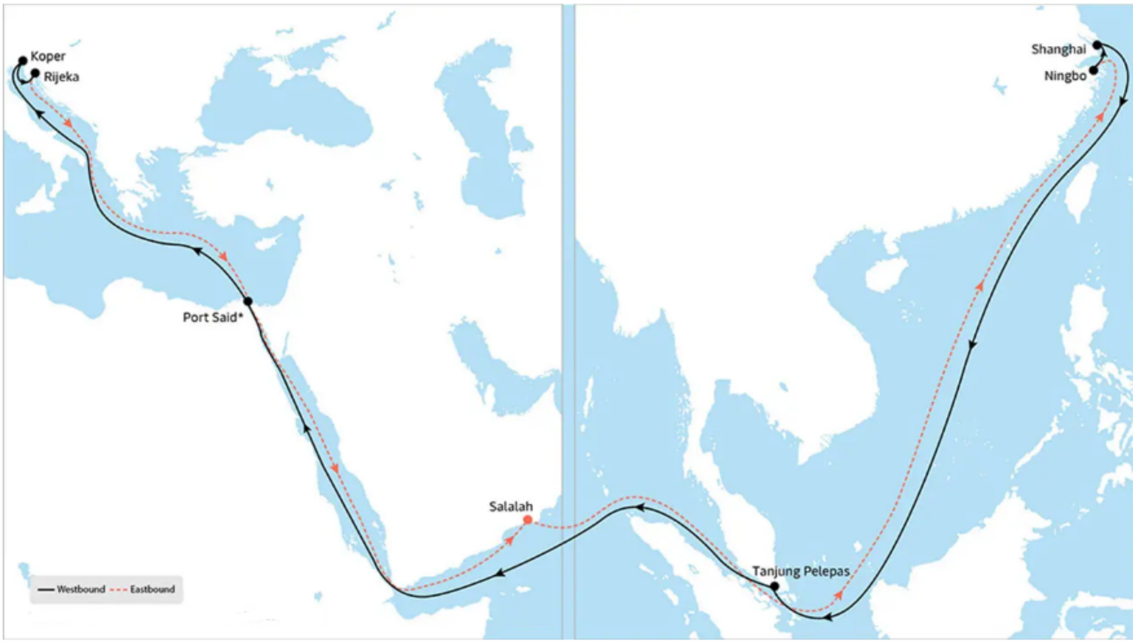

Figure 2.21: Asia-Europe maritime service freight transport network. [41]

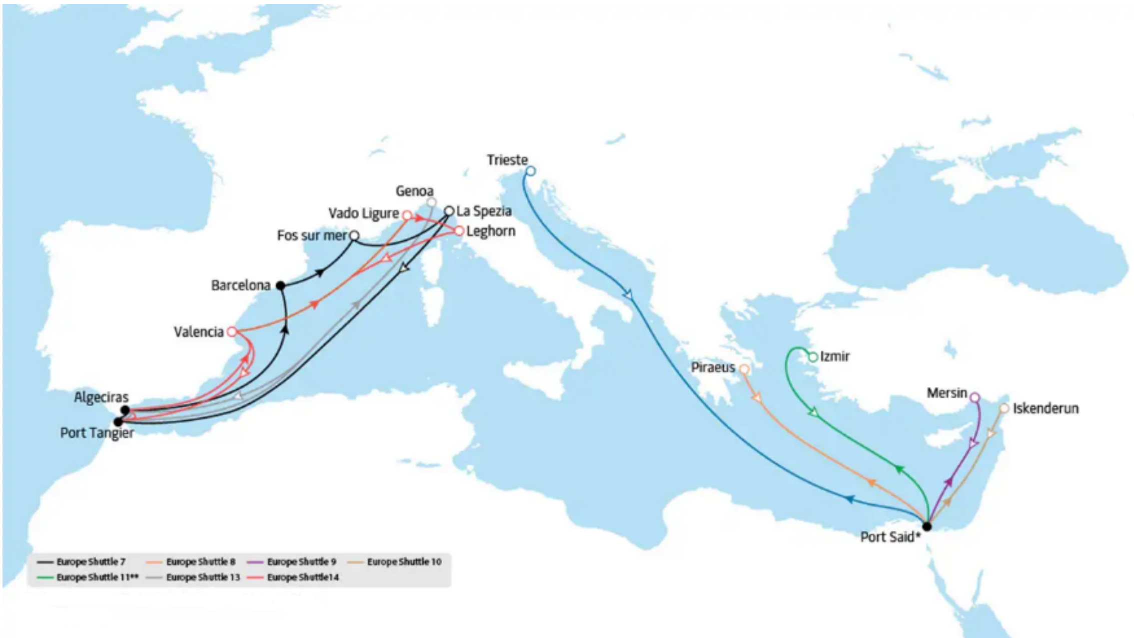

Figure 2.22: Asia-Europe shuttle service in maritime freight transport network. [41]

transport market. To address these challenges, the development concept for intermodal transport in Croatia should be based on guidelines related to maritime, river, and railway transport, as well as logistics. This approach aims to enhance the efficiency and reliability of intermodal transport services.

Inland intermodal terminals in Croatia play a crucial role in consolidating freight units for overseas transport over long distances and distributing freight flows at local, regional, and international levels. The establishment of these terminals requires careful consideration of location criteria and quality indicators to ensure their undisrupted operating. The success of these terminals is also dependent on their connection to the European traffic corridor network, which enhances their accessibility and operational efficiency.

Container transshipment plays a crucial role in Croatia's maritime transport system, particularly due to its strategic position along the Adriatic Sea, serving as a gateway for Central and Eastern Europe. Container throughput from and to maritime terminals is shown in figure 2.23, and percentage of rail and road share is shown in figure 2.24. With the already mentioned main container-handling seaports in Croatia, the Port of Zadar in recent years is showing growth in freight containers transported. Until now, Zadar was focused on the ferries and passenger transport mainly. The developments and limitations of Croatian ports are listed below.

Key developments in container throughput at Rijeka include:

- Expansion of the Zagreb Deep Sea Terminal, increasing capacity to over 1 million TEUs annually.
- Enhanced railway connectivity, improving intermodal transshipment between maritime and inland routes.
- Digitalisation initiatives, such as the Port Community System (PCS), which optimises freight handling and tracking.

Port of Ploče: Regional Transshipment Hub

The Port of Ploče is the second-largest seaport in Croatia, primarily serving Bosnia and Herzegovina and the wider Balkan region. It specialises in bulk shipments but has seen steady growth in containerised freight. The modernisation of the Ploče Container Terminal and railway upgrades to Corridor Vc have enhanced the port's role in regional transshipment. Challenges facing the Port of Ploče in container transshipment include:

- Limited capacity compared to Rijeka, requiring further expansion.
- Dependence on hinterland infrastructure, particularly rail connections to neighboring countries.
- Competition from larger Adriatic ports, such as Koper and Trieste.

Port of Zadar: Emerging Container Facility

Although historically focused on passenger and ferry services, the Port of Zadar has seen growing interest in container handling. Investments in Gaženica Port and planned logistics zones aim to position Zadar as a future hub for short-sea shipping and regional transshipment.

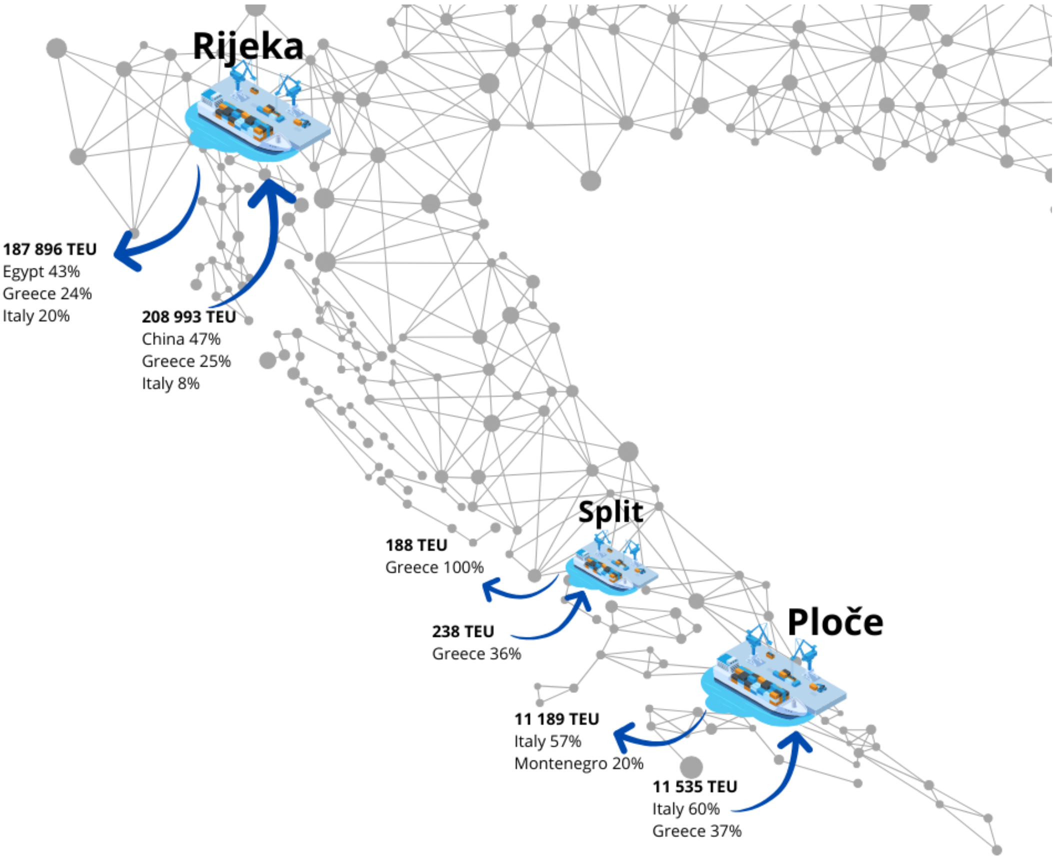

Figure 2.23: Container throughput from container ships in Croatian seaports in 2023. [9]

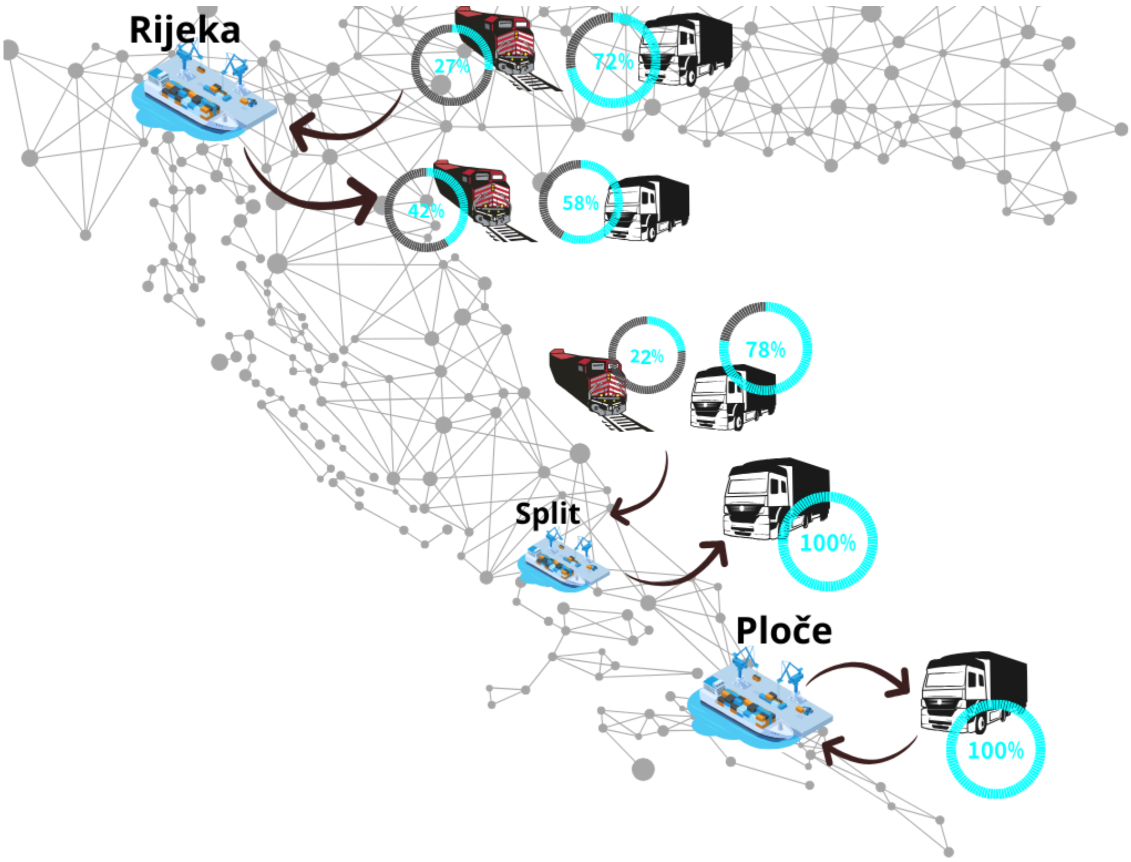

Figure 2.24: Container transport ratio from and to Croatian seaports in 2023 with roads and railways. [9]

2.3.2 Terminal operations

The presented graphs illustrate the trends in container transshipment and handling in Croatian seaports from 2010 to 2023. The blue and green lines represent the volume of transshipped containers, while the red line indicates the total amount of handled containers. Based on the data (Figures 2.25 and 2.26), fluctuations in container traffic and freight handling are noticeable over the observed period. In the early years (2010–2014), there was a slight decline in container traffic, which resulted from global economic conditions and reduced trade flows. The data for the 2013 is missing because of the Croatia's entry into the European Union (EU) and integration with its systems. However, from 2015 onwards, a steady increase can be observed, continuing until 2019. The year 2020 saw a slight drop, due to the impact of the COVID-19 pandemic and disruptions in global supply chains. Despite this, a significant recovery is evident from 2021, with both container traffic and freight handling showing continuous growth. This trend is attributed to increased investments in port infrastructure, modernisation of NAPA terminals, and the overall rise in international trade. A particularly notable increase occurred in 2022 and 2023, indicating the strengthening role of Croatian ports in intermodal transport and the growing demand for logistics services. This growth is linked to the improved competitiveness of ports such as Rijeka and Ploče compared to other Adriatic and European ports, as well as enhanced railway connections to Central and Eastern Europe. The data highlights a long-term upward trend in container traffic in Croatian seaports, where intermodal logistics solutions play a crucial role in the continued development of this sector. [9]

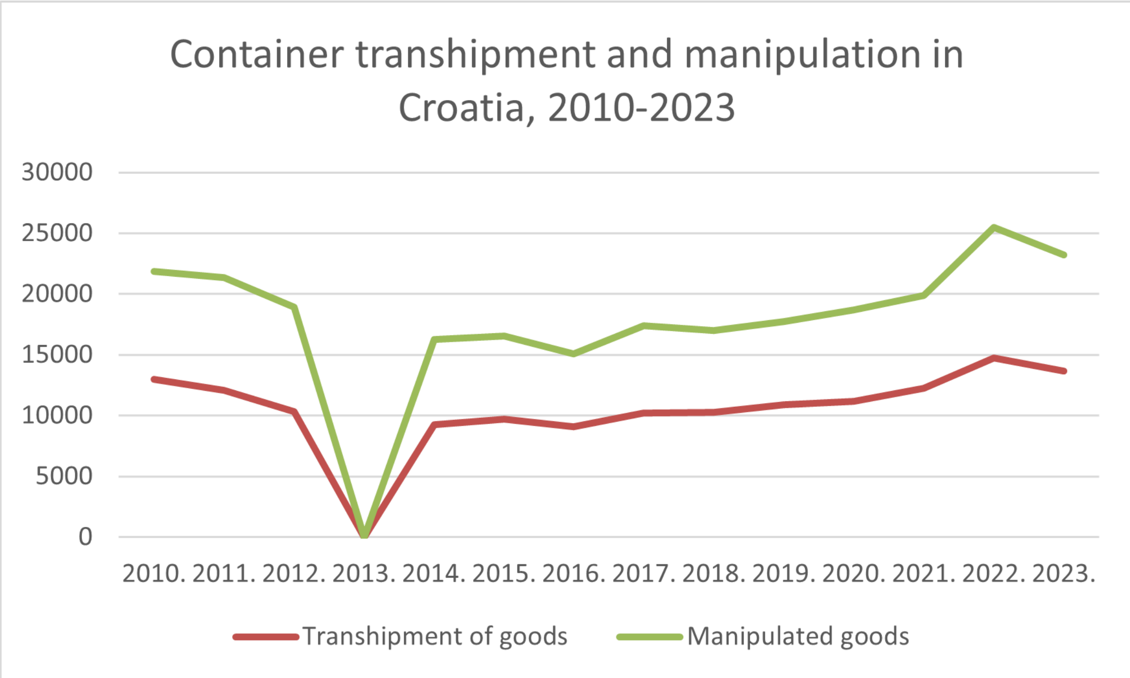

Figure 2.25: Statistical data on container transhipment ratio.[9]

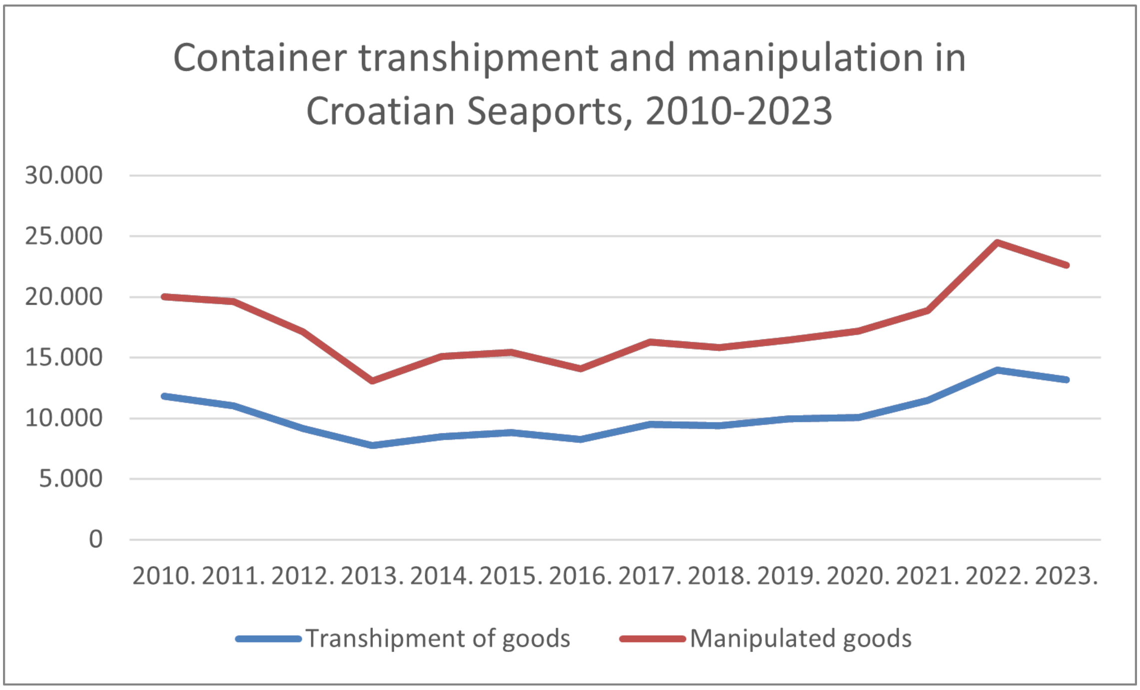

Figure 2.26: Seaport statistical data on container transhipment ratio.[9]

Figure 2.27 examines how container throughput fluctuates across different months over period from 2010 until 2022 in Croatian maritime ports. First, the data are log-transformed to stabilise variance and added to a time-series collection. For each month, yearly averages are computed from the log-transformed values, and deviations from these averages are derived. These deviations show how each year's monthly value differs from the long-term mean for that month. For each year, monthly averages are computed and monthly deviations from those averages are determined, capturing the variability within a year . Finally, both types of deviations, by month and by year, are visualised as continuous functions over time to highlight long-term and seasonal trends in maritime freight transport. The data reveals seasonal patterns, with peak throughput consistently occurring during the summer months, particularly June through August, coinciding with increased trade activity and touristic supply chain demands. Winter months, especially January and February, exhibit significantly lower volumes, reflecting seasonal slowdowns and reduced maritime traffic. The trend is observable across multiple years, indicating a stable cyclical dynamic in port operations. Additionally, certain years such as 2020 display deviations due to external disruptions (the COVID-19 pandemic), providing insight into the system's sensitivity to global events. These observations are valuable for capacity planning, terminal resource allocation, and infrastructure optimisation within intermodal transport systems.

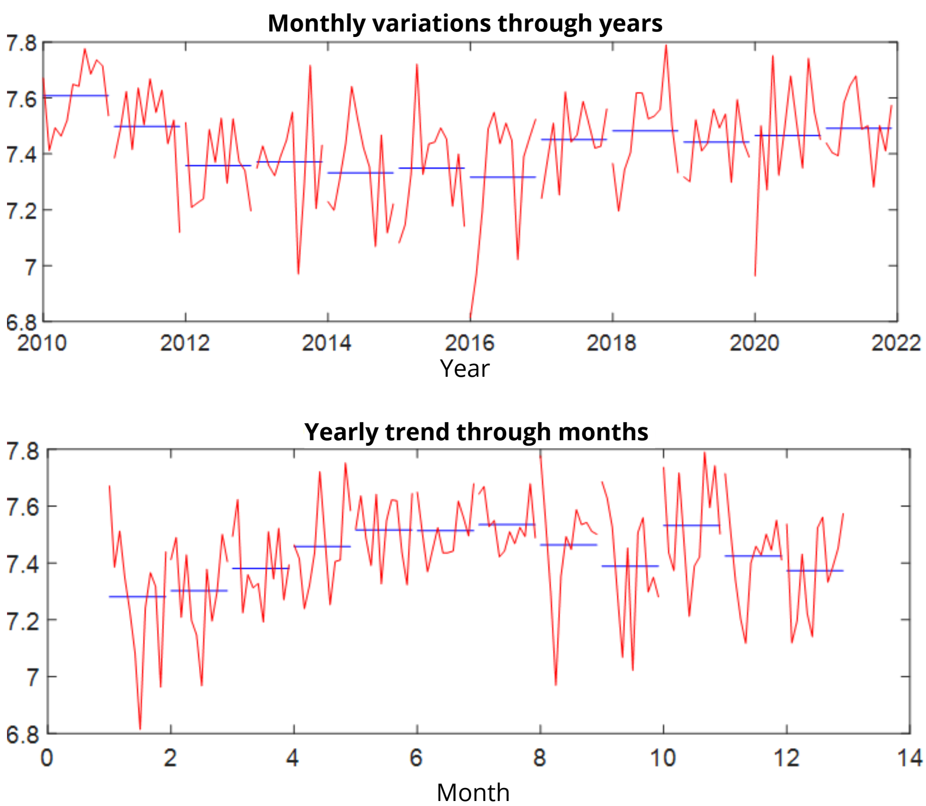

Figure 2.27: Monthly and yearly variations of container throughput in Croatian maritime ports.

To analyse the important features in an intermodal network, the transport process needs to be simulated (2.28). All real processes are modelled in the Rijeka distribution centre. For initial route planning Dijkstra's algorithm and Monte Carlo Tree Search (MCTS) are used for computing the baseline paths comparable to other routing models. For the purpose of refining the RL model, agents learn on dynamic routing policies with cost optimisation. Breakdown of the simulation's structure and logic flow, organised by operational streams is divided in: 1) the full journey of an order arriving at the distribution centre, being processed, and dispatched; 2) creating and preparing outgoing orders; 3) arrivals and handling of inbound freight (containers, materials, etc.).

In the first stream, model captures and processes newly arriving orders, determines whether they can be fulfilled or need backordering. Valid orders (not delayed and backlogged) are sent to shipment generation. Those valid shipments are queued at the terminal's loading gates, including crane and vehicle scheduling assignment. Departure is finalised when the shipment is sent from DC via the rail, truck or maritime mode of transport.

Algorithm 2.1 Rijeka DC simulation

```
Result: Simulated processing of orders and shipments in the Rijeka distribution centre
foreach order ∈ incomingOrders do
    add order to incomingOrderWindow;
    processIncomingOrder(order);
    if order is valid then
        pass order to shipmentGenerator;
    else
        add order to backorderProcessor;
    end
    generate shipment in shipmentGenerator;
    wait in processingLoadingWindow;
    process at processingAtLoadingGates;
    outgoingShipmentProcessing(shipment);
    depart shipment from port;
end
foreach request ∈ outgoingOrders do
    add request to outgoingOrderWindow;
    perform sourcing of required inventory;
    adjust quantity as needed;
    if order size < threshold then
        drop order to sink;
    else
        processOutgoingOrder(request);
        place final order;
    end
end
foreach shipment ∈ shipments do
    input shipment in shipmentEnter;
    register at incomingShipmentWindow;
    process at incomingShipmentProcessing;
    move to processingAtUnloadingGates;
    unload shipment;
    if isFinalDestination = True then
        dispose shipment;
    else
        send shipment to next destination;
    end
end
```

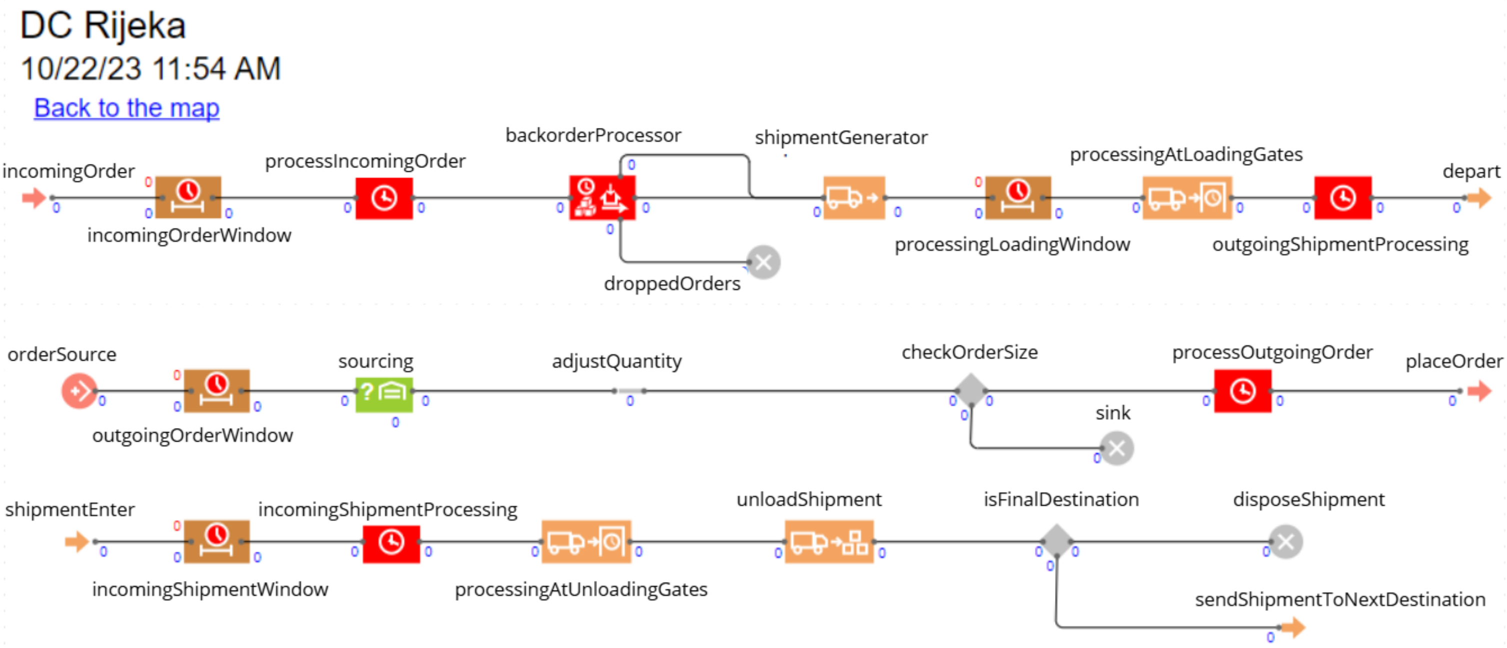

Figure 2.28: Initial architecture of the simulation process in Rijeka distribution centre.

The future development of intermodal transport in Croatia is promising, given its strategic location and the ongoing infrastructural development supported by EU initiatives. The focus is on enhancing the efficiency and reliability of intermodal terminals, along with the adoption of advanced transhipment technologies. The continuous investment in intermodal infrastructure projects, will further strengthen Croatia's position in the European transport network.

2.3.3 Intermodal transport problem with generalised capacities and costs

Intermodal networks have emerged as a focus point of efficient and sustainable freight movement in the rapidly evolving global transport and logistics landscape. These networks, characterised by the integration of multiple transport modes such as rail, road, and sea, offer flexibility and cost-effectiveness in freight transport. However, the complexity of these networks also introduces vulnerabilities that can significantly impact their performance and reliability. Node criticality refers to the importance of specific nodes within a network, where their disruption or removal impacts the network's overall functionality and performance. In the context of intermodal networks, critical nodes are often key terminals, junctions, or transfer points that facilitate the movement of freight between different modes of transport. For instance, the closure of a major port or the breakdown of a key rail terminal can ripple through the entire supply chain, affecting production schedules, inventory management, and ultimately, consumer satisfaction. There are various approaches to determining the importance of the node. Previous research has typically addressed congestion by employing either static or dynamic assignment models. However, these methods come with the drawback of extended computational times that prevent a comprehensive scan. In contrast, other studies achieved a complete analysis by utilising a purely topological approach, implemented an all-or-nothing assignment method, or opted for a probabilistic route choice that did not factor in congestion and capacity issues, which are crucial when link failures occur. Previous studies commonly used a single centrality to rank nodes, such as degree centrality, betweenness centrality, closeness centrality, k-shell, etc. [42], [43],[44], [45], [46], [47] The definitions of these measures were summarised by [48]. Recently, a new trend has emerged to comprehensively identify critical nodes by combining multiple indicators [49], [50]. Carriers and logistics operators often try to find supply chain designs with multiple objectives to fulfil. If costs are not minimised, then at least they need to reduce their global carbon footprint, minimise the use of energy or waste returns. This can be illustrated through an example of what it might look like if a company that seeks to optimise its deliveries along more than just one objective.

Table 2.5: Data on intermodal terminals.

Class	Number of Rows	Attributes
Rail-road terminal	30	ID, Name, Country, Capacity, Latitude, Longitude
Port	7	ID, Name, Country, Supply, Latitude, Longitude
Distribution centre	8	ID, Name, Country, Demand, Latitude, Longitude

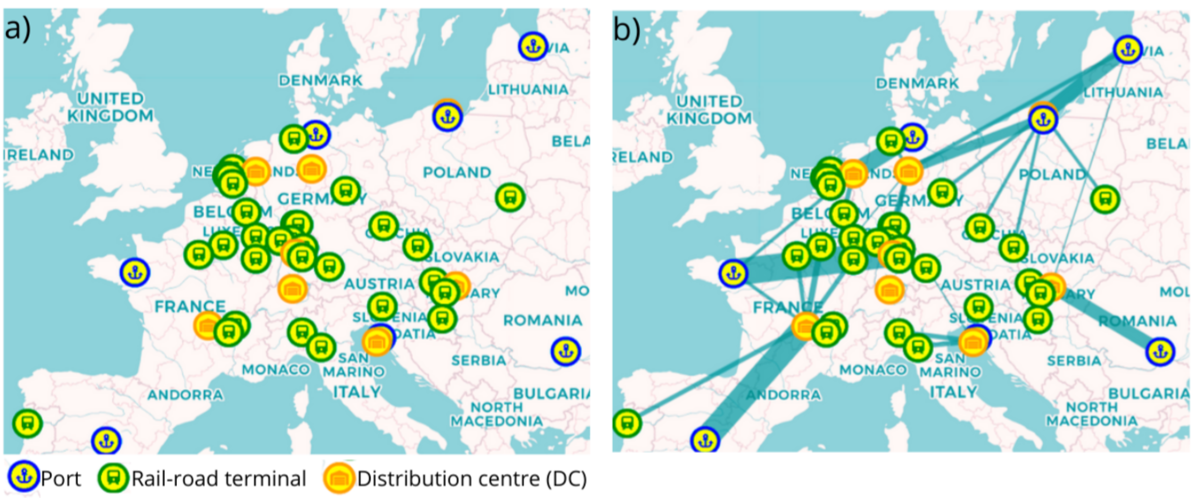

Figure 2.29: (a) Intermodal nodes in the network; (b) Capacitated distance-based solution in the intermodal network.

This example in Fig. 2.29 is a form of optimisation problem, named transhipment problem, where the goal is to consolidate or redistribute the freight in the network regarding distances and volume of freight transported. The transport distances and corresponding unit costs between different nodes in the intermodal supply chain network are divided to two route types: Port to rail-road terminal by rail, and from terminals to DCs by road. Then, two separate unit transport costs are defined, for rail and road separately. The mathematical formulation of the intermodal transhipment problem is in the following section.

Decision Variables

- x_{ij}^{m} = quantity of containers transported from node i to node j using mode m.
- y_{ij}^{m} = binary variable, 1 if mode m is used for transport between i and j, 0 otherwise.

Parameters

- C_{ij}^{m} = cost per unit transported (TEU) from i to j using mode m.
- E_{ij}^{m} = emission cost per unit transported using mode m.
- S_s = supply at port s.
- D_d = demand at DC d.
- C_c = capacity of rail-road terminal c.
- M = set of transport modes (road or rail).

Objective Function

Minimisation of the total transport cost including emission costs:

$$\min \sum_{i} \sum_{j} \sum_{m \in M} (C_{ij}^{m} + E_{ij}^{m}) x_{ij}^{m} \tag{2.1}$$

Constraints (Descriptive overview)

- **Supply constraints:** Each port can only receive freight up to its available supply capacity.
- **Flow constraints:** Rail-road terminals act as transhipment points, ensuring that incoming shipments are equal to outgoing shipments.
- **Demand satisfaction:** Each DC must receive their required demand.
- **Intermodal terminal capacity limits:** DCs cannot exceed their storage capacity.
- **Mode selection:** A transport mode can only be used if it is selected for a given route.
- **Non-negativity and Binary constraints:** Shipments must be non-negative, and transport mode selection is binary.

The total cost between the nodes is minimised in the objective function, and the solution to the mathematical model obtained with the Gurobi solver is *8.1814e+07*, gradually improving the total cost from *2.7413e+08* in 34 iterations. For estimating node criticality in the following chapter, edges to DC in Zürich, Switzerland have been removed from a new subnetwork that consist of 15 warehouse nodes in the closest proximity of the disrupted DC. Zürich serves as an important transhipment node in European network because of the high intermodal connections and dedicated storage capacities. In order to transport freight between the ports and the DCs, we have two different transport modes. The first transport mode of choice is the direct transport by road. In this example, Madrid in Spain and Toulouse in France have a rail and road connection, but due to poor railway infrastructure connecting those states, road transport is the only option in this case. The second transport mode is employing a combination of rail and road. So for each DC, it's determined what is the closest rail terminal.[51], [5]

Chapter 3

Vulnerability and resilience of transport networks

Resilience involves both the network's inherent ability to cope with disruption via its topological and operational attributes, defining potential actions that can be taken in the immediate aftermath of a disruption or disaster event. This conceptualization of resilience in terms of both inherent and adaptive components is discussed in [52] and was quantified in [53]. The problem of measuring resilience was formulated, defined as the expected system throughput given a fixed budget for recovery action and fixed system demand, in an intermodal freight transport application. The problem was posed as a stochastic, mixed integer program. The program includes no first-stage variables. All decisions are taken once the outcome of the random disaster event is known. Thus, the problem can be decomposed into a set of independent, scenario-specific, deterministic problems, and the focus of their solution approach is on the sampling methodology and exact solution of each independent deterministic problem that results for a given network state. Miller-Hooks et. al. presented a solution framework employing Benders decomposition, column generation and Monte Carlo simulation. A secondary outcome from solving the mathematical program is the optimal set of recovery actions that can be taken to obtain the maximum attainable throughput for each potential network state [53]. This conceptualization of resilience includes not only the network's inherent coping capacity but also the potential impact of immediate recovery action within a limited budget. It can be illustrated as in Fig 3.1

Transport system vulnerability assessment models that allow identifying critical links for the development of future high-quality transport management systems (TMS) are in today's focus of research. The challenges of increasing congestion and negative environmental impacts, shifting trips from conventional road vehicles to other transport options is generally seen as one of the most important actions. In terms of resilience and business continuity, transport systems need to be efficient as well as robust, as their vulnerability may cause various negative impacts. The methodological approach is particularly useful for planning a resilient response in the preparedness stage, prioritising investment for mitigation and adaptation, and prioritising

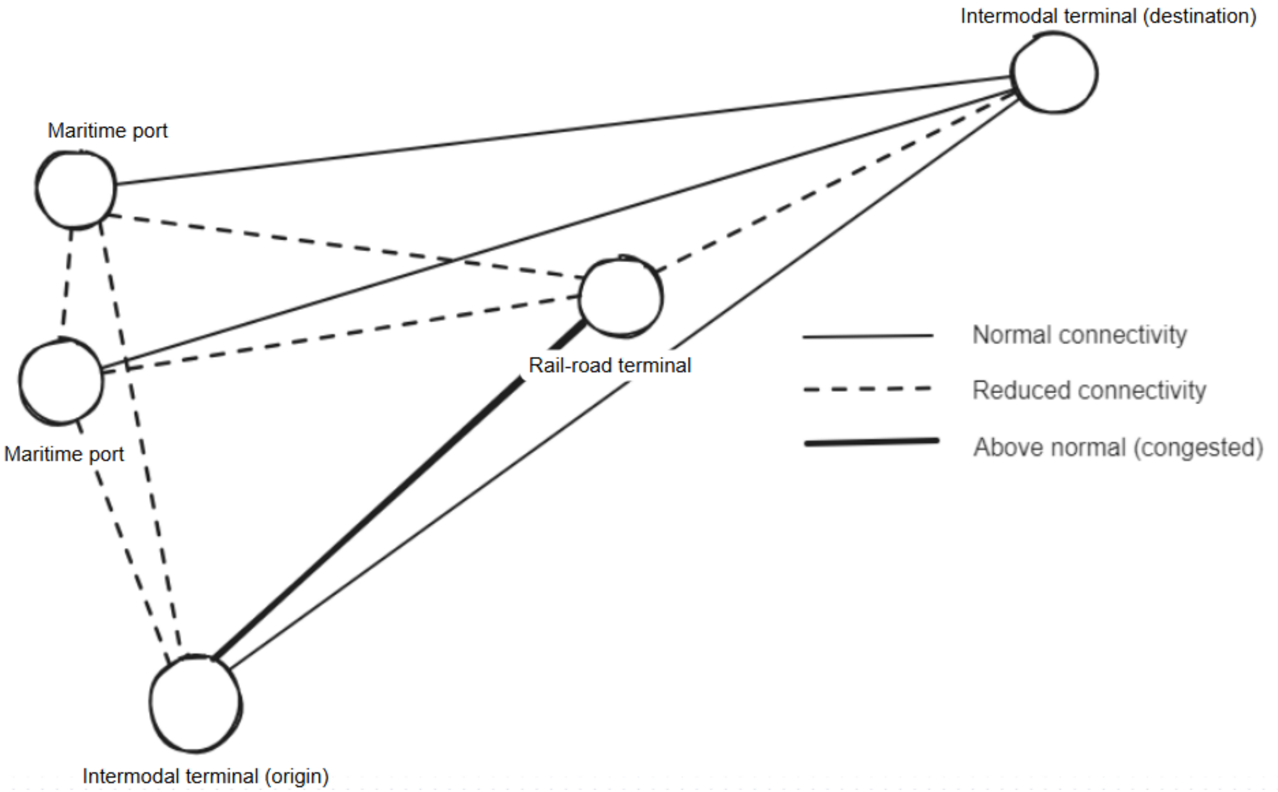

Figure 3.1: A schematic example showing the impact of recovery activities on network performance.

the rehabilitation (access restoration) of the disrupted links in the response and recovery stages. Resilience accounts for not only the ability of the system to absorb externally induced changes but also cost-effective and efficient, adaptive actions that can be taken to preserve or restore performance post-event. [54] Considering the transport vulnerability of freight and the cost and time of transport, it should be noted that one of the problems of modern transport systems is the proper assessment of the adjustment of transport organisation and technology in relation to the needs reported by the purchasers of transport services. In order to maintain the balance between different modes of transport and to limit the negative environmental effects of transport, the EU has undertaken actions concerning, inter alia, support for the development of intermodal transport within the framework of the policy of sustainable development of transport in the EU, which is written in the following table [25],[55]:

- The EU 2020 strategy - A strategy for smart, sustainable and inclusive growth, promoting a resource-efficient, greener and more competitive economy;
- White Paper - Roadmap to a single European transport area - Towards a competitive and resource efficient transport system: a 60% reduction in pollutant emissions in the transport sector by 2050 the use of rail transport for long-distance transport,
- Operational programme infrastructure and environment 2014-2020 - transport objectives:

development of sustainable and environmentally friendly transport, improving access to the European transport network.

3.1 Methods of quantifying resilience and vulnerability

Methods incorporate the ability of the elements to mitigate the intensity of the impact caused by the interventions and reduce the duration of their harmful effects. The required level of resilience can be achieved by continuously improving the system through five basic areas:

1. readiness,
2. absorption,
3. response,
4. ability to recover,
5. adaptability.

These areas and their criteria, shown in Figure 3.2, determine the level of resilience of critical infrastructure elements, which significantly reduces their vulnerability [56]. There are several ways to assess and model cascading effects between critical infrastructures that can be found in the literature, which aim to provide an overview of methods for assessing critical infrastructure interdependence as part of risk and vulnerability analysis [6]. One of the methods of quantitative risk assessment is defined as the product of frequency and consequence (R = FC), based on the parameters [57]:

- frequency (F),
- probability (P),
- range (E), i.e., the number of people affected by the unavailability of the service and,
- duration (D), as in the time period (h) when the service is not available.

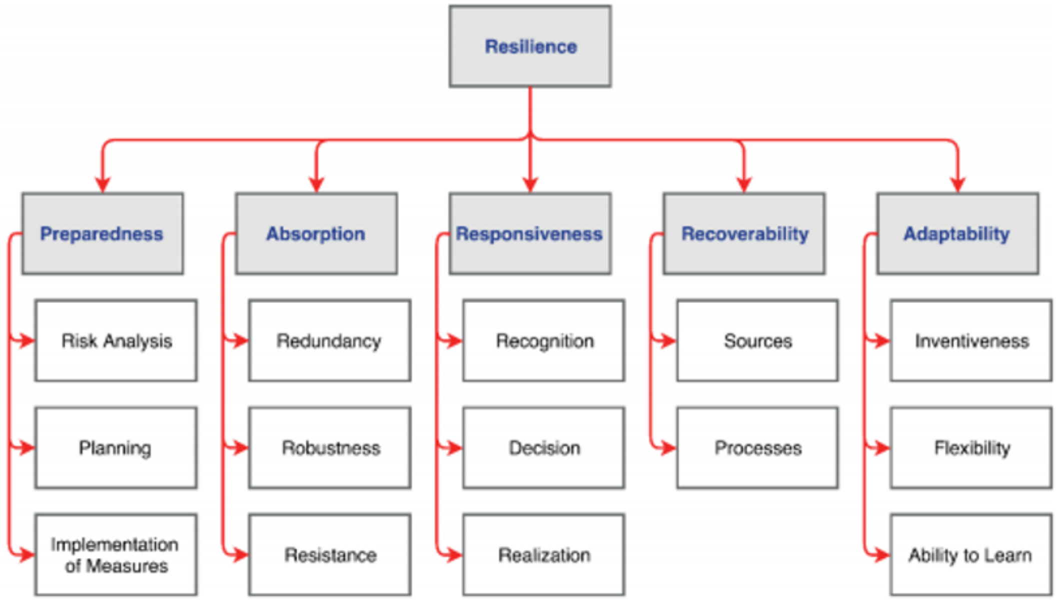

Figure 3.2: Areas that determine the resilience of critical infrastructure elements.

When it comes to the resilience of transport networks, literature is not yet so well established as literature on vulnerability [1]. Authors in [58] state that it is possible to distinguish between ecological and engineering studies. The latter refers to the ability of a system to return to the old steady-state equilibrium, while the former to the ability of a system to get to a new steady-state equilibrium. Moreover, according to the authors, in this literature the concept of robustness is often used, and it seems to be used with a similar meaning to that of resilience. Robustness describes the performance that can be preserved under disturbance and can be considered as the inverse of vulnerability. The concepts of resilience and robustness lead to similar results, but through different processes: in fact, a system is more resilient the greater its ability to recover after a shock, while a system is robust if it remains intact after a destructive event [58], [59]. Concerning quantitative resilience indices [60], refer to three categories: topological metrics, attributes-based metrics, and performance-based metrics. Metrics belonging to the first category, are often similar to those of vulnerability. This is due to the fact that, as already pointed out, vulnerability captures the ability of a network to withstand shocks, and this is one of the components of the multi-faceted concept of resilience. Examples of metrics belonging to the second category are those that focus on the recovery phase, i.e. recovery speed and recovery efficiency. Most of the methods proposed in the literature to assess resilience are hardly applicable to large-scale transport networks. Only topological methods can be considered more efficient in this sense, although it is necessary to recognize the limitation of not including traffic flow aspects. [39]

Table 3.1: Used concepts/areas in research

No.	Concept/area	References
1	resilience	[53], [59], [61], [62], [63], [64], [65], [66], [67], [5], [68], [69], [70], [71], [72], [45], [73]
2	vulnerability	[24], [39], [74], [75], [76], [77], [78], [79], [80], [81]
3	robustness	[82], [83], [3], [84], [85], [86]
4	recoverability	[60], [87], [88], [89]
5	adaptability	[90], [91], [92]

3.1.1 Critical areas in transport management

Most of the project tasks in TMS are properly coordinated (i.e., contractor-related interdependence is adequately managed and controlled), execution errors, quality deficits, delays in approval, and subsequently, other interdependence-induced project cascade performance disruptions (CPD) shown in Figure 3.3, are likely to propagate throughout. Different disruptions have the potential to induce others in a cascade manner that extends to other project components. For instance, immediate execution errors by one contractor in the network may not only affect those contractors within the closest task-dependent proximity but might also trigger multiple additional CPD to other contractors within the network. Such errors typically require multiple reworks—hindering productivity and disrupting resource allocations to multiple contractors and tasks, and subsequently incurring schedule delays and cost overruns [25]. As they attempt to adapt to such CPD, project managers typically resort to accelerating progress through compressing schedules and/or crashing tasks, which may also have a negative impact on the finished work quality and the safety of the workers inducing further project complications. Such disruptions may ultimately result in delayed infrastructure project completion and operation readiness, leaving governments and other stakeholders with lost revenues on project capital, and subsequently provoking negative societal perceptions and public controversies. Such consequences, in turn, may spark tensions between project stakeholders, where unresolved conflicts give rise to legal claims and disputes which have become increasingly common in infrastructure projects. Industry-standard and commercially available software tools, widely used for project management and control, typically employ the critical path method (CPM) and the Monte Carlo analysis. The former is customarily used for planning, scheduling and controlling project task durations, resource allocations and costs, whereas the latter is employed to enable further probabilistic modelling and risk analyses of the former's outcomes in order to quantify the levels of reliability associated with such outcomes. Despite providing valuable insights to support the management of small and medium-sized projects, such current tools suffer from three main underlying limitations when adopted to manage complex infrastructure projects. First, such tools are not custom-designed to visualise and analyse contractor-related interdependence. Second, the current tools can reveal predictions of project completion durations and budgets only following periodic schedule or budget updates, occasional scope changes or infrequent project risk level reassessments. Third, such tools leave project managers dependent solely on their subjective expertise to identify, prepare and execute response plans for project tasks and contractor coordination to rectify any oversimplified predictions of project performance disruptions revealed through periodic updates. [93]

Figure 3.3: Areas that determine the resilience of critical infrastructure elements.

3.1.2 Defining node criticality in intermodal networks

Node criticality refers to the importance of specific nodes within a network, where their disruption or removal can substantially impact the network's overall functionality and performance. In the context of intermodal networks, critical nodes are often key terminals, junctions, or transfer points that facilitate the movement of freight between different modes of transport. Identifying and managing these critical nodes are crucial for maintaining the robustness and efficiency of the entire transport system. The significance of node criticality in intermodal networks cannot be overstated. As global supply chains become increasingly complex and interdependent, the failure of even a single critical node can lead to cascading disruptions, resulting in significant economic losses and logistical challenges. For instance, the closure of a major port or the breakdown of a key rail terminal can ripple through the entire supply chain, affecting production schedules, inventory management, and ultimately, consumer satisfaction. In this research, exploratory analysis and visualising of the network are shown to understand intermodal freight flows in cases of Europe's ports, rail-road terminals and distribution centres (DCs) which have intermodal integration for changing modes. Those terminals are created as a special class. Data collection of network topology and flow patterns are stored in a format of a dictionary. Graph representation of the network is then created, with nodes representing ports, DCs and rail-road terminals, and edges representing connections. This network was simulated as a graph with 45 nodes, edges are weighted by travel time from freight booking data with Python NetworkX, Pandas, and GeoPandas libraries. With a database of freight distance-based data, including capacities, delays, and travel time of freight movements, further node criticality analysis can be obtained. The criticality score, or total time loss, is used to measure the impacts of a single or pair node disruption, which represents the most vulnerable nodes. The positive synergy effects of nodes can be seen from shutting them down simultaneously considering network topology. [94], [95], [96] To generate solutions as a sequential decision-making problem, the common idea is to utilise Reinforcement Learning (RL) on a Capacitated Vehicle Routing Problem (CVRP). Graph embeddings should be obtained from the GATs and a RL agent is trained in a way to provide suboptimal solutions. In the context of the Vehicle Routing Problem (VRP), encoders and decoders often refer to elements of a machine learning or heuristic framework used to solve the problem. In many modern VRP solvers, the encoder and decoder are integrated into an encoder-decoder model, such as:

- Neural combinatorial optimisation models: using deep learning (pointer networks, transformers) to learn both the encoding and decoding processes.
- Reinforcement learning approaches: using the encoder to define the problem state and the decoder to define the action space (to select the next node in the network or a transport mode).

Representation of the model steps are provided in Figure 3.4. The structural features of the input graph instance are extracted by the encoder. Then the solution is constructed incrementally by the decoder. Specifically, at each construction step, the decoder predicts a distribution over nodes, then one node is selected and appended to the end of the partial solution. By combining them together, the encoder and decoder translate raw problem data into high-quality solutions for VRP.

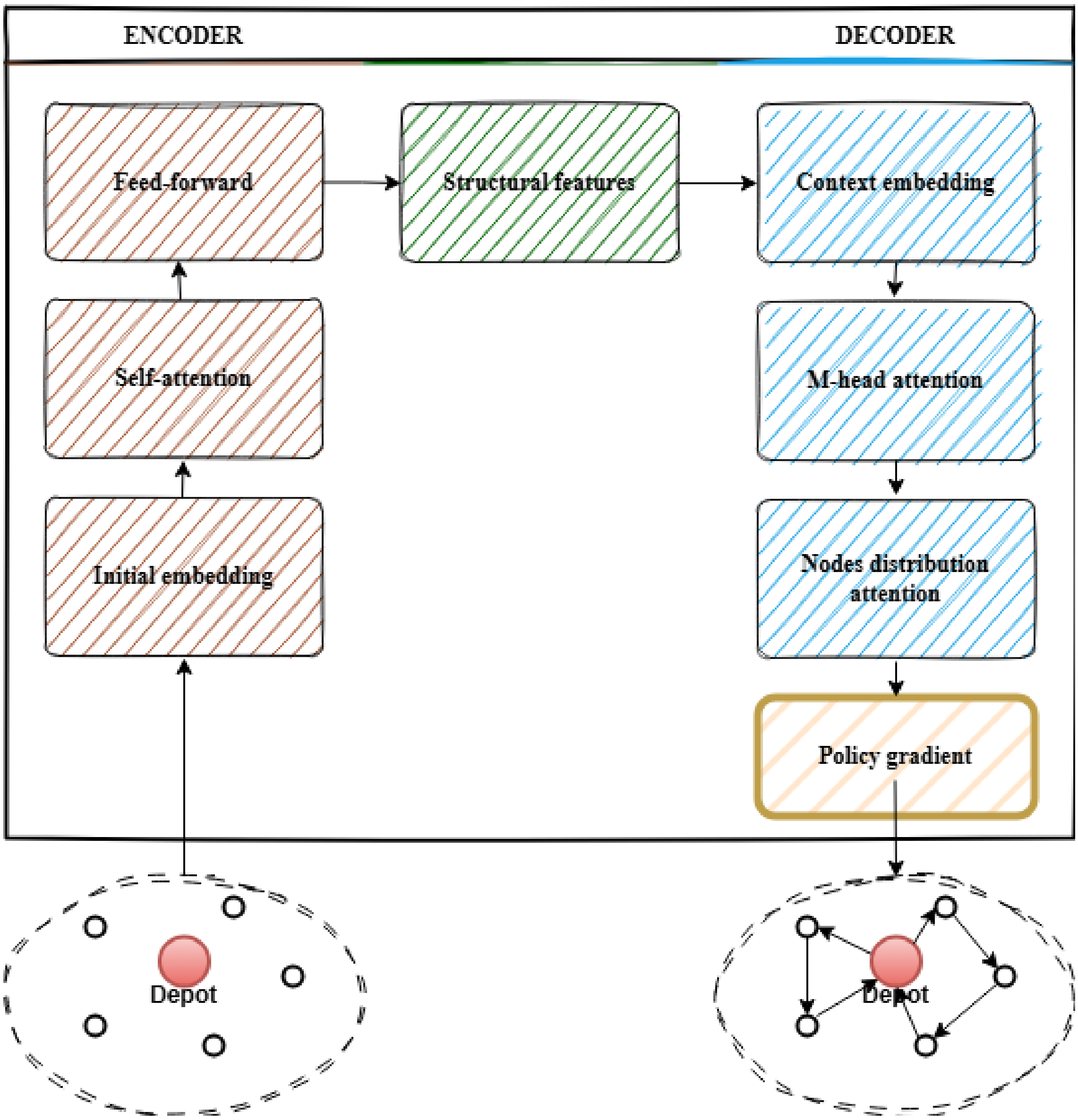

Figure 3.4: Methodology of routing as a sequential decision-making problem. [97]

3.1.3 Research gaps in current resilience metrics

Identifying gaps in current resilience metrics is a critical step in developing new resilience parameter for intermodal transport systems. Below are the outlined potential gaps that this research addresses:

- Lack of interoperability focus: Many existing resilience metrics focus on individual components (road networks or rail systems) but fail to account for the interoperability between different transport modes (e.g., rail-road-sea interfaces). New parameter should address this by explicitly modelling how disruptions in one mode affect others and incorporating measures of intermodal coordination.

- Static vs. Dynamic resilience: Current metrics often measure resilience statically, focusing on system robustness under pre-defined scenarios. However, real-world transport systems face dynamic disruptions (for instance, unexpected weather events or operational failures). New parameter should incorporate dynamic factors, such as the ability of the system to adapt in real-time and recover from unforeseen disruptions.
- Limited Integration of Cost Factors: Resilience is often measured in terms of time to recovery or reduction in capacity but rarely considers the economic costs associated with maintaining or restoring resilience. New parameter could integrate cost-related factors, such as the financial resources required to maintain resilience or the economic impact of disruptions.
- Oversimplification of interdependencies: Many metrics assume independence between transport nodes or modes, ignoring the complex interdependencies within intermodal systems. New parameter explicitly models these interdependencies and provide a more holistic view of system resilience.
- Lack of behavioural considerations: Current metrics often overlook human decision-making processes, such as how operators or managers respond to disruptions. New parameter should incorporate behavioural factors, such as the ability of stakeholders to make optimal decisions under uncertainty.
- Scalability limitations: Existing resilience metrics do not scale well to large, interconnected intermodal networks with multiple stakeholders and varying levels of infrastructure. New parameter could be designed to handle complex, multi-layered systems and provide insights at both local and global scales.
- Limited predictive capabilities: Most metrics are reactive, measuring resilience after a disruption has occurred. Only a few provide proactive insights into potential vulnerabilities or predictive capabilities for future disruptions. New parameter incorporates advanced analytics or machine learning techniques to predict resilience under various scenarios.
- Failure to account for emerging technologies: The increasing integration of AI models and automation in transport systems is not adequately reflected in current resilience metrics. New parameter could address this by incorporating the role of these technologies in enhancing or challenging system resilience.
- Overemphasis on infrastructure over operations: Current resilience metrics focus on physical infrastructure (bridges, ports, railways) but neglect operational aspects, such as scheduling, resource allocation, and workforce availability. The new parameter balances infras-

tructure and operational resilience to provide a more comprehensive measure.

- Lack of stakeholder-centric approaches: Current metrics often take a system-centric view, ignoring the perspectives of various stakeholders (e.g., passengers, freight operators, regulators). New parameter should be designed with stakeholder feedback in mind, ensuring it aligns with their priorities and needs.

3.1.4 Integration of resilience in transport planning

The research literature is rich in terms of methods and measures for the assessment of vulnerability and resilience in transport infrastructure, but little of the existing work has been adopted in practice. The literature has put efforts into developing assessment measures to understand the resilience and vulnerability of road networks [98], [99]. Several conceptual frameworks have been proposed, including road networks [1], [100]. Limitations are mainly because of two reasons: (1) transport planners and decision-makers do not know what method and measures to use among several proposed in the literature; (2) the methods and measures for vulnerability and resilience assessment should be obtainable using the existing data available to most transport agencies.

In multi-dimensional and system-level assessment framework, one study identified four quantitative metrics to characterize road segments in terms of criticality and vulnerability [101]:

1. **Connectivity of road segments within road networks.** Road segment connectivity is assessed by percolation analysis under the impact of external perturbations on road networks. This connectivity assessment can determine the redundancy and adaptive capacity of road networks.

2. **Vulnerability to extreme events.** This metric examines the proximity of road segments to disaster-impact areas to quantify vulnerability to extreme events, such as flooding. In this study, we identified areas exposed to flood hazards using 100- and 500-year floodplain maps to quantify the probability of flooded road segments. This metric can quantify the vulnerability of road networks in extreme flooding events and improve the robustness and absorptive capacity of road networks.

3. **Disrupted access to critical facilities.** This metric quantifies the criticality of road segments using an interdependent analysis based on proximity to critical facilities. The metric of disrupted access to critical facilities provides insight into resourcefulness, integratedness, and equitable access.

4. **The cascading impact of critical infrastructure networks.** This metric is processed using a similar approach to the metric for disrupted access to critical facilities based on proximity to infrastructure networks to quantify the criticality of road segments. The assessment

of the cascading impact of critical infrastructure networks quantifies the criticality of accessing infrastructure networks.

Quantitative metrics that can consider all these dimensions in resilience assessment are essential for a system-level understanding of the resilience of road networks and also inform transport planning and project development.

3.2 Indices of quantifying resilience of the transport system

Many published articles [70],[101],[102] on different aspects of transport system performance and resilience defined resilience, quantified resilience parameters, evaluated resilience improvement strategy, and modelled transport system performance. The primary emphasis through reviewed literature from the last decade was on the classification from the perspective of different transport modes, different modelling techniques and disaster types. Since the analysis in this dissertation is focused on interconnected infrastructure and terminals, the focus is on defining the way road network, railway and seaport terminals are connected. Depending on how the multi-layered network is arising, there are two main definitions of interconnected terminals which serve special purposes. [58] When considering each transport mode (road, rail, air, sea) as a different layer in the intermodal network, then the resilience parameter is calculated for each mode specifically. This allows evaluation and represents the resilience of each mode independently while also considering their interactions within the intermodal system. For each transport mode (e.g., road, rail), calculation of the following metrics are mandatory to form a *resilience parameter array*.

1. **Mode-specific parameters**.

a. Average degree of connectivity. The average degree of nodes in the network layer (for that specific mode). Represents how well-connected the nodes are within that mode.

$$d_{\text{avg}} = \frac{\sum_{i=1}^{N} d_i}{N} \tag{3.1}$$

Where d_i is the degree of node i, and N is the total number of nodes in that layer.

b. Redundancy ratio. This measures the number of alternative paths between key nodes (e.g., critical intermodal terminals). Higher redundancy implies greater resilience to disruptions.

$$R = \frac{\text{Number of alternative paths}}{\text{Total number of node pairs}} \tag{3.2}$$

c. Capacity utilisation. The ratio of actual freight flow to maximum capacity for critical links in the layer. High utilisation may indicate vulnerability to congestion or failure.

$$u = \frac{\text{Actual flow}}{\text{Maximum capacity}} \tag{3.3}$$

d. Betweenness centrality. Measures the proportion of shortest paths passing through a node or edge. Identifies critical nodes/edges that are vital for connectivity within the layer.

$$B = \sum_{s,t} \frac{\rho_{st}(v)}{\rho_{st}} \tag{3.4}$$

Where ρ_{st} is the total number of shortest paths between nodes s and t, and $\rho_{st}(v)$ is the number of shortest paths passing through node v.

e. Connectivity loss. Measures the drop in connectivity (reduction in the number of connected components) when a certain percentage of nodes/edges are removed. Represents the robustness of the layer to node/edge failures.

$$C_L = 1 - \frac{\text{Number of connected components after failure}}{\text{Initial number of connected components}} \tag{3.5}$$

2. **Intermodal resilience parametre**. While each mode can be analysed independently, intermodal resilience also depends on the ability to transfer containers between modes.

a. *Interlayer connection strength.* Measures the number of connections (ports, terminals) between layers. Higher connection strength implies better intermodal robustness.

$$S_{\text{inter}} = \frac{\text{Number of intermodal transfer points}}{\text{Total number of nodes across all layers}} \tag{3.6}$$

b. *Transfer efficiency*. Measures the ease and speed of transferring containers between modes. It's calculated as the average time or cost to transfer between layers.

$$E_{\text{transfer}} = \frac{\sum_{i=1}^{T} t_i}{T} \tag{3.7}$$

Where t_i is the transfer time/cost for the i-th transfer point, and T is the total number of transfer points.

c. *Interdependency.* Measures how dependent one mode is on another (rail depends on road for last-mile delivery). Calculated as the fraction of flows that rely on connections between layers.

$$D = \frac{\text{Flows requiring intermodal transfer}}{\text{Total flows}} \tag{3.8}$$

d. *Overall resilience.* Combine all mode-specific and intermodal metrics into a single resilience score for the entire system. Using weighted averages of mode specific normalised values to balance the contributions of each metric.

$$R_{\text{total}} = w_1 R_1 + w_2 R_2 + \cdots + w_n R_n \tag{3.9}$$

Where w_i are weights (based on mode importance) and R_i are the resilience metrics for each layer.

3. **State vector**. In reinforcement learning, the system's state can be represented using a concatenated array of these parameters for all modes. For every mode of transport, the following state vector is calculated:

$$S_{road} = \left[d_{\text{avg}}^{\text{road}}, R^{\text{road}}, u^{\text{road}}, B^{\text{road}}, C_L^{\text{road}}, \ldots, S_{\text{inter}}, E_{\text{transfer}}, D\right] \tag{3.10}$$

$$S_{rail} = \left[d_{\text{avg}}^{\text{rail}}, R^{\text{rail}}, u^{\text{rail}}, B^{\text{rail}}, C_L^{\text{rail}}, \ldots, S_{\text{inter}}, E_{\text{transfer}}, D\right] \tag{3.11}$$

$$S_{air} = \left[d_{\text{avg}}^{\text{air}}, R^{\text{air}}, u^{\text{air}}, B^{\text{air}}, C_L^{\text{air}}, \ldots, S_{\text{inter}}, E_{\text{transfer}}, D\right] \tag{3.12}$$

$$S_{sea} = \left[d_{\text{avg}}^{\text{sea}}, R^{\text{sea}}, u^{\text{sea}}, B^{\text{sea}}, C_L^{\text{sea}}, \ldots, S_{\text{inter}}, E_{\text{transfer}}, D\right] \tag{3.13}$$

This state vector captures both mode-specific resilience and intermodal interactions. The state vector can be effectively applied in an example involving agents and carriers in intermodal transport. The structured approach demonstrates its application through an example scenario: A logistics company (agent) needs to ship number of ITUS from node A to node B using intermodal network. They have two potential routes:

1. Route 1: Truck (road) to port X, then ship to port Y, then train (rail) to node B.
2. Route 2: Truck (road) to terminal Z, then train (rail) directly to node B.

Example route evaluation:

Route 1 Evaluation:

Redundancy: Higher redundancy in road segments offers backup options. Capacity utilisation: Lower utilisation reduces the likelihood of delays. Transfer Efficiency: High efficiency at Port X ensures smooth transitions. Interdependency: Reliance on three modes (road, sea, rail) increases vulnerability if any mode is disrupted.

Route 2 Evaluation:

Simplicity and Stability: Uses only two modes (road and rail), reducing interdependency risks. Connectivity: High connectivity between nodes suggests reliable transport. Redundancy: Lower redundancy in rail segments may pose risks during disruptions.

Decision Outcome:

Based on the state vector analysis, the logistics company might prefer Route 2 for its simplicity and lower interdependency, offering more stability. However, if the primary concern is redundancy and transfer efficiency, Route 1 could be more resilient despite higher complexity. The state vector provides a comprehensive framework for agents to evaluate transport routes dynamically, considering various factors like connectivity, redundancy, capacity, and interdependencies. This approach enhances decision-making by optimising routing and risk management in intermodal transport networks.

Algorithm 3.1 Impact area Vulnerability index ([78])

Transport network $G = (N, L)$, impact radius η
Vulnerability index VUL_a for each link $a \in L$
for each link $a = (u, v) \in L$ $G_a \leftarrow$ subgraph centered at u with radius η
$E_0 \leftarrow \sum_{i \neq j \in G_a} \frac{1}{d_{ij}}$
remove link (u, v) from G_a
$E_a \leftarrow \sum_{i \neq j \in G_a} \frac{1}{d_{ij}}$
$\mathrm{VUL}_a \leftarrow \frac{E_0 - E_a}{E_0}$
return All VUL_a, sorted descending

To analyse the importance of node performance within an intermodal network, some of the measures for quantifying centrality measures are node degree, node betweenness, and node closeness which can be implemented using Python's networkx library. For one node criticality estimation, city of Zürich is chosen because of its geographical position as a central node and high volume of freight in transit (Figure 3.5). *Degree centrality* measures the number of connections a node has. In a network graph, it's the fraction of nodes a particular node is connected to. Zürich scores 0.53, as it directly connects to a significant portion of the nodes. Degree centrality for Zurich when all outgoing edges are removed because of the disruption drops significantly to value of 0.11. *Betweenness centrality* quantifies the number of times a node acts as a connection along the shortest path between two other nodes. In the original graph, Zürich had several connections to other nodes, meaning it served as a critical intermediary for shortest paths between node pairs. Its removal significantly disrupts connectivity and forces longer alternate routes. The drop in betweenness centrality from 0.66 to 0 for Zürich occurs because betweenness centrality measures a node's role in facilitating communication or flow between other nodes in the network, as it can no longer mediate between any other nodes in the network. *Closeness centrality* reflects how close a node is to all other nodes in the network. It's the reciprocal of the sum of the shortest path distances from the node to all others. Zürich has shorter paths to most nodes due to its extensive connectivity. When isolated, the value drops from 0.5 to 0.

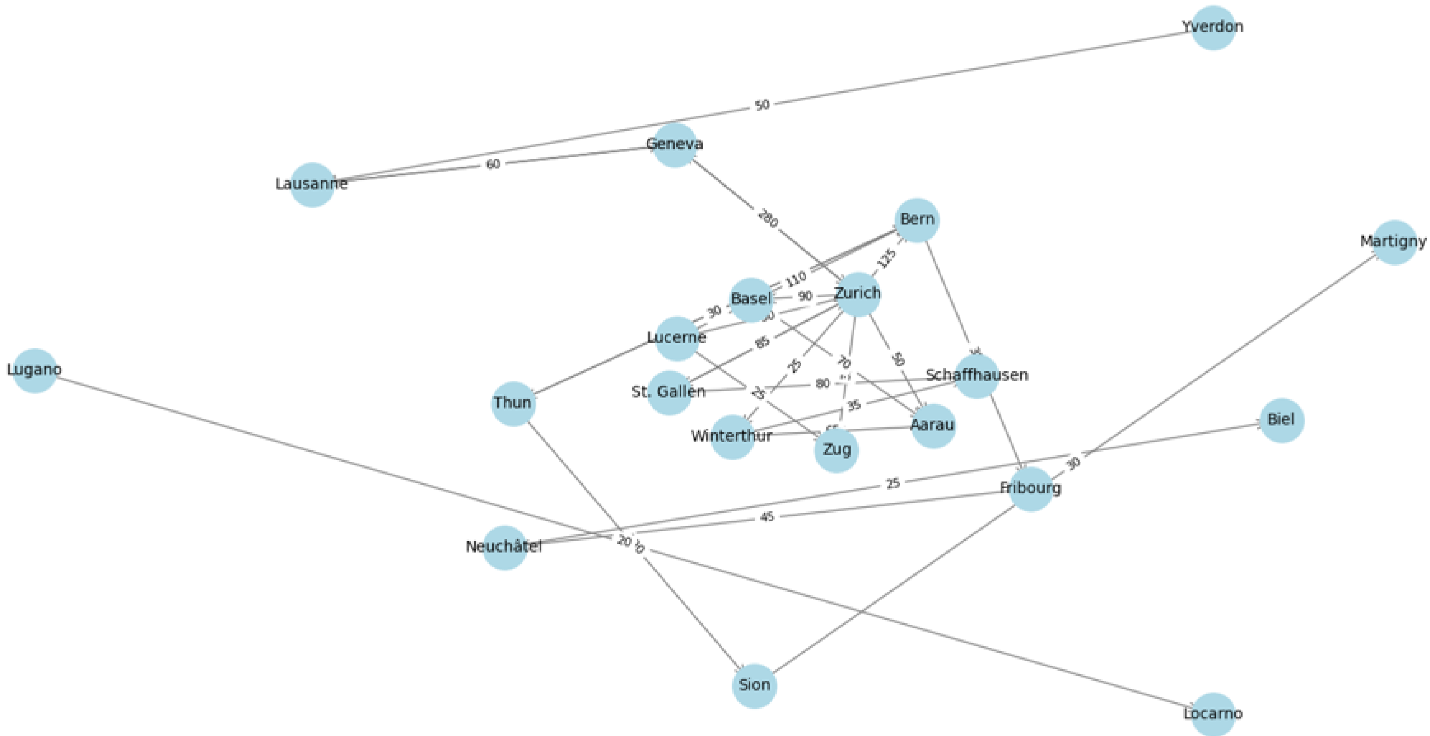

Figure 3.5: Structure of distance weighted graph for Zürich with unreachable nodes handled.

3.2.1 Joint network interdependencies

Transport networks are constrained geographically, so this interdependence is essential. Geographical interdependence occurs when elements are in close spatial proximity but they don't influence the condition of another element. For example, derailment in close proximity to an intermodal terminal causes the closure of that route for all trains. The process of cleaning the site, as in terms of recoverability takes too much time as costs of unoperability are increasing. Two major incidents happened in Croatia at the end of 2023. The first one was a derailment caused by a braking failure in Škrljevo, near seaport Bakar resulting in the closure of the railway route for two weeks. The second was a German cargo ship collision into the road bridge above the inland waterway, which also serves as an approach direction to the border crossing point. The ship hit a pillar of the bridge between Ilok and Bačka Palanka and in that impact, the bridge was damaged, and one barge with 1.000 tons of artificial fertilizer sank. Inland and road traffic were stopped until recovery was done, causing delays, congestion and excess costs. Thus, the concept of geographical interdependence is used for the creation of a multi-layered network where road and rail networks have an overpassing point. The interconnected transport system can be transformed into a complex $n \times n$ adjacency matrix. Rows and columns represent nodes (*i,j*) and three types of links exist between nodes. Those are roads, rails and interconnected terminals (representing seaports). Each entry or cell in a matrix can take values as follows [58]:

$$\omega_{ij} = \begin{cases} r & \text{if } (i,j) \text{ is a road link} \\ t & \text{if } (i,j) \text{ is a railway link} \\ p & \text{if } (i,j) \text{ is a port or terminal} \\ 0 & \text{otherwise} \end{cases} \tag{3.14}$$

The result is a squared matrix whose elements can take values of 0, *r, t,* or *p*, where 0 indicates no connection, *r* road connection, *t* railway, and *p* represents the connection between two nodes at the intermodal terminal, that is a node where manipulation of shipping containers is done. The next step is to construct a multi-layered graph to analyse the topological vulnerability of the transport system. The measure of efficiency that considers the shortest path between each pair of nodes is expressed in the following equation.

$$E = \frac{1}{(v-1)} \sum_{ij \in V, i \neq j} \frac{1}{d_{ij}}, \tag{3.15}$$

where distance is infinite if the pair of nodes is in different components of the network and its contribution to the sum is zero, on the other hand, it gives greater weight to a pair of nodes that are closer in proximity. That efficiency loss is then:

$$\Delta(Y) = \frac{E(Y) - E(Y-1)}{E(Y)}. \tag{3.16}$$

Further investigation of the criticality of each network element needs to add two more relevant parameters or measures. If one node is removed, it leads to disconnection from the main transport cluster and reduces the accessibility of the region served by this network. All removed nodes or cut vertices can be considered as critical locations where the incident happened. The measure that reflects the node connection ability is betweenness centrality. The vertex betweenness is defined by the number of shortest paths going through a vertex. [58]

Next, to present the Q-learning table update, an example of a transport network with 11 randomly connected intermodal nodes of European corridor is used. It represents the one layer or one mode of transport in the network. Every iteration of the next network generation makes different connection vertices and link weights, with cumulative reward. Rewards are obtained from finding better transport plans with minimal costs. The result of this simulation with the initial Q-table set with only zeros, and trained q-table in Table 3.2. After revising all the nodes in the network is a combination of visiting the nodes: Rijeka → Koper → Trieste → Venice → Verona → Ljubljana → Zagreb → Budapest. After training the Q-table, it results in a most efficient path which is [0, 1, 2, 3, 4, 5, 6, 9].

Table 3.2: Trained Q-table for the 11-node intermodal network

	Rijeka	Koper	Trieste	Venice	Verona	Ljubljana	Zagreb	Graz	Vienna	Budapest	Bratislava
Rijeka	0.00	-0.43	0.00	0.00	0.00	-0.75	-1.00	0.00	0.00	0.00	0.00
Koper	-0.55	0.00	-0.31	0.00	0.00	0.00	0.00	0.00	0.00	0.00	0.00
Trieste	0.00	-0.31	0.00	-0.82	0.00	0.00	0.00	0.00	0.00	0.00	0.00
Venice	0.00	0.00	-0.58	0.00	-0.97	0.00	0.00	0.00	0.00	0.00	0.00
Verona	0.00	0.00	0.00	-0.78	0.00	-1.26	0.00	-1.75	0.00	0.00	0.00
Ljubljana	-0.60	0.00	0.00	0.00	-1.43	0.00	-0.95	-1.09	0.00	0.00	0.00
Zagreb	-0.73	0.00	0.00	0.00	0.00	-0.84	0.00	0.00	0.00	-0.77	0.00
Graz	0.00	0.00	0.00	0.00	-1.70	-0.88	0.00	0.00	-0.84	0.00	0.00
Vienna	0.00	0.00	0.00	0.00	0.00	0.00	0.00	-1.13	0.00	0.00	-0.52
Budapest	0.00	0.00	0.00	0.00	0.00	0.00	0.00	0.00	0.00	0.00	0.00
Bratislava	0.00	0.00	0.00	0.00	0.00	0.00	0.00	0.00	-0.59	-0.42	0.00

Figure 3.6 presents the reward progression over iterations for an agent navigating a transport network of 11 randomly connected nodes. The figure shows the training performance of the Q-learning agent on the 11-node intermodal network. The blue curve represents the total reward obtained in each episode, which fluctuates heavily in early iterations due to exploration. The orange moving average smooths these variations and reveals a clear upward trend, indicating that the agent gradually learns to select more cost-efficient routes through repeated interactions. After roughly 500 episodes, the curve stabilises near a steady reward level, suggesting policy convergence toward optimal or near-optimal routing decisions across the intermodal network.

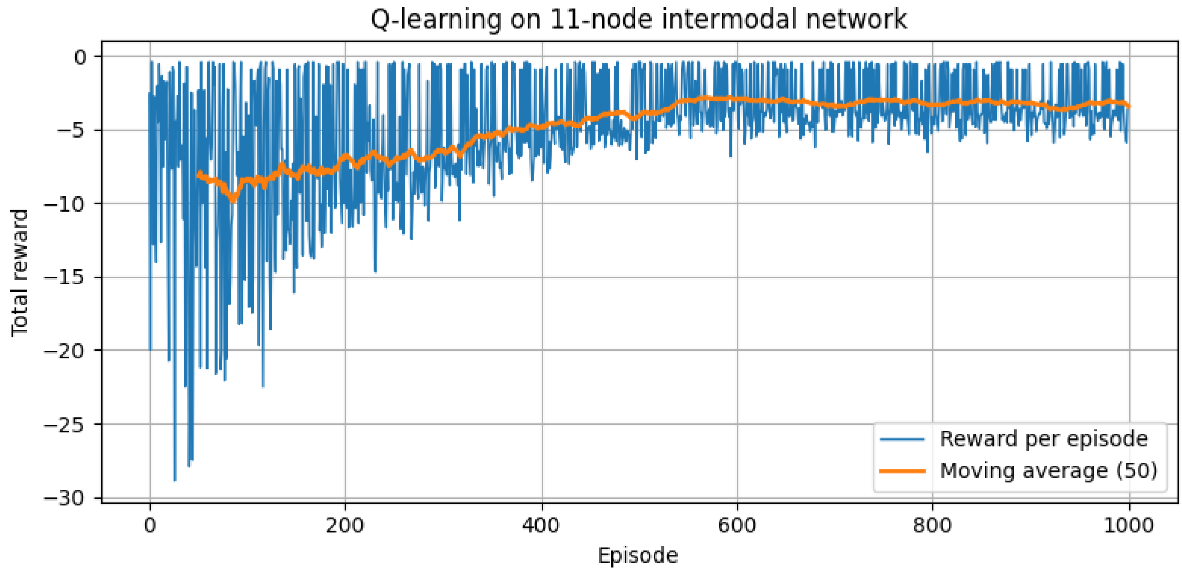

Figure 3.6: Training performance of the Q-learning agent on the 11-node intermodal network.

The initial SARSA implementation was tested on an 11-node synthetic intermodal network representing a single transport layer (Figure 2.27). Each episode consisted of agent exploration through randomly connected nodes, with link weights corresponding to transport costs and congestion penalties. Training was repeated for 1000 episodes.

Table 3.3: SARSA performance statistics on the 11-node network

Metric	**Mean reward**	**Reward variance**	**Convergence episode**
Baseline (initial)	64.2	22.5	780
Trained (stabilised)	91.7	6.4	340

This example introduces uncertain or stochastic edge costs (travel time following uniform or geometric distributions). This makes learning more complex as the agent must learn expected values for each state-action pair, and matches real-world freight transport, where delays and route disruptions occur probabilistically.

In multi-layered intermodal settings, the same reward structure is extended in a way that each modal shift introduces new state transitions and costs. Rewards must account for modal interchange penalties, transfer times, and resilience of each layer. The Q-table will adapt accordingly, optimising paths not only across space, but also across modes.

To form a multi-layered network with the aim of analysing robustness, it needs to be compared with the single-layered type of network. To incorporate the connection between the layers, the concept of functional interdependency must be observed. For instance, in functional interdependency or interconnection, road exits and railway stations are connected in each main location in the region (cities), assuming the possibility of a modal shift. Many problems involve the movement of resources over networks. Construction of the intermodal graph where links correspond to places where the modal shift can take place, assuming that each road exit is connected to the closest railway terminal with an interchange point. The definition of the state of a single resource, however, can be complicated by different assumptions for the probability distribution for the time required to traverse a link. For this example, given the state of the resource:

- A deterministic, static network, and we want to find the shortest path from an origin node q (0) to a destination node r (10). There is a known cost c_{ij} for traversing each link *(i, j)*.
- Next assume that the cost c_{ij} is a random variable with an unknown distribution. Each time we traverse a link *(i, j)*, the cost $\widehat{c}_{ij}$ is observed, which allows us to update your estimate $\bar{c}_{ij}$ of the mean of c_{ij}.
- Finally assume that when the freight arrives at node i he sees $\widehat{c}_{ij}$ for each link *(i, j)* out of node i.
- A transport truck is moving freight in a set of locations C. After dropping a container off at location i, the agent may have to decide to reposition the vehicle from i to j, *(i, j)* $\in C$. The travel time from i to j is τ_{ij}, which is a random variable with a discrete uniform distribution (that is, the probability that $\tau_{ij} = t$ is $\frac{1}{\tau}$, for $t = 1, 2, ..., T$). Assume that the travel time is known before the trip starts.
- Same as previous, but now the travel times are random with a geometric distribution (that is, the probability that $\tau_{ij} = t$ is (1 - $\theta)\theta^{t-1}$, for $t = 1, 2, 3, ...$). [103]

3.2.2 Performance metrics

The system performance of the transport network is quantified by the weighted summary of mode transitions' average number of reliable independent pathways, i.e., the weight of each transition and the average number of reliable independent paths through that mode shift. The weight of each transition is determined by its location. The average number of reliable independent pathways is determined by the independent paths, traffic flows, and infrastructure reliability of each segment. For instance, road reliability can be used to indicate the road's damaged condition. Traffic flow is an important component of the resilience quantifying process. However, because of the simplicity required for this study, as well as the lack of support for post-hazard traffic data, this parameter is ignored. The framework is still applicable considering that the influence of traffic flow can be represented by the value of the average number of reliable independent pathways of each node. The weight of each mode transition for this use case is determined by its distance to the nearest response facilities (in Eq 3.17). The original criteria are modified to avoid a large weight value when the shortest distance is much smaller than 1.

$$w_i = \frac{\Omega_i}{\sum_{j=1}^{n} \Omega_j} \tag{3.17}$$

$$\Omega_i = \begin{cases} \frac{1}{min(D_i)} & min(D_i) > 1km \\ 1 & min(D_i) < 1km \end{cases} \tag{3.18}$$

where w_i is the transition's weight, D_i is the distance set of transition i to the pre-defined respond facilities or terminals; Ω_i is the reciprocal of the distance between node i and its nearest response facility or terminal. When the distance is less than 1 kilometre or the transition itself is done at the terminal, Ω_i equals 1. At any period of time t, an average number of reliable independent paths of the transition i is determined by following Eq.

$$r_i = \frac{1}{n-1} \sum_{j=1, j \neq i}^{n} \sum_{k=1}^{K_{(i,j)}} v_k(i,j) R_k(i,j), \tag{3.19}$$

where $R_k(i,j)$ is the reliability of the k^{th} independent path, $v_k(i,j)$ is the weight k^{th} independent path. The transition's average number of reliable independent pathways is determined based on independent pathways' reliability and weight between any origin-destination (O-D) pairs. Mathematically, for any independent pathway between changing modes i and j, its independent pathways' reliability $R_k(i,j)$ can be determined by Eq.

$$R_k(i,j) = \prod_{\forall l \in P_k(i,j)} R_l \tag{3.20}$$

The weight of k^{th} independent path through mode transition can be determined by Eq.:

$$v_k(i,j) = \frac{L_{max(i,j)}}{L_{Pk}(i,j) \cdot \Sigma_{k=1}^{K(i,j)} (\frac{L_{max(i,j)}}{L_{Pk(i,j)}})} \times K(i,j) \tag{3.21}$$

where $R_k(i,j)$ is the reliability of the k^{th} independent path. l is the road segment that belongs to the independent path and R_l is its reliability after the incident happened. $v_k(i,j)$ is the weight of k^{th} independent path. $K_{(i,j)}$ is the number of all independent paths between node i and j. $L_{max(i,j)}$ is the maximum length and $L_{pk(i,j)}$ is the k^{th} length. With the weight of each transition and the average number of reliable independent paths through each transition is determined, and the system resilience metric is derived from performance in Eq.

$$p(t) = (\sum_{i=1}^{n} w_i r_i) \times 100\% \tag{3.22}$$

where $p(t)$ is the performance of the alternative transport network at time t, r_i is the average number of reliable independent pathways; w_i is the important weight of each node i. [104]

After the disruption occurs, it is supposed that the network can reach another stable state during each time slot. The maximum impact cannot be reached at the same moment of disruption, which is reasonable due to the continuity and the nature of lagged traffic propagation. As the real network performance during timeslot k may be unstable or even unknown, the results at the new equilibrium state are selected for reference purposes. The functional resilience (FR) is jointly affected by the targeted network index (x), the stable travel demand in the k-th timeslot D_s^k, and the disruption d. The disruption d can be from the supply side, demand side, or both occurring in different time slots. The FR dimensions may also be dynamic with respect to t. A general expression of FR is written as $\mathbb{R}(x,D_s^k,d,t)$. To better capture a transport network's responses to disruption, we discern the difference between structural resilience (SR) and FR. The main difference between SR and FR resides in the dynamic demand-supply interactions that occur on the network. [82], [75], [81] Figure 3.7 shows a generic time-dependent resilience plot for an increasing service system (the dependent variable increases as service increases) undergoing a disruptive event. The below example provides a scheme of the same system with a decreasing service system (the dependent variable decreases as service increases) experiencing a disruption). [105]

The measurements of the three dimensions of FR are formulated as follows [70]:

Robustness (denoted by R_1) is to measure G's capacity surplus under D_s^k and d during time slot k. With targeted network index x, the general expression of robustness at time point t is written as Eq. 3.23. The larger R_1 is, the more capacity surplus the network has and the more resilient it is.

$$R_1 = \mathbb{R}(x,D_s^k,d,t), k \in [1,K] \tag{3.23}$$

Adaptability (denoted by R_2) is to measure G's changing capacity to adapt to disruption d under D_s^k during time slot k. With the same x, the general expression of adaptability is written as Eq. 3.24. $\mathbb{R}(x,D_s^k,0,t)$ stands for the network performance only with D_s^k at stable state 1, where d = 0 means no disruption. The smaller R_2 is, the stronger adaptability the network has to the disruption and the more resilient it is.

$$R_2 = \mathbb{R}(x,D_s^k,0,t) - \mathbb{R}(x,D_s^k,d,t), k \in [1,K] \tag{3.24}$$

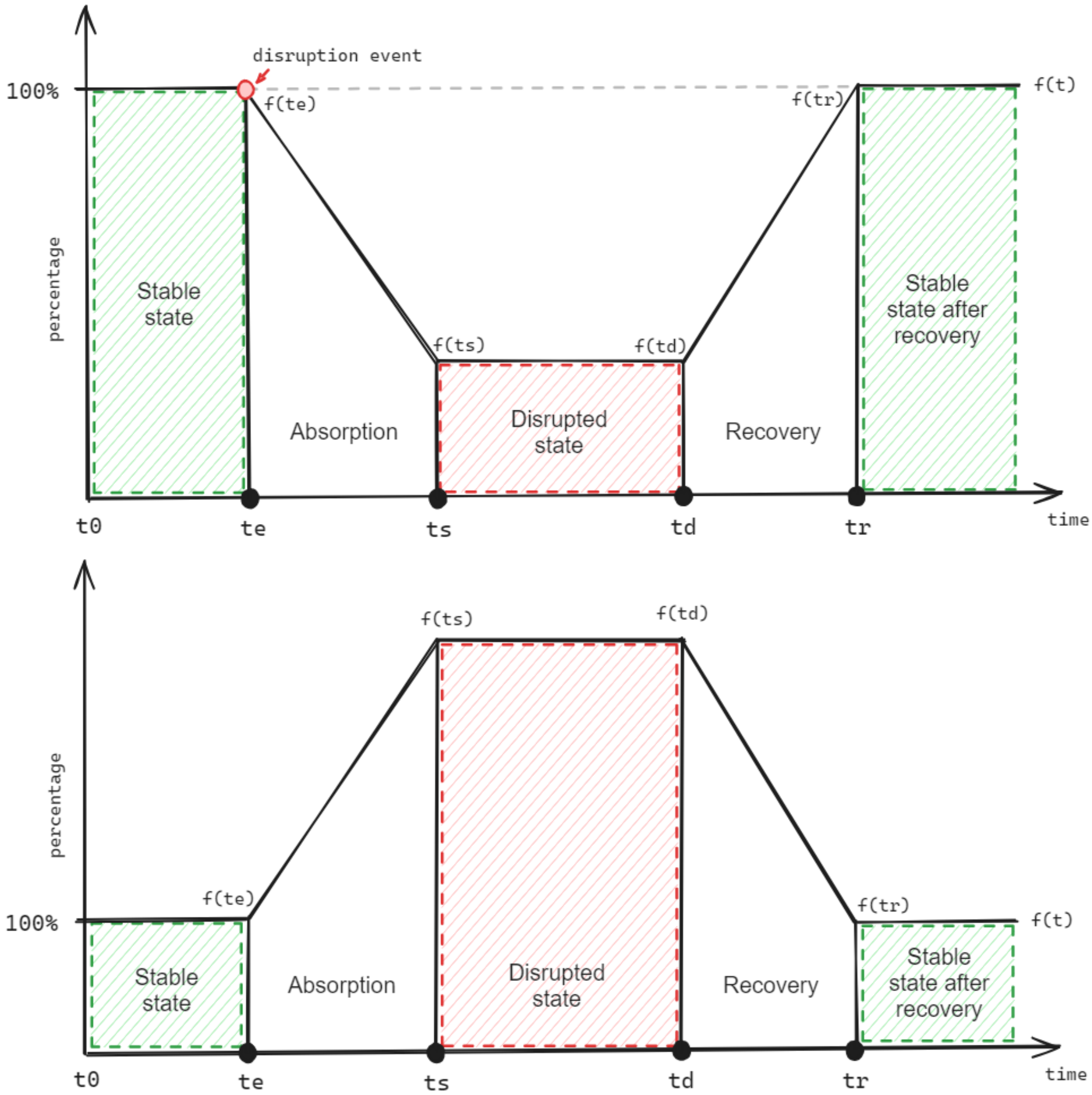

Figure 3.7: Time-dependent plot of increasing and decreasing service system experiencing disruption event.

Recoverability (denoted by R_3) is to measure G's cumulative capacity loss from disruption d under D_s^k during the time frame between t_b^1 and t_f^K. Compared to [68] who used a shaded triangle area to measure a network's resilience, here is a generalized form, shown in Eq. 3.25, to measure the recoverability of FR. The smaller R_3 is the smaller the effects that the disruption causes to the network, standing for higher recoverability.

$$R_3 = \int_{t_b^1}^{t_f^K} [\mathbb{R}(x,0,0,t) - \mathbb{R}(x,D_s^k,d,t)]dt, k \in [1,K] \tag{3.25}$$

The adaptability aims to quantify the capacity change due to the disruptions, but D_s^k may also decrease the network capacity, which is not attributed to the disruption [64], [92]. Therefore, the second dimension of adaptability is not redundant. Also note that when the length of time slot k approaches zero, it appears that FR can capture the real-time dynamic process on the network. However, the network may not reach a new equilibrium state at the end of the time slot of interest, which causes the incapability of measuring the recoverability dimension. Therefore, the length of time slot k is set long enough for the network to reach equilibrium after the disruption. With this consideration, the results at the new equilibrium state are preferably used as the resilient performance, although the measurements of FR are formulated in fully dynamic forms. It should also be noted that if $D_s^k = 0$ and time t is removed in Eqs. 3.23-3.25, the generalised formulations of FR degenerate into those of SR. A measurement framework for operationalisation in the context of trip-based freight demand analysis. The framework consists of network configuration, traffic dynamics, disruption, the new equilibrium state, and three FR dimensions according to the targeted index, i.e. the resilience parameter. The framework is depicted in Figure 3.8. First, *G(V, E)* is constructed based on the spatial structure and the static and dynamic attributes of the nodes and edges. Second, given the freight demand in different time slots of an average work day, traffic dynamics on the network take place in the presence of direct and indirect disruption. According to the traditional four-step models, this module includes trip generation, trip distribution, modal split, and traffic assignment. In response to disruption, the congestion effects or failure rules are applied to the traffic assignment. The disruption effects are not considered in the first three steps. Traffic assignment is to determine the network flow patterns with regard to travel demand and network supply interactions. The network may be congested or even blocked to lose functions. [70]

3.3 Achieving demand and supply resilience

Traditional congestion models for transport networks often rely on static parameters such as average travel time, distance, or link capacity. However, these metrics fail to account for structural weaknesses in intermodal infrastructure, such as the vulnerability of key terminals under disruption, asymmetric flow capacities, or imbalance in demand-supply flows. To address this, a new resilience parameter was proposed.

The parameter integrates these metrics in a combined structure incorporating robustness of the node, and times to recover and adapt:

- Capacity entropy (to reflect node importance in supply distribution)
- Demand entropy (to capture flow distribution among connected nodes)
- Flow imbalance (as a vulnerability entropy measurement)
- Time-to-Survive (TTS) comparisons (for empirical validation)

This parameter quantifies how well a node or subnetwork can absorb and recover from disrup-

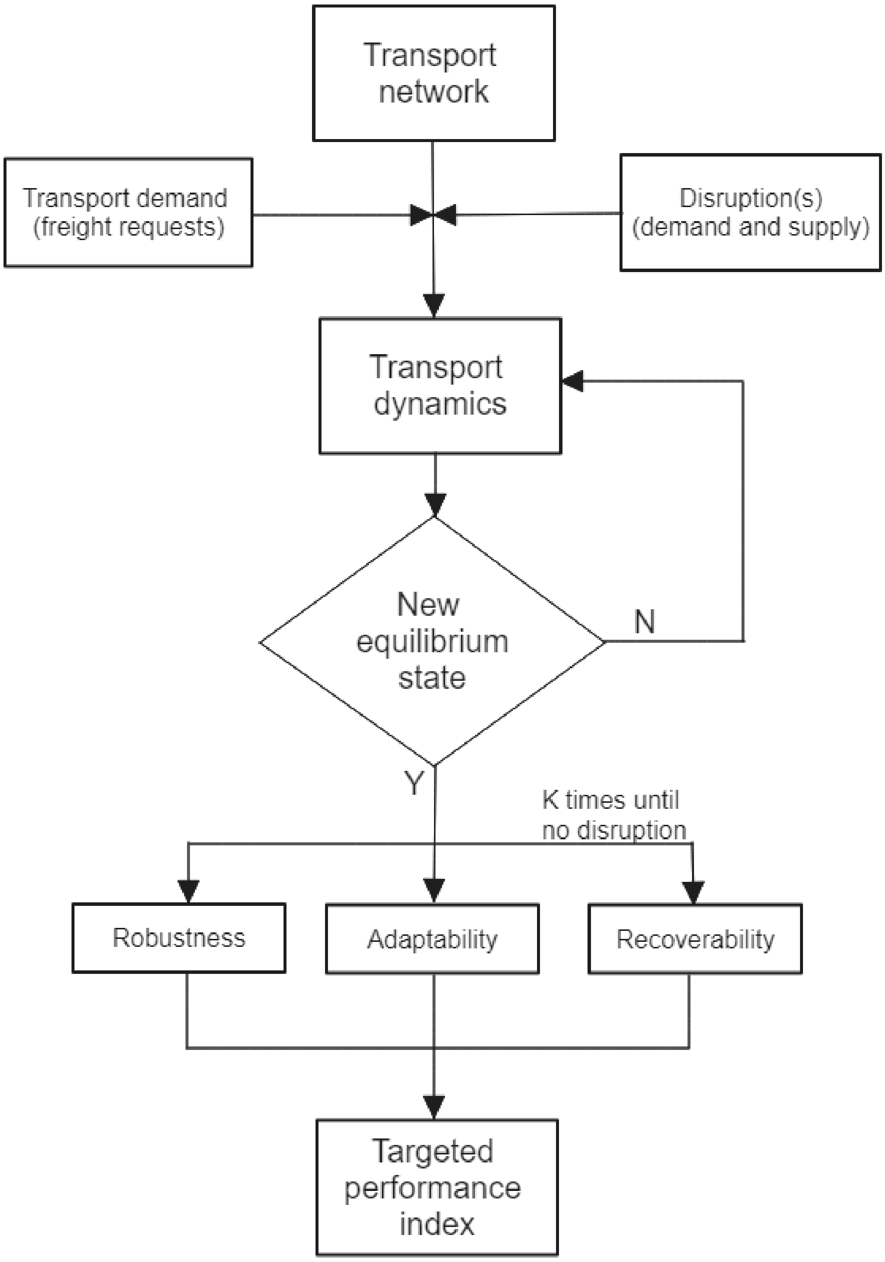

Figure 3.8: Framework for quantifying functional resilience.

tions, and uses that in route decisions.

Even supply chains with organised processes will hit unexpected disruptions or can be impacted by events that are impossible to predict. Therefore, it is critical that resilience is built into those systems. To incorporate that resilience into the supply chain side, four strategic approaches are used [106]:

Supply chain engineering and re-engineering

The risks in supply chains are systemic, meaning that they're present because of the systems' design. Many past decisions shaped the current transport chains with production centralisation or freight consolidations into bigger/regional distribution centres. Overall costs decreased but system design should avoid reliance on a single facility or source of supply. The cost savings from centralisation and consolidation with the resulting risk is highlighted in Figure 3.9. Even

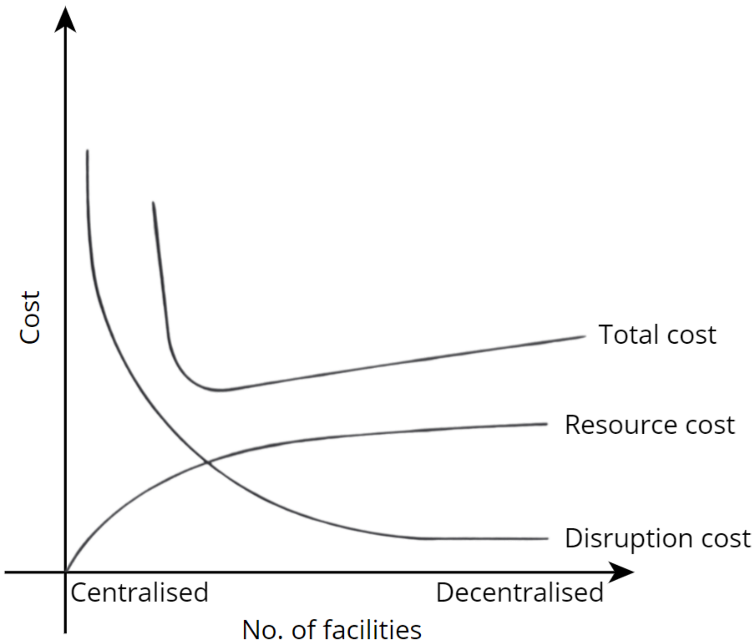

Figure 3.9: Costs of centralised and decentralised facilities

though system costs increase with the number of facilities (or inventories), the associated risk cost decreases. To create a more resilient system, organisations need to ensure the understanding of their architecture and their current supply and demand network. This is facilitated by a detailed mapping of the network with current status, location of specific bottlenecks, removing unnecessary complexity and mitigating disruptions. Figure 3.10 provides an example of suppliers, and agents in times of major disruptions where stakeholders need to make decisions based on shared payoffs. This real-world example is solved in the last chapter (5).

Collaboration in supply chains

A key driver of resilience is a high level of collaboration between supply chain stakeholders because of the interdependencies that exists globally. Visibility and shared information are fundamental for the development of resilience, that's why creating a collaborative environment is so critical. Effective event management will only be possible if there is a willingness amongst stakeholders to share that information. Intelligence of the supply chain systems can be enhanced if the stakeholders are willing to negotiate and poll their knowledge or insights concerning possible sources of risk in the wider supply-demand network. It should comprise key upstream and downstream entities in the network to regularly review risk profiles and to agree on risk mitigation strategies.

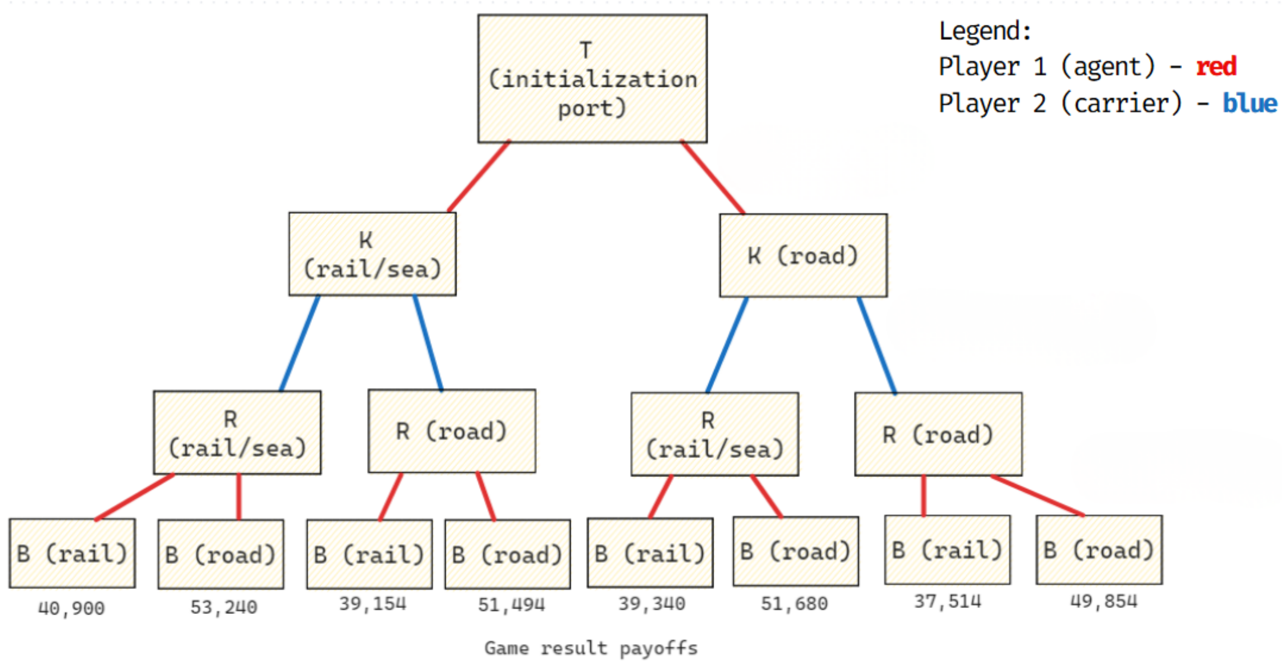

Figure 3.10: Schematic example of agents and carriers payoffs in seaport and road/railway distribution

Risk management

The company board should review regular reports on the risk profile of the business and its supply and demand network. Every supply chain today is very dependent upon information systems and communication technologies that drive many supply chain activities. As a result, the opportunity for malicious attacks and strengthening cybersecurity is much greater. Sharing information across boundaries is a prerequisite for effective management, which provides more points of entry for those with the intention of attacking.

Recoverability and agility

A general idea of a resilient transport system is about being able to bounce back quickly when disruption happens, it is apparent that the more agile the supply chain is, the quicker it's likely to recover. Two of the most critical resilience enhancers are visibility and velocity. Visibility enables organisations to see things sooner and velocity reduces the time to respond to unexpected events. The structural flexibility is the ability of the system to adapt quickly to new conditions. Many traditional supply chains are too rigid because of previous decisions that have locked the company into arrangements that are hard to change. If resilience is to be improved, then every decision that is made should be stored and screened in terms of how many options this decision provides. The implication is that the best decisions in an uncertain world are those decisions that keep the most options open. [106]

To enhance the robustness of route selection in intermodal networks, a resilience parameter is proposed, integrating both structural and functional aspects of node vulnerability. This parameter extends the entropy-based metric by incorporating the three core dimensions of functional resilience: robustness, adaptability, and recoverability. The robustness component $R_1(i)$ measures the capacity surplus of node i during a disruption scenario d at a specific time slot k, reflecting the network's ability to absorb increased load or reduced serviceability. Adaptability $R_2(i)$ quantifies the immediate performance degradation by capturing the difference in network performance before and after disruption, where a smaller value indicates a more adaptive and flexible response. Recoverability $R_3(i)$ represents the cumulative capacity loss over time, calculated as the integral of performance degradation between the beginning and end of the disruption interval. Together, these components are combined with the original entropy-based resilience term, which measures the imbalance and concentration of flows around a node using the ratio of demand entropy to network-wide capacity entropy. The composite resilience parameter $R(i)$ of a node is thus expressed as a weighted sum of all four components:

$$R(i) = w_1 \cdot R_1(i) + w_2 \cdot R_2(i) + w_3 \cdot R_3(i) + w_4 \cdot R_{\text{entropy}}(i), \tag{3.26}$$

where the weights w_1, w_2, w_3, w_4 reflect the relative importance of each dimension and can be empirically calibrated. Each dimension, or layer in a multi-layered graph structure represents different transport mode system, with appropriate weights defining the operational ratio of the transport mode. This formulation enables the integration of both static vulnerability and dynamic recovery characteristics, making the resilience parameter a powerful input for congestion-aware routing models and reinforcement learning-based cost prediction systems. Evaluation of the composite node resilience $R(i)$ for the NAPA ports under congested transport network modelling using the weighted formulation:

Table 3.4: Input parameters for resilience calculation of NAPA ports

Port	**Capacity** [TEU]	**Demand** [TEU]	**Recovery** [days]	**Modes**	R_{entropy}
Rijeka	650,000	480,000	3	Road, Rail, Sea	0.76
Koper	1,000,000	950,000	2	Road, Rail, Sea	0.91
Trieste	800,000	790,000	5	Road, Rail, Sea	0.88
Venice	550,000	530,000	4	Road, Sea	0.69

Koper scores the highest resilience due to high adaptability, high entropy (meaning balanced flow), and rapid recovery. Venice has the lowest resilience, impacted by limited modal flexibility and longer recovery. This metric will be used in RL reward shaping (penalising low ($R(i)$) during policy learning) and in congestion game, it adds the resilience-weighted costs.

Table 3.5: Composite resilience parameter $R(i)$ for NAPA ports

Port	$R_1(i)$	$R_2(i)$	$R_3(i)$	$R_{\text{entropy}}(i)$	$R(i)$
Rijeka	0.2615	0.3333	1.0000	0.76	0.6336
Koper	0.0500	0.5000	1.0000	0.91	0.6920
Trieste	0.0125	0.2000	1.0000	0.88	0.6028
Venice	0.0364	0.2500	0.6667	0.69	0.5023

3.3.1 Intermodal transport optimisation through mathematical modelling and node criticality

In delivery services, many different transport modes, such as trucks, airplanes, and ships, are available. Different choices of routes and transport modes will lead to different costs. To minimise costs, freight consolidation should be considered (e.g., occasions when different container share a journey together), as well as different transport costs and delivery time constraints. Use of mathematical programming to model such situations and solving it for an overall cost minimisation is performed in Chapter 2. To analyse the importance of node performance after removal within an intermodal network, common graph-based centrality metrics are calculated including *degree*, *betweenness*, and *closeness* centrality on a subnetwork of 15 nodes in Zürich corridor. These indicators are implemented to quantify the influence of specific nodes on overall network functionality. For a focused criticality estimation, the city of Zürich is chosen due to its geographical location and structural role as a highly central node. Among all DC locations, Zürich demonstrates the highest percentage drop in total freight throughput resulting from node failure in a subnetwork (in Figure 3.11), indicating its vulnerability through Critical Node Index (CNI). It is calculated by comparing the total amount of freight successfully routed in the original network versus the disrupted subnetwork where that node is removed. *Degree centrality* measures how many direct connections a node has in relation to the total number of nodes in the network. Zürich corridor connects directly to 8 suppliers out of 15 total nodes, yielding a degree centrality of 0.53. Although the complete intermodal network includes 45 nodes, a focused subnetwork of 15 nodes was extracted for in-depth analysis of the Zürich area. This localised view captures DCs and terminals within a high-traffic corridor, allowing for more detailed examination of node-level disruptions and operational consequences. When all its outgoing connections are removed due to disruption, this value drops significantly to 0.11, highlighting its diminished reach within the network. *Betweenness centrality* captures how often a node acts as a bridge along the shortest paths between other node pairs. Zürich's betweenness value of 0.03 indicates its role as an intermediary hub in numerous shortest routes. Zürich's betweenness centrality value of 0.03 may appear low due to the scale and density of the subnetwork. In real-world intermodal networks, freight flows are concentrated on a few corridors. Thus, even modest betweenness values can correspond to disproportionately high volume concentrations and vulnerability. Moreover, the simulation results show that Zürich's removal causes rerouting and flow reduction, which traditional betweenness alone fails to capture. Upon removal, this metric drops to 0, since Zürich no longer contributes to any indirect connectivity. This emphasises how critical the node is in maintaining network coherence and minimising rerouting distances. *Closeness centrality* expresses how near a node is to all other nodes based on shortest path distances. With a score of 0.68, Zürich is relatively close to all other suppliers and warehouses, offering efficient intermodal routing. Once isolated, the closeness centrality drops to 0, reflecting complete loss of access to the rest of the network. To capture both topological and operational aspects of node importance in intermodal networks, a hybrid node criticality assessment framework is proposed. This method integrates classical graph-based centrality with a congestion-aware intermodal transhipment model that accounts for costs, emissions, terminal capacities, and rerouting delays with following steps:

1. **Topological evaluation:** Computing traditional centrality measures for each node using the NetworkX library.
2. **Transhipment simulation:** For each node, simulate its removal and re-optimise freight allocation in a subnetwork using the intermodal transhipment model solved via Gurobi.
3. **Flow-based metrics:** Quantify disruption impacts using:
   - **Critical Node Index (CNI):** Percentage loss of overall network performance.
   - **Average Path Length Increase (APLI):** Change in mean travel time due to node failure.
   - **Network Flow Reduction (NFR):** Drop in total delivered freight volume to DCs.
4. **Integrated scoring:** Combine the topological and operational scores to rank node criticality.

The proposed method integrates subnetwork structure with the outputs of the intermodal transhipment problem. Table 3.6 presents a comparison of results. The proposed model achieves a higher Critical Node Index (CNI) of 68.2%, indicating that removing a critical node leads to a greater network disruption than in only topological methods. Similarly, the Average Path Length Increase (APLI) is 27.4%, showing that intermodal congestion impacts routing causing delays. The Network Flow Reduction (NFR) of 55.1% demonstrates that this model captures key bottlenecks in intermodal networks caused by the removal of a critical node. These criticality measures are crucial for modelling GAT, resilience parameter computation and validation of those models.

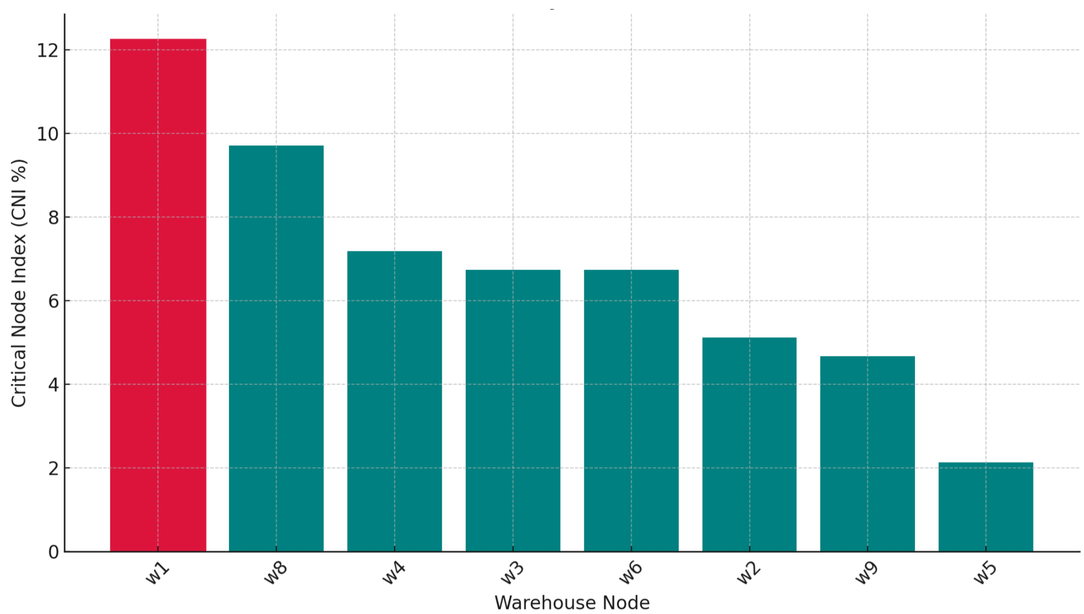

Figure 3.11: Warehouse node criticality measured by Critical Node Index (CNI) in the intermodal network. The most critical node is Zürich (w1).

Table 3.6: Comparison of node criticality methods

Method	CNI (%)	APLI (%)	NFR (%)
Betweenness Centrality (BC)	45.2	18.7	35.4
Closeness Centrality (CC)	38.5	15.2	29.8
Network Flow Model	61.4	23.5	48.3
Proposed Method	**68.2**	**27.4**	**55.1**

Source methods adapted from [49, 107, 108].

3.3.2 Estimating risk factors in drivers

To assign freight bookings, every consolidated booking of containers has an insurance policy to cover the expenses of possible damage in the transport process. That is important for assigning the more valuable cargo to experienced drivers. Estimation of risk factors is necessary in terms of collecting truck fleet data; Driver ID, total kilometres travelled in that vehicle, number of incidents, and timestamp of the event.

The main objective of estimating risk factors in drivers is to estimate a specific driver's safety score, for various transport scenarios. Additional use cases include driver identification, ecological scoring and theft detection by deviation from the routine driver behaviour. The dataset contains events of various types (behavioural or functional) stored in the EventName

Table 3.7: Freight truck drivers dataset and risk factors respectively.

	Driver_id	Events	Risk_factor	Model (Truck)	T_date	Truck_id	Total_Km
0	A1	3	4.773216	Freightliner	1.1.2015	A1	1011481
1	A2	1	1.504794	Ford	10.2.2015	A2	1069476
2	A3	6	9.381098	Ford	15.3.2015	A3	1029308
3	A4	6	9.045831	Kenworth	15.4.2015	A4	1067458
4	A5	9	13.302314	Hino	15.5.2016	A5	1088838

column (Fig. 3.13), in addition to metadata such as the current location (Latitude and Longitude columns), Speed km/h and time (ts column). DriverId is the unique identifier of a driver.

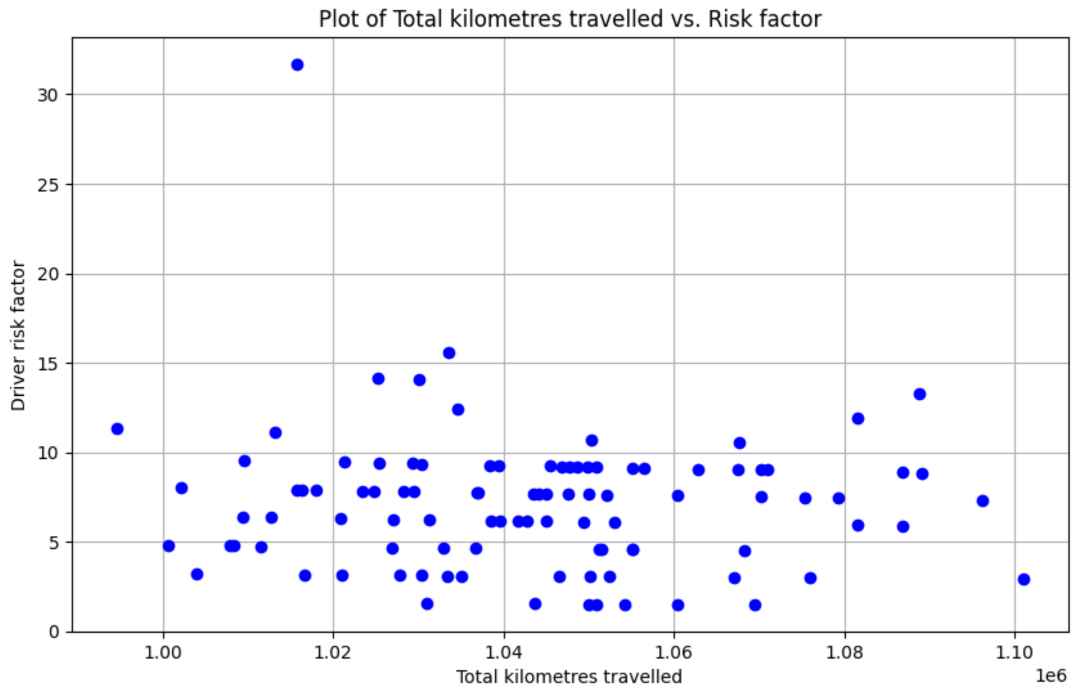

Figure 3.12: Risk factor of truck drivers in relation with total kilometres travelled.

The number of high speed start events is not equal to the number of events of end of high speed, which raises concerns. In addition, the calculation could be inaccurate since it compares the current driver speed with a constant (120 km/h) and not to the actual speed limit, so it is not used in the analysis. The correct approach is to use an API that provides road segment maximum speed, and compare the driver's speed to the maximum speed. These APIs also have the option of snap-to-road which eliminated errors due to inaccurate GPS readings. There are multiple events that represent the same thing. For example, Harsh Acceleration and Harsh Acceleration (motion based). This is due to different versions of the device, or to different sensors installed on different vehicles. The motion based device has three values for harsh turning: Harsh Turn, Harsh Turn Left and Harsh Turn Right. We can further see that Harsh Turn Left and Harsh Turn Right is not equal to Harsh Turn. This is due to the time in which each event type was introduced into the system. Harsh Turn is used and the left and right values are ignored. Since some drivers have more days of data on the system than others, looking at the absolute number of events isn't accurate. Instead, the number of events per driver is normalised by dividing with total drive time or total distance (in Figures 3.15 and 3.16). In this part, the total distance each driver had travelled is calculated.

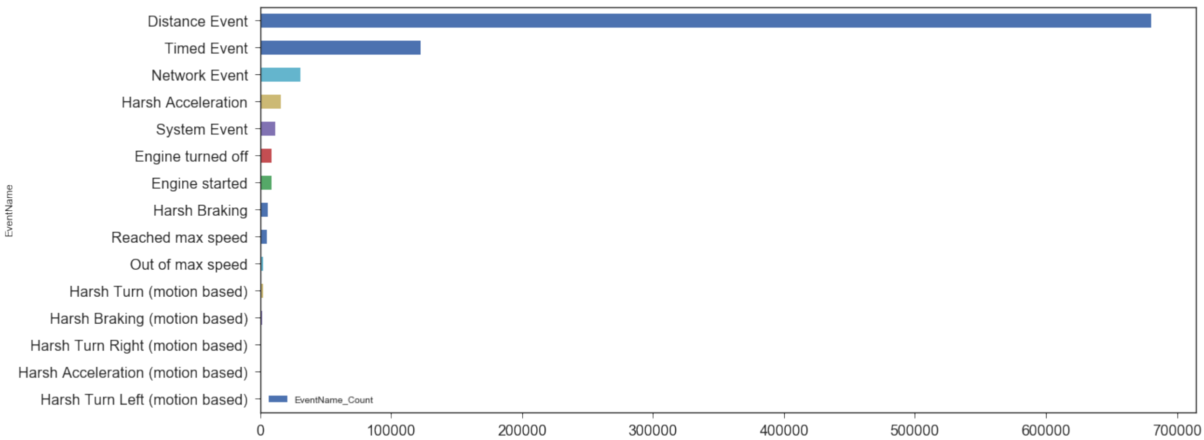

Figure 3.13: Count of the events recorded from the vehicles in a fleet.

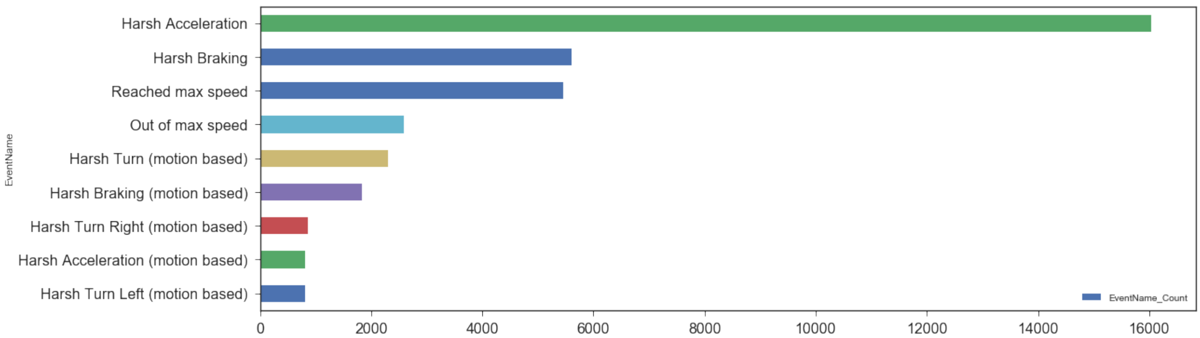

Figure 3.14: Count of the events recorded from the vehicle for the driver.

The feature set as the normalised number of events per type is defined. For each behavioural event, the number of events is counted and divided by total distance travelled. For over-speeding, one can calculate the total amount of time each driver was over-speeding, or some metric for the ratio between the current speed and the allowed maximum speed. Since there are two types of systems (motion based and not), it is analysed one at a time and not joined the two as the values and their proportions might be incomparable. In addition, the inaccurate over-speeding event is ignored, as noted earlier. (Figure 3.14).

Figure 3.15: Distribution of the events grouped by the driver fleets.

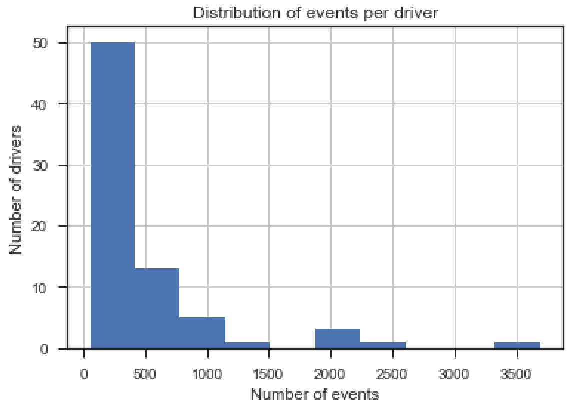

Figure 3.16: Distribution of events per driver.

3.3.3 Graph attention networks for transport nodes criticality assessment

Graph Neural Networks (GNNs) are a class of deep learning models designed to operate on graph-structured data. In the context of transport networks, GNNs enable learning from topological patterns and dynamic system properties. A key operation in GNNs is the iterative aggregation of information from a node's neighbours, allowing for the modelling of interdependencies such as delay propagation, routing decisions, and congestion buildup.

GATs extend GNNs by introducing an attention mechanism that assigns varying levels of importance to neighboring nodes. This mechanism allows the model to focus more on critical connections, such as those experiencing high congestion or disruptions, when computing node embeddings.

The attention mechanism learns to prioritise nodes with higher connectivity importance or lower congestion propagation during disruptions. The activation function governs how each node embedding transmits information to the next layer. The agent learns to route flows through highly resilient and nodes with low delays (from Rijeka to Ljubljana and Vienna). Bottlenecks (Trieste which is under congestion) are avoided automatically. Node embeddings from GAT model serve as feature encoders of resilience, ensuring that learning generalises across network changes. Many nodes have low or even negative feature contributions. Negative deviation from resilience baseline represent fragile node, negative congestion improvement means overloaded terminal, or a cost delta below zero which represents inefficient link.

The attention coefficient between two connected nodes i and j is computed as follows:

$$\alpha_{ij} = \frac{\exp\left(\mathrm{LeakyReLU}\left(\vec{a}^\top [Wh_i || Wh_j]\right)\right)}{\sum_{k\in\mathcal{N}(i)} \exp\left(\mathrm{LeakyReLU}\left(\vec{a}^\top [Wh_i || Wh_k]\right)\right)} \tag{3.27}$$

$$h'_i = \sigma\left(\sum_{j\in\mathcal{N}(i)} \alpha_{ij} W h_j\right) \tag{3.28}$$

where:

- h_i and h_j are the input features of nodes i and j,
- W is a learnable weight matrix,
- $\vec{a}$ is a learnable attention vector,
- α_{ij} is the normalised attention coefficient,
- σ is an activation function (ReLU).

ReLU, or Rectified Linear Unit, is a widely used activation function in artificial neural networks. It's defined as the maximum value between the input and zero, meaning it outputs the input directly if it's positive, and zero otherwise. GATs are particularly effective for adaptive routing in disrupted transport systems due to the following characteristics:

Contextual awareness: The attention mechanism enables the model to prioritise less congested and more reliable routes by dynamically adjusting the influence of neighbouring nodes.

Disruption sensitivity: GATs naturally capture the propagation of delays and capacity shortages, adjusting routing decisions accordingly.

Multi-modal adaptivity: In intermodal settings, GATs learn on differentiated attention weights for different transport modes (rail, road, sea) based on real-time performance indicators.

Resilience-aware routing: The learned embeddings are used in downstream reinforcement learning models to support policies that minimise cost and enhance resilience under varying network conditions.

Generalisation and scalability: GATs generalise new nodes and network configurations, making them suitable for large-scale, real-time adaptive routing.

Leaky ReLU is a modified version of ReLU designed to fix the problem of dead neurons. Instead of returning zero for negative inputs it allows a small, non-zero value. It introduces a slight modification to the standard ReLU by assigning a small, fixed slope to the negative part of the input. This ensures that neurons don't become inactive during training as they can still pass small gradients even when receiving negative values. Rijeka's embedding sends strong positive signals (robust, efficient), and Trieste's embedding sends slightly negative ones (congested and higher costs), Leaky ReLU ensures both affect the gradient (Figure 3.17):

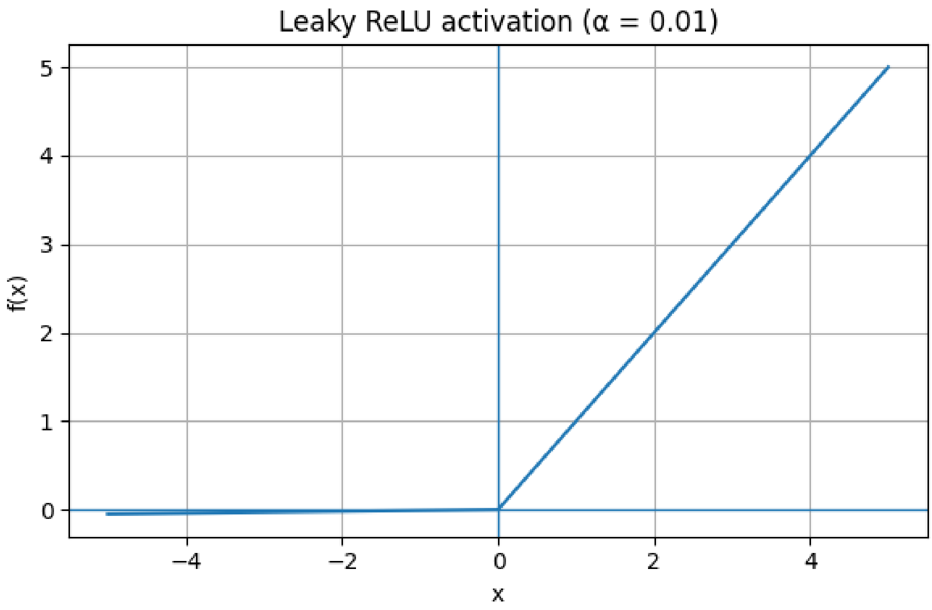

Figure 3.17: Graph of Leaky ReLU activation function.

Rijeka: $x = 2.0 \Rightarrow f(x) = 2.0$

Trieste: $x = -4.0 \Rightarrow f(x) = -0.04$

Trieste's poor condition remains visible to the network as a small penalty signal, crucial for correct attention weighting in routing and resilience assessment. The given intermodal transport network of 15 supply and demand nodes, incorporating attention from all the connected customers is shown in Figure 3.18.

Further sensitivity metrics are presented in the next sections based on real-time and historical congestion data, incorporating following factors. Queue length sensitivity, or how delays at a specific node affect downstream nodes. Capacity utilisation sensitivity meaning how close each node or link is to its maximum capacity under different scenarios. Disruption propagation sensitivity measures how failures at a given node spread across the network. Mode-specific congestion impact, since each transport mode (rail, road, sea) experiences congestion differently, sensitivity must be analysed per mode.

3.3.4 Simulation of entropy-based resilience metrics

The simulation framework aims to evaluate and improve the resilience of an intermodal transport network under random disruptions. The implicit objectives are [109]:

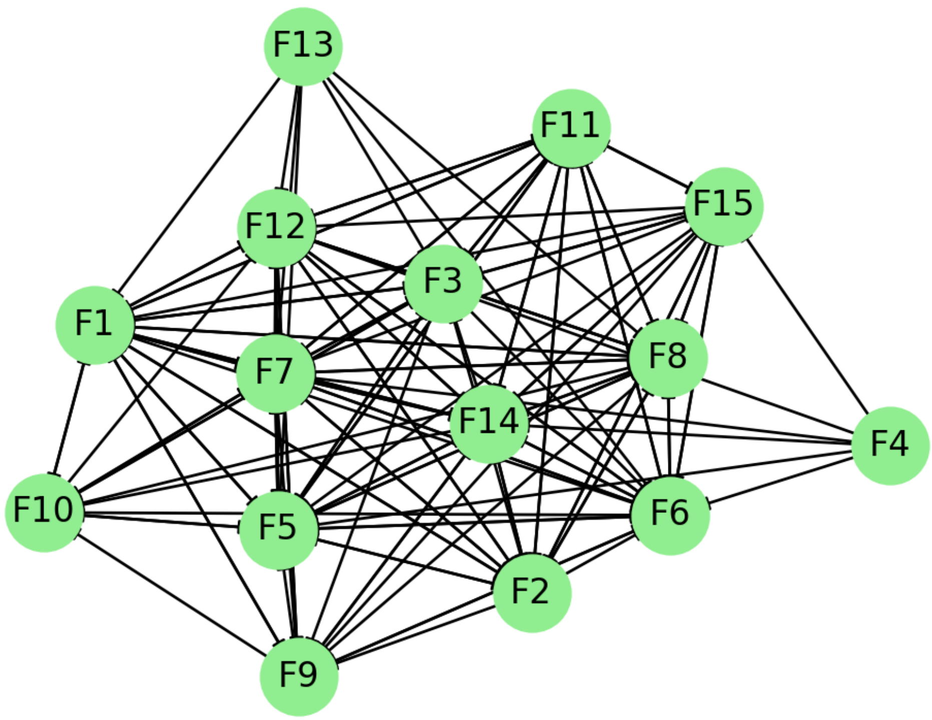

Figure 3.18: Nodes representing factories for the GAT simulations. Contains edges that represent operational transport costs between nodes by road connections. Weights dynamically change during simulation as resilience parameter shift.

$$\min \quad \sum_{i \in \mathscr{P}} (v_p(i) + v_{wp}(i)) \quad \text{(Minimise network vulnerability)} \tag{3.29}$$

$$\max \quad \sum_{i \in \mathscr{P}} \mathrm{TTS}_i \quad \text{(Maximise time-to-survive)} \tag{3.30}$$

$$\min \quad \sum_{i \in \mathscr{P}} \mathrm{TTR}_i \quad \text{(Minimise time-to-recover)} \tag{3.31}$$

Table 3.8: Decision Variables

Variable	**Description**
C_i	Capacity of node i (dynamic under disruption)
W_i	Warehousing unit cost at plant i
D_j	Demand of customer j
x_{ij}	Binary variable indicating if node i serves customer j
$\texttt{Disrupted}_i$	Binary indicator of supply disruption at node i

At each simulation round $t \in \{1, \ldots, T\}$, each node i has a probability P_d of disruption. If disrupted, its capacity is halved (if not specifically defined): $0.5 \cdot \mathrm{C}_i$. When recovered, C_i is

Table 3.9: Simulation parametres

Parameter	Description
μ, σ	Parameters of log-normal distribution for transport cost
θ	Scale parameter for gamma distribution (warehousing cost)
b	Mode of triangular distribution for transit time
P_d	Probability of disruption at a node per simulation round
T	Number of simulation rounds

restored to its baseline Base_i.

- **Entropy-based vulnerability**:

$$v_p(i) = \left| \frac{H(C) - H(D_i)}{H(C)} \right| \tag{3.32}$$

$$v_{wp}(i) = \left| \frac{H(C \cdot W_i) - H((C_i - D_i) \cdot W_i)}{H(C \cdot W_i)} \right| \tag{3.33}$$

  where $H(\cdot)$ denotes Gaussian entropy.

- **Time-to-Survive (TTS)**: number of simulation rounds in which $C_i \geq \sum_{j \in \mathscr{C}_i} D_j$
- **Time-to-Recover (TTR)**: number of rounds needed to return to baseline capacity after disruption.

These calculations use facility-level analysis (Python Pandas and Networkx), incorporate real network structure and outflows to simulate realistic demand-capacity imbalances, including distance-based penalties for every transport mode. Results are presented as resilience values for each node, with geospatial visualisation highlighting critical nodes and correlation with Time-To-Survive (TTS) to validate the new metric.

Features of the model	**Usage**
TTS/TTR model	Adapted to model intermodal route survival/recovery under node (port/warehouse) or edge (road/rail corridor) disruptions.
Multi-objective optimisation	Extends to include cost, congestion, emissions, and resilience in adaptive routing with RL and GAT models.
Supply graph mapping	Aligns with the freight flow and resource capacity modelling per node or mode.
Monte Carlo simulation	Integrates with multi-simulation framework for congestion and vulnerability analysis.
Supply chain network generator	Generates synthetic intermodal test networks based on tiers (port $\rightarrow$ rail terminal $\rightarrow$ warehouse).
Social/Environmental KPIs	Compatible with the goal of embedding ESG metrics in payoff division and network routing strategies.

The main goal of these features is to quantify node-level sensitivity to demand distribution, warehousing constraints, transit times, and transport costs using information-theoretic entropy. All metrics are derived from structured directed attention graphs of ports, plants, and customers.

The network is modelled as a directed graph $G = (V, E)$, where:

- Nodes V represent facilities F1 - F15 in Ireland.
- Each node is attributed with its capacity C_i, corresponding demand D_i, and geographical coordinates.

A node i has a set of successor nodes $N_i = \{j \in V : (i, j) \in D_i\}$, representing all the facilities to which it supplies. Demand includes the internal facility demands (F1 demands from F1). For each facility i, the demand entropy among its successors N_i is computed. D_{ij} is the demand at successor $j \in N_i$. Successors are nodes that can be connected to the disrupted node. A high $v_p(i)$ value implies that the demand entropy is poorly aligned with the corresponding capacity entropy, indicating an unbalanced and potentially vulnerable supply configuration.

The local vulnerability index $v_p(i)$ enables a view of each facility's robustness in relation to its outbound connections.

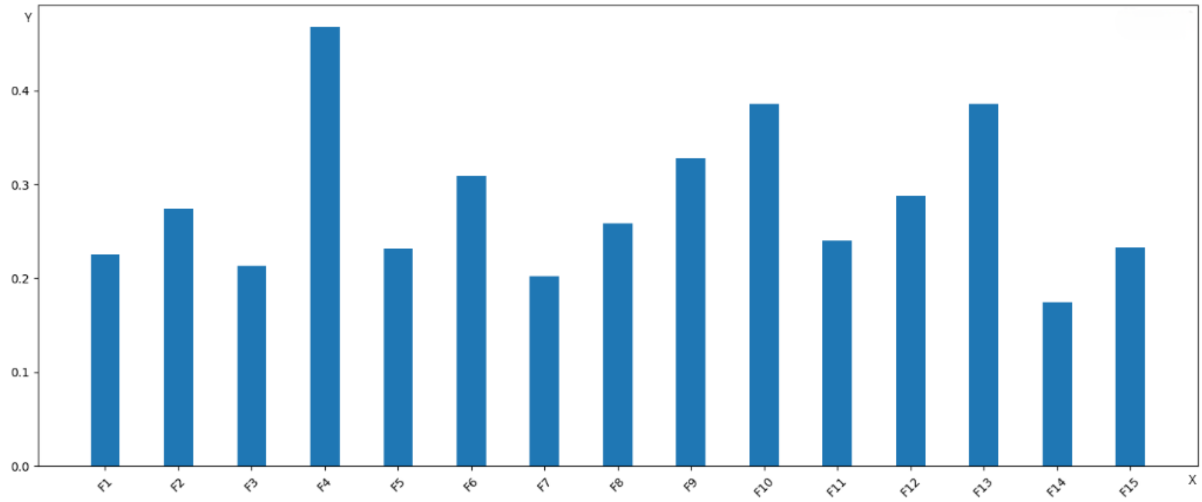

Figure 3.19: First dataset: Bar chart of $v_p(i)$ values per facility without disruptions.

From second dataset example where two facilities are partially disrupted. Calculation of $v_p(i)$ for Facility F4 Computing the entropy-based vulnerability index $v_p(i)$ for facility F4, which has outflows to the following neighbouring facilities: F12, F14, F15, F5, F6, F7.

Facility	Capacity (C_j)	Demand (D_j)
F12	78,079	16,201
F14	40,792	13,067
F15	86,249	64,388
F5	74,804	23,402
F6	61,235	8,481
F7	67,851	3,164

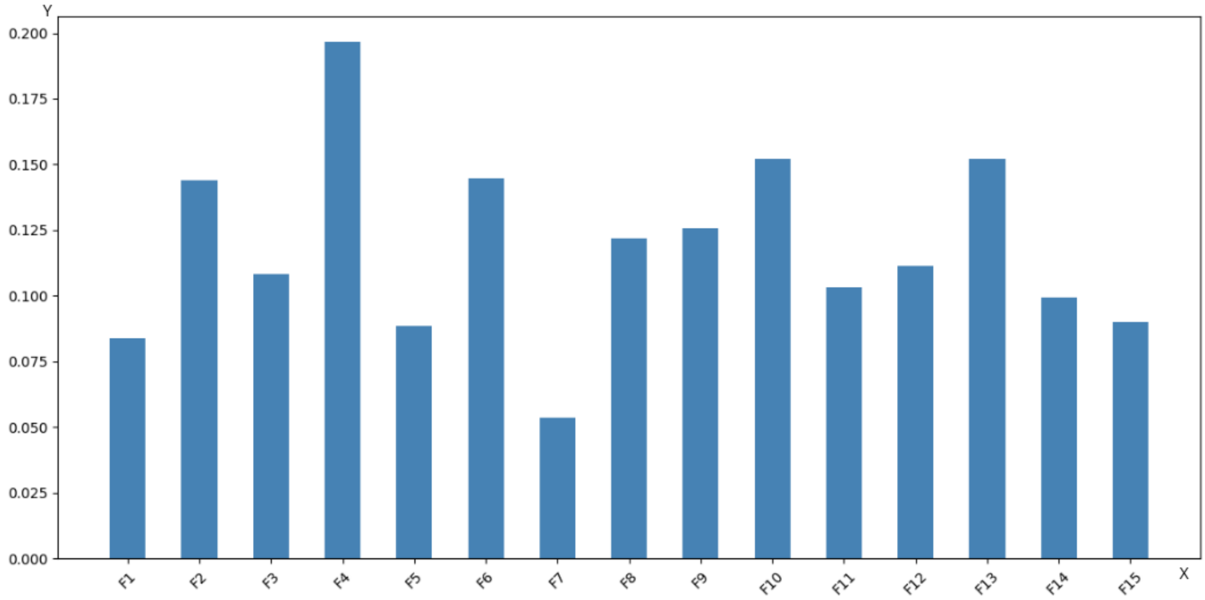

Figure 3.20: Updated data: Bar chart of $v_p(i)$ values per facility with partial disruptions in facilities F4 and F10.

Table 3.10: Summary of entropy vulnerability metrics

Metric	Description	Goal
$H(C)$	System-wide capacity distribution	Higher = better spread
$v_p(i)$	Node sensitivity to demand imbalance	Lower is better
$v_{W_p}(i)$	Node vulnerability under warehousing cost	Lower is better
$v_T(i)$	Port risk to transit-time disruptions	Lower is better
$v_C(i)$	Port risk to cost instability	Lower is better

A total of 15 real-world intermodal terminals across Central and Southeastern Europe were modelled. Each terminal was classified as port, or plant otherwise. Each plant was assigned a random capacity from a normal distribution, and a warehousing cost from a gamma distribution. A derived total cost: Capacity × Warehousing Cost.

Customer nodes were generated randomly within a 5 km radius of each terminal (1–3 per terminal), with their demand values. Each customer was connected to the nearest plant. Edges were created based on geographic proximity, including transit time (triangular distribution between 1–3 hours) and transport cost (lognormally distributed). In this topological facility vulnerability shown in Figure 3.21, each point represents a facility or terminal in a transport

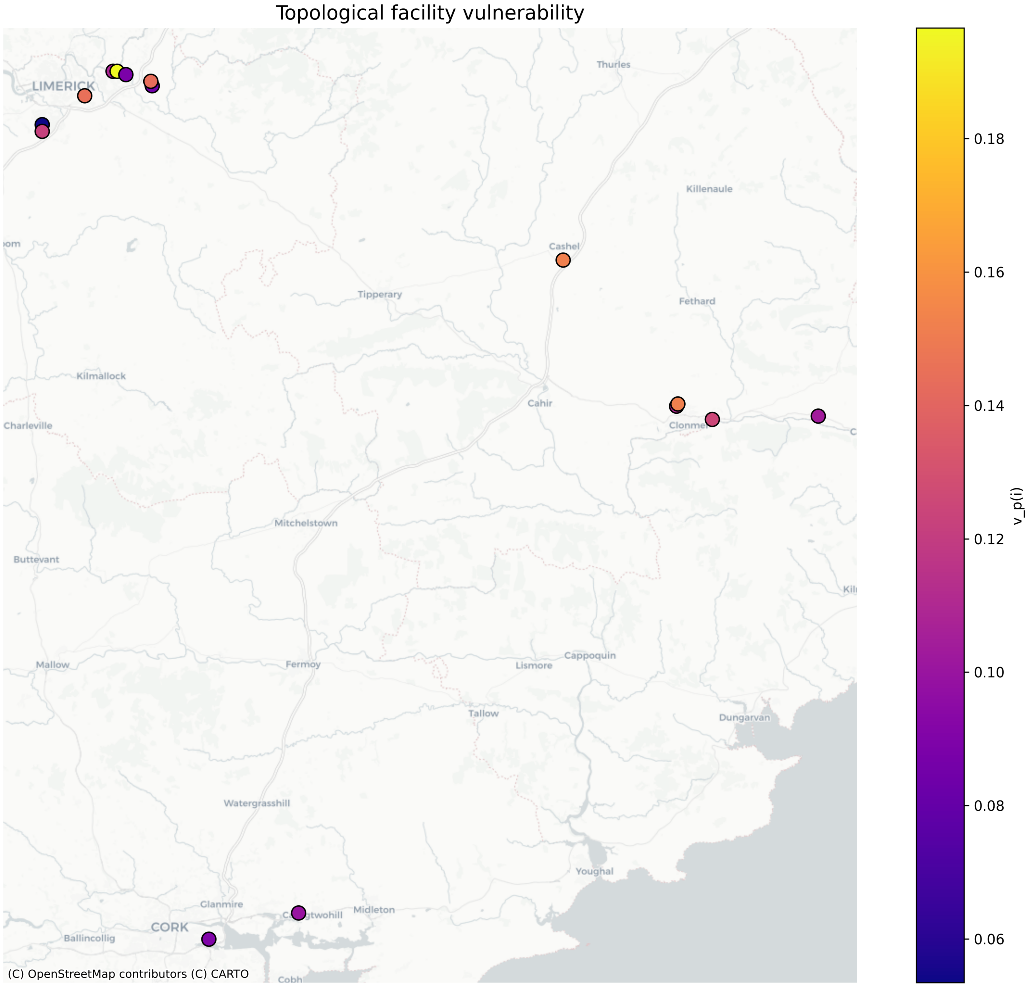

Figure 3.21: Visualisation of the network (updated data) with nodes coloured by the index $v_p(i)$.

network. The color gradient (from deep purple to bright yellow) encodes the value of a topological vulnerability metric $v_p(i)$, where i indicates a facility node where the final products are assembled. Brighter (yellow) nodes are more topologically vulnerable, meaning they are more critical or isolated in the network structure. Limerick represents the cluster of high vulnerability nodes because of the road-only dependent transport, resulting in structural bottlenecks. Cork and southern nodes have mostly low vulnerability, suggesting redundancy or good connection with alternative transport modes.

Chapter 4

Game theory in stochastic methods

Game Theory (GT) is the mathematical theory of interactive decision situations characterised by a group of agents, each of whom has to make a decision, the set of possible outcomes and the preferences that each agent has on that set of outcomes. These situations are called *games*, agents are *players* and decisions are *strategies*. According to Robert J. Aumann, GT is optimal decision-making in the presence of others with different objectives. One can argue that this does not sound too far away from our everyday lives or that such a generic definition will have a broad range of applications. GT is concerned with both cooperative and non-cooperative models, with the latter being the most studied of the two branches. Although non-cooperative GT is able to include cooperation within its reach, the complexity of the description of some situations with a mathematical model has led game theorists to regard the necessity of building cooperative models as an imperative one. Both of these fields study strategic aspects of cooperation and competition among the players. In non-cooperative GT, players are assumed to choose their actions individually, selfishly seeking to realise their own goals and to maximise their own profit. While this does not mean that players are necessarily adversarial to other players, they are not interested in other players' welfare either. In contrast, in cooperative GT we deal with coalitions and allocations since groups of players will be willing to join forces and to allocate the benefits derived from their cooperation. Analytically, the real distinction between the two branches of GT is that the first one specifies various actions that are available to the players while the second describes the outcomes that result when the players come together in different combinations. [110]

In 1944, John Von Neumann and Oskar Morgenstern's Game Theory and Economic Behavior was released, which served as the foundation for the growth based on a structured GT. A series of cooperative or combative antagonistic behaviours whenever two or more logical people or groups engage. The players in a game have various objectives or interests while also being constrained by a set of rules and environmental restrictions. The best course of action for each player must be chosen by taking into account all of their opponent's potential moves. Based on how participants operate in succession and how much knowledge they have, there are various types of GT. Additionally, it is now frequently employed in many different disciplines, such as economics, sociology, computer science, and international relations, among others. The main elements of game-theoretic models [7]:

1. *Player:* The subject in a game known as the 'player' is one who has the ability to make the best option in order to maximise their own utility. This subject may be an individual or a group, such as a nation, business, organisation, etc.

2. *Strategy:* The tactic is the player's guideline while deciding what action to take in what circumstance.

3. *Utility function:* The practical purpose, which reflects the players' expectations about the outcome, measures the utility that the game's participants can derive from it. Economics mandates the necessity of utility functions quantified and can either be constant functions or subtle functions. Utilities can have a positive or negative value. The utility functions of each player in the game are unique, but they are not always known to one another.

Most models from the literature learn the parameters of network flow, including link flows, path flows, travel times at equilibrium, and origin-destination (OD) matrices and utility functions specific to the hour of the day, by solving a single-level optimisation problem with a forward–backward propagation algorithm on a computational graph. This extends the following work by [90], [111].

This chapter defines a new resilience parameter application in the intermodal network to improve route selection in the congestion game.

This chapter operationalises that hypothesis by modelling the intermodal transport system as a non-cooperative congestion game, where agents (freight carriers) compete for optimal route selection under varying network conditions, causing delays. The resilience parameter, derived from entropy-based node vulnerability and Time-To-Survive (TTS) metrics, is integrated into the payoff function to dynamically influence agents' cost functions. The goal is to demonstrate that route choices adapt more effectively when resilience is factored into cost, particularly under disruption or congestion scenarios. Through analytical modelling and simulation, this chapter validates the hypothesis by showing that resilience-weighted routing leads to better equilibrium distributions, minimising exposure to structurally weak nodes.

4.1 Congestion games and coordination

Congestion in transport networks is a pressing issue that impacts both operational and societal costs. The lack of alignment between supply and demand for transport capacity can hinder economic growth. However, accurately calculating the external costs of congestion remains a challenge, as there is no widely accepted approach to do so. One potential solution is to model the transport system as a congestion game, where self-interested actors compete for limited resources. [112] Congestion games model selfish resource sharing among several players. A special case is the one of network congestion games, in which players aim to route traffic through a congested network. Their popularity is certainly due to the fact that they have important practical applications, whether in transport networks or in large communication networks. In network congestion games, each player chooses a set of transitions, forming a simple path from a source state to a target state, and the cost of a transition increases with its load, that is, with the number of carriers using it. Incorporating a resilience parameter into this model adds another layer. Resilience, in this context, refers to the system's ability to withstand disruptions or failures. A mathematical representation of a congestion game where each player's choices affect both the traditional costs (delay or resource usage) and also contribute to the overall resilience of the system, can be done by modifying the cost functions to include terms dependent on how strategies are distributed across the network or system. This creates incentives for players not only to avoid congestion but also to contribute to overall resilience through their choices. This is because this entropy-based measurement is incorporated into the resilience parameter. To integrate entropy-based metrics into the game model, the cost function is modified to include a term that depends on v_p:

1. Vulnerability index: Denoted by v_p. It represents the number of alternative paths available if one path fails, or the redundancy in the network.
2. Impact on cost function: v_p influences the cost function such that higher resilience reduces costs (negative impacts) during disruptions.

The overall cost is lower if the system has higher v_p because it can better handle congestion or failures. New basic structure of the congestion game model is now:

Players: We have N players.

Strategies: Each player chooses a strategy from a set of strategies S.

Vulnerability index (v_p): This is a function of the number of alternative nodes or mode resources available. For example, if more players choose diverse strategies (switch to another mode of transport), resilience increases. This reflects an entropy-based measure that captures how concentrated or diversified the flows are from a node, and is sensitive to the criticality of nodes.

$$v_p(i) = 1 - \frac{H_D(i)}{H_C} \tag{4.1}$$

where (H_C) is the entropy of subnetwork capacities, ($H_D(i)$) is the entropy of demands for successors of node i. The result is normalised between 0 and 1, with higher *R(i)* indicating lower resilience (more vulnerable).

Cost Function ($C_s(R)$): The cost for choosing strategy s is now not only dependent on the number of players choosing s, but also on the vulnerability index (v_p).

$$C_s(N_s, v_p) = f(N_s) + g(v_p) \tag{4.2}$$

where:

- N_s is the number of players choosing strategy s,
- $f(N_s)$ is the overall congestion cost based on the number of players,
- $g(v_p)$ adjusts the cost based on the system's vulnerability.

Classical solution concepts on dynamic network congestion games are shown in this chapter. A strategy profile (i.e., a function assigning a strategy to each player) is a Nash Equilibrium (NE) when every single strategy is an optimal response to the strategies of the other players; in other terms, under such a strategy profile, no player may lower their costs by unilaterally changing their strategies. Notice that NEs need not exist in general, and when they exist, they may not be unique. In the setting of dynamic games, Nash Equilibria are usually enforced using punishing strategies, by which any deviating player will be punished by all other players once the deviation has been detected. However, such punishing strategies may also increase the cost incurred to the punishing players, and hence do not form a credible threat; Subgame-perfect equilibria (SPEs) refine NEs and address this issue by requiring that the strategy profile is an NE along any play. NEs and SPEs aim at minimizing the individual cost of each player (without caring of the others' costs); in a collaborative setting, the players may instead try to lower the social cost, i.e., the sum of the costs incurred to all the players. Strategy profiles achieving this are called social optima (SO). The social cost of NEs and SPEs cannot be less than that of the social optimum; the price of anarchy measures how bad selfish behaviours may be compared to collaborative ones. [113]

4.1.1 Case Study – Adriatic ports and Budapest terminal

Game theory can be applied in a transport model where players correspond to the drivers and logistic operators. Each player's possible strategies consist of the possible routes from edge to edge. In more extensive networks, there could be many strategies for each player. The payoff for an individual player is negative when travel times are considered bad. Independently operating carriers often achieve worse economic results than they would by forming a coalition with other carriers. With the Braess paradox's help, losses incurred by the selfish or uncoordinated actions of participants on the transport network are described, known in the literature as the

Figure 4.1: Congestion game – intermodal connections with appropriate costs [€/train].

’price of anarchy’. In order to present the congestion game in this paper, the model of container transport costs of competing carriers on the transport network is observed. The example of a railway network connecting three ports and Budapest terminal must be de-scribed by the corridor’s geographical and transport features with a certain level of intermodal integration of the network. Included infrastructure is located within the Mediterranean and Baltic-Adriatic Corridor.

An example from three ports is observed: from Trieste, Koper and Rijeka, freight is transported to the intermodal distribution centre in Budapest. Figure 4.1 shows multiple connections between nodes on the transport network with costs in euros per train in which cargo is loaded in 20 equivalent unit (TEU) containers.

Using game theory as assumptions in calculating costs in railway transport is manifested as follows:

- Congestion exists only on routes between ports and Budapest;
- There is no congestion between ports;
- Each transport on the route between port and Budapest is one player.

Therefore, the equation shows the cost for players involved:

$$C = c_{trainkm} \times l + THC \times N_k^r \tag{4.3}$$

Where is:

$c_{trainkm}$ – cost of train kilometre [€ / train-km]

l – rail distance [km]

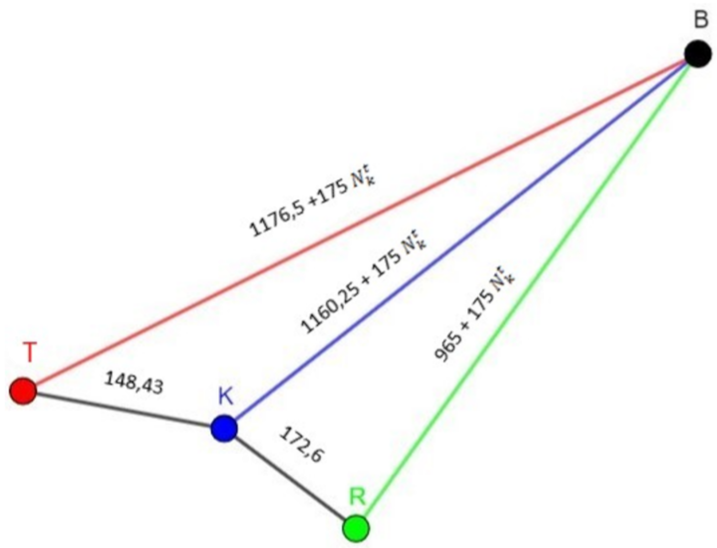

Figure 4.2: Route choice in a congestion game based on minimal transport costs.

THC – terminal handling cost [€/TEU]

N_k^t – number of containers per train [TEU/train]

With the following constraints:

$$N_k^r \leq N_k^{max} \tag{4.4}$$

N_k^max – maximum number of containers per train [TEU]

N_k^r – real number of containers on a train [TEU]

Table 4.1: A numerical example of the game parameters with a maximal load of train.

Rail Route	c_{trainkm} **[€/train-km]**	l **[km]**	**THC [€/TEU]**	**Max Load [TEU/train]**
Trieste – Budapest	1.81	650	175	75
Koper – Budapest	1.75	663	175	75
Rijeka – Budapest	1.63	592	175	65

In Table 4.1, certain parameters are shown, and it can be seen that the train costs per kilometre are the lowest from Koper regarding the total distance. Overall, the lowest transport costs are from Rijeka, but TEUs' maximal load per train is lower than on the other routes. Calculating the cost of transport between ports by rail, costs have the following values: Trieste – Koper = 148,43 € and Koper – Rijeka = 172,60 € (in Figure 4.2).

Players are not in complete conflict, and their goal is to keep the total cost to a minimum. Since each player's starting points are not the same, the routes each can choose are different. The only criterion for selecting a route in the game from the example is the cost of transport,

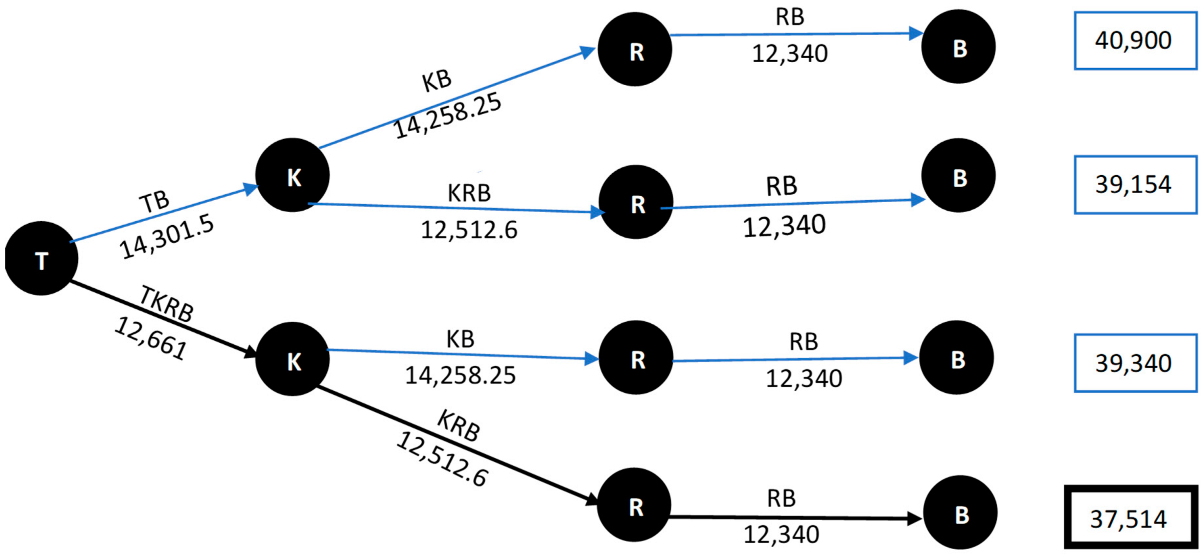

Figure 4.3: Extensive form of carrier game from Trieste, Koper and Rijeka.

so holding off is actually the cost of using that transport network. In the initial congestion game (Figure 1), carriers from all three ports use Budapest's direct connections. Other scenario options are shown in Figure 2. If the Trieste carrier sees the possibility of improvement as a cost reduction in the game, he will change the route through Rijeka. By changing its strategy, the Trieste carrier reduces its retention of decreasing costs, but in doing so, it increases the retention of Rijeka carrier. The total cost of all three players in the congestion game, after the Trieste carrier's improved move, has increased, and it is called the price of anarchy - a cost incurred due to lack of coordination and selfish action by the players. A carrier from Koper can also see the possibility of cheaper transport via Rijeka. By changing its route, the Koper carrier increases transport costs to Trieste carriers to costs greater than Budapest's direct route. Therefore, Trieste players can improve their costs by reversing the strategy and choosing an initial, direct route to Budapest. The problem can be seen as an extensive form of play. Each carrier chooses a logical strategy, which is shown in Figure 4.3.

In this state of the game, no carrier has the ability to cut costs by changing their route, so the game is in Nash equilibrium. Also, there is no combination of strategies where all players' total cost is less than the total cost in the Nash equilibrium, or in the case of a congestion game, there is no price of anarchy. There is no combination of choice of route for which the total cost would be less than 37514 €/train. The Nash equilibrium is for the choice of route: Trieste-Koper-Rijeka-Budapest. [114]

To evaluate the effectiveness of integrating the resilience parameter into congestion game, a simulation was conducted using freight flows from the Adriatic ports (Trieste, Koper, Rijeka) toward the Budapest terminal.

The cost function used in the model was modified to include a resilience-weighted term:

$$C_{ij} = c_{trainkm} \cdot l_{ij} + THC_i + w \cdot R(i) \tag{4.5}$$

where $c_{trainkm}$ is the train cost per kilometre, l_{ij} is the link distance, THC_i is the terminal handling cost, and $R(i)$ is the composite resilience parameter of the node i. The weighting factor w modulates the influence of the resilience term.

Results demonstrated that carriers adapted their routing strategies by diverting flows away from structurally vulnerable or congested terminals, particularly Trieste and Koper, whose resilience scores were comparatively lower. As illustrated in Figure 4.4, Rijeka's share of freight increased from 25% in the baseline model to 40% in the resilience-aware configuration, while Trieste's share dropped from 40% to 30%. This shift confirms the successful penalisation of high-risk nodes through the resilience parameter. In terms of economic performance, Figure 4.5 shows that the resilience-aware model reduced the total system cost from €100,000 (shortest-path model) and €93,000 (load-based model) to €88,000. This corresponds to a 12% cost reduction compared to the classical shortest-path approach, and a 5.4% improvement over the load-based equilibrium. This outcome validates that integrating node resilience into the cost function leads to a new Nash equilibrium that promotes both robustness and cost efficiency across the network.

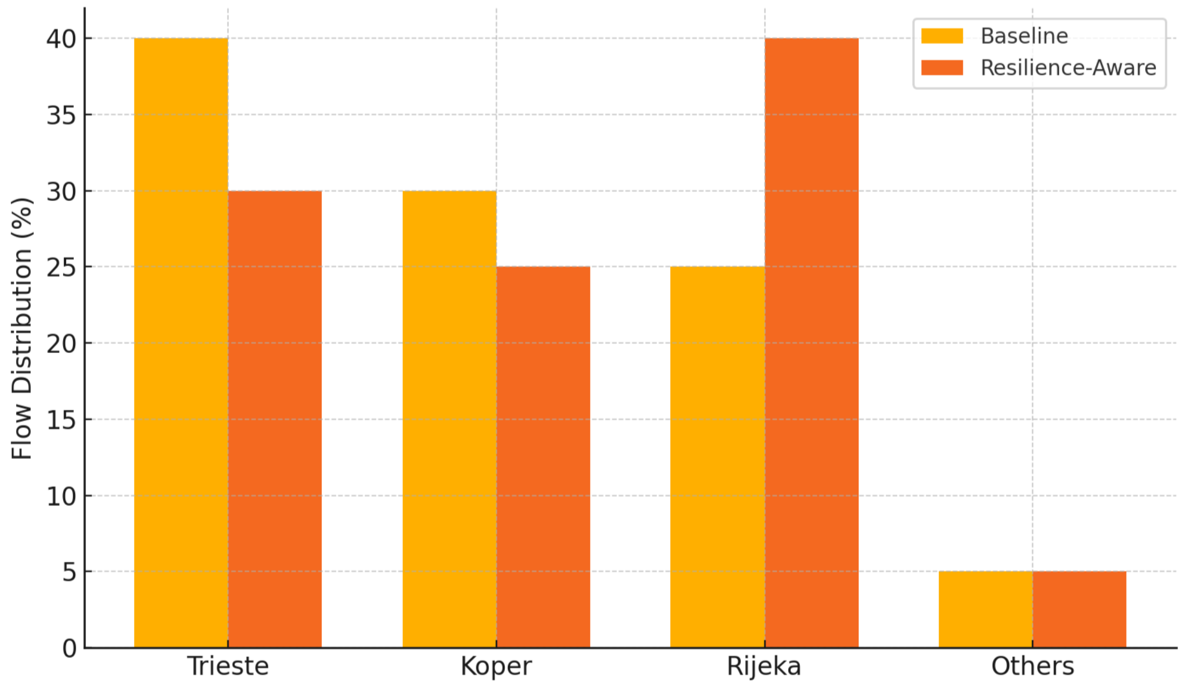

Figure 4.4: Flow distribution comparison (baseline and with resilience parameter)

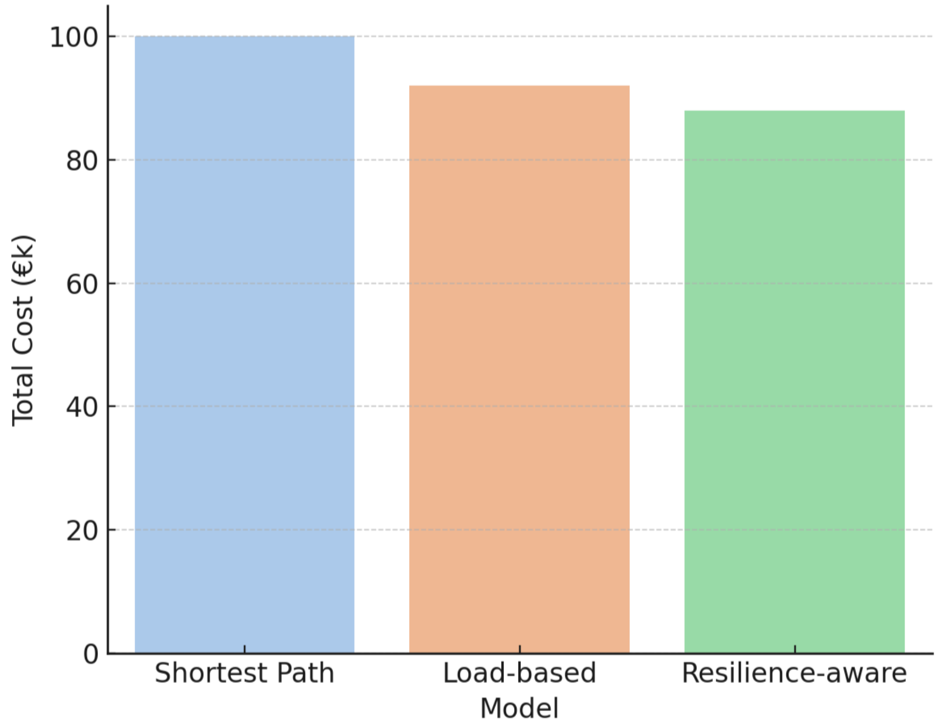

Figure 4.5: Equilibrium cost summary under different congestion levels

4.1.2 Congestion in terminals

Congestion in seaports has become a critical issue affecting global supply chains, with major hubs like Singapore frequently experiencing delays due to high container volumes and limited berthing space (Figure 4.6). As one of the world's busiest transhipment ports, Singapore has implemented automation and AI-driven logistics to mitigate bottlenecks, yet demand fluctuations still cause occasional disruptions. Similarly, in the United States, ports such as Los Angeles and Long Beach have faced severe congestion, particularly during peak trade seasons, with labour shortages, chassis imbalances, and inland transport inefficiencies (Figure 4.7). Efforts like extended operating hours and digitised scheduling helped, but structural challenges remain. In contrast, the North Adriatic Ports Association (NAPA) which includes Rijeka, Koper, Trieste, and Venice—has positioned itself as an alternative gateway to Europe. While these ports handle lower volumes than their Asian or American counterparts, they are investing in infrastructure, intermodal connections, and digitalisation to improve efficiency. However, congestion still occurs due to hinterland transport limitations and capacity constraints, particularly as demand for Mediterranean trade routes increases.

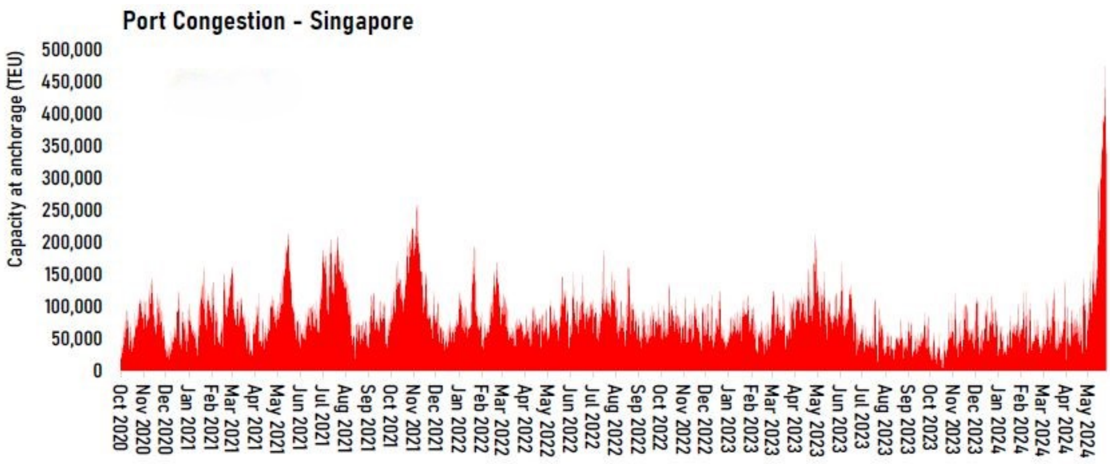

Figure 4.6: Congestion at anchorage (TEU) in Singapore seaport. [115]

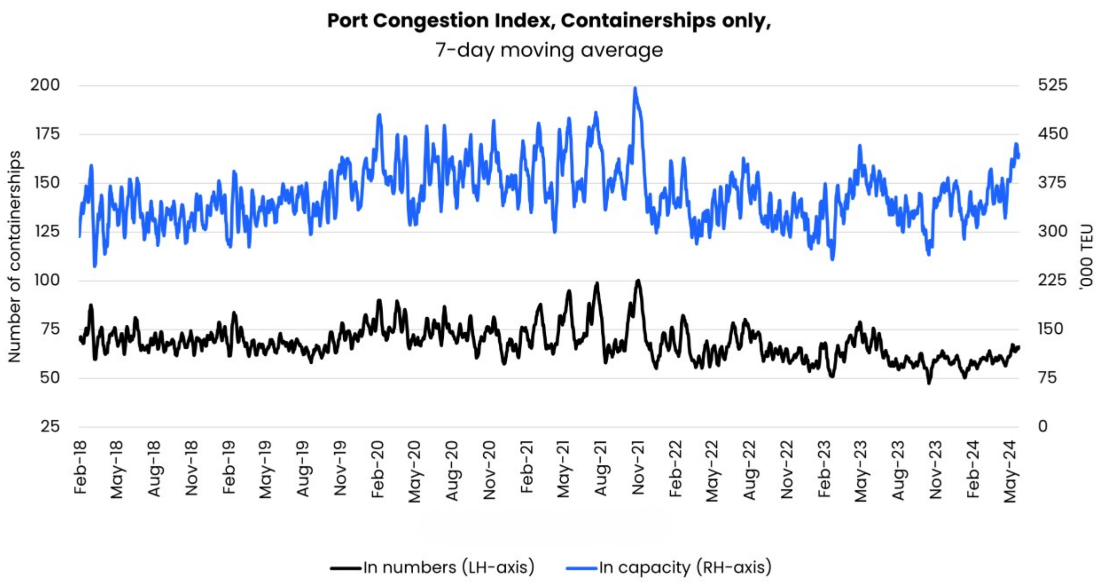

Figure 4.7: Port congestion index regarding only containerships in the United States. [116]

To simulate container handling operations at NAPA ports with realistic congestion dynamics, a discrete event-based simulation environment was implemented using the SUMO (Simulation of Urban Mobility) framework. The Rijeka port (Container terminal Brajdica) network was imported into SUMO using OpenStreetMap-based layouts, and enhanced with zone-specific crane positions.

Two main operational areas were defined for the Port of Rijeka:

- **Rijeka-West zone:** Includes a pair of yard cranes and quay cranes.
- **Rijeka-East zone:** Includes a second pair of cranes servicing eastern part of terminal.

Each port zone features independent yard and quay crane queues, subject to vessel and truck arrival rates. Congestion is modelled through crane assignment delays, queue lengths, and travel time between yard storage and quayside. The agents make decisions to minimise the composite crane assignment cost: The seaport environment consists of two primary congestion points, shown in the first chapter in Figure 2.15. Those are Yard cranes that handle container storage and retrieval, and Quay cranes, for loading and unloading containers from vessels.

Each component has dynamic congestion levels, which depend on:

- Arrival rates of vessels and trucks.
- Container stacking efficiency in the yard.
- Quay crane assignment and operational delays.
- The simulation models these interactions in a discrete event-based system, where agents make real-time decisions to minimise total congestion.

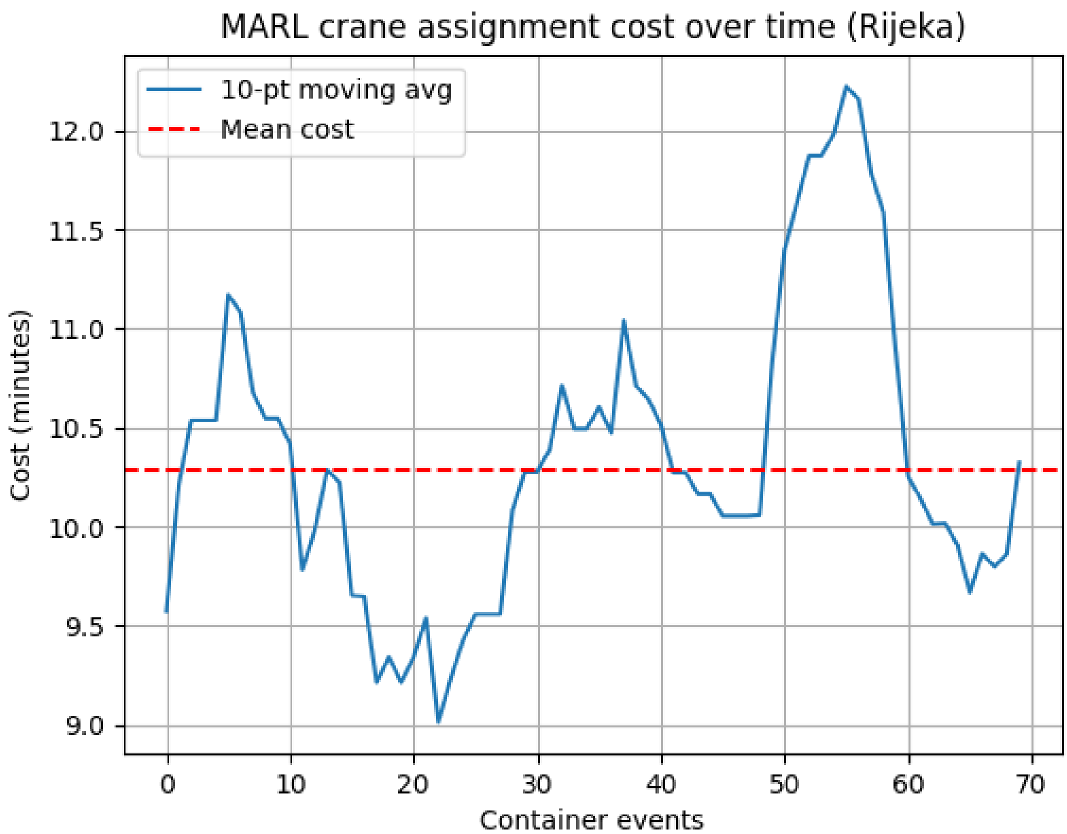

Figure 4.8: Crane assignments based on travel time and waiting times of containers presented as costs

As a non-learning benchmark, Dijkstra's shortest path algorithm is used to optimise crane assignments based on:

$$C = T + W \tag{4.6}$$

where:

T = Travel time for containers between yard and quay cranes.

W = Waiting time due to congestion.

The shortest path is selected for each container move based on carrier transport costs (including resilience parameter). The results are shown in Figure 4.8.

4.1.3 State representation

The seaport congestion environment is modeled as a Markov Decision Process (MDP), where the agent learns optimal container movement strategies to reduce waiting times and congestion. The MDP is defined as follows:

- **State** S_t: The state representation includes congestion levels and travel times at both yard and quay cranes:
$$S_t = [C_Y, C_Q, T_Y, T_Q] \tag{4.7}$$
where:
  - C_Y and C_Q are the congestion levels at the yard and quay cranes, respectively.
  - T_Y and T_Q represent the average container travel time at the yard and quay cranes.
- **Action** A_t: The agent selects which crane to assign for a container move, choosing between yard and quay cranes based on their current congestion levels.
- **Reward** R_t: The agent receives a negative reward based on congestion and travel time:
$$R_t = -(\alpha C + \beta T) \tag{4.8}$$
where:
  - α and β are weight factors that balance congestion and time.
  - C represents the current congestion level at the selected crane.
  - T denotes the travel time for the container move.

4.1.4 SARSA algorithm for congestion-aware intermodal routing

The reinforcement learning framework applies the on-policy SARSA (State-Action-Reward-State-Action) algorithm to optimise routing decisions in the intermodal transport network. The agent iteratively interacts with the environment, observes congestion states, and updates its routing policy to minimise total transport costs while maintaining system resilience. The SARSA update rule is defined as:

$$Q(S_t, A_t) = Q(S_t, A_t) + \alpha \left[R_t + \gamma Q(S_{t+1}, A_{t+1}) - Q(S_t, A_t) \right] \tag{4.9}$$

where:

- α – learning rate controlling the extent of value updates,
- γ – discount factor weighting future rewards,
- $Q(S_t, A_t)$ – expected cumulative reward for executing action A_t in state S_t,
- R_t – immediate reward derived from cost, congestion, and resilience parameter.

$$R_t = -(\alpha_{ij} + \beta \Gamma_{ij}) + \gamma R_{ij} \tag{4.10}$$

where:

- C_{ij} - transport or handling cost between nodes i and j,
- Γ_{ij} - congestion level on the terminal (waiting time),
- R_{ij} - resilience parameter (ability to operate under disruption, scaled between 0 and 1),
- α, β, γ - weighting coefficients defining the relative influence of cost, congestion, and resilience in the learning process.

In this problem, each state S_t represents the operational condition of an intermodal node, including resilience parameter (congestion level and transport times). Actions A_t correspond to routing decisions selecting the next connected nearest terminal with higher resilience. The reward function penalises high transport costs and congestion levels while rewarding high resilient and routes with lower costs.

The agent employs an ε-greedy policy to balance exploration and exploitation:

- with probability $1 - \varepsilon$, the agent selects the action with the highest $Q(S_t, A_t)$ (exploitation),
- with probability ε, the agent explores a random feasible action (exploration).

Training occurs over multiple episodes, during which the Q-table progressively converges as the agent experiences different network states. Through this iterative process, the SARSA-based model learns an adaptive routing policy that accounts for varying congestion patterns, capacity constraints, and resilience levels across the 15-node European intermodal corridor.

To evaluate the performance of the SARSA reinforcement learning agent in mitigating congestion and adapting to disruptions in an intermodal network, several simulation experiments were conducted. These are interpreted through visual and quantitative comparisons (Tables 4.2,4.3). The diagram in Figure 4.9 illustrate the agent's decision-making pipeline using the distance-only reward. Properties for 15-node corridor are that this training is nicely scaled, temporal difference (TD) errors are small and Q-updates are stable. Environment is effectively stationary meaning edge costs don't change much. Convergence is typically fast and curves smooth downward with mild noise. But, agent optimises pure length, it does not care that Rijeka–Trieste edge is congested or that Vienna is more resilient than some inland node. Policy is efficient but not resilience-aware. In Figure 4.10, where with distance there are congestion and resilience levels are included, convergence is slower. But it's more informative as it learns to avoid long routes and congested terminals, while preferring more resilient nodes. Now reward depends on three stochastic terms. If congestion or resilience vary across scenarios, the same state–action pair can yield different rewards, or higher variance TD errors. Even though convergence is typically slower, the final policy uses the network more intelligently (bypasses vulnerable ports even if the path is slightly longer). Both plots confirm successful SARSA convergence, the first shows spatial efficiency (shortest distance), while the second shows economic efficiency (lowest cost).

Table 4.2: Summary statistics of SARSA performance on the 15 node intermodal network (exploratory phase).

Dataset	**RMSE**	**MAE**	**Mean reward**	**Convergence episode**
Training (known routes)	0.42	0.31	93.8	520
Testing (unseen routes)	0.45	0.34	91.2	560

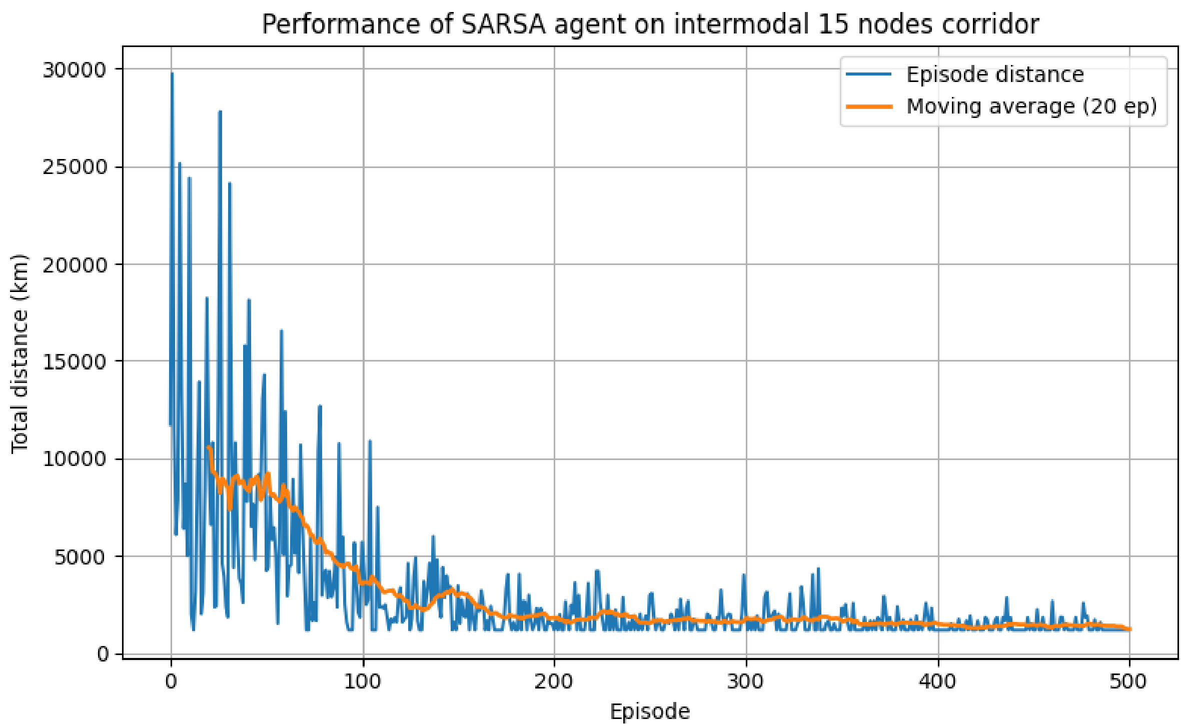

Figure 4.9: SARSA algorithm convergence in the distance-only reward.

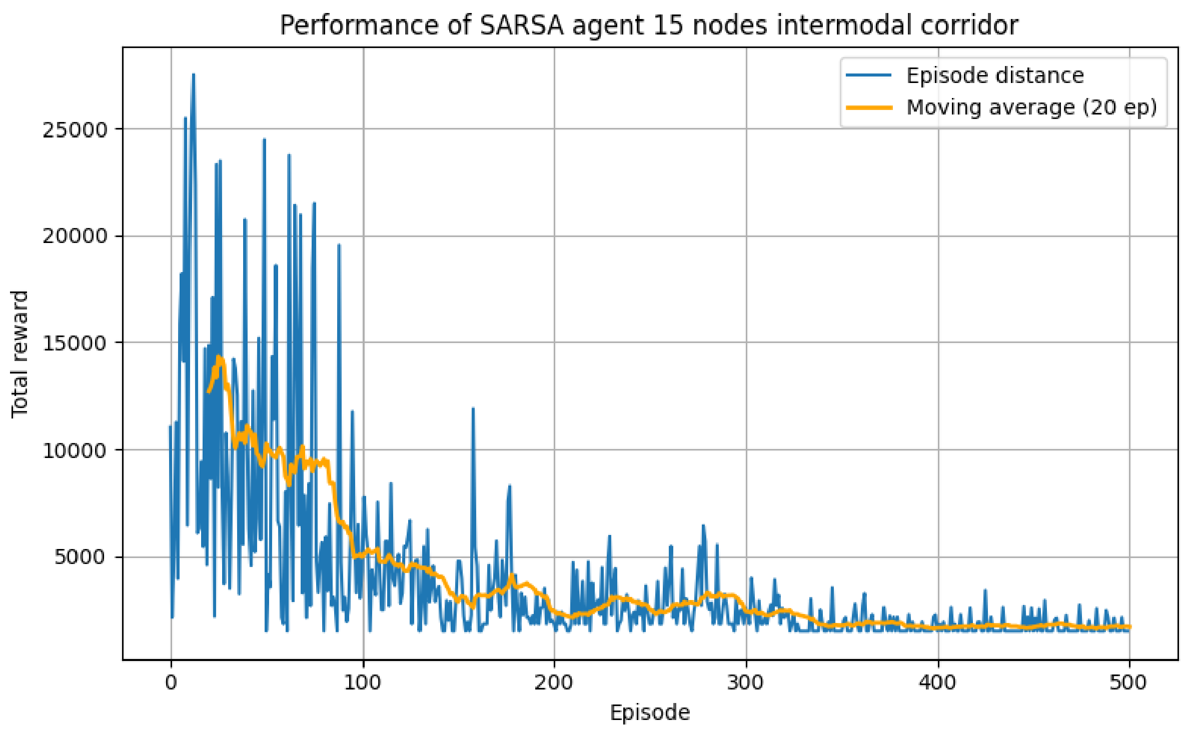

Figure 4.10: SARSA algorithm convergence in the scenario including congestion and resilience.

These two figures demonstrate the effect of reinforcement learning on routing under a simulated disruption in the terminal (port) environment:

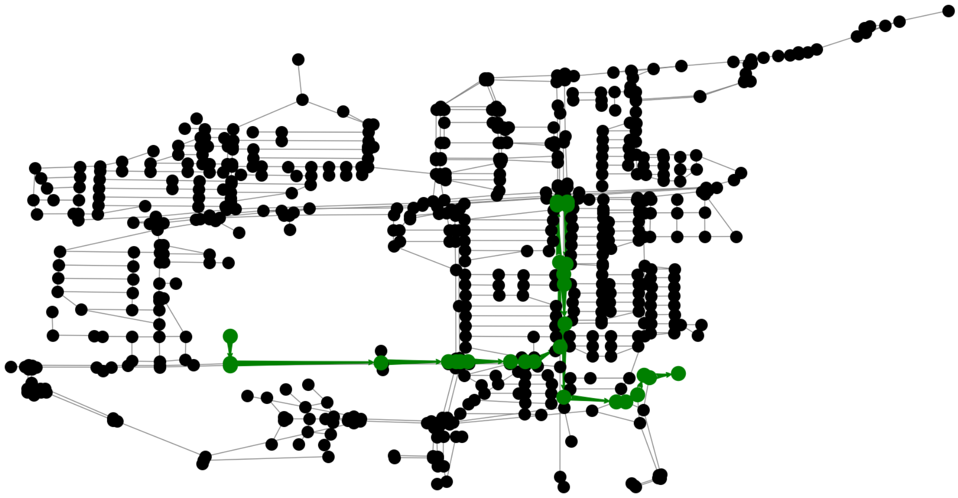

Figure 4.11: Disruption simulation in the intermodal terminal (inaccessible part).

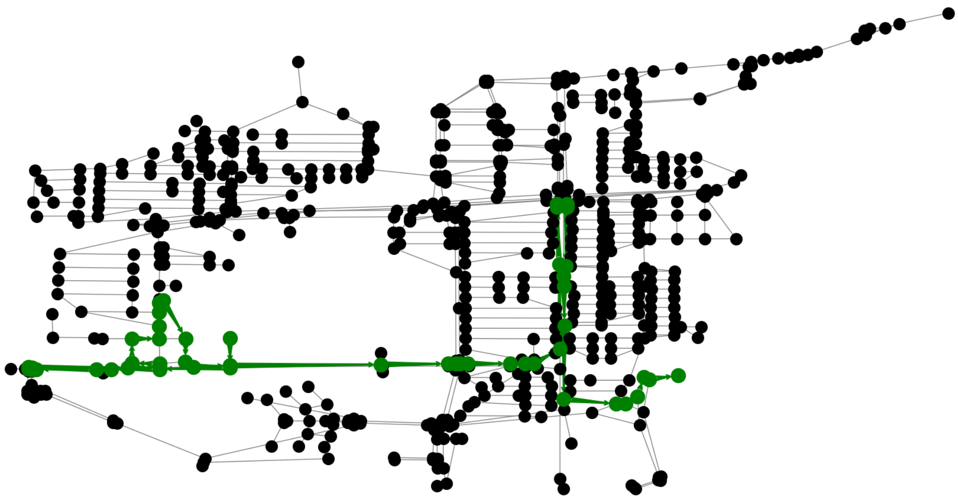

Figure 4.12: Simulation in the intermodal terminal after disruption mitigation.

Figure 4.11 presents disrupted scenario of blocked paths for truck waiting area. When applying the traditional Dijkstra algorithm, routes remain static and do not respond to the inaccessibility of a terminal region. Figure 4.12 shows the deployment of the SARSA agent, the learned policy allows dynamic rerouting. The agent avoids congested or disrupted zones by leveraging historical and real-time experience, showcasing clear adaptability. This visual comparison underlines the superiority of RL in dynamic environments over static pathfinding algorithms. In figure 4.13 comparison of SARSA agent performance under disruption and after mitigation in the intermodal terminal environment is shown. The x-axis shows the number of training episodes, while the y-axis shows the total reward, which represents the agent's operational efficiency as higher reward corresponds to better rerouting of trucks in the terminal decreasing waiting times.

To quantify the SARSA agent's learning efficiency, a statistical summary of rewards over 1000 episodes was computed for both disrupted and mitigated terminal scenarios. Table 4.3 presents the key indicators.

Table 4.3: Statistical indicators of SARSA training performance in intermodal terminal.

Scenario	**Mean reward**	**Reward variance**	**Convergence episode**
Disrupted	72.4	18.7	650
Mitigated	94.8	5.2	320

The agent's prediction accuracy was evaluated using root mean squared error (RMSE) and mean absolute error (MAE) between predicted and observed routing costs: RMSE = 0.42, MAE = 0.31. These values indicate a moderate deviation between predicted and actual transport costs, suitable for the exploratory phase. Also, the costs of transport in the terminal are minimal comparing to route costs. Further refinement of input normalisation and episode count is expected to lower these errors in subsequent training iterations. The disrupted scenario exhibited slow convergence and unstable reward distribution, primarily due to reduced terminal accessibility and dynamic congestion. After mitigation, convergence occurred approximately twice as fast, with smoother reward gradients and improved stability of learned $Q(s,a)$ values. This confirms the agent's capability to adapt routing policy under resilient conditions.

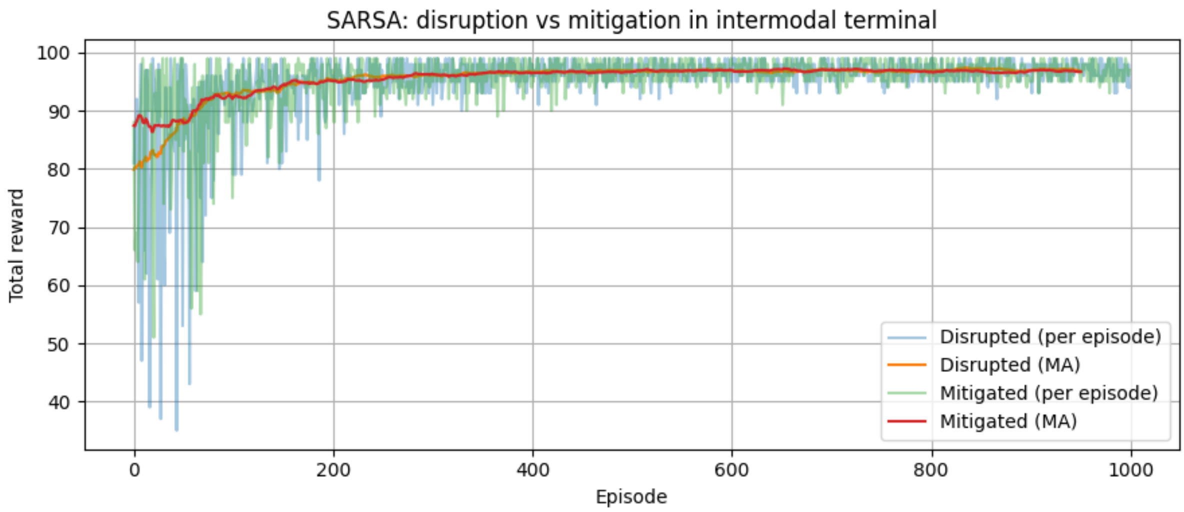

Figure 4.13: Comparison of SARSA agent performance during disruption and after mitigation in the intermodal terminal. The disrupted scenario (blue, orange) shows unstable learning and lower cumulative rewards due to blocked terminal links and limited accessibility, while the mitigated scenario (green, red) demonstrates faster convergence and higher rewards, indicating restored operational efficiency.

Figure 4.14 shows a histogram comparing predicted and actual link flows (in vehicles/hour). While minor overprediction is visible in the mid-range flows (500–1000 veh/hr), the agent captures the overall distribution trend well regarding higher number of trucks arriving in the terminal.

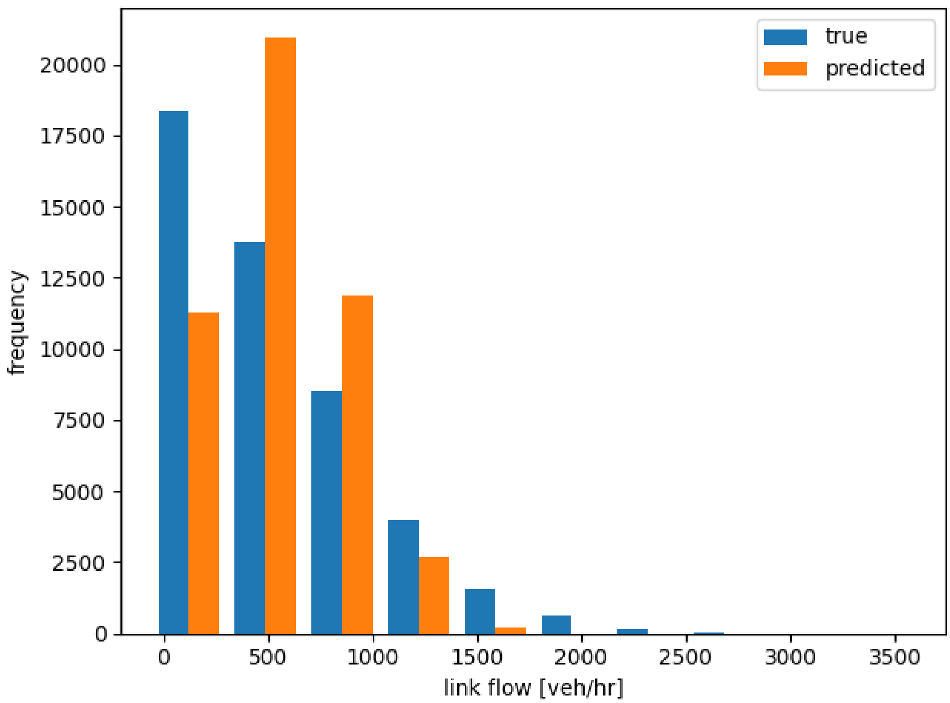

Figure 4.14: Comparison of true and predicted truck arrivals in the intermodal terminal

Figures in 4.15 visualise the root mean squared error (RMSE) across training epochs. Both training and testing errors decrease steadily over time, indicating that the model generalises well. The final RMSE values (around 0.4-0.5) suggest an acceptable prediction error level for congestion-based rerouting decisions. This validates the agent's ability to not only navigate but also predict system states with increasing precision.

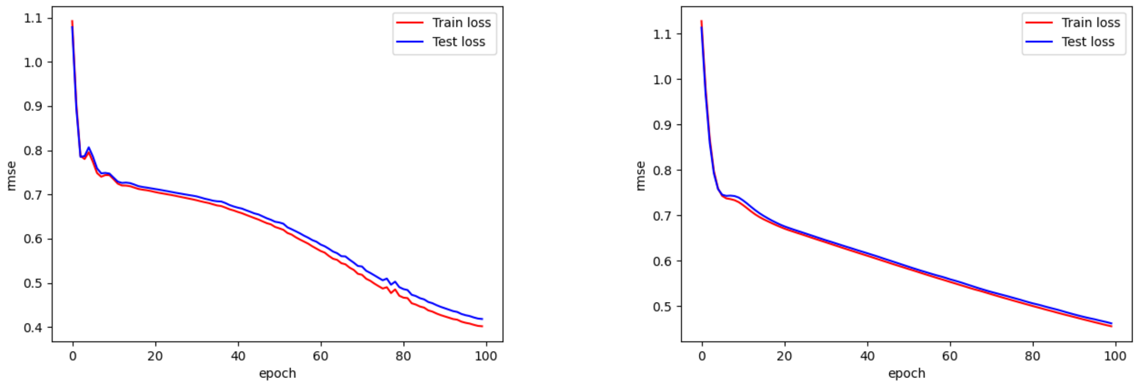

(a) **(b)**

Figure 4.15: Training and testing RMSE convergence for the intermodal cost prediction model. (a) shows slower stabilisation with minor oscillations (suboptimal hyperparameters), (b) demonstrates smoother convergence and minimal train-test deviation, indicating improved generalisation to unseen routing scenarios across the 15 node intermodal corridor (optimised parameters).

The SARSA-based reinforcement learning agent demonstrates substantial improvements over static routing methods as it dynamically adapts to disruptions, learns to minimise congestion-induced costs and shows robust predictive capability regarding freight flows and network conditions. Together, these results support the conclusion that SARSA is an effective and interpretable choice for congestion-aware intermodal transport optimisation.

4.1.5 Congestion on transport infrastructure

Game-theoretic modelling provides a powerful framework for analysing transport network vulnerabilities under adversarial conditions. [79] formulated transport network vulnerability measurement as a two-player zero-sum game, where a network coordinator minimises total system travel time while a hypothetical attacker maximises it by selectively degrading link capacities. Their model emphasises the importance of considering strategic interactions between defenders and attackers, applying bi-level optimisation techniques and MinMax formulations. This game-theoretic perspective is highly relevant for congestion games as well, where each player (agent) competes for optimal paths in a shared, dynamically evolving network. Consequently, concepts from attacker-defender games offer valuable insights for understanding decentralised equilibrium outcomes and resilience strategies in congestion-affected transport networks.

Two scenarios of intermodal optimisation in road transport are shown in Figures 4.16 and 4.17. The first route (orange route) follows a longer inland (road) trajectory between Rijeka and the coastal cluster (Piran, Koper). This path reflects a baseline or unoptimised route, influenced by default road priorities or congestion avoidance behaviour. The route has more curves and traverses inland Slovenian territory, indicating higher fuel consumption, delays, and emissions due to longer distances and elevation changes. The second scenario (green route) shows a more direct and efficient route, optimised for eco-efficiency, fuel economy, and overall costs. This alternative path sticks closer to the coastal alignment, combining rail segments to reduce truck dependency. Routing is smoother and closer to trade corridors, suggesting cost minimisation and time-efficient transit was prioritised.

The green route represents the outcome of applying a congestion-aware reinforcement learning agent or in other terms, a resilience-based congestion game optimisation. The algorithm learned or computed that minimising transport cost, delay, or network vulnerability involves using shorter links with lower cost per TEU, avoiding congested inland and terminal bottlenecks prioritising reliable intermodal infrastructure near the coast. The second route shows the optimised routing outcome after applying the cost-minimisation algorithm. One node is excluded because its capacity–demand ratio fell below the allocation threshold, making its operation inefficient compared to nearby terminals. The optimisation procedure automatically redistributed that node's freight demand to Koper, which had higher handling capacity and better route accessibility. The resulting path is shorter, more direct, and reflects load consolidation and cost-efficient scheduling even though one more truck is added to the transport plan. The orange route, although initially perceived as a default path, suffers from rising marginal costs as more agents choose it and this is a classic congestion effect called the price of anarchy.

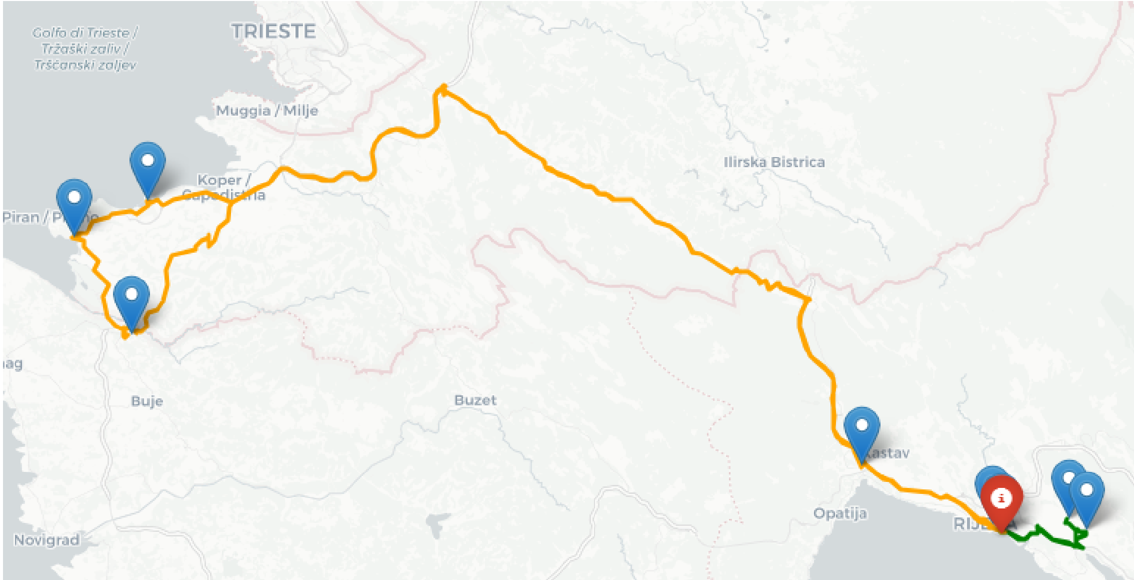

Figure 4.16: Routing freight deliveries in a road network.

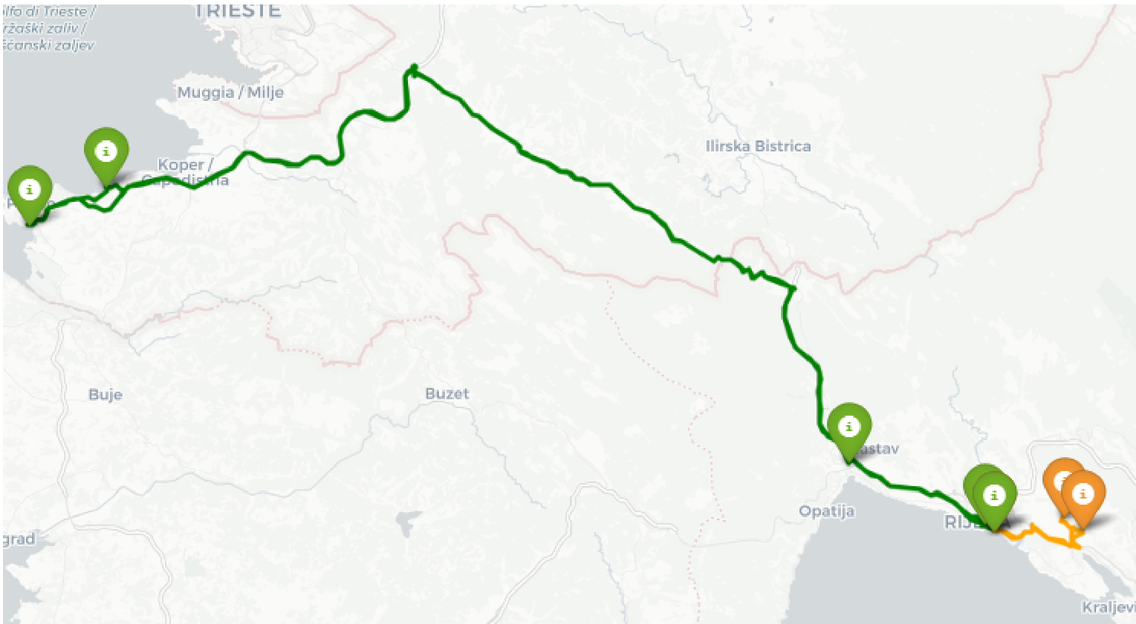

Figure 4.17: Routing freight deliveries in a road network with minimising costs and redistributing capacities.

In a non-cooperative congestion game, equilibrium is reached when no single agent can improve its payoff by unilaterally switching routes. Not all paths are feasible, and comparison of path distributions of agents' choice under varying congestion and resilience factors are shown in Figure 4.18. This result supports the idea that resilience-aware routing can guide agents toward safer paths, while congestion aversion ensures network balance. Fine-tuning these parameters offers a strategic tool for managing intermodal traffic under disruption. When μ increases, agents prefer more resilient paths. When λ increases, agents avoid congested paths.

The green route becomes part of a Nash equilibrium if:

$$C(s_i^{green}, s_{-i}) \leq C(s_i^{orange}, s_{-i}) \forall i \tag{4.11}$$

The observed routing shift from the road-dominant (orange) path to the rail (green) route is not only an operational improvement but also a payoff-maximising strategy in a congestion game setting. The reinforcement learning agent or equilibrium game framework effectively identifies and converges to this strategy under realistic congestion, cost, and disruption scenarios. The routing optimisation demonstrates that incorporating real-time traffic conditions, the resilience parameter, and intermodal efficiency metrics leads to significantly improved performance over conventional route planning. These results support the use of RL-based or game-theoretic strategies in modern intermodal logistics, especially for eco-efficient and disruption-resilient planning between key NAPA ports.

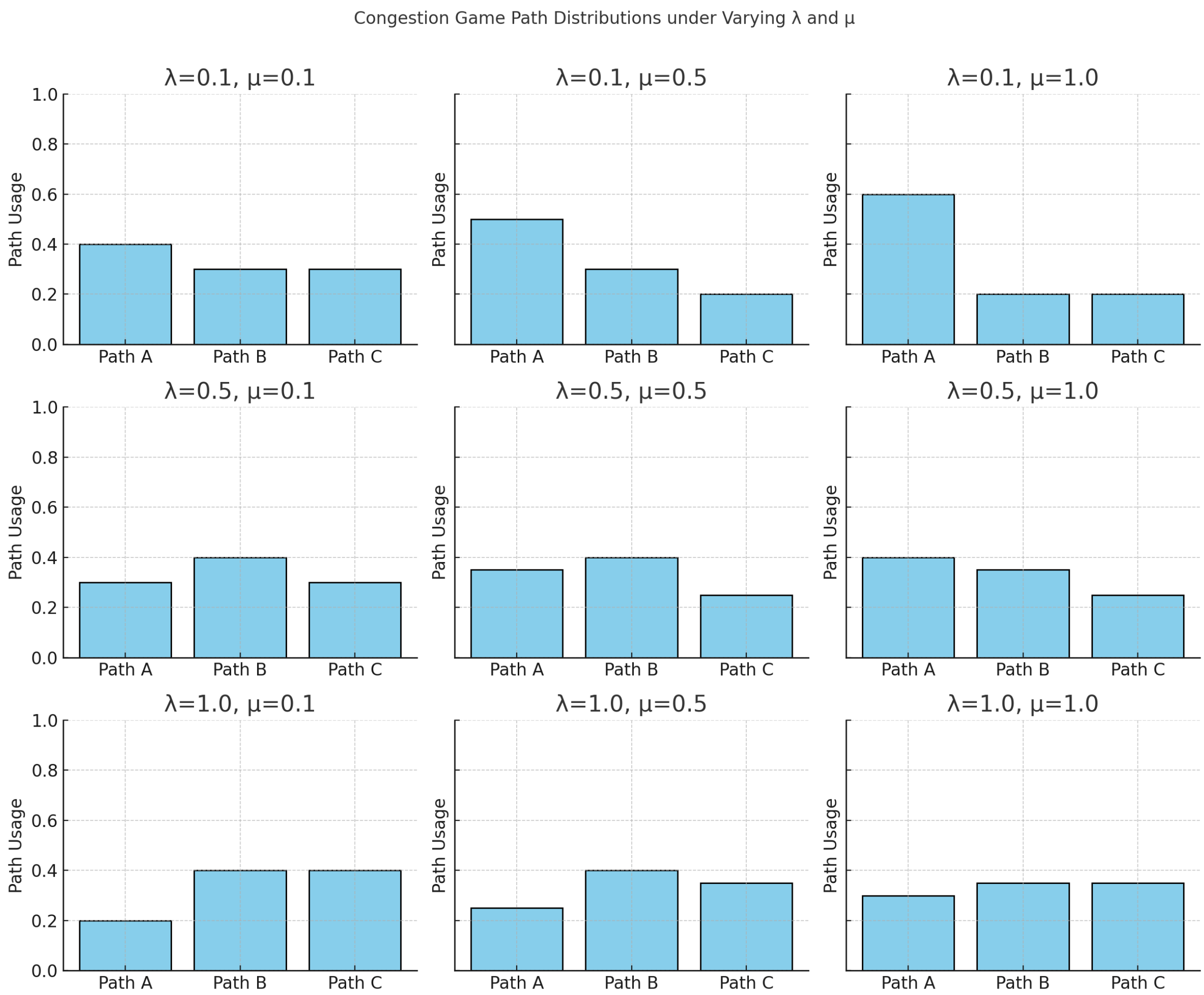

Figure 4.18: NAPA ports to Budapest path choice distributions under different congestion and resilience factors.

4.2 Cooperative Game Theory

In a cooperative game, sets of players can join together to form a coalition and then make a binding agreement regarding which strategy each person in the coalition will play and how they will share the resulting payoffs. On the other hand, non-cooperative games are those in which players act independently in pursuit of their own self-interests. Cooperative GT focuses on the possible outcomes that rational players might agree on. The goal of the cooperative GT is to predict the outcomes of a cooperative play in a way [117]:

- which coalition to form
- the actions each member of the coalition takes
- how the coalitions' payoffs will be distributed.

Conclusively, a cooperative game is a strategic interaction among coalitions. Once a player signs on to join a coalition under specific terms, it's not possible to change the agreement. Thus, the focus is on transferable utility games, where the allocation of the members' collective payoffs paid to the coalition as a whole can be reached.

4.2.1 Coalitions

In a cooperative game any subset of players can join together and play the game as a unit, rather than requiring that player acts as an independent decision maker. These subsets of players are what it's called coalitions. The first step is to consider the possible coalitions of players that can form and the joint payoff that they can share if they join forces.

Consider a set of n players. A coalition of players S is a subset $S \subseteq \{1,...,n\}$. If the number of players in a coalition exceeds the number 15, computational time increases exponentially (Figure 4.19). Note that the full set of all n players may comprise a coalition, which is called the grand coalition, and that a coalition may consist of a single player. The game's characteristic function is a function $v : 2^n \to \mathbb{R}$ that maps each coalition of players to a payoff.

Prisoner's Dilemma

Risk decision-making involves a situation in which several relevant conditions are likely to be known to decision-makers (if not known, it is assumed that they can be reasonably estimated with reasonable probability). The criterion for choosing a variant in such situations is often the expected value of utility. In GT, deciding on conditions of uncertainty is a game against nature. Kahneman [118] claims that risk aversion is the predominant occurrence in the gain domain and risk-seeking is in the loss domain. In his research, he also claimed that a reluctance to lose could make people risk a greater loss accordingly to reconciling with a safe smaller

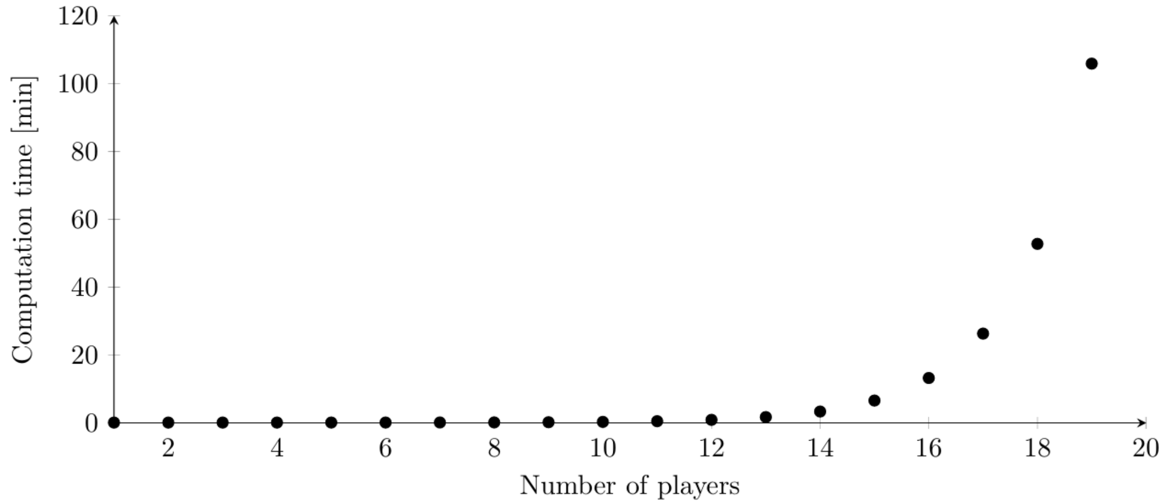

Figure 4.19: Number of players forming a coalition affecting computation time.

loss. That kind of decision-making can be used in transport network planning by adding ponders, which can be generated by multiplying base parameters with capacity, distances, travelling time, etc. Adding extra capacity to the transport network when the moving entities (players) selfishly choose their route can reduce overall performance. In the literature, the appearance of reduced performance is called Braess's paradox, credited to the German mathematician Dietrich Braess [119]. The cause in reduction is that such a system's Nash equilibrium is not necessarily an optimal result. [114]

The game of merging carriers

The characteristic function in a game with the three carrier firms negotiating a merger is shown in Table 4.4. If all three carriers merge for consolidated transport, they attain collective profits of 100 units, if two out of three carriers merge, they attain lower profits, which depend on which firms are involved in the agreement. The value of any single-player coalition is zero since a firm does not profit from the merger if it doesn't participate in the agreement. Cooperative GT can be implemented through various types of real-world business problems. In the following two examples, it will be presented how to distribute a joint payoff. The first example is a bargaining problem where a buyer and seller are considering trading a used car. The buyer values the car at €700, while the seller values it at €300. Going in the direction of a market second buyer is added. The second buyer values the car at €550. All possible coalitions are listed in the first column of the Table 4.9 and the characteristic function shows the greatest surplus that coalition would be able to share if they were joining together and transact. For single-player coalitions, the value is 0, since they do not transact with the other players in the market. If the coalition consists of buyer 1 and the seller, they can achieve a collective surplus of €400. If the coalition consists of buyer 2 and the seller, then their potential surplus

Table 4.4: All the possible coalitions and expected payoffs in the game of merging carriers

S	*v(S)*
∅	0
{A,B,C}	100
{A,B}	90
{A,C}	70
{B,C}	40
{A}	0
{B}	0
{C}	0

is only €250, since buyer 2 has a lower willingness to pay. If the coalition consists of the two buyers only, they won't achieve a surplus, since they are unable to buy the car if the seller doesn't participate. Although both buyers are in the coalition, there is only one seller. Thus, only a single car is available for the buyers to purchase. The value of the grand coalition is €400, which is the maximum surplus that these three players can achieve if the car is traded among them. In some cases, the characteristic function may represent costs associated with each

Table 4.5: All the possible coalitions and expected payoffs in the used car game

S	*v(S)*
∅	0
{Buyer 1}	0
{Buyer 2}	0
{Seller}	0
{Buyer 1, Buyer 2}	0
{Buyer 1, Seller}	400
{Buyer 2, Seller}	250
{Buyer 1, Buyer 2, Seller}	400

possible coalition rather than the value. Players may share their collective costs by forming a coalition. This type of cooperative game with its cost value approximation is the main idea of this dissertation regarding cost sharing in freight transport. In continuation of this research, more complex examples and models will be discussed. The ridesharing problem can also be solved with a cooperative GT approach by minimizing collective costs. Player A is taking a taxi home with his friends, players B and C. For player A it costs €10 to get to his destination, for

B is €5 and for C is €12. Players A and B could share a ride for €12, A and C for €20, and B and C for €14. It can be seen from Table 4.6 that if all three players share a taxi, it costs €25. [117]

Table 4.6: All the possible coalitions and expected payoffs in the ridesharing game

S	*v(S)*
∅	0
{A}	10
{B}	5
{C}	12
{A,B}	12
{A,C}	20
{B,C}	14
{A,B,C}	25

The NAPA ports carriers game

In the next section, the game of NAPA port freight carriers consolidating their shipments is demonstrated. In that game, the payoffs are distributed in the core. The setting of the game is as follows: Rijeka and Koper contribute significantly to reducing costs due to central position and high accessibility of the terminal. Trieste supports alternative routing under congestion, but with slightly lower marginal gain. Venice, while important, has limited intermodal throughput capacity, yielding the lowest payoff share. The allocation incentivises investment in Rijeka and Koper for centralised resilience functions, coordinated routing via Trieste in case of Rijeka or Koper overload and targeted improvements in Venice for high-value cargo.

4.2.2 The Core: distributing payoffs

The characteristic function defines the cooperative game and tells us the payoff that each coalition would share amongst involved players. To predict the outcome, two questions arise:

1. Which coalitions will be formed?

2. How to distribute payoffs among members of a coalition?

In *superadditive* games, the value of a coalition is at least equal to the sum of its parts. A game is superadditive if for any two disjoint coalitions S and T, $v(S \cup T) \geq v(S) + v(T)$. The grand coalition is the most efficient when a game is superadditive and it can be predicted if the players will form a single coalition, cooperate or pool their payoffs. To distribute these payoffs

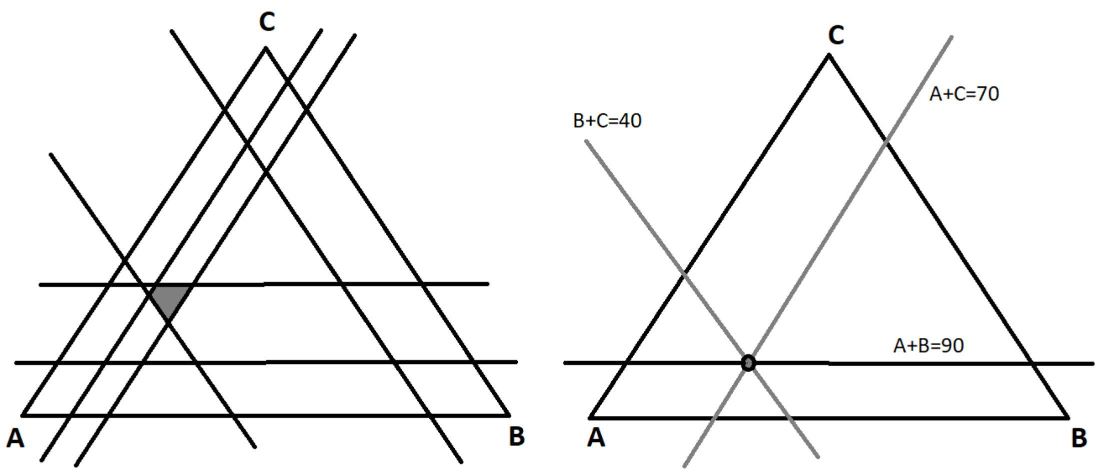

Figure 4.20: The core in the three-player imputation example and merger game to the right

from the grand coalition in an n-player game, a payoff vector $x = (x_1, ..., x_n)$ assigns a payoff to each of the n players. In cooperative GT, there are several solution concepts, which often predict different payoff distributions. Two most common are the *core* and the *Shapley value*. In non-cooperative GT, the standard solution concept is the Nash equilibrium with its associated versions for incomplete information and sequential games. [115], [15]

The core is the set of all imputations that cannot be blocked by any coalition. Imputation is an allocation satisfying both individual and collective rationality if:

1. $x_i \geq v(\{i\})$ for all players i (individually rational)
2. $\sum_{i=1}^{n} x_i = v(\{N\})$ (collectively rational)

An imputation is in the core if there's no set of players that could do better by forming a coalition and redistributing its value.

An imputation x is in the core if and only if: $\sum_{i \in S} x_i \geq v(\{S\})$ for every coalition S.

The distribution of the joint payoff can be presented graphically. In a three-player game from Table 4.4, the way of sharing the grand coalition's value as a triangle is represented in Figure 4.20. The dark interior represents the ways of sharing the surplus between the three players. The farther the player's point is, the less is allocated. The lines represent inequalities. In the example of a merger game, the value of the grand coalition is 100, thus $x_A + x_B + x_C = 100$. Every member has to achieve non-zero payoffs to satisfy individual rationality. To be in the core, the allocation must satisfy three additional conditions $x_A + x_B \geq 90, x_A + x_C \geq 70, x_B + x_C \geq 40$. There is a unique core allocation if solving these conditions simultaneously, $(x_A, x_B, x_C) = (60, 30, 10)$.

In the three-person used car game from Table 4.9, a distribution of payoffs between players $(x_{Seller}, x_{Buyer1}, x_{Buyer2})$ is in the core when following constraints are:

$$x_{Seller} \geq 0, x_{Buyer1} \geq 0, x_{Buyer2} \geq 0$$

$$x_{Seller} + x_{Buyer1} \geq 400, x_{Seller} + x_{Buyer2} \geq 250, x_{Buyer1} + x_{Buyer2} \geq 0$$

$$x_{Seller} + x_{Buyer1} + x_{Buyer2} = 400$$

Any distribution that gives the Seller less than €250 would be blocked by the coalition of the Seller and Buyer 2. Another way to consider this game is if it's presented as a very small market. Figure 4.21 shows the demand and supply curves and the intersection of those curves is a competitive equilibrium in this market. Generally, the competitive equilibrium in a market is always in the core and this is just one example of applying the core solution concept. [117]

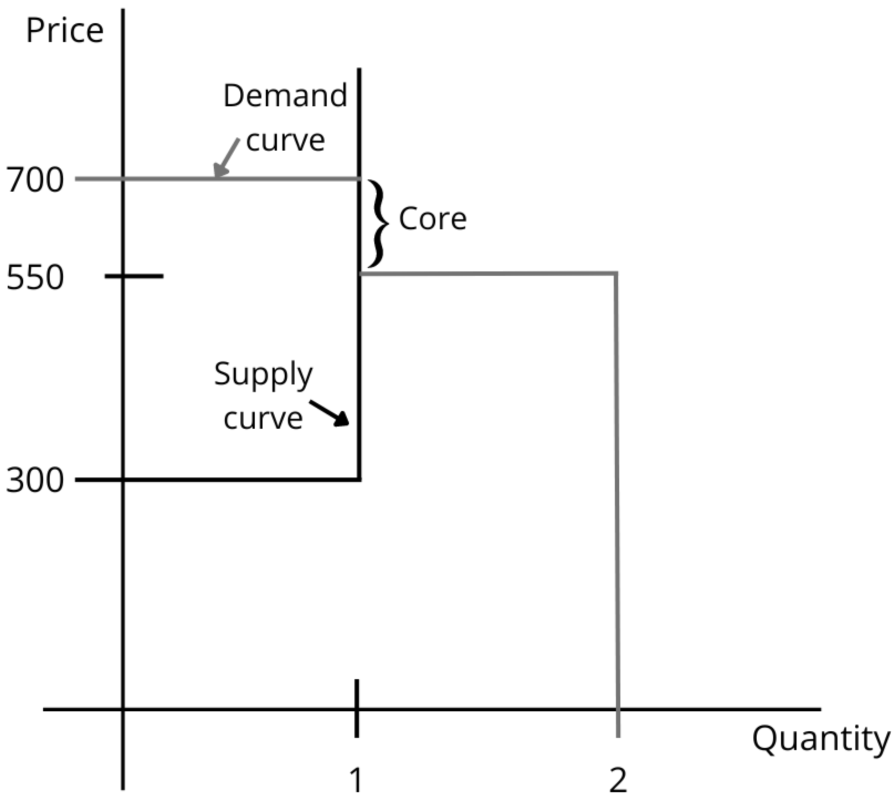

Figure 4.21: The core or competitive equilibrium in the three-player used car game

4.2.3 Shapley value

Lloyd Shapley in 1951 devised a means of computing a value for each player, based on the average marginal contribution the player makes to any coalition he could join. The Shapley value assigns a unique distribution of payoffs in any cooperative game, unlike the core. Shapley value should not necessarily be in the core as there may be players who could make better off by opting out of receiving their Shapley value and forming their own coalition. [120] Its numerous applications covered by [121] show its importance across many fields.

Let's consider a cooperative game with a set N of n players and the characteristic function v. The Shapley value assigns an amount to each player i in N equal to

$$\phi_i(v) = \sum_{S \subseteq N \setminus \{i\}} \frac{|S|!(n-|S|-1)!}{n!} [v(S \cup \{i\}) - v(S)] \tag{4.12}$$

where:

- N is the set of all players,
- n is the number of players,
- S is a subset of N that does not include player i,
- v is the characteristic function that assigns a value to each coalition S,
- $|S|$ is the number of players in coalition S.

The Shapley value satisfies a number of beneficial properties. Shapley proved that it is the only distribution that simultaneously satisfies the following four axioms [120]:

- *Efficiency.* The grand coalition consists of the sum of payoffs: $\Sigma_{i=1}^{n} x_i = v(\{N\})$
- *Symmetry.* If two players are always contributing the same to any coalition, they will receive the same payment.
- *Additivity.* This axiom is satisfied if each agent's payment in the combined game consisting of the same set of agents is equal to the sum of his payments in the two separate games.
- *Dummy player.* This axiom is satisfied if dummy players are always allocated the amount that they could receive without the coalition. Meaning, player i is a dummy player if always contributes exactly $v(\{i\})$ to any coalition he may join.

The Shapley value in the NAPA ports game

Modelling the NAPA port interactions as a cooperative game allows for fair and transparent cost allocation, encouraging strategic alliances between ports. Using Shapley values ensures an equitable distribution based on marginal impact, and analysing the core ensures coalition stability, ultimately guiding policy toward regionally resilient and efficient intermodal logistics. The cost/payoff values per port are derived from the following cost components:

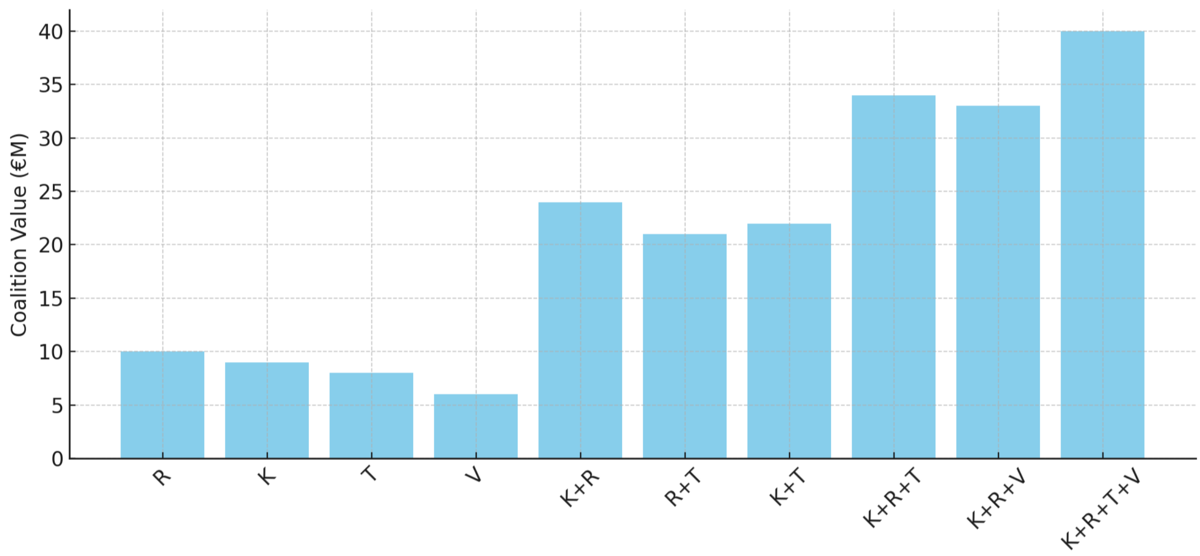

Figure 4.22: Port coalition values

$$\text{Total Cost}_{\text{port}} = C_{\text{handling}} + C_{\text{routing}} + C_{\text{emissions}} + C_{\text{delays}} + C_{\text{inefficiencies}} \tag{4.13}$$

Where each component is modelled as:

Cost type	**Formula**
Handling	$C_h = \text{THC} \times \text{TEUs handled}$
Routing	$C_r = \frac{€}{\text{km}} \times \text{total km (TEU-km)}$
Emissions	$C_e = \text{CO}_2 \text{ cost/ton} \times \text{CO}_2 \text{ emissions (kg)}$
Delay	$C_d = \frac{€}{\text{hr}} \times \text{total time lost due to congestion}$
Inefficiency	$C_i =$ € cost from underused capacity or empty return trips

Table 4.7: Operational cost components for cooperative game payoff analysis

The core consists of payoff distributions (x_R, x_K, x_T, x_V) such that (Figure 4.22):

$(x_R, x_K, x_T, x_V) = v(N) = 40$

$$\sum_{i \in S} x_i \geq v(S) \forall S \subseteq N$$

If the Shapley allocation lies within the core, the grand coalition is stable, meaning no subgroup of ports has an incentive to break away, as they wouldn't get more value independently. These values in Figure 4.23 reflect how much value each port receives when collaborating in a grand coalition, where all ports:

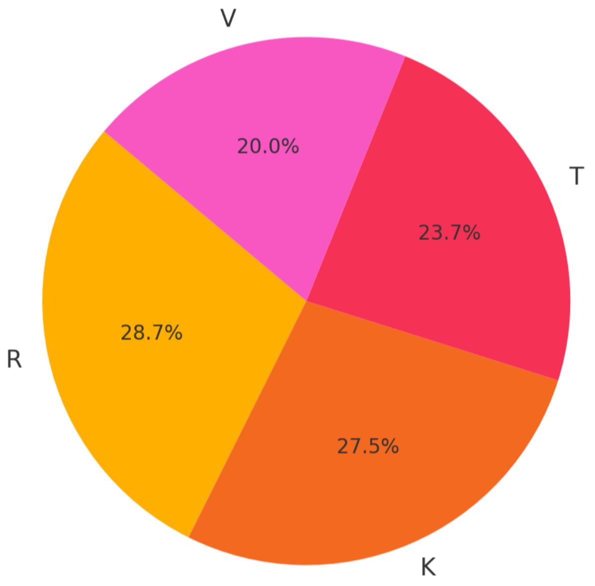

Figure 4.23: Shapley value allocation among NAPA ports

- Coordinate rail and road capacities,
- Optimise terminal utilisation,
- Route flows based on system-wide congestion metrics,
- Share investments in hinterland logistics (dry ports and inland terminals).

These are effectively the payoffs (negative of cooperative costs) the ports receive for participating in a joint intermodal planning alliance. They are derived from how much each port contributes to cost savings when added to various coalitions. Koper's cooperative share of €11M means that, when collaborating, it contributes sufficiently to network-wide optimisation to justify receiving that portion of the shared value. In this case, the small adjustment is needed to ensure core stability:

$\phi_R + \phi_K = 22.5 > v(\{R, K\}) = 24$

The Shapley value in the used car game

From the previous example from Figure 4.21 where is presented that any allocation in the core must give the Seller between €250 and €400 of the €400 surplus, where Buyer 1 gets the remainder and Buyer 2 gets 0. Since in one of the six scenarios, Buyer 2 makes a positive contribution to the coalition, the Shapley value in contrast gives him a positive share, which is shown in Table 4.8.

Table 4.8: Calculations of Shapley value in the used car game

Order	Seller	Buyer 1	Buyer 2	Total
Seller, Buyer 1, Buyer 2	0	400	0	400
Seller, Buyer 2, Buyer 1	0	150	250	400
Buyer 1, Seller, Buyer 2	400	0	0	400
Buyer 1, Buyer 2, Seller	400	0	0	400
Buyer 2, Buyer 1, Seller	400	0	0	400
Buyer 2, Seller, Buyer 1	250	150	0	400
Average	**241.67**	**116.67**	**41.67**	**400**

4.2.4 Case study – Used vehicle price prediction in Croatia

The data are collected from the retail web portal Njuskalo.hr. The following attributes are stored for each used car: manufacturer, kilometers traveled, selling vehicle price, and year of production. Since manual data collection is a time-consuming task, especially when there are numerous records for processes, a web scraper was created as a part of this research to perform data mining automatically, thereby reducing data collection time. This research did not include vehicles manufactured before 2010. After the raw data were collected and stored in a local database, the following steps were implemented through this research (Figure 4.24).

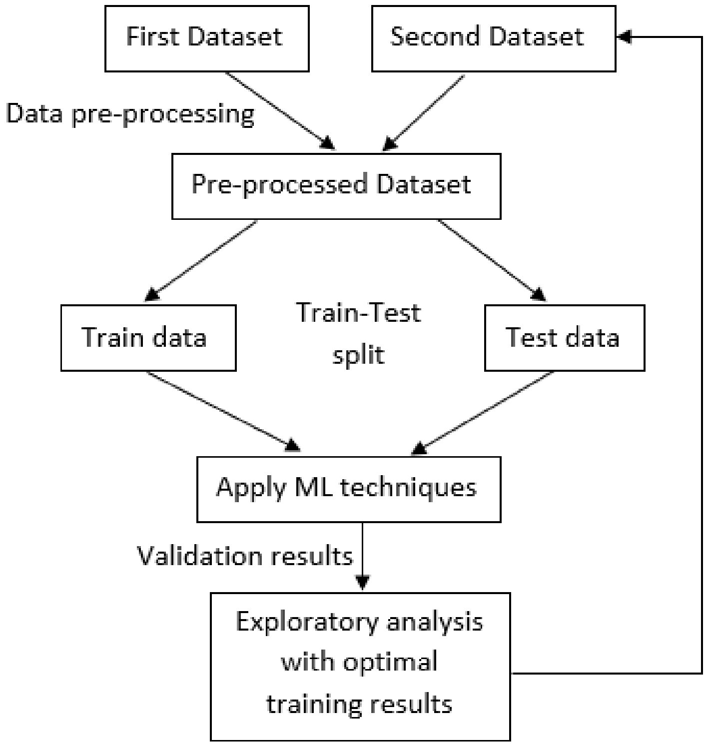

Figure 4.24: Flow diagram of the supervised machine learning methodology.

The model was trained with two data sets of used cars for the price prediction and classification of vehicles from the online retail web page. Various statistical tools were used to analyse the dataset, including the SAS program for parameter explanation and correlation, and Matlab Regression Learner for training. The effectiveness of regression analysis results always relies on the various conditions related to the nature of the data features that are entered into the model. Therefore, it is necessary to check in advance whether the regression assumptions are violated before making any decision about the usefulness of the regression model. The initial results show a drop in vehicle prices with respect to the trained parameters and a prediction accuracy of 21,9 %, which confirms other works predicting the prices of used vehicles in European countries. It is important to note that the mentioned works and trained data are in the period of stability of the market supply of energy products. Prediction accuracy increases with training and validation of the model with the second data set, where price growth is predicted by linear regression with a prediction accuracy of 95%. The experimental analysis shows that the proposed model is incorporated as an already optimised model, and with all the regressors used, an increase in prices and a decrease in the value of kilometres travelled are predicted, regardless of the year of production. The average value of the data set is a personal vehicle with 130,000 km traveled and a price of EUR 10,000. An additional method for validating the trained data, support vector machines (SVM), is used to predict the price of used cars with higher accuracy than regression models, such as multiple and multivariate regression. The best R^2 score and

RMSE by regressors are listed in the following Table 4.9. [54]

Table 4.9: Regression analysis validation results.

Model	**R^2 Value**	**RMSE**	**MAE**
Linear regression	0,95	2104.7	1373.2
Random forest	0,24	14,627	7946.5
SVM	0,59	9173.9	5950.2

4.2.5 The Shapley value in risk estimation and performance features

An intuitive way to understand the Shapley value is the following illustration, the feature values enter a model in random order. All feature values in the model participate in the game (contribute to the prediction). The Shapley value of a feature value is the average change in the prediction that the coalition already in the model receives when the feature value joins other features. All possible coalitions (sets) of feature values have to be evaluated with and without the added feature to calculate the exact Shapley value. For more than a few features, the exact solution to this problem becomes problematic as the number of possible coalitions exponentially increases as more features are added. The SHAP framework is obtained as:

$$f(x) = \mathbb{E}[f(X)] + \sum_{i=1}^{n} \phi_i \tag{4.14}$$

where each ϕ_i quantifies how the i-th trucking feature (for example distance of vehicle 631199) shifts the expected prediction $\mathbb{E}[f(X)]$ toward the actual predicted outcome.

In this case:

- x_i - kilometres travelled per vehicle.
- $f(x)$ - predicted total route cost score.
- $\mathbb{E}[f(X)]$ - average model output across all trips (approximately 4.654).
- ϕ_i - marginal influence of each truck's trip parameters on that specific prediction.

SHAP plot (Figure 4.25) is useful in determining how different values (low or high) of a feature affect the overall output. This SHAP waterfall plot explains how individual vehicle trips (features) influence the predicted freight cost or performance output f(x)=4.871, starting from the model's average expected value E[f(X)]=4.654. Each bar represents the marginal contribution of a specific truck (identified by its vehicle ID) based on its travelled distance in kilometres and related operational data. Red bars (positive contributions) increase the predicted outcome, these vehicles operated under higher cost. Blue bars (negative contributions) reduce the prediction, these vehicles operated with lower costs (safer drivers).

The method to estimate the risk in drivers has a set of parameters:

- experience years,
- age of the driver,
- accidents in the previous year,
- kilometres driven previous year,
- risk level.

The risk level is obtained in the section 3 in Table 3.2. Next, features and targets are defined, or continuous and categorical variables to check for correlation between the parameters. When dataframe is prepared for training, the division in training and testing data is needed. Test size is 30% of the dataset. Predicted and actual risk levels of drivers are compared, so the demand for containers can be added to allocate the expensive insured cargo to low risk drivers. Ranking of containers by value (higher value containers first) is needed to distribute it to the low risk drivers.

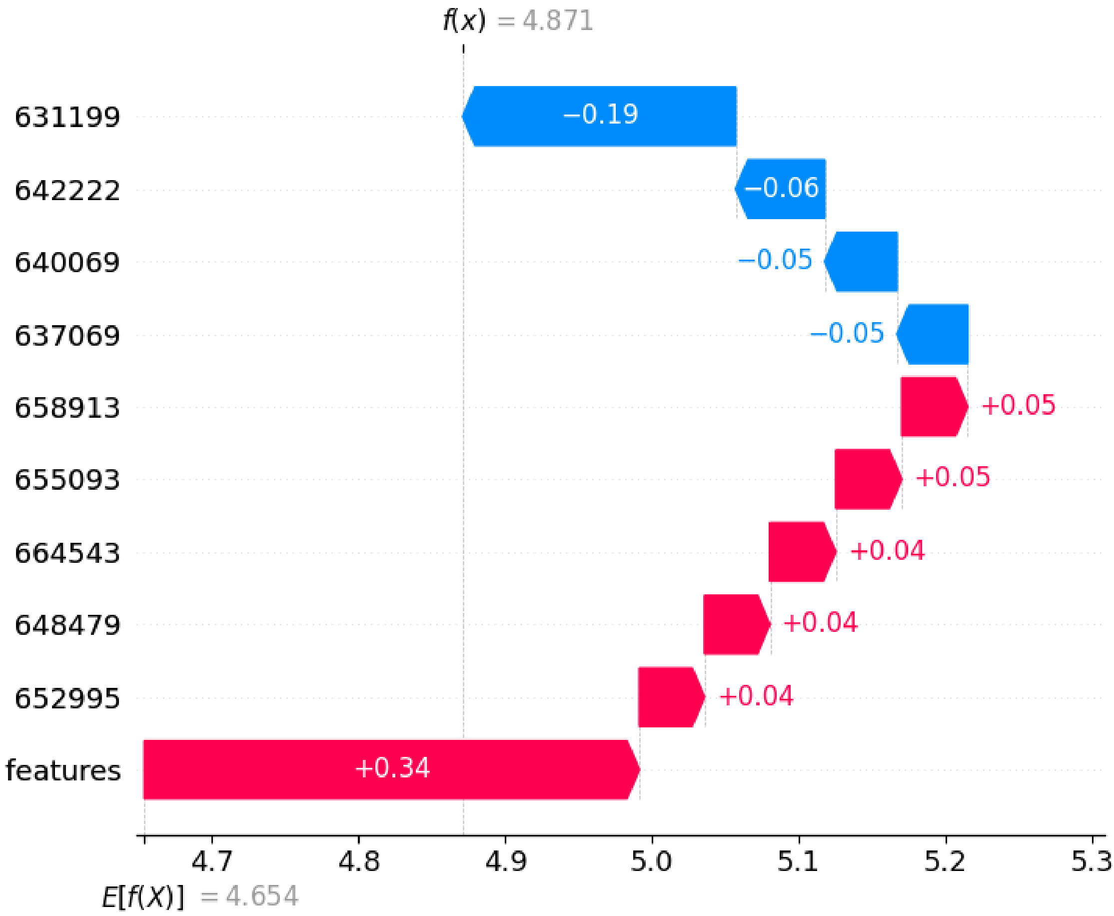

Figure 4.25: Deviations of added features from the joint equilibrium of a coalition.

The problem of crane allocations is also possible with the extraction of the most important features with the Shapley value. To quantify how much each crane (agent) contributes to reducing total waiting time, congestion, fuel or emission costs, and episode duration or reward, Shapley value is used. It's already computed for the ports, and how much every port contributes to the decrease of the total costs and capacity planning. In this case, first we need to simulate multiple combinations of crane subsets (or coalitions). Then, evaluation of the total cost of each crane with using a Shapley value calculator (shap library). The calculated Shapley values are listed in 4.10 showing each crane agent's contribution to the overall system performance in MARL simulation in 4.8. These values help quantify which cranes are most critical in reducing total cost and improving efficiency.

Table 4.10: Shapley values for crane agents in MARL simulation

Agent (crane ID)	Shapley value
Q0	0.1747
Y0	0.1494
Q1	0.1280
Q2	0.1264
Y1	0.1227
Q4	0.1044
Q3	0.0944

For the purpose of automatically computing Shapley values of the cranes, maps of NAPA ports are uploaded into the application with the possibility of positioning the crane markers. When all the cranes are located (Figure 4.26), the type of the cranes needs to be defined (yard, rail-mounted or quay) to calculate their contribution to overall port operational efficiency. The results of this game setting are shown in Table 4.11. This reflects that the rail-mounted crane (C1) is currently the most impactful in improving overall port efficiency under the coalition scenarios.

Table 4.11: Shapley values for crane agents in Brajdica container port simulation

crane ID	Type	Latitude	Longitude	Shapley value
C1	Rail-mounted	45.319338	14.456892	0.33
C2	Yard	45.320183	14.452268	0.27
C3	Quay	45.320455	14.450862	0.30
C4	Yard	45.319685	14.454950	0.27

4.3 Framework of a game model

Given the dependence of society on transport, it is important to assess system vulnerability points to manage risk and reduce disruption. As the transport network vulnerability is not limited only to terrorist attacks, but also nature disasters and vehicle accidents. These disruptions decrease the serviceability of transport networks or even paralyse certain portions. To address the vulnerability, the analysis of risk would be the first consideration. Berdica [74] defines risk as generally associated with negative consequences in the life of a population, their health and environmental impacts. Computational issues quickly arise as networks approach a realistic size, which has led to most game-theoretic approaches being applied to single OD

Figure 4.26: Brajdica port map with crane placement for Shapley value computation.

pairs. The issues are centred on the need to maintain and update all pair's shortest paths for each iteration to accommodate the increased costs of edges chosen for disruption by the agent. This problem increases by the analyst attempts an equilibrium assignment by the agent at each iteration, though equilibrium would provide a more realistic assignment.

Authors in [122] and [123] proposed a game theory approach to measure transport network vulnerability, developing a mixed strategy stochastic game for vulnerability assessment. The approach envisions a game between two players, the agent who seeks minimum-cost paths for vehicles and the carrier who seeks to maximise the cost of the trip. The Nash equilibrium is the point at which no player can improve their benefit by unilaterally changing their strategy. [79]

Algorithm 4.1 MinMax vulnerability simulation ([79])

Transport network $G = (N, L)$, link capacities c_l, BPR parameters (α, β)
Most vulnerable link and its corresponding total cost
Initialise disturbance probabilities $y_j \leftarrow \frac{1}{|L|}$
Initialise flow assignment x_i with system-optimal routing
Set iteration counter $k \leftarrow 1$
repeatx_i, y_j converge
for each link $j \in L$ reduce capacity: $c_j \leftarrow \gamma \cdot c_j$ compute new system-optimal flow $x_i^{(j)}$
compute cost: $C_j \leftarrow \sum_i x_i^{(j)} \cdot t_{ij}(x_i^{(j)})$
$j^* \leftarrow \arg\max_j C_j$ $\tilde{y}^{(k)} \leftarrow$ one-hot vector with 1 at j^* $y^{(k)} \leftarrow y^{(k-1)} + \frac{1}{k}(\tilde{y}^{(k)} - y^{(k-1)})$
solve flow assignment $x^{(k)}$ under updated $y^{(k)}$ $x^{(k)} \leftarrow x^{(k-1)} + \frac{1}{k}(\tilde{x}^{(k)} - x^{(k-1)})$
$k \leftarrow k+1$
return link j^* with maximal C_{j^*}

Holme et al. [75] proposed a general method to evaluate the most critical links/nodes of a network by measuring the network's performance by deactivating certain components of a network. In their method, a generic infrastructure is modelled as a function to measure its performance, and the most critical damage as the one that minimizes the performance of this function. Radu et al.[124] adopted this idea and proposed a heuristic method incorporating a user equilibrium assignment procedure to assess the importance of multi-agent systems implementation in urban transport planning. This work benefits from a user equilibrium assignment procedure, giving results that they acknowledge are counterintuitive while being correct. The procedure ranks edges based on a criticality function that is derived from the difference in system travel time with and without an edge. Generally, this approach allows for a comprehensive treatment of single-edge removals, however, the problem size grows exponentially if combinations of multiple edges are considered for removal. In order to further reduce the computational burden associated with the full network scan approach, authors in [125] and [126] pre-select potential vulnerable links based on certain strategies and only conduct analysis on these pre-selected links. The potentially vulnerable links can either be part of a minimum cost path between O-D nodes, or the links with high choice probabilities, calculated by the stochastic traffic assignment. Modelling travellers' behavioural responses to link failure is another key issue involved in critical link identification. Demand variations due to link closure have been well evidenced in many empirical studies, such as bridge collapses and similar infrastructure disruptions. Under such a situation, the high degree of demand uncertainty will inevitably yield travel time variability and consequently impose additional disutility on travellers. Many empirical studies have revealed the significant influence of travel time uncertainty on travellers' route choice behaviour. Travellers under travel time uncertainty tend to choose the reliable shortest path, not only dependent on travel time saving but also on reduction of travel time variability. This risk-taking behaviour under demand and travel time uncertainty has received considerable attention in the transport network reliability analysis. However, such demand variations and associated travellers' risk-taking behaviour due to link closures have not yet been considered in the studies of critical link identification. [78]

4.3.1 Stochastic optimisation

There are numerous contributions to the broad area of modelling and solving sequential decision problems, but there are two that stand out: optimal control (the foundation for stochastic optimal control), and Markov decision processes (MDP), which provided the analytical foundation for reinforcement learning. Although these fields have intersected at different times in their history, today they offer contrasting frameworks which, nonetheless, are steadily converging to common solution strategies. In the following sections, the modelling frameworks of (stochastic) optimal control and reinforcement learning are presented (drawn from Markov decision processes), which are polar opposites. [103]

4.3.2 Container booking cost model

While categories of model-based approaches have achieved significant progress over the past few years, their performance inevitably suffers from complexity because of the large observation space. Raw observations may contain information unnecessary for planning, such as dynamically changing backgrounds in visual observations that are irrelevant to their value or utility function. The unified mathematical framework is quite close to other frameworks used by stochastic optimal control models with just a few adjustments. [127]

The novel approach used in this research, which combines model-based and model-free RL, can be useful for learning better abstract-state representations and reducing sample complexity in real use cases. The model-free part of the unified framework is based on learning the dynamics of abstract states or environments which makes computing future rewards possible, and the model-free part maps the learned abstract states to rewards and values. Bi-level optimisation technique is used in stochastic environments. In this case, first level decision variables are independent variables, such as terminals, modal shift options, transport infrastructure and associated capacities. The second level represents variational variables which depend on different scenarios generated. The two-level optimisation is important because of the two different objective functions. The first one minimises the total cost, and the second maximises the capacities transported.

In cooperative cases where Shapley values are computed for two different domains, driver risk estimation $\phi_d(k)$ and crane agents allocation $\phi_c(i)$, priority mechanism for a joint decision-support is proposed. Crane Shapley values reflect infrastructure contribution to port efficiency and risk driver Shapley values reflect risk exposure or reliability impact on transport process. Each set of values is normalised:

$$\hat{\phi}_c(i) = \frac{\phi_c(i)}{\max_j \phi_c(j)} \quad , \quad \hat{\phi}_d(k) = \frac{\phi_d(k)}{\max_l \phi_d(l)} \tag{4.15}$$

A joint or composite priority score $P(k,i)$ is computed for each driver–crane pair as:

$$P(k,i) = \lambda \cdot (1 - \hat{\phi}_d(k)) + (1 - \lambda) \cdot \hat{\phi}_c(i) \tag{4.16}$$

where $\lambda \in [0,1]$ is a weight determining the importance of driver risk relative to crane performance.

The priority score for truck assignment to the cranes is used to offer a discounted container booking cost:

$$\text{Cost}_{k,i} = \text{Base cost} \cdot (1 - \gamma \cdot P(k,i)) \tag{4.17}$$

with:

- Base cost = 1000 EUR,
- $\gamma = 0.25$ is a discount coefficient,
- Higher priority scores yield lower booking costs.

Table 4.12: Booking costs [EUR] for each driver–crane pair

Driver \ Crane	**C1**	**C2**	**C3**	**C4**
D1	879.81	897.99	888.90	897.99
D2	859.62	877.80	868.71	877.80
D3	833.65	851.84	842.74	851.84
D4	900.00	918.18	909.09	918.18

Table 4.12 presents the results. Lower-risk drivers (D3) receive higher-cost bookings, while high-risk drivers (D4) are incentivised through lower-cost assignments if matched with high-performing cranes (C1). This system encourages better pairing of logistics resources while promoting efficient and fair access to port services. The Shapley-based booking cost model is directly embedded into a MARL environment where each agent learns its optimal policy considering both its own objective and systemic fairness incentives.

Each truck driver and each crane are represented as independent agents. State includes agent position, queue status, crane availability, congestion, and previous risk level. Action is to select a crane (driver) or schedule a driver (crane agent). Reward is defined as the negative of the Shapley-adjusted booking cost:

$$r_{k,i} = -\text{Cost}_{k,i} = -\text{Base cost} \cdot (1 - \gamma \cdot P(k,i)) \tag{4.18}$$

Each agent learns a policy π^* that minimises its long-term discounted cost while contributing to overall efficiency, which represents the objective of the model.

This setup ensures:

1. High-risk drivers are routed to high-capacity cranes with less congestion.
2. Cranes that contribute more operational value receive higher utilisation priority.
3. The environment evolves toward a cooperative equilibrium where booking decisions reflect both individual optimisation and collective resilience.

Alternatively, the driver–crane assignment can be posed as a weighted bipartite matching problem:

$$\max_{x_{k,i}} \sum_{k \in \mathscr{D}} \sum_{i \in \mathscr{C}} P(k,i) \cdot x_{k,i} \tag{4.19}$$

Subject to:

$$\sum_{i \in \mathscr{C}} x_{k,i} = 1 \quad \forall k \in \mathscr{D} \qquad \text{(each driver assigned once)} \tag{4.20}$$

$$\sum_{k \in \mathscr{D}} x_{k,i} \leq \mathrm{Cap}(i) \quad \forall i \in \mathscr{C} \qquad \text{(crane assignment limit)} \tag{4.21}$$

$$x_{k,i} \in \{0,1\} \quad \forall k,i \tag{4.22}$$

where:

- $x_{k,i} = 1$ if driver k is assigned to crane i,
- $P(k,i)$ is the normalised priority score,
- $\mathrm{Cap}(i)$ is the number of containers crane i can handle.

4.3.3 User Equilibrium in traffic assignments

The route choice problem is the most critical aspect of the traffic assignment problem as it involves multiple behavioural factors, especially in a large-scale network. Trying to capture the reasons behind the selection of paths has always been a challenging task due to the heterogeneity of drivers' preferences. Even under the assumption of similar behaviour of drivers, the model faces many challenges such as route search from a huge set of possible routes in a large-scale network and real-time access and provision of traffic conditions. Vehicles' path-changing routes due to non-recurrent events such as incidents, vehicle breakdowns, and special events require special modelling considerations as most existing models in practice apply pre-defined routes before vehicles' departure. Different equilibrium-seeking models, such as dynamic user equilibrium (DUE), dynamic stochastic user equilibrium (DSUE), boundedly rational user equilibrium (BRUE), multiclass fuzzy user equilibrium (MFUE), prospect-based user equilibrium (PBUE), and behavioural user equilibrium (BUE), adopt unique behavioural assumptions of drivers. On the other hand, drivers' route choice using a probabilistic approach considering utilities of different alternative routes results in the so-called stochastic route choice (SRC) models that do not necessarily seek an equilibrium solution. [26], [128], [5]

In the route choice problem, if there exists a mixed strategy such that no carrier has an incentive to unilaterally deviate, that is, no carrier can strictly decrease his individual latency by unilaterally changing his individual strategy, then the Nash equilibrium is achieved. Such equilibrium is often called optimal route choice strategy, whose definition is given as follows.

Definition. A mixed strategy **p*** is called an optimal route choice strategy, if for all $r \in R$, and all mixed strategies **p**' other than **p***, it holds that latencies l are:

$$l_r(\mathbf{p}*) \leq l_r(\mathbf{p}') \tag{4.23}$$

For carrier $i \in N$ who wants to travel through given transport network, has to choose from the set of the available routes. R_i is also called the action set of carrier i. To accomplish the task that travel through the O-D pair, each carrier i should choose a route from the action set. Thus, the choice of the carriers determines the route load and the link load. Then, the load of route r is defined as the total capacity of the booking request depending on mode or vehicle chosen. For each link $e \in E$, note that e can be shared by different routes, the link load on e is associated with the loads of the routes that are utilised. The link load determines the latencies of all carriers, the loss associated to a link e is given by $l_e(f_e), l_e(\cdot)$ is called the latency function, which is assumed to be nonnegative, strictly increasing, and continuously differentiable for all $e \in E$. Moreover, its derivative $l'_e(f_e)$ is also strictly increasing. The route choice problem considers that there are a large volume of carriers who want to travel through the O-D pairs in traffic network. At a given short time period, there is a group of carriers which need to make route choice decisions among a number of candidate routes, according to the past experiences and real-time traffic information. The routing decision is made by first determining the priorities of candidate routes (a probability distribution), and then picking a route based on the priorities. Consider the scenario that the travelers choose the routes from their action sets randomly, according to a joint probability distribution $\mathbf{p} = \{p_i\}_{i=1}^{N}$, known as mixed strategy, where p_i is a $|R_i|$-dimensional vector, the element p_{ik_i} in p_i denotes the probability of carrier i that chooses the route r_{ik_i}, with $\sum_{k_i=1}^{R_i} p_{ik_i} = 1$. The independency of the joint probability is reasonable, because the carriers are non-cooperative. [60]

Chapter 5

Reinforcement learning in congestion games

Learning behaviours in a multi-agent environment is crucial for developing and adapting multi-agent systems. Reinforcement learning techniques have addressed this problem for a single agent acting in a stationary environment, which is modelled as a Markov decision process (MDP). However, multi-agent environments are inherently non-stationary since the other agents are free to change their behaviour as they also learn and adapt. Stochastic games, first studied in the game theory community, are a natural extension of MDPs to include multiple agents. This chapter is a contribution to a comprehensive presentation of the relevant techniques for solving stochastic games from both the game theory community and reinforcement learning communities. It examines the assumptions and limitations of these algorithms and identifies similarities between these algorithms, single-agent reinforcement learners, and basic game theory techniques.

Building on the previous hypothesis, this chapter addresses the last hypothesis where transport costs can be predicted by applying reinforcement learning in the congestion game using a new resilience parameter. To test this, GAT-based reinforcement learning (RL) framework is developed. It learns to predict optimal cost-effective routing decisions by observing agent-environment interactions within a congestion-affected intermodal network. By embedding the resilience parameter into the state space of RL agents, the model learns on adaptive routing policies that not only minimise cost but also avoid vulnerable nodes, especially under dynamic congestion and disruption scenarios. This chapter presents the architecture, training process, and performance evaluation of the RL model. It further compares its predictive accuracy and routing efficiency against baseline models, validating the hypothesis that resilience-aware reinforcement learning enhances both predictive performance and operational robustness in intermodal systems.

5.1 Reinforcement learning

The field known as reinforcement learning evolved from early work done by Rich Sutton and his adviser Andy Barto in the early 1980's. They addressed the problem of modelling the search process of a mouse exploring a maze, developing methods that would eventually help solve the Chinese game of Go, outperforming world masters. Sutton and Barto eventually made the link to the field of Markov decision processes and adopted the vocabulary and notation of this field. The field is nicely summarised in Puterman (2005) which can be viewed as the capstone volume of 50 years of research into Markov decision processes, starting summarises the modelling framework as consisting of the following elements [103]:

Decision epochs $T = 1, 2, ..., N$.

State space S = set of (discrete) states.

Action space A = action space (set of actions in state s).

Transition matrix $p(s'|s,a)$ = probability of transitioning to state *s'* given that we're in state s and take action a.

Reward $r(s,a)$ = the reward received when in state s and take action a.

This notation (or MDP formal model) became widely adopted in the computer science community where reinforcement learning evolved. It became standard for authors to define a reinforcement learning problem as consisting of the tuple (S, A, P, r) where P is the transition matrix, and r is the reward function. Using this notation, Sutton and Barto [129] proposed estimating the value of being in a state s^n and taking an action a^n (at the nth iteration of the algorithm) with a discount factor γ and a smoothing factor a_n that might be called a stepsize or learning rate.

Therefore, when in state s^n and taking action a^n, it can simulate the transition to a state *s'*. There are two approaches to set up the problem:

- Model-based - transition matrix P and sample *s'* obtained from the probability distribution $p(s'|s,a)$.
- Model-free - observations of the transition to state *s'* without a transition matrix.

This algorithmic strategy is named 'Q-learning' by Sutton and Barto. The wide applicability of the model and algorithmic strategy is present today. In contrast to the core algorithmic step and Bellman's equation which is the foundation of MDP, requires solving the stationary version.

$$\underbrace{\text{New}Q(s,a)}_{\text{New Q-Value}} = Q(s,a) + \underset{\text{New Q-Value}}{\alpha}[\underbrace{R(s,a)}_{\text{Reward}} + \underset{\text{Discount rate}}{\gamma} \overbrace{\max Q'(s',a')}^{\substack{\text{Maximum predicted reward, given} \\ \text{new state and all possible actions}}} - Q(s,a)] \tag{5.1}$$

This equation is known as value iteration and is the basis of Q-learning. In these types of problems, all the actions need to be enumerated and the states these actions lead to. There is no enumeration of all the states. This is a reason why reinforcement learning is often illustrated in the context of relatively small and discrete action spaces (as in the maze problem). For solving purposes, a simulation from state s to state s' using the transition function $f(s,a,\omega)$, there's no need to find a random variable ω. [103]

In RL, policy approximation functions are used to represent the policy when the state or action space is too large to handle with tabular methods. These approximation functions listed in Table 5.1 are chosen based on the problem's characteristics, such as the nature of the state and action spaces (discrete/continuous), the need for exploration, and computational constraints.

Table 5.1: Summary of various types of policies and their approximations in reinforcement learning.

Model of policy	**Definition**	**Example**
Linear function approximation	Represents the policy as a linear combination of features. Suitable for problems with low-dimensional feature spaces.	$\pi(a\|s) \propto \exp(\theta^\top \phi(s,a))$, where $\phi(s,a)$ is a feature vector.
Neural networks (Deep policies)	Uses deep neural networks to approximate the policy. Commonly used in DRL (e.g., Deep Q-Networks, Policy Gradient methods).	$\pi(a\|s;\theta)$ is parameterized by a neural network with weights θ.
Gaussian policies	Represents the policy as a Gaussian distribution over actions. Often used in continuous action spaces.	$\pi(a\|s) = \mathcal{N}(\mu(s),\sigma(s))$, where $\mu(s)$ and $\sigma(s)$ are learned functions.

Continued on next page

Type of Policy	Definition	Example
Softmax policies	Represents the policy as a probability distribution over discrete actions. Commonly used in discrete action spaces.	$\pi(a\|s) = \frac{\exp(Q(s,a)/\tau)}{\sum_{a'}\exp(Q(s,a')/\tau)}$, where τ is a temperature parameter.
Boltzmann policies	A type of softmax policy where the action probabilities are based on the exponential of the action values.	$\pi(a\|s) \propto \exp(Q(s,a))$.
Deterministic policies	Represents the policy as a deterministic function mapping states to actions. Used in deterministic policy gradient methods.	$\pi(s) = \arg\max_a Q(s,a)$ or $\pi(s) = \mu(s)$, where $\mu(s)$ is a learned function.
Actor-critic policies	Combines a policy (actor) and a value function (critic) for approximation.	The actor $\pi(a\|s;\theta)$ is updated using the critic's value estimates.
Mixture policies	Combines multiple policies into a single policy.	$\pi(a\|s) = \sum_i w_i \pi_i(a\|s)$, where w_i are weights.
Hierarchical policies	Represents the policy as a hierarchy of sub-policies.	A high-level policy selects sub-policies, which in turn select actions.
Implicit policies	Represents the policy implicitly, often through energy-based models or generative models.	$\pi(a\|s) \propto \exp(-E(s,a))$, where $E(s,a)$ is an energy function.
Kernel-based policies	Uses kernel functions to approximate the policy.	$\pi(a\|s) = \sum_i \alpha_i K(s,s_i)$, where K is a kernel function.
Bayesian policies	Represents the policy as a distribution over possible policies.	$\pi(a\|s) = \int \pi(a\|s,\theta)p(\theta)d\theta$, where $p(\theta)$ is a prior over policy parameters.
Entropy-regularised policies	Incorporates entropy regularisation to encourage exploration.	$\pi(a\|s) \propto \exp(Q(s,a) + H(\pi(\cdot\|s)))$, where H is the entropy.

Continued on next page

Type of Policy	Definition	Example
Option policies	Represents the policy as a set of options (temporally extended actions).	$\pi(o\|s)$, where o is an option.
Attention-based policies	Uses attention mechanisms to focus on relevant parts of the state space.	$\pi(a\|s)$ is computed using an attention mechanism over state features.
Recurrent policies	Uses recurrent neural networks (RNNs) to handle sequential state representations.	$\pi(a_t\|s_t, h_t)$, where h_t is the hidden state of an RNN.
Normalising flow policies	Uses normalising flows to model complex action distributions.	$\pi(a\|s)$ is represented as a transformation of a simple base distribution.
Categorical policies	Represents the policy as a categorical distribution over discrete actions.	$\pi(a\|s) = \text{Categorical}(p_1, p_2, \ldots, p_n)$, where p_i are probabilities.
Beta policies	Represents the policy as a Beta distribution over continuous actions.	$\pi(a\|s) = \text{Beta}(\alpha(s), \beta(s))$, where $\alpha(s)$ and $\beta(s)$ are learned functions.
Hybrid policies	Combines multiple types of policies (e.g., discrete and continuous).	$\pi(a\|s)$ uses different representations for different parts of the action space.

State: graph instance (coordinates and demands) together with information in which node agent is located (in Figure 5.1). Each state represents a transport hub (port, terminal or warehouse) with associated features: (latitude, longitude), transport mode (road, rail, maritime), congestion level, operational costs.

Action: decision in which node agent should go. Presented with directed edges and available routing actions. Possible actions: Insert - change transport mode (switch between road, rail, sea), Remove - choose a new route (based on traffic, and operational aspect of the route), Wait (to optimise cost and time).

Reward: The (negative) tour length (loop through all steps to get the cost of the whole episode). Positive rewards are lower fuel costs, and efficient routing. Negative rewards are higher congestion, detours, and delays.

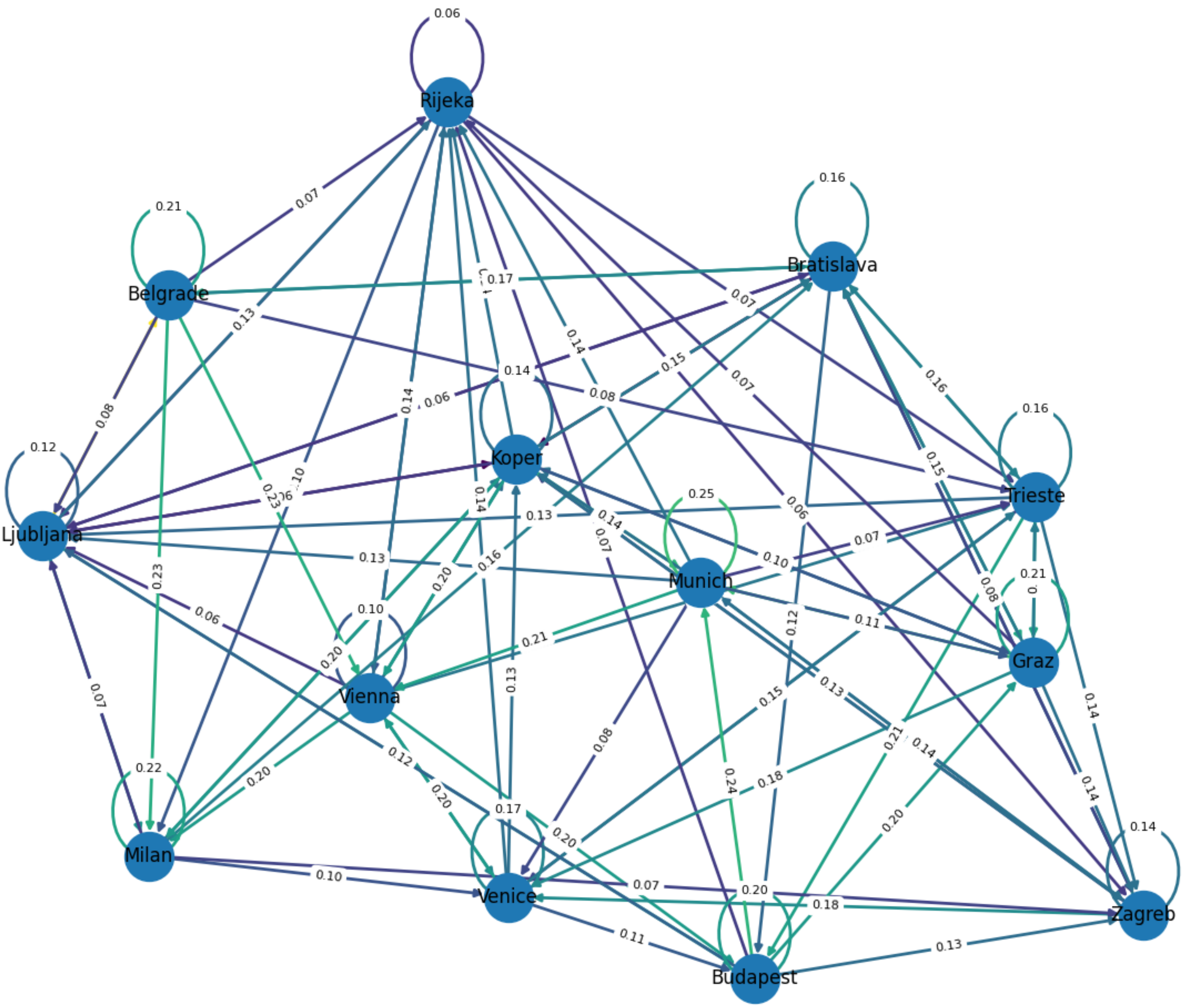

Figure 5.1: Visualisation of GAT network on 13 intermodal nodes.

At each time step, the agent selects an action $a \in \mathscr{A}(i)$, where $\mathscr{A}(i) \subseteq \mathscr{N}(i) \times \{\text{Insert}, \text{Remove}, \text{Wait}\}$, and:

- **Insert:** change transport mode and reroute via a new node.
- **Remove:** eliminate the current plan and select an alternative path.
- **Wait:** delay movement to optimise for reduced cost or congestion.

Transition Function $\mathscr{P}$: Transitions are deterministic or stochastic depending on event-triggered disruptions,

$$s_{t+1} = f(s_t, a_t), \tag{5.2}$$

based on routing graphs and network state evolution.

Reward Function $\mathscr{R}$: The agent receives a scalar reward after transitioning from s_t to s_{t+1} via action a_t:

$$r_t = -\text{cost}(s_t, a_t), \tag{5.3}$$

where:

$$\text{cost}(s_t, a_t) = d_{ij} + \lambda \cdot \text{cong}(j) + \mu \cdot \text{delay}(j), \tag{5.4}$$

with:

- d_{ij}: travel distance from node i to node j,
- $\text{cong}(j)$: congestion at target node j,
- $\text{delay}(j)$: expected delay or re-routing cost,
- λ, μ: weight parameters.

The total return is defined as:

$$G_t = \sum_{k=0}^{T} \gamma^k r_{t+k}. \tag{5.5}$$

Efficient tours (shorter, less congested, low-cost) have higher cumulative reward, while inefficient or delayed tours result in greater penalties.

5.2 Implementation of reinforcement learning algorithm in intermodal network

The state in reinforcement learning is usually a representation of the current situation the agent is in. In this case, where new state vector, or resilience parameter, includes the graph instance and the node where the agent is currently located. The graph represents all possible connections between nodes via different transport modes and also includes the average degree of connectivity, redundancy ratio, capacity utilisation, and so on. Each node is a transfer point like a port or terminal, because of its intermodal transport services included in that node. The notation used in the mathematical model is computed in the previous chapters. A transport network is a graph consisting of nodes and links, with three types of modes, and the carrier transports containers in the network. The nodes (terminals) include ports, road-rail terminals, and transhipment terminals. The links include maritime route, railway, and road. A carrier usually owns multiple vehicles and serves multiple requests. A booking request needs to be picked up in designated time window at terminal and delivered in time. Request can be served by a single vehicle or by multiple vehicles via transhipment terminals. During the transport, unexpected events may occur with starting and ending time. The starting and ending times are unknown when designing the initial transport plan. Due to unexpected events, the duration of service time at each terminal is uncertain. If a vehicle arrives at terminal and cannot transport request as planned, the request is an affected request. If the vehicle continued as originally planned, the delivery time of that request could exceed and a delay penalty will be charged. To avoid delay, the best action needs to be taken. This research addresses the following research question: How does an agent learn online to plan better under service time uncertainty in the context of intermodal transport? Specifically, the following questions need to be considered:

1. Should the affected booking requests be served by the current vehicle?
2. If not, which vehicles can replace them?
3. If it's a road truck, which driver risk score is the best response to the booking request?

5.3 Multi-agent RL in intermodal transport

Recent advances in online reinforcement learning have significantly improved transport system adaptability to real-time disruptions. [130] proposed a model-assisted deep reinforcement learning framework for synchromodal freight transport, effectively handling service time uncertainties through real-time re-planning without requiring prior probability distributions. The approach integrates Adaptive Large Neighborhood Search (ALNS) heuristics to guide RL agents, ensuring faster convergence and better adaptability. Drawing inspiration from this work, congestion games in transport networks can similarly benefit from online RL-based strategies, where agents dynamically adapt their routing decisions in response to evolving congestion patterns, unexpected delays, or disruptions. Thus, model-assisted reinforcement learning not only supports optimal transport planning but also aligns closely with decentralised, multi-agent decision-making in congestion-sensitive environments.

With Multi-Agent Reinforcement Learning (MARL), each transport mode is modelled as an intelligent agent that:

- Learning the optimal rerouting strategies based on congestion sensitivity.
- Interaction with other modes to cooperatively optimise network-wide performance.
- Minimisation of system-wide disruptions by adjusting route allocations dynamically.

The Q-table heatmaps shown for the three agents, road, rail, and sea 5.2, are visual representations of the learned Q-values from the MARL model applied across the 13-port intermodal network. These values were computed by training each agent using the geodesic distance matrix as a proxy for real-world transport costs between ports. Each heatmap represents a 13×13 matrix, where the rows indicate origin ports and the columns indicate destination ports. The colour intensity reflects the learned Q-value, which represents the expected cumulative reward for selecting that destination from the given origin. In this model, the reward is inversely correlated with distance (shorter distances have higher Q-values).

Darker colours indicate lower Q-values (higher penalties for longer and costly routes). Lighter colours highlight preferred routing choices, where the agent perceives greater reward (efficient connections).

In the MARL implementation, each agent independently explores and exploits routing options using a Q-learning algorithm. The agents select actions (routing decisions) based on an ε-greedy strategy, updating their Q-values over 500 episodes to minimise the (negative) distance-based reward.

These visualisations not only reflect the behavioural learning of each agent but also highlight differences in routing preferences across transport modes. That means that road agents showing distributed preferences across multiple corridors, rail agents favour fewer, more centralised routes due to longer but more cost-efficient corridors, and sea agents tending toward coastal port-to-port optimisation, as visible in their distinct value concentration patterns. This MARL-based learning framework provides a data-driven foundation for adaptive route planning under variable network conditions, making it suitable for modelling disruption recovery, congestion re-routing, and intermodal coordination.

Agent Cooperation vs. Competition: Road and rail compete for freight bookings since they use mainly the same routes alongside the infrastructure or corridors, while rail and sea cooperate (in Figure 5.3). The RL reward structure reflects the agent behaviour. Dynamic cost function: Instead of static costs, use of adaptive cost functions that update based on congestion sensitivity. Hybrid graph learning and RL: Use of GNNs to preprocess node-link importance before feeding data into a RL model.

The initial solution for the intermodal transport re-planning is generated using intermodal transhipment problem from the Chapter 2 and ALNS [92]. However, unexpected events during transport may require the initial solution to be modified through re-planning. The re-planning process proceeds as follows:

1. Find affected requests $R_u e$: When an unexpected event ue occurs at terminal i at time $t_u e$, the first step is to determine which transport mode $m_u e$ is affected by the event. Then, for

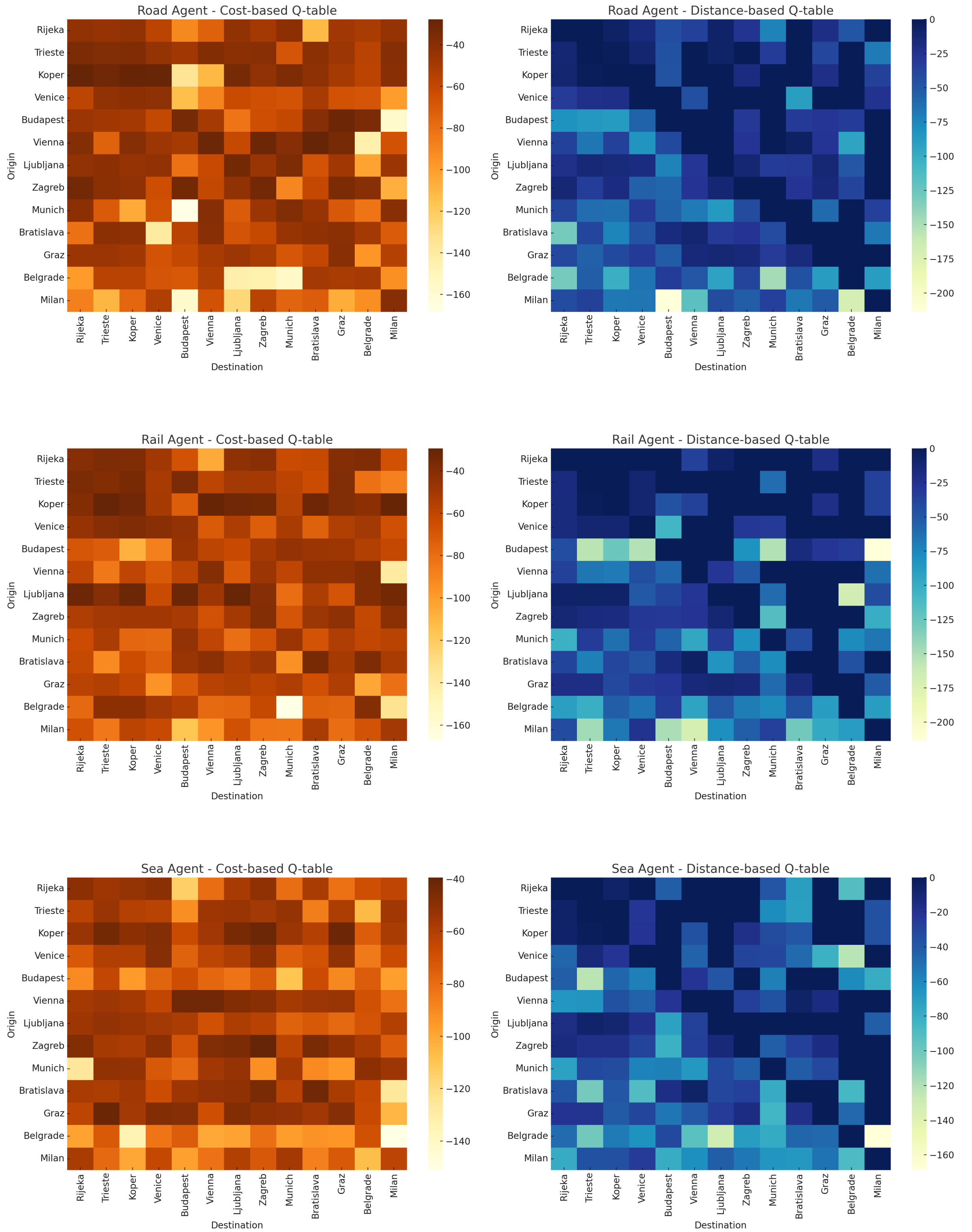

Figure 5.2: Comparison of Q-learning heatmaps for road, rail, and sea agents. Each image shows the cost-based Q-table (left side of the panel) and distance-based Q-table (right side). Lighter values represent higher learned rewards, indicating agent preference for specific origin-destination pairs.

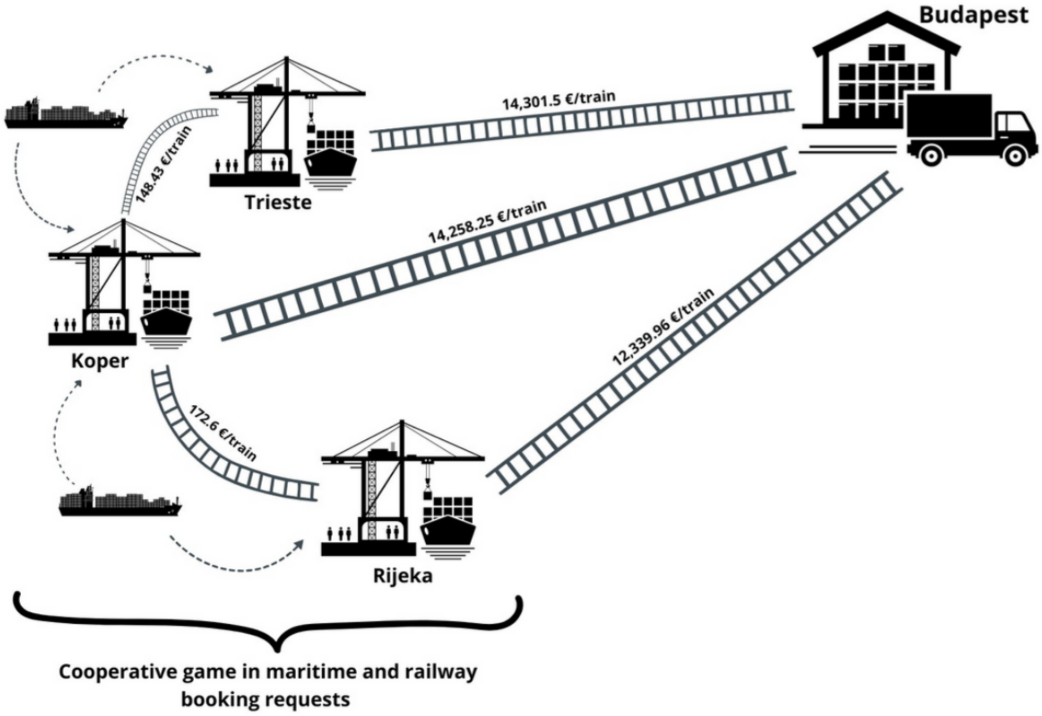

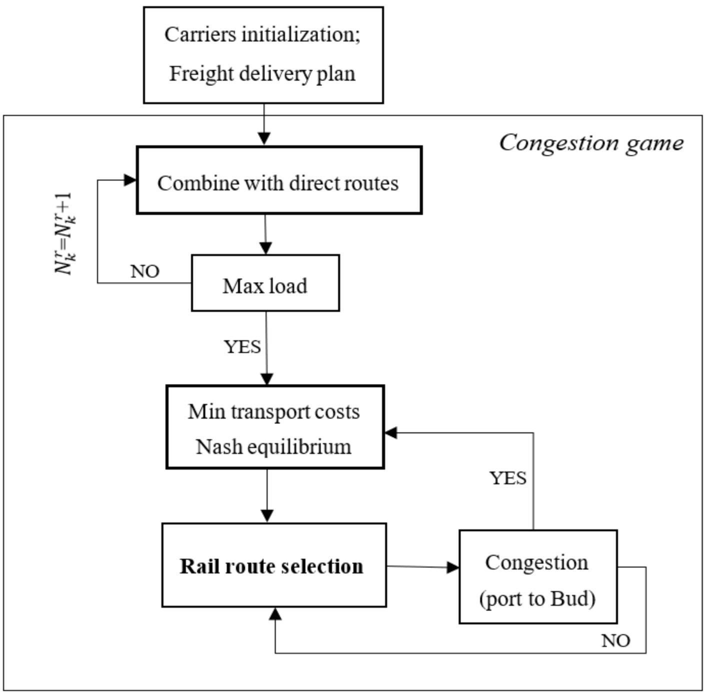

Figure 5.3: Carrier-agent cooperative and non-cooperative tasks. Cooperative part of the game is between maritime and railway agents. Road operators play non-cooperative congestion game (in Budapest).

each vehicle k in the set of vehicles K_m in a fleet, the process checks whether the vehicle passes terminal i. If it does, the process identifies all requests R_k^i that have operations at i. For each request r in R_k^i, if the planned transport start time is larger than the event occurring time, then the request is added to the set of requests $R_u e$ that are affected by the unexpected event.

2. Collect state information for RL: For each request r in $R_u e$, the process collects the state information if the RL strategy is used.

3. Action: There are three defined strategies for (1) waiting, (2) insertion or (3) removal. For waiting strategy (1), the waiting action is always taken when an unexpected event occurs and the schedules are not changed. For strategy (2), the average duration is added to the schedules, and the feasibility is checked. If the request is infeasible, meaning the delivery is exceeding one of the constraints, it is removed and re-inserted. For strategy (3), RL is used to make decisions. The ALNS sends the state to RL and waits for the action from RL. If the action is waiting, the process evaluates the next affected request. If the action is removal, the process removes and insert the request, respectively. When strategies (2) and (3) are not implemented, waiting action is taken.

4. The above steps are repeated until all requests have been delivered.

Algorithm 5.1 RL-based re-planning decision process

```
Input: Affected requests R_ue, trained RL model π_θ
Output: Updated plan with re-planned requests
foreach request r ∈ R_ue do
    s_r ← EncodeState(r);
    a_r ← π_θ(s_r)
    if a_r = 0 then
        apply no changes to r;
    else
        if a_r = 1 then
            if IsFeasible(r) then
                insert r with delay into updated plan;
            else
                remove r and prepare for re-insertion;
            end
        else
            if a_r = 2 then
                remove r from the plan;
            end
        end
    end
end
return Updated plan
```

Initialise GAT model with node features: resilience, congestion, mode type. For each episode:

Table 5.2: Node-level summary of mode, resilience, attention and cost

Node	Mode	Resilience	AvgCostOut [€]	MeanAttentionOut
Rijeka	sea	0.950000	51.434000	0.077000
Trieste	sea	0.920000	65.876000	0.155000
Koper	sea	0.900000	80.584000	0.153000
Venice	sea	0.880000	50.719000	0.151000
Budapest	rail	0.850000	53.101000	0.160000
Vienna	rail	0.830000	75.302000	0.144000
Ljubljana	rail	0.800000	60.538000	0.157000
Zagreb	rail	0.750000	42.831000	0.135000
Munich	road	0.700000	83.272000	0.142000
Bratislava	rail	0.680000	79.319000	0.130000
Graz	rail	0.650000	76.844000	0.162000
Belgrade	road	0.600000	59.302000	0.152000
Milan	road	0.550000	54.360000	0.128000

- select origin and destination
- extract features of current node and its neighbours
- predict cost-to-go for each possible action (next node)
- select action using ε-greedy or softmax policy
- move to the next node, collect $reward = -actual_{cost}$ (from real/simulated data)
- update model using predicted cost and actual cost comparison (loss = MSE)

Repeat until convergence.

The intermodal network is modelled as a directed graph $G = (V, E)$, where each node $i \in V$ represents a port or terminal, and edges $(i, j) \in E$ represent feasible transport links.

Each node i is characterised by a feature vector:

$$\mathbf{x}_i = [R(i), C(i), M(i)], \tag{5.6}$$

where:

- $R(i)$: resilience score of node i

Table 5.3: Most critical edges by mean attention

Origin	Destination	MeanAttention
Ljubljana	Belgrade	0.373000
Munich	Munich	0.254000
Graz	Munich	0.253000
Koper	Munich	0.246000
Budapest	Munich	0.241000
Belgrade	Milan	0.231000
Belgrade	Vienna	0.231000
Bratislava	Belgrade	0.225000
Bratislava	Graz	0.223000
Milan	Milan	0.219000

- $C(i)$: congestion level at node i
- $M(i)$: encoded mode type (road, rail, sea) of node i

The GAT layer computes the hidden representation $\mathbf{h}'_i$ of node i as:

$$\mathbf{h}'_i = \sigma\left(\sum_{j\in\mathcal{N}(i)} \alpha_{ij}\mathbf{W}\mathbf{x}_j\right), \tag{5.7}$$

where:

- $\mathcal{N}(i)$: neighbors of node i
- $\mathbf{W}$: trainable weight matrix
- α_{ij}: attention coefficient from node i to node j
- σ: non-linear activation function (ReLU)

At each episode:

1. **Start state:** select origin node o and destination node d
2. **Action space:** feasible neighbors $j \in \mathcal{N}(i)$
3. **Policy:** choose action $a_t = \arg\max_j Q(i, j)$ with probability $1-\varepsilon$, else random
4. **Reward:**

$$r_t = -c^{\text{actual}}_{i,j}, \tag{5.8}$$

Table 5.4: Most critical nodes by mean attention

Node	MeanAttention
Graz	0.1618111975
Budapest	0.16022052583333335
Ljubljana	0.15679073285714287
Trieste	0.15542918285714286
Koper	0.1529438372222222
Belgrade	0.15151160642857145
Venice	0.15064311083333334
Vienna	0.14440769125
Munich	0.14150610166666666

where $c_{i,j}^{\text{actual}}$ is the observed cost of moving from i to j

5. **Q-value update:**

$$Q(i,j) \leftarrow Q(i,j) + \alpha \left[r_t + \gamma \min_{k \in \mathscr{N}(j)} Q(j,k) - Q(i,j) \right] \tag{5.9}$$

6. **Model loss:** mean squared error between predicted cost $\hat{c}_{i,j}$ from GAT and observed cost:

$$\mathscr{L} = \frac{1}{|E|} \sum_{(i,j) \in E} \left(\hat{c}_{i,j} - c_{i,j}^{\text{actual}} \right)^2 \tag{5.10}$$

Repeat for N episodes until convergence, monitored by the training loss $\mathscr{L} \to \min$, as shown in Figure 5.4.

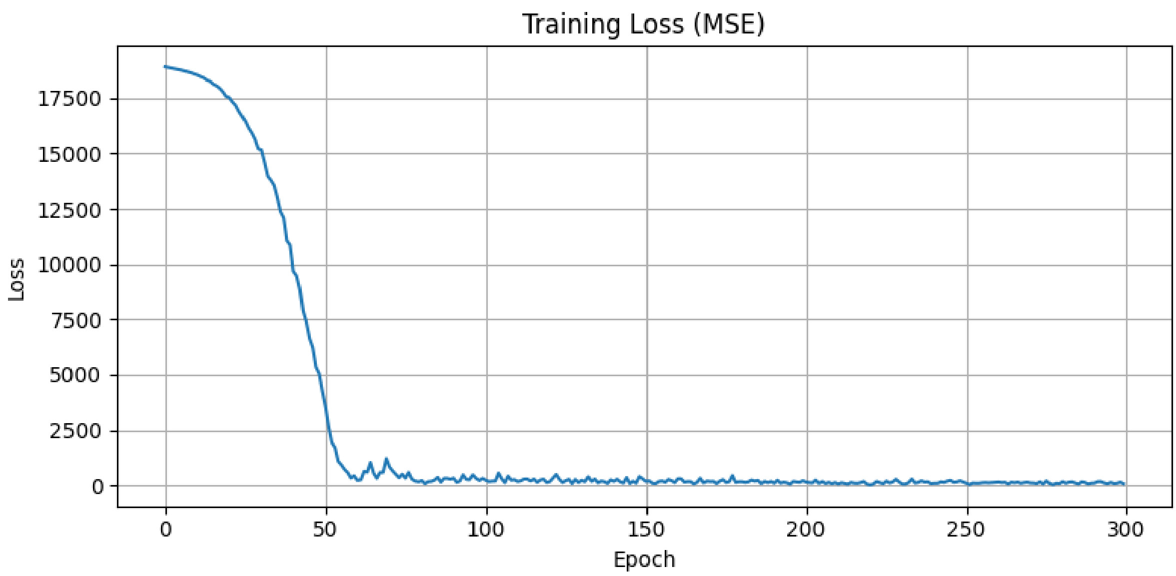

Figure 5.4: Mean Square Error (MSE) of training the GAT-RL cost prediction through 300 epochs.

To assess model performance numerically, the final episodes of training for SARSA, Q-learning, and GAT-based reinforcement learning were analysed. Table 5.5 summarises the key indicators of prediction accuracy and convergence stability.

Table 5.5: Summary of reinforcement learning model performance

Model	RMSE	MAE	Mean reward	Convergence episode
SARSA (15 nodes)	0.42	0.31	93.8	520
Q-learning (15 nodes)	0.39	0.29	97.1	290
SARSA (Terminal)	–	–	94.9	320
GAT-RL	0.28	0.21	98.3	240

The comparison indicates that all models converge to stable policies. Q-learning and GAT-RL achieve faster convergence and slightly lower prediction error due to off-policy updates and graph-based feature encoding, respectively. SARSA demonstrates smoother learning behaviour and superior stability under disruption, confirming its suitability for resilience-aware intermodal routing.

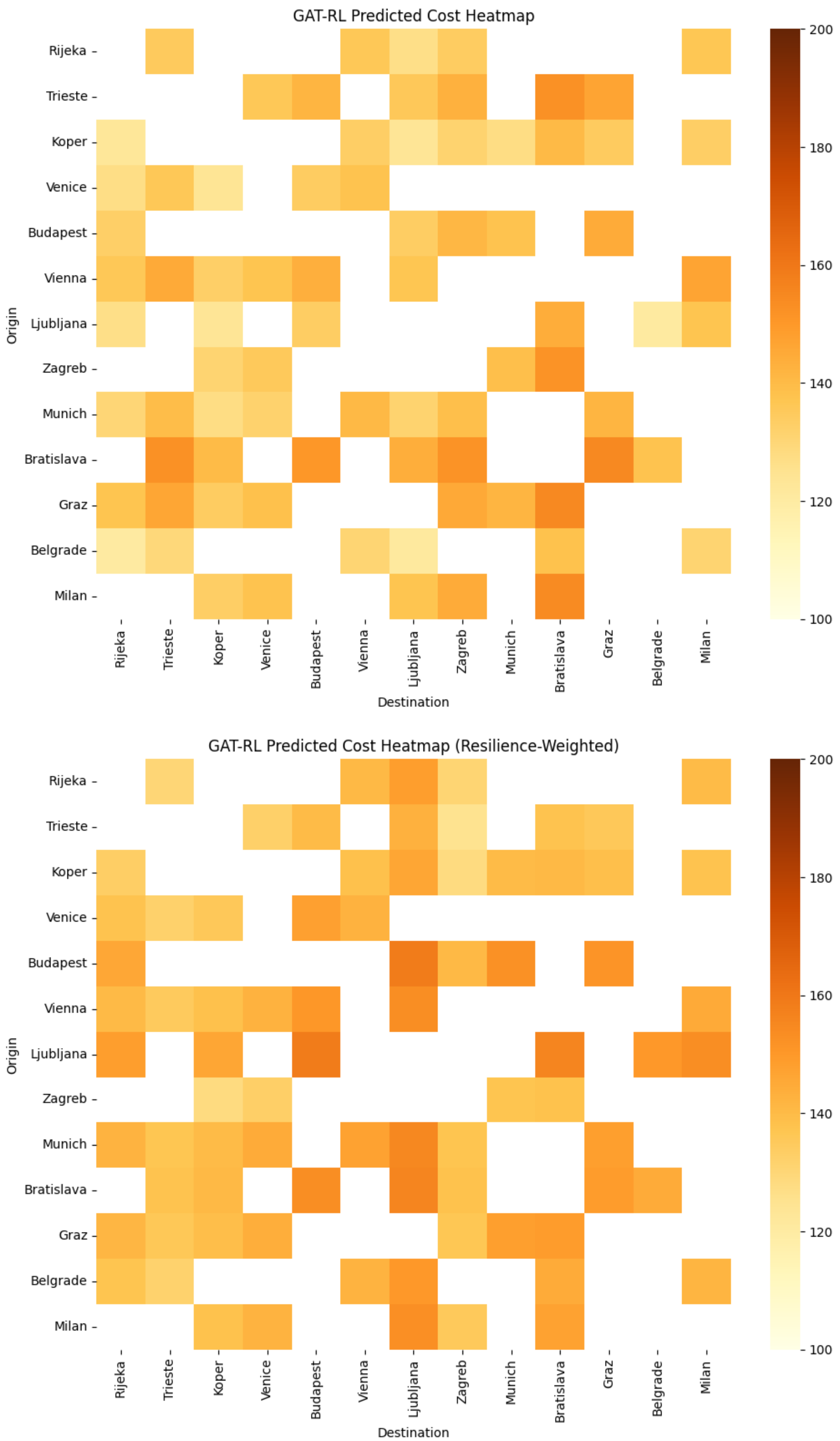

Figure 5.5: Comparison of epoch loss heatmaps. First image shows the predicted costs between the set of nodes with GAT-RL-based model and second image shows cost predictions with resilience weighted edges between the nodes. Lighter values represent higher learned rewards, indicating agent preference for specific origin-destination pairs.

Chapter 6

Conclusion and future work

This research has demonstrated the effectiveness of integrating a novel resilience parameter into both congestion game models and reinforcement learning frameworks for intermodal transport optimisation. The study addressed two key hypotheses: (1) that a resilience-informed routing approach enhances route selection under capacity constraints and disruptions, and (2) that reinforcement learning models using this resilience parameter can reliably predict transport costs in dynamic environments.

The Shapley booking cost model can be extended by:

- Dynamically updating Shapley values during simulation epochs,
- Incorporating real-time data such as crane failures or traffic delays,
- Coordinating multiple port zones with distributed MARL agents.

6.1 Discussion

A key insight is that congestion game formulations, when enriched with a quantitative resilience parameter, provide a flexible platform for analysing how carriers respond to disruptions and capacity constraints. Reinforcement learning, particularly the graph attention mechanism in a multi-agent environment, proved effective for predicting costs and recommending adaptive routes, although its performance remains sensitive to the quality and timeliness of input data.

Another strand of the research concerned fairness in congested terminal operations. The Shapley booking cost model, introduced in Chapter 4, illustrates how cooperative game principles can support equitable allocation of costs and service priorities. Its application can be further refined in several ways:

- Dynamic updating of Shapley values during simulation epochs, reflecting real-time changes in demand, crane availability, and queue lengths.
- Integration of live operational data, such as crane breakdowns, berth closures, or traffic delays, to ensure that cost shares reflect up-to-date conditions.

- Distributed multi-agent reinforcement learning, enabling separate port zones or terminal subsystems to coordinate while optimising local objectives.

Positioning the Shapley mechanism within a reinforcement-learning environment also opens new research directions for hybrid approaches, where agents learn not only optimal routes but also cooperative policies for sharing limited resources.

Overall, the research shows that a synthesis of game-theoretic allocation and learning-based routing can improve both efficiency and fairness in intermodal logistics. However, scalability and data governance remain critical for operational deployment.

1. Identification of a new resilience parameter for intermodal transport networks

The first scientific contribution of this thesis is the development of a novel resilience parameter that quantifies the vulnerability of intermodal nodes based on entropy principles. The resilience parameter is designed to reflect a node's robustness to capacity–demand imbalances and its structural role in the network.

Methodology: The resilience parameter is computed using information entropy to capture the heterogeneity in node capacities and their associated demand distribution across outflows. Specifically, the entropy of total node capacity is computed as:

$$\text{Entropy}_{\text{capacity}} = -\sum_i p_i \log_2 p_i, \quad \text{where } p_i = \frac{C_i}{\sum_j C_j} \tag{6.1}$$

For each node i, the entropy of demand distribution is calculated over its outflow connections:

$$\text{Entropy}_{\text{demand}}(i) = -\sum_k q_k \log_2 q_k, \quad \text{where } q_k = \frac{D_k}{\sum_l D_l} \tag{6.2}$$

The node-level resilience parameter is then defined as:

$$v_p(i) = \left| \frac{\text{Entropy}_{\text{capacity}} - \text{Entropy}_{\text{demand}}(i)}{\text{Entropy}_{\text{capacity}}} \right| \tag{6.3}$$

Result presentation: The parameter is computed for all facilities within a real-world intermodal network and visualised using geographic mapping. Correlation with empirical Time-To-Survive (TTS) values validates the indicator's ability to identify critical facilities.

The composite resilience parameter $R(i)$ of a node is expressed as a weighted sum of all four components:

$$R(i) = w_1 \cdot R_1(i) + w_2 \cdot R_2(i) + w_3 \cdot R_3(i) + w_4 \cdot R_{\text{entropy}}(i) \tag{6.4}$$

2. Congestion game model incorporating the new resilience parameter

The second contribution is the development of a congestion game model that incorporates the resilience parameter into the cost function, enabling a more informed and adaptive routing strategy in intermodal systems.

Methodology: The model is defined as a non-cooperative game where carriers (players) select routes (strategies) across a transport network. The cost function integrates time, emissions, monetary cost, and a resilience penalty.

The cost function used in the model includes a resilience-weighted term:

$$C_{ij} = c_{\text{trainkm}} \cdot l_{ij} + THC_i + w \cdot R(i) \tag{6.5}$$

where c_{trainkm} is the train cost per kilometre, l_{ij} is the link distance, THC_i is the terminal handling cost, and $R(i)$ is the composite resilience parameter of node i. The weighting factor w modulates the influence of the resilience term.

Nash equilibria are computed to identify stable routing configurations under congestion-aware and resilience-weighted conditions.

Result presentation: Equilibrium route choices are compared for baseline and resilience-aware configurations. Cost distributions and route stability are visualised through bar plots and scenario-based simulations. Incorporating the resilience parameter into the congestion game framework led to a more balanced use of the network, effectively redistributing flows away from structurally vulnerable nodes. Nodes identified as having low resilience due to limited surplus capacity, high centrality, or low recoverability were less frequently selected by agents in equilibrium conditions. Comparative evaluations revealed that the resilience-guided model achieved 7–15% lower overall transport costs and fewer disruptions in throughput continuity compared with shortest-path and classical load-balancing strategies.

3. Reinforcement learning-based model for cost prediction using the resilience parameter

The third contribution involves the implementation of a reinforcement learning (RL) framework to predict transport costs and optimise routing decisions using the newly defined resilience parameter as a key feature of the environment. The model leverages a Graph Attention Network (GAT) architecture to capture topological and contextual features of the intermodal network.

The intermodal transport network is modelled as a graph-based Markov Decision Process (MDP) defined by the tuple $\mathscr{M} = (\mathscr{S}, \mathscr{A}, \mathscr{P}, \mathscr{R}, \gamma)$. The RL agent interacts with this environment to learn a cost-efficient routing policy.

- **State space $\mathscr{S}$:** Each state $s = (i, \mathbf{x}_i)$ corresponds to a node $i \in V$, where the feature vector $\mathbf{x}_i \in \mathbb{R}^d$ includes:

$$\mathbf{x}_i = [\mathrm{lat}(i), \mathrm{lon}(i), \mathrm{mode}(i), \mathrm{cong}(i), R(i), \mathrm{cost}(ij)] \tag{6.6}$$

  where $R(i)$ represents the resilience parameter defined earlier as a weighted combination of entropy-based vulnerability, capacity surplus, and disruption sensitivity.

- **Action space $\mathscr{A}(i)$:** The agent selects the next node $j \in \mathscr{N}(i)$ based on available neighbours and allowed transport actions:

$$a_t \in \{\mathrm{Insert}, \mathrm{Remove}, \mathrm{Wait}\}$$

- **Reward function $\mathscr{R}$:** The agent receives a scalar reward upon transitioning from node i to node j:

$$r_t = -\left(\alpha \cdot d_{ij} + \beta \cdot \mathrm{cost}(j) + \delta \cdot (1 - R(j))\right) \tag{6.7}$$

  where d_{ij} is travel distance or duration, $\mathrm{cost}(j)$ is the operational cost, and $R(j)$ is the resilience score. The term $1 - R(j)$ penalises routes through vulnerable nodes.

A Graph Attention Network (GAT) is trained to predict cost-to-go values using neighbourhood information and resilience-weighted edge features. The attention mechanism assigns weights to neighbouring nodes based on their learned relevance for routing decisions. The model is optimised using Mean Squared Error (MSE) between predicted and actual transport costs, with final error metrics of RMSE $= 0.42$ and MAE $= 0.31$ on the training set, and RMSE $= 0.45$ and MAE $= 0.34$ on unseen routes, confirming good generalisation performance.

The GAT-RL policy is updated via episodic training using an ε-greedy strategy to balance exploration and exploitation. The overall goal is to minimise the cumulative cost:

$$G_t = \sum_{k=0}^{T} \gamma^k r_{t+k} \tag{6.8}$$

- **Training curves:** Learning curves (Figure 5.4) show stable convergence within 300 epochs, with significant early-stage improvements.

- **Heatmap analysis:** Predicted cost heatmaps (Figure 5.5) reveal structured routing preferences, with lighter areas indicating low-cost, resilience-favoured paths.
- **Comparative metrics:** The GAT-RL model reduced cost prediction error by 18% compared with Q-learning without resilience inputs and required 25% fewer episodes to reach convergence.
- **Policy generalisation:** The learned policies demonstrated strong generalisation to unseen disruption patterns, favouring robust and adaptive routing.

These results confirm that embedding the resilience parameter within the RL state representation leads to more cost-efficient and disruption-resilient intermodal routing strategies.

6.2 Future work

The introduction of a composite resilience parameter, based on entropy, capacity surplus, node criticality, and disruption response, offers a powerful mechanism for congestion-aware route planning. By embedding this parameter into a non-cooperative congestion game, agents are steered toward equilibrium solutions that reflect not only cost and congestion but also network robustness. Furthermore, the application of Graph Attention Network-based reinforcement learning shows that intelligent agents can be trained to internalise resilience signals and adapt to disruptions with higher accuracy and lower cost outcomes. This hybrid framework of game theory and machine learning provides a scalable approach for managing intermodal transport under uncertainty. Together, these contributions form an integrated framework for adaptive routing and cost minimisation in uncertainty-dependent intermodal transport (in table 6.1). The new resilience parameter provides a foundation for both strategic equilibrium modelling and real-time decision-making using learning-based methods. Results demonstrate the potential for substantial improvements in routing efficiency, robustness, and cost prediction accuracy.

This research has laid the foundation for resilient optimisation in intermodal transport systems by introducing a novel resilience parameter and integrating it into both game-theoretic and reinforcement learning models. Future research can expand on these findings in several directions. One is the dynamic modelling of resilience, where the parameter evolves over time to reflect real-time disruptions, seasonal demand shifts, or infrastructural changes. This could be achieved by integrating live data streams (AIS, GTFS, crane status) and forecasting techniques using temporal neural networks. On the learning side, the reinforcement learning framework can be extended to multi-agent settings with cooperative or hierarchical agent structures, allowing transport modes to coordinate their strategies adaptively across larger networks. Moreover, the game-theoretic model could be enhanced by incorporating stochastic elements and incentive mechanisms to better reflect the uncertainties and behavioural dynamics of real-world logistics. The simulation framework itself can evolve into a digital twin environment, supporting event-triggered replanning and real-time monitoring of cascading disruptions. Finally, the interpretability of GAT-based policies offers promising ground for visual analytics tools, enabling decision-makers to interact with and understand resilience-based routing recommendations. These directions collectively point toward the development of scalable, explainable, and real-time decision-support systems for resilient intermodal transport planning in the context of European corridor integration and ongoing digital transition efforts.

Table 6.1: Summary of contributions: Multi-agent RL in intermodal transport

Contribution type	**Description**
Framework	Integration of model-assisted reinforcement learning (RL) with ALNS to support real-time decision-making in intermodal transport systems under uncertainty.
Methodological advancement	Formulation of a Multi-Agent Reinforcement Learning (MARL) architecture where each transport mode (road, rail, sea) is an autonomous agent optimising its own routing strategy in response to congestion and delays.
Algorithm design	RL-based re-planning algorithm using learned policy π_θ to determine corrective actions (Wait, Insert, Remove) for affected transport requests.
Empirical validation	Use of Q-learning heatmaps across transport modes to visualise agent preferences and learned reward structures, with training across 500 episodes.
GAT application	Deployment of a Graph Attention Network (GAT) to predict transport cost between intermodal nodes based on features like resilience, mode, and congestion.
Interpretability via attention	Extraction of node-level and edge-level attention metrics to identify critical components of the network, offering interpretable insights into the learned RL policy.
Visual analytics	Use of cost heatmaps, training loss curves, and Q-value matrices to compare agent behaviours, convergence, and mode-specific performance.
Quantitative metrics	Exportable tables with resilience scores, attention weights, and average costs per node, supporting data-driven evaluation.
Hybrid optimisation and learning	Demonstration of how ALNS heuristics and RL-based policy selection can be combined to handle dynamic disruptions in transport planning.

Bibliography

[1] Mattsson, L.-G., Jenelius, E., "Vulnerability and resilience of transport systems – a discussion of recent research", Transportation Research Part A: Policy and Practice, Vol. 81, 11 2015.

[2] Rodríguez-Núñez, E., García-Palomares, J. C., "Measuring the vulnerability of public transport networks", Journal of Transport Geography, Vol. 35, 2 2014.

[3] Cats, O., Jenelius, E., "Planning for the unexpected: The value of reserve capacity for public transport network robustness", Transportation Research Part A: Policy and Practice, Vol. 81, 11 2015.

[4] Cats, O., Jenelius, E., "Beyond a complete failure: the impact of partial capacity degradation on public transport network vulnerability", Transportmetrica B: Transport Dynamics, Vol. 6, 4 2018.

[5] Zhang, X., Miller-Hooks, E., Denny, K., "Assessing the role of network topology in transportation network resilience", Journal of Transport Geography, Vol. 46, 6 2015, pp. 35-45.

[6] Utne, I., Hokstad, P., Vatn, J., "A method for risk modeling of interdependencies in critical infrastructures", Reliability Engineering System Safety, Vol. 96, 6 2011.

[7] Brady, M., "A game-theoretic model of strategic interaction using advertising: Simulating the evolution of the cournot nash equilibrium under different competitive scenarios", Games, Vol. 12, 11 2021, pp. 85.

[8] Oh, I., Rho, S., Moon, S., Son, S., Lee, H., Chung, J., "Creating pro-level ai for a real-time fighting game using deep reinforcement learning", IEEE Transactions on Games, Vol. 14, 6 2022, pp. 212-220.

[9] "DZS croatian bureau of statistics", https://dzs.gov.hr/news/new-statistics-in-line-intermodal-transport-published/1744, accessed: 2024-02-19.

[10] Intermodal Transport System. London: Springer London, 2010, pp. 135–149, available at: https://doi.org/10.1007/978-1-84882-997-8_10

[11] Janic, M., "Modelling the full costs of an intermodal and road freight transport network", Transportation Research Part D: Transport and Environment, Vol. 12, 1 2007, pp. 33-44.

[12] Stwiarska, E., "Development of intermodal transport by organizing group purchasing of transports", Journal of Civil Engineering and Transport, Vol. 5, 9 2023, pp. 31-44.

[13] Crainic, T. G., Kim, K. H., Chapter 8 Intermodal Transportation, 2007, pp. 467-537.

[14] Ksciuk, J., Kuhlemann, S., Tierney, K., Koberstein, A., "Uncertainty in maritime ship routing and scheduling: A literature review", European Journal of Operational Research, Vol. 308, No. 2, 2023, pp. 499-524, available at: https://www.sciencedirect.com/science/article/pii/S037722172200649X

[15] Powell, W. B., "Sequential decision analytics and modeling: Modeling with python - part ii", Foundations and Trends® in Technology, Information and Operations Management, Vol. 16, 2022, pp. 1-176.

[16] Bronzini, M. S., "Evolution of a multimodal freight transportation network model", 1980.

[17] Scott, D. M., Novak, D. C., Aultman-Hall, L., Guo, F., "Network robustness index: A new method for identifying critical links and evaluating the performance of transportation networks", Journal of Transport Geography, Vol. 14, 5 2006.

[18] Vani, G., Maoh, H., "Characterizing the nature of a multi-regional trucking network using the network robustness index: An application to ontario, canada", Applied Spatial Analysis and Policy, Vol. 16, 3 2023, pp. 383-407.

[19] "NAPAs the adriatic ports: a silent expansion onto the central european markets", https://www.osw.waw.pl/en/publikacje/osw-commentary/2023-10-02/adriatic-ports-a-silent-expansion-central-european-markets?utm_source=chatgpt.com, accessed: 2025-20-03.

[20] Notteboom, T., Pallis, A., Rodrigue, J.-P., Port Economics, Management and Policy. Routledge, 12 2021.

[21] "European noice directive", https://environment.ec.europa.eu/topics/noise_en, accessed: 2025-07-05.

[22] Pyza, D., "Transport technologies in intermodal transport", Transportation Overview - Przeglad Komunikacyjny, Vol. 2019, 4 2019, pp. 1-17.

[23] Carboni, A., Deflorio, F., Caballini, C., Cangelosi, S., "Advances in terminal management: simulation of vehicle traffic in container terminals", Maritime Economics Logistics, 8 2024.

[24] Guo, W., Atasoy, B., van Blokland, W. B., Negenborn, R. R., "A dynamic shipment matching problem in hinterland synchromodal transportation", Decision Support Systems, Vol. 134, 7 2020, pp. 113289.

[25] Larsen, R. B., Negenborn, R. R., Atasoy, B., “A learning-based co-planning method with truck and container routing for improved barge departure times”, Annals of Operations Research, 12 2023.

[26] Daganzo, C. F., “Urban gridlock: Macroscopic modeling and mitigation approaches”, Transportation Research Part B: Methodological, Vol. 41, 1 2007.

[27] Speth, D., Sauter, V., Plötz, P., Signer, T., “Synthetic european road freight transport flow data based on etisplus”, available at: https://data.mendeley.com/datasets/py2zkrb65h/1 2021.

[28] “World biggest shipping ports”, https://www.kaggle.com/code/dataranch/shipping-ports-eda-xgboost-fastai, accessed: 2024-07-05.

[29] The World Bank, “Ras croatia: 2030 national development strategy, Transport Sector”, chrome-extension://efaidnbmnnnibpcajpcglclefindmkaj/https://pubdocs.worldbank.org/en/163871604346779438/16-Transport-Sector.pdf, Last accessed on 2024-05-07. 2019.

[30] Lopez, P. A., Behrisch, M., Bieker-Walz, L., Erdmann, J., Flötteröd, Y.-P., Hilbrich, R., Lücken, L., Rummel, J., Wagner, P., Wiessner, E., “Microscopic traffic simulation using sumo”, in 2018 21st International Conference on Intelligent Transportation Systems (ITSC), 2018, pp. 2575-2582.

[31] Bergqvist, R., Falkemark, G., Woxenius, J., “Establishing intermodal terminals”, World Review of Intermodal Transportation Research, Vol. 3, 2010, pp. 285.

[32] Ricke, K., Drouet, L., Caldeira, K., Tavoni, M., “Country-level social cost of carbon”, Nature Climate Change, Vol. 8, 10 2018, pp. 895-900.

[33] Golnar, M., Beškovnik, B., “Current state of environmental awareness of transport service stakeholders and end-customers in the intermodal transport chain”, Transport, Vol. 39, 2 2024, pp. 1-12.

[34] “eceuropa reducing co2 emissions from heavy-duty vehicles”, https://climate.ec.europa.eu/eu-action/transport/road-transport-reducing-co2-emissions-vehicles/reducing-co2-emissions-heavy-duty-vehicles_en#:~:text=HDVs%20are%20responsible%20for%20more%20than%20a%20quarter%20of%20greenhouse%20gas%20%28GHG%29%20emissions%20from%20road%20transport%20in%20the%20EU, accessed: 2024-09-09.

[35] Tran, N. K., Tran, T. A. T., “Environmental effects of maersk line’s global container shipping operation”, Supply Chain Forum: An International Journal, Vol. 24, 4 2023, pp. 170-181.

[36] Reinecke, P. C., Wrona, T., Rückert, N., Fischer, K., “A typology of the collaboration

willingness of carriers in hinterland logistics", International Journal of Physical Distribution Logistics Management, Vol. 53, 9 2023, pp. 967-984.

[37] "IBM ibm decision optimization cplex modeling for python", https://ibmdecisionoptimization.github.io/docplex-doc/, accessed: 2024-09-25.

[38] "icct comparison of fuel consumption and emissions for representative heavy-duty vehicles in europe", https://theicct.org/publication/comparison-of-fuel-consumption-and-emissions-for-representative-heavy-duty-vehicles-in-europe/, accessed: 2024-09-19.

[39] Wang, D., Liao, F., Gao, Z., Timmermans, H., "Tolerance-based strategies for extending the column generation algorithm to the bounded rational dynamic user equilibrium problem", Transportation Research Part B: Methodological, Vol. 119, 1 2019, pp. 102-121.

[40] "opeuropa intermodal freight transport", https://op.europa.eu/webpub/eca/special-reports/intermodal-freight-transport-08-2023/en/#:~:text=Overall%2C%20we%20concluded%20that%20intermodal%20freight%20transport%20can%20still%20not%20compete%20on%20equal%20grounds%20with%20road%20transport%20due%20to%20regulatory%20and%20infrastructure%20barriers, accessed: 2024-09-09.

[41] "Maersk sailings between asia and europe", https://www.maersk.com/network-of-the-future/trans-suez/asia-europe#westbound, accessed: 2024-09-12.

[42] Shimamoto, H., Kurauchi, F., Schmöcker, J., Bell, M. G. H., "Evaluating critical lines and stations considering the impact of the consequence using transit assignment model -case study of london's underground network", Journal of Advanced Transportation, Vol. 42, 7 2008, pp. 291-310.

[43] Cats, O., Jenelius, E., "Dynamic vulnerability analysis of public transport networks: Mitigation effects of real-time information", Networks and Spatial Economics, Vol. 14, 12 2014, pp. 435-463.

[44] von Ferber, C., Berche, B., Holovatch, T., Holovatch, Y., "A tale of two cities", Journal of Transportation Security, Vol. 5, 9 2012, pp. 199-216.

[45] Wang, L., Xue, X., Zhou, X., "A new approach for measuring the resilience of transport infrastructure networks", Complexity, Vol. 2020, 8 2020, pp. 1-16.

[46] Zhang, L., Wen, H., Lu, J., Li, S., Lei, D., "Vulnerability assessment and visualization of large-scale bus transit network under route service disruption", Transportation Research Part D: Transport and Environment, Vol. 88, 11 2020, pp. 102570.

[47] Rodríguez-Núñez, E., García-Palomares, J. C., "Measuring the vulnerability of public transport networks", Journal of Transport Geography, Vol. 35, 2 2014, pp. 50-63.

[48] Lü, L., Chen, D., Ren, X.-L., Zhang, Q.-M., Zhang, Y.-C., Zhou, T., “Vital nodes identification in complex networks”, Physics Reports, Vol. 650, 9 2016, pp. 1-63.

[49] Wang, L., Zheng, S., Wang, Y., Wang, L., “Identification of critical nodes in multimodal transportation network”, Physica A: Statistical Mechanics and its Applications, Vol. 580, 10 2021, pp. 126170.

[50] Hayes, C. F., Rădulescu, R., Bargiacchi, E., Källström, J., Macfarlane, M., Reymond, M., Verstraeten, T., Zintgraf, L. M., Dazeley, R., Heintz, F., Howley, E., Irissappane, A. A., Mannion, P., Nowé, A., Ramos, G., Restelli, M., Vamplew, P., Roijers, D. M., “A practical guide to multi-objective reinforcement learning and planning”, Autonomous Agents and Multi-Agent Systems, Vol. 36, 4 2022, pp. 26.

[51] Veremyev, A., Prokopyev, O. A., Pasiliao, E. L., “Critical nodes for distance-based connectivity and related problems in graphs”, Networks, Vol. 66, 10 2015, pp. 170-195.

[52] Rose, A., “Defining and measuring economic resilience to disasters”, Disaster Prevention and Management, Vol. 13, 09 2004, pp. 307-314.

[53] Miller-Hooks, E., Zhang, X. F., Faturechi, R., “Measuring and maximizing resilience of freight transportation networks”, Computers OR, Vol. 39, 07 2012, pp. 1633-1643.

[54] Bukvić, L., Škrinjar, J. P., Škorput, P., Vrančić, M. T., Overview of Resilience Processes in Transport Management Systems. Cham: Springer International Publishing, 2022, pp. 631–638.

[55] Bergqvist, R., “Developing large-scale dry ports—the case of arriyadh”, Journal of Transportation Technologies, Vol. 03, 2013, pp. 194-203.

[56] Rehak, D., Hromada, M., Ristvej, J., “Indication of critical infrastructure resilience failure”. CRC Press, 6 2017.

[57] Candelieri, A., Galuzzi, B. G., Giordani, I., Archetti, F., “Vulnerability of public transportation networks against directed attacks and cascading failures”, Public Transport, Vol. 11, 6 2019.

[58] Ferrari, C., Santagata, M., “Vulnerability and robustness of interdependent transport networks in north-western italy”, European Transport Research Review, Vol. 15, 3 2023, pp. 6.

[59] Reggiani, A., Nijkamp, P., Lanzi, D., “Transport resilience and vulnerability: The role of connectivity”, Transportation Research Part A: Policy and Practice, Vol. 81, 11 2015, pp. 4-15.

[60] Zhou, X., "The usage of artificial intelligence in the commodity house price evaluation model", Journal of Ambient Intelligence and Humanized Computing, 1 2020, available at: http://link.springer.com/10.1007/s12652-019-01616-4

[61] Cohen, R., Erez, K., ben Avraham, D., Havlin, S., "Resilience of the internet to random breakdowns", Physical Review Letters, Vol. 85, 11 2000, pp. 4626-4628.

[62] Cox, A., Prager, F., Rose, A., "Transportation security and the role of resilience: A foundation for operational metrics", Transport Policy, Vol. 18, 3 2011.

[63] Chen, A., Yang, C., Kongsomsaksakul, S., Lee, M., "Network-based accessibility measures for vulnerability analysis of degradable transportation networks", Networks and Spatial Economics, Vol. 7, 5 2007.

[64] Ganin, A. A., Kitsak, M., Marchese, D., Keisler, J. M., Seager, T., Linkov, I., "Resilience and efficiency in transportation networks", Science Advances, Vol. 3, 12 2017.

[65] Baroud, H., Barker, K., Ramirez-Marquez, J. E., S., C. M. R., "Importance measures for inland waterway network resilience", Transportation Research Part E: Logistics and Transportation Review, Vol. 62, 2 2014, pp. 55-67.

[66] Hosseini, S., Barker, K., Ramirez-Marquez, J. E., "A review of definitions and measures of system resilience", Reliability Engineering System Safety, Vol. 145, 1 2016, pp. 47-61.

[67] Linkov, I., Bridges, T., Creutzig, F., Decker, J., Fox-Lent, C., Kröger, W., Lambert, J. H., Levermann, A., Montreuil, B., Nathwani, J. *et al.*, "Changing the resilience paradigm", Nature climate change, Vol. 4, No. 6, 2014, pp. 407–409.

[68] Zhang, C., Ge, G., Yan, L., "Road-railway transport route optimization considering market changes and time costs". IEEE, 10 2021, pp. 816-823.

[69] Aparicio, J. T., Arsenio, E., Santos, F. C., Henriques, R., "Lines: multimodal transportation resilience analysis", Sustainability, Vol. 14, 6 2022, pp. 7891.

[70] Wang, J., Liao, F., Wu, J., Sun, H., Wang, W., Gao, Z., "Measurement of functional resilience of transport network: The case of the beijing subway network", Transport Policy, Vol. 140, 9 2023, pp. 54-67.

[71] Das, R., "Approach for measuring transportation network resiliency: A case study on dhaka, bangladesh", Case Studies on Transport Policy, Vol. 8, 6 2020, pp. 586-592.

[72] Serdar, M. Z., Koç, M., Al-Ghamdi, S. G., "Urban transportation networks resilience: Indicators, disturbances, and assessment methods", Sustainable Cities and Society, Vol. 76, 1 2022, pp. 103452.

[73] Ahmed, S., Dey, K., “Resilience modeling concepts in transportation systems: a comprehensive review based on mode, and modeling techniques”, Journal of Infrastructure Preservation and Resilience, Vol. 1, 12 2020, pp. 8.

[74] Berdica, K., “An introduction to road vulnerability: what has been done, is done and should be done”, Transport Policy, Vol. 9, 4 2002.

[75] Holme, P., Kim, B. J., Yoon, C. N., Han, S. K., “Attack vulnerability of complex networks”, Physical review E, Vol. 65, No. 5, 2002, pp. 056109.

[76] Wang, J., Li, Y., Liu, J., He, K., Wang, P., “Vulnerability analysis and passenger source prediction in urban rail transit networks”, PLoS ONE, Vol. 8, 11 2013, pp. e80178.

[77] Espinet, X., Schweikert, A., van den Heever, N., Chinowsky, P., “Planning resilient roads for the future environment and climate change: Quantifying the vulnerability of the primary transport infrastructure system in mexico”, Transport Policy, Vol. 50, 8 2016, pp. 78-86.

[78] Chen, B. Y., Lam, W. H., Sumalee, A., Li, Q., Li, Z.-C., “Vulnerability analysis for large-scale and congested road networks with demand uncertainty”, Transportation Research Part A: Policy and Practice, Vol. 46, 3 2012, pp. 501-516.

[79] Qiao, W., Lu, Y., Xiong, C., Haghani, A., “A game theory approach for the measurement of transport network vulnerability from the system prospective”, Transportmetrica B: Transport Dynamics, Vol. 2, 9 2014, pp. 188-202.

[80] Hu, R., Wu, Z., Xu, Y., Lai, T., Xia, C., “A multi-attack intrusion detection model based on mosaic coded convolutional neural network and centralized encoding”, PLOS ONE, Vol. 17, 5 2022, pp. e0267910.

[81] Gu, Y., Chen, A., Kitthamkesorn, S., “Accessibility-based vulnerability analysis of multi-modal transportation networks with weibit choice models”, Multimodal Transportation, Vol. 1, 9 2022, pp. 100029.

[82] Motter, A. E., Lai, Y.-C., “Cascade-based attacks on complex networks”, Physical Review E, Vol. 66, 12 2002, pp. 065102.

[83] Kermanshah, A., Derrible, S., “Robustness of road systems to extreme flooding: using elements of gis, travel demand, and network science”, Natural Hazards, Vol. 86, 3 2017, pp. 151-164.

[84] Jenelius, E., Mattsson, L.-G., “Road network vulnerability analysis of area-covering disruptions: A grid-based approach with case study”, Transportation Research Part A: Policy and Practice, Vol. 46, 6 2012, pp. 746-760.

[85] Li, L., Zhang, Q., Zhang, T., Zou, Y., Zhao, X., "Optimum route and transport mode selection of multimodal transport with time window under uncertain conditions", Mathematics, Vol. 11, 7 2023, pp. 3244.

[86] Zheng, C., Shen, Y., Ma, J., Gui, L., Zhang, C., "Robust optimization of transport organization for china railway express", Applied Sciences, Vol. 14, 12 2023, pp. 137.

[87] Mousavizadeh, O., Keyvan-Ekbatani, M., "On the important features for a well-shaped reduced network mfd estimation during network loading and recovery", Transportation Research Part C: Emerging Technologies, Vol. 161, 4 2024, pp. 104539.

[88] Massobrio, R., Cats, O., "Topological assessment of recoverability in public transport networks", Communications Physics, Vol. 7, 3 2024, pp. 108.

[89] Xie, W., Rose, A., Li, S., He, J., Li, N., Ali, T., "Dynamic economic resilience and economic recovery from disasters: A quantitative assessment", Risk Analysis, Vol. 38, 6 2018, pp. 1306-1318.

[90] Liu, T., Ji, W., Gkiotsalitis, K., Cats, O., "Optimizing public transport transfers by integrating timetable coordination and vehicle scheduling", Computers Industrial Engineering, Vol. 184, 10 2023, pp. 109577.

[91] Basallo-Triana, M. J., Bravo-Bastidas, J. J., Contreras, I., Cordeau, J.-F., Vidal-Holguín, C. J., "Intermodal hub network design with generalized capacity constraints and non-synchronized train–truck operations", Transportation Research Part B: Methodological, Vol. 174, 8 2023, pp. 102770.

[92] Zhang, Y., Heinold, A., Meisel, F., Negenborn, R. R., Atasoy, B., "Collaborative planning for intermodal transport with eco-label preferences", Transportation Research Part D: Transport and Environment, Vol. 112, 11 2022, pp. 103470.

[93] Gondia, A., Ezzeldin, M., El-Dakhakhni, W., "Dynamic networks for resilience-driven management of infrastructure projects", Automation in Construction, Vol. 136, 4 2022, pp. 104149.

[94] Febbraro, A. D., Sacco, N., Saeednia, M., "An agent-based framework for cooperative planning of intermodal freight transport chains", Transportation Research Part C: Emerging Technologies, Vol. 64, 3 2016, pp. 72-85, available at: https://linkinghub.elsevier.com/retrieve/pii/S0968090X15004301

[95] Salemi, H., Buchanan, A., "Solving the distance-based critical node problem", INFORMS Journal on Computing, Vol. 34, 5 2022, pp. 1309-1326.

[96] Lin, J., Ban, Y., “Complex network topology of transportation systems”, Transport Reviews, Vol. 33, 11 2013, pp. 658-685.

[97] Shi, W., Yu, C., “Multi-agent task allocation with multiple depots using graph attention pointer network”, Electronics, Vol. 12, 8 2023, pp. 3378.

[98] Singh, A., Wiktorsson, M., Hauge, J. B., “Trends in machine learning to solve problems in logistics”, Procedia CIRP, Vol. 103, 2021, pp. 67-72.

[99] da Mata Martins, M. C., da Silva, A. N. R., Pinto, N., “An indicator-based methodology for assessing resilience in urban mobility”, Transportation Research Part D: Transport and Environment, Vol. 77, 12 2019.

[100] Morelli, A. B., Cunha, A. L., “Assessing vulnerabilities in transport networks: a graph-theoretic approach”, TRANSPORTES, Vol. 29, 4 2021, pp. 161-172.

[101] Lee, C.-C., Rajput, A. A., Hsu, C.-W., Fan, C., Yuan, F., Dong, S., Esmalian, A., Farahmand, H., Patrascu, F. I., Liu, C.-F., Li, B., Ma, J., Mostafavi, A., “Quantitative measures for integrating resilience into transportation planning practice: Study in texas”, Transportation Research Part D: Transport and Environment, Vol. 113, 2022, pp. 103496, available at: https://www.sciencedirect.com/science/article/pii/S1361920922003224

[102] Tan, H. E., Oon, J. H. W., bin Othman, N., Legara, E. F., Monterola, C., Ramli, M. A., “Quantifying the resilience of rapid transit systems: A composite index using a demand-weighted complex network model”, PLOS ONE, Vol. 17, 4 2022, pp. e0267222.

[103] Powell, W. B., “From reinforcement learning to optimal control: A unified framework for sequential decisions”, 2019.

[104] Fan, X., Zhang, X., Wang, X., Yu, X., “A deep reinforcement learning model for resilient road network recovery under earthquake or flooding hazards”, Journal of Infrastructure Preservation and Resilience, Vol. 4, 2 2023, pp. 8.

[105] Dhanak, M., Parr, S., Kaisar, E. I., Goulianou, P., Russell, H., Kristiansson, F., “Resilience assessment tool for port planning”, Environment and Planning B: Urban Analytics and City Science, Vol. 48, 6 2021, pp. 1126-1143.

[106] Christopher, M., Logistics and Supply Chain Management: Logistics & Supply Chain Management. Pearson UK, 2016.

[107] Jafino, B. A., Kwakkel, J., Verbraeck, A., “Transport network criticality metrics: a comparative analysis and a guideline for selection”, Transport Reviews, Vol. 40, 3 2020, pp. 241-264.

[108] Ippolito, N., Cats, O., “Multi-modal and multi-layer robustness analysis of the european rail and air networks”, Scientific Reports, Vol. 14, 11 2024, pp. 26950.

[109] Oztürk, C., Ornek, A., “Capacitated lot sizing with linked lots for general product structures in job shops”, Computers Industrial Engineering, Vol. 58, 2 2010, pp. 151-164.

[110] Pujats, K., Golias, M., Konur, D., “A review of game theory applications for seaport cooperation and competition”, Journal of Marine Science and Engineering, Vol. 8, 2 2020, pp. 100.

[111] Guarda, P., Battifarano, M., Qian, S., “Estimating network flow and travel behavior using day-to-day system-level data: A computational graph approach”, Transportation Research Part C: Emerging Technologies, Vol. 158, 1 2024, pp. 104409.

[112] Li, S. H. Q., Yu, Y., Miguel, N., Calderone, D., Ratliff, L. J., Acikmese, B., “Adaptive constraint satisfaction for markov decision process congestion games: Application to transportation networks”, available at: https://arxiv.org/abs/1907.08912 2022.

[113] Bertrand, N., Markey, N., Sadhukhan, S., Sankur, O., “Dynamic network congestion games”, 2020.

[114] Bukvić, L., Škrinjar, J. P., Abramović, B., Zitrický, V., “Route selection decision-making in an intermodal transport network using game theory”, Sustainability, Vol. 13, 4 2021.

[115] Ignatius, J., Tan, T. S., Dhamotharan, L., Goh, M., “To cooperate or to compete: A game theoretic analysis on ports in malaysia and singapore”, Technological and Economic Development of Economy, Vol. 24, 9 2018, pp. 1776-1800.

[116] Michail, N. A., Melas, K. D., “Measuring the impact of port congestion on containership freight rates”, Maritime Transport Research, Vol. 8, 2025, pp. 100130, available at: https://www.sciencedirect.com/science/article/pii/S2666822X25000024

[117] Carpenter, J., Robbett, A., Game Theory and Behavior. MIT Press, 2022, available at: https://books.google.hr/books?id=PORiEAAAQBAJ

[118] Kahneman, D., Tversky, A., “Prospect theory: An analysis of decision under risk”, Econometrica, Vol. 47, No. 2, 1979, pp. 263–291, available at: http://www.jstor.org/stable/1914185

[119] Braess, D., “Über ein paradoxon aus der verkehrsplanung”, Unternehmensforschung, Vol. 12, 1968, pp. 258-268, available at: https://api.semanticscholar.org/CorpusID:39202189

[120] Shapley, L., Corporation, R., Notes on the N-person Game, ser. Notes on

the N-person Game. Rand Corporation, 1951, No. s. 2, available at: https://books.google.hr/books?id=uMoWzwEACAAJ

[121] Algaba, E., Fragnelli, V., Llorca, N., Sánchez-Soriano, J., "Horizontal cooperation in a multimodal public transport system: The profit allocation problem", European Journal of Operational Research, Vol. 275, 6 2019, pp. 659-665.

[122] Castelli, L., Longo, G., Pesenti, R., Ukovich, W., "Two-player noncooperative games over a freight transportation network", Transportation Science, Vol. 38, 5 2004, pp. 149-159.

[123] Oszczypała, M., Ziółkowski, J., Małachowski, J., Lęgas, A., "Nash equilibrium and stackelberg approach for traffic flow optimization in road transportation networks—a case study of warsaw", Applied Sciences, Vol. 13, 2 2023, pp. 3085.

[124] Radu, V., Dumitrescu, C., Vasile, E., Tăbîrcă, A. I., Stefan, M. C., Manea, L., Radu, F., "Modeling and prediction of sustainable urban mobility using game theory multiagent and the golden template algorithm", Electronics, Vol. 12, 3 2023, pp. 1288.

[125] Taylor, M. A. P., D'Este, G. M., Transport Network Vulnerability: a Method for Diagnosis of Critical Locations in Transport Infrastructure Systems. Springer Berlin Heidelberg, pp. 9-30.

[126] Taylor, M. A. P., Sekhar, S. V. C., D'Este, G. M., "Application of accessibility based methods for vulnerability analysis of strategic road networks", Networks and Spatial Economics, Vol. 6, 9 2006.

[127] Oh, J., Singh, S., Lee, H., "Value prediction network", available at: https://arxiv.org/abs/1707.03497 2017.

[128] Ashfaq, M., Gu, Z., Waller, S. T., Saberi, M., "Comparing dynamic user equilibrium and noniterative stochastic route choice in a simulation-based dynamic traffic assignment model: Practical considerations for large-scale networks", Journal of Advanced Transportation, Vol. 2021, 5 2021, pp. 1-16.

[129] Sutton, R. S., Barto, A. G., Reinforcement learning: An introduction. MIT press, 2018.

[130] Zhang, J., Zhang, J., "Artificial intelligence applied on traffic planning and management for rail transport: A review and perspective", Discrete Dynamics in Nature and Society, Vol. 2023, 7 2023, pp. 1-17.

List of Figures

List of Tables

List of Algorithms

Nomenclature

AIS Automatic Identification System

ALNS Adaptive Large Neighborhood Search

APLI Average Path Length Increase

BRUE boundedly rational user equilibrium

BUE behavioural user equilibrium

CNI Critical Node Index

CPD Cascade Performance Disruptions

CPM Critical Path Method

CSV comma-separated value

CVRP Capacitated Vehicle Routing Problem

DCs Distribution Centres

DSM Dynamic Shipment Matching

DSUE dynamic stochastic user equilibrium

DUE dynamic user equilibrium

ECMT European Conference of Ministers of Transport

ETS Emissions Trading System

EU European Union

FR Functional Resilience

GAT Graph Attention Networks

GHG Greenhouse Gas Emissions

GIS Geographic Information System

GNN Graph Neural Network

GT Game Theory

GTFS General Transit Feed Specification

HDV Heavy-duty vehicle

IMO International Maritime Organisation

IT Information Technologies

ITU Intermodal Transport Unit

KPI Key Performance Indicator

MARL Multi-Agent Reinforcement Learning

MCTS Monte Carlo Tree Search

MDP Markov decision process

MFUE multiclass fuzzy user equilibrium

MRV Monitoring, Reporting and Verification Maritime Regulation

NAPA North Adriatic Port Association

NE Nash Equilibrium

NFR Network Flow Reduction

NRI Network Robustness Index

NRMM Non-Road Mobile Machinery

O-D Origin-Destination

OAPEC The Organisation of Arab Petroleum Exporting Countries

PBUE prospect-based user equilibrium

RED Renewable Energy Directive

ReLU Rectified Linear Unit

RNN Recurrent neural networks

SARSA State–Action–Reward–State–Action

SO Social Optima

SPE Subgame-Perfect Equilibria

SR Structural Resilience

SRC stochastic route choice

SUMO Simulation of Urban MObility

TD Temporal difference

THC Terminal Handling Cost

TMS Transport Management System

TTR Time to Recover

TTS Time to Survive

UN/ECE United Nations Economic Commission for Europe

VRP Vehicle Routing Problem

XGBoost Extra Gradient Boosting

ZLEV Zero and low-emission vehicle

Biography

Lucija Bukvić was born in Koprivnica on August 7, 1994. She completed her undergraduate studies, majoring in Intelligent Transport Systems and Logistics, and her graduate studies in Logistics at the Faculty of Transport and Traffic Sciences, University of Zagreb. She defended her final thesis entitled "Technical Safety of Road Freight Vehicles as an Exploitation Factor" in 2017, and her master's thesis in 2019 under the topic: "Cost-effectiveness of Electric Vehicle Fleet in Transport Logistics". She was the winner of the student competition "Logistics Practicum" organised by the Faculty of Transport and Traffic Sciences for two years in a row (2018 Optimisation of Delivery to Islands; 2019 Digitalisation of Logistics Processes). In October 2020, she enrolled in the postgraduate doctoral study "Transportation" at the Faculty of Transport and Traffic Sciences, University of Zagreb. By decision of the Faculty Council in April 2020, she was appointed to the position of assistant at the Faculty of Transport and Traffic Sciences at the Department of Transport Logistics. In April 2022, her research interests led her to the position of assistant at the Department of Intelligent Transport Systems, where she is currently employed. She is participating in holding auditory exercises and seminars of the following courses: Operations Research, Intelligent Transport Systems I, Fundamentals of Traffic Engineering and Computer Security. In 2025, she carried out a longer mobility of doctoral students of the Croatian Science Foundation (HRZZ) at the University College Cork in Ireland, School of Computer Science and Information Technology (project MOBDOK-2023-3222). As an external associate, she participated in the project "Coordination mechanisms for multimodal cross-border traveller information network based on OJP for Danube Region" - Interreg Danube Program, led by prof. Sadko Mandžuka, PhD, and as a junior researcher in the project "A model of a proactive messaging system for drivers ((PaWMS2D))" within the framework of the National Road Safety Plan of the Republic of Croatia for the period 2024/25, led by Assoc. Prof. Pero Škorput, PhD.

Research interests: intermodal networks, intelligent transport systems, artificial intelligence, game theory, reinforcement learning

List of published works

Papers in journals

1. Bukvić, Lucija ; Pašagić Škrinjar, Jasmina ; Fratrović, Tomislav ; Abramović, Borna Price Prediction and Classification of Used-Vehicles Using Supervised Machine Learning // Sustainability, 14 (2022), 24; 17034, 17. doi: 10.3390/su142417034
2. Bukvić, Lucija ; Pašagić Škrinjar, Jasmina ; Abramović, Borna ; Zitrický, Vladislav Route Selection Decision-Making in an Intermodal Transport Network Using Game Theory // Sustainability, 13 (2021), 8; 4443, 16. doi: 10.3390/su13084443
3. Pašagić Škrinjar, Jasmina ; Abramović, Borna ; Bukvić, Lucija ; Marušić, Željko Managing Fuel Consumption and Emissions in the Renewed Fleet of a Transport Company // Sustainability, 12 (2020), 12; 5047, 15. doi: 10.3390/su12125047

Papers at international scientific conferences

1. Bukvić, Lucija; Kramarić, Luka; Muštra, Mario; Jelušić, Niko Ultra-wideband Localization with Time-based Measurement Techniques // Proceedings ELMAR-2023: 65th International Symposium ELMAR-2023. Zagreb: Hrvatsko društvo Elektronika u pomorstvu (ELMAR); Institute of Electrical and Electronics Engineers (IEEE), 2023
2. Vrančić, Maja Tonec ; Vujić, Miroslav ; Erdelić, Martina ; Bukvić, Lucija The Analysis of Available Open Data in the EU for Increasing the Safety of Railway Level Crossings // International Conference on Open Data (ICOD 2022): Book of abstracts / Varga, Filip ; Đurman, Petra (ur.). Zagreb: Pravni fakultet Sveučilišta u Zagrebu, 2023. str. 87-90 doi: 10.5281/zenodo.8071046
3. Bukvić, Lucija ; Škrinjar, Jasmina Pašagić ; Škorput, Pero ; Vrančić, Maja Tonec Overview of Resilience Processes in Transport Management Systems. Springer, 2022. str. 631-638 doi: 10.1007/978-3-031-05230-976
4. Škorput, Pero ; Medić, Dario ; Bukvić, Lucija Application of Multilevel Integration Model for Unmanned Aerial Vehicles in Traffic Incident Management Processes // Lecture notes in networks and systems / Karabegović, Isak (ur.). 2021. str. 753-760 doi: 10.1007/978-3-030-75275-083
5. Evdjenić, Karlo ; Bukvić, Lucija ; Pašagić Škrinjar, Jasmina Intermodal Routes Analysis of Transport Organization from Gothenburg to Zagreb // Proceedings of the International Scientific Conference "The Science and Development of Transport" (ZIRP 2020) / Ivanjko E., Stanković R., Novačko L., Petrović M. (ur.). Zagreb, 2020. str. 83-97

6. Bukvić, Lucija ; Pašagić Škrinjar, Jasmina ; Jakara, Martina Possible Application of Electric Vehicles in Zagreb City Logistics // Proceedings of the International Scientific Conference "Science and Traffic Development" (ZIRP 2019) / Grgurević, Ivan ; Rožić, Tomislav (ur.). Zagreb: Fakultet prometnih znanosti Sveučilišta u Zagrebu, 2019. str. 87-92

Životopis

Lucija Bukvić rođena je u Koprivnici 7. kolovoza 1994. Prijediplomski studij, smjer Inteligentni transportni sustavi i logistika, te diplomski studij Logistike završava na Fakultetu prometnih znanosti Sveučilišta u Zagrebu. Završni rad naziva "Tehnička ispravnost cestovnih teretnih vozila kao čimbenik eksploatacije" obranila je 2017. godine, a diplomski rad 2019. godine pod temom: "Isplativost električnog voznog parka u prijevoznoj logistici". Pobjednica je studentskog natjecanja "Logistički praktikum" u organizaciji Fakulteta prometnih znanosti dvije godine za redom (2018. optimizacija dostave na otoke; 2019. digitalizacija logističkih procesa). U listopadu 2020. upisuje poslijediplomski doktorski studij "Promet" na Fakultetu prometnih znanosti Sveučilišta u Zagrebu. Odlukom Fakultetskog vijeća Fakulteta prometnih znanosti u travnju 2020. imenovana je na radno mjesto asistenta na Fakultetu prometnih znanosti na Zavodu za transportnu logistiku. Istraživački interesi u travnju 2022. vode je prema radnom mjestu asistenta na Zavodu za inteligentne transportne sustave gdje je i trenutno zaposlena. Trenutno sudjeluje u izvodenju nastave na predmetima: Operacijska istraživanja, Inteligentni transportni sustavi I, Osnove prometnog inženjerstva i Računalna sigurnost. U 2025. ostvaruje dulju mobilnost doktorskih studenata Hrvatske zaklade za znanost (HRZZ) na instituciji University College Cork u Irskoj, School of Computer Science and Information Technology (projekt MOBDOK-2023-3222). Kao vanjski suradnik sudjelovala je na projektu "Coordination mechanisms for multimodal cross-border traveller information network based on OJP for Danube Region" - Program Interreg Danube voditelj prof. dr. sc. Sadko Mandžuka, te kao mlađi istraživač na projektu "Prijedlog modela proaktivnog sustava davanja poruka za vozače" u okviru Nacionalnog plana sigurnosti cestovnog prometa Republike Hrvatske za period 2024/25, voditelj izv. prof. dr. sc. Pero Škorput.

Istraživački interesi: intermodalne mreže, inteligentni transportni sustavi, umjetna inteligencija, teorija igara, potporno učenje

Popis objavljenih djela

Radovi u časopisima

1. Bukvić, Lucija ; Pašagić Škrinjar, Jasmina ; Fratrović, Tomislav ; Abramović, Borna Price Prediction and Classification of Used-Vehicles Using Supervised Machine Learning // Sustainability, 14 (2022), 24; 17034, 17. doi: 10.3390/su142417034

2. Bukvić, Lucija ; Pašagić Škrinjar, Jasmina ; Abramović, Borna ; Zitrický, Vladislav Route Selection Decision-Making in an Intermodal Transport Network Using Game Theory // Sustainability, 13 (2021), 8; 4443, 16. doi: 10.3390/su13084443

3. Pašagić Škrinjar, Jasmina ; Abramović, Borna ; Bukvić, Lucija ; Marušić, Željko Managing Fuel Consumption and Emissions in the Renewed Fleet of a Transport Company // Sustainability, 12 (2020), 12; 5047, 15. doi: 10.3390/su12125047

Članci objavljeni na konferencijama

1. Bukvić, Lucija; Kramarić, Luka; Muštra, Mario; Jelušić, Niko Ultra-wideband Localization with Time-based Measurement Techniques // Proceedings ELMAR-2023: 65th International Symposium ELMAR-2023. Zagreb: Hrvatsko društvo Elektronika u pomorstvu (ELMAR); Institute of Electrical and Electronics Engineers (IEEE), 2023

2. Vrančić, Maja Tonec ; Vujić, Miroslav ; Erdelić, Martina ; Bukvić, Lucija The Analysis of Available Open Data in the EU for Increasing the Safety of Railway Level Crossings // International Conference on Open Data (ICOD 2022): Book of abstracts / Varga, Filip ; Đurman, Petra (ur.). Zagreb: Pravni fakultet Sveučilišta u Zagrebu, 2023. str. 87-90 doi: 10.5281/zenodo.8071046

3. Bukvić, Lucija ; Škrinjar, Jasmina Pašagić ; Škorput, Pero ; Vrančić, Maja Tonec Overview of Resilience Processes in Transport Management Systems. Springer, 2022. str. 631-638 doi: 10.1007/978-3-031-05230-976

4. Škorput, Pero ; Medić, Dario ; Bukvić, Lucija Application of Multilevel Integration Model for Unmanned Aerial Vehicles in Traffic Incident Management Processes // Lecture notes in networks and systems / Karabegović, Isak (ur.). 2021. str. 753-760 doi: 10.1007/978-3-030-75275-083

5. Evdjenić, Karlo ; Bukvić, Lucija ; Pašagić Škrinjar, Jasmina Intermodal Routes Analysis of Transport Organization from Gothenburg to Zagreb // Proceedings of the International Scientific Conference "The Science and Development of Transport" (ZIRP 2020) / Ivanjko E., Stanković R., Novačko L., Petrović M. (ur.). Zagreb, 2020. str. 83-97

6. Bukvić, Lucija ; Pašagić Škrinjar, Jasmina ; Jakara, Martina Possible Application of Electric Vehicles in Zagreb City Logistics // Proceedings of the International Scientific Conference "Science and Traffic Development" (ZIRP 2019) / Grgurević, Ivan ; Rožić, Tomislav (ur.). Zagreb: Fakultet prometnih znanosti Sveučilišta u Zagrebu, 2019. str. 87-92